Eur. J. Mineral.
1998, **10**, 693-812

Elastic anomalies in minerals due to structural phase transitions

MICHAEL A. CARPENTER and EKHARD K.H. SALJE

Department of Earth Sciences, University of Cambridge, Downing St., Cambridge CB2 3EQ, England

Abstract: Landau theory provides a formal basis for predicting the variations of elastic constants associated with phase transitions in minerals. These elastic constants can show substantial anomalies as a transition point is approached from both the high-symmetry side and the low-symmetry side. In the limiting case of proper ferroelastic behaviour, individual elastic constants, or some symmetry-adapted combination of them, can become very small if not actually go to zero. When the driving order parameter for the transition is a spontaneous strain, the total excess energy for the transition is purely elastic and is given by:

$$G_{\text{elastic}} = \frac{1}{2}\sum_{i,k} C_{ik}e_ie_k + \frac{1}{3!}\sum_{i,k,l} C_{ikl}e_ie_ke_l + \frac{1}{4!}\sum_{i,k,l,m} C_{iklm}e_ie_ke_le_m + \ \ldots$$

which has the same form as a Landau expansion. In this case, the second-order elastic constant C_{ik} softens as a linear function of temperature with a slope in the low-symmetry phase that depends on the thermodynamic character of the transition. If the driving order parameter, Q, is some structural feature other than strain, the excess energy is given by:

$$G = \frac{1}{2}a(T - T_c)Q^2 + \frac{1}{4}bQ^4 + \ \ldots \ + \sum_{i,m,n}\lambda_{i,m,n}e_i^mQ^n + \frac{1}{2}\sum_{i,k} C_{ik}^{o}e_ie_k$$

In this case, the effect of coupling, described by the term in λe^mQ^n, is to cause a great diversity of elastic variations depending on the values of m and n (typically 1, 2 or 3), the thermodynamic character of the transition and the magnitudes of any non-symmetry-breaking strains. The elastic constants are obtained by taking the appropriate second derivatives of G with respect to strain in a manner that includes the structural relaxation associated with Q.

The symmetry properties of second-order elastic constant matrices can be related to the symmetry rules for individual phase transitions in order to predict elastic stability limits, and to derive the correct form of Landau expansion for any symmetry change. Selected examples of "ideal" behaviour for different types of driving order parameter, coupling behaviour and thermodynamic character have been set out in full in this review. Anomalies in the elastic properties on a macroscopic scale can also be understood in terms of the properties of acoustic phonons. These microscopic processes must be considered if elastic anomalies due to dynamical effects are to be accounted for

0935-1221/98/0010-0693 $ 30.00

correctly. Such additional anomalies are characterised by softening of the form $\Delta C_{ik} = A_{ik}|T - T_c|^K$ as the transition is approached from the high-symmetry side. The A coefficient is a property of the material, and K depends on how the branches of the critical acoustic mode soften in three dimensions.

Adopting this approach allows the quantitative description of elastic variations in "real" systems. Albite provides a likely example of proper ferroelasticity in minerals, and values for the required coefficients, extracted from experimental data, yield a complete picture of the expected elastic properties. The $\beta \rightleftharpoons \alpha$ transition in quartz provides an example of co-elastic behaviour. Data for TeO_2, $BiVO_4$ and $KMnF_3$ (a perovskite) have been reviewed to illustrate the full range of elastic anomalies that should be expected at structural phase transitions in natural minerals.

Key-words: phase transitions, elastic constants, ferroelasticity, Landau theory, albite, quartz, perovskite.

Contents

1. Introduction

The elastic constants of many geological materials show a smooth and approximately linear increase with falling temperature (T) or increasing pressure (P). Minerals which undergo phase transitions can show dramatic variations in their elastic properties, however, and the influence of a transition can extend over a wide P, T range on either side of the transition point. Illustrations of these two extremes are provided by the elastic constants of olivine, showing a "normal" pattern (Fig. 1), and of quartz, showing significant anomalies associated with the $\beta \rightleftharpoons \alpha$ transition (Fig. 2). Exactly at a transition point individual elastic constants and specific combinations of elastic constants can go to zero, or at least become very small. The effects of such anomalies must have some influence on the seismological and rheological properties of rocks – hence the interest, for example, in whether or not $(Mg,Fe)SiO_3$ perovskite remains orthorhombic with increasing depth in the mantle (*e.g.* Hemley & Cohen, 1992; Wentzcovitch *et al.*, 1995; Warren & Ackland, 1996; and references therein).

From a thermodynamic point of view there are two sound reasons for suggesting that the variations of elastic constants at phase transitions in minerals warrant closer investigation. Firstly, the elastic energy change associated with a phase transition, G_{elastic}, can be a significant quantity in relation to the total free-energy change, G_{excess}, due to that transition. This elastic energy is usually expressed formally as $\frac{1}{2}\sum_{i,k} C^{\circ}_{ik} e_i e_k$ where C°_{ik} represents the "bare" elastic constants of the crystal (*i.e.* those which do not include the influence of the transition), and e_i, e_k are components of the spontaneous strain. In the case of the $C2/m \rightleftharpoons C\bar{1}$ transition in albite, $|G_{\text{elastic}}|$ is a substantial fraction of $|G_{\text{excess}}|$ (Salje *et al.*, 1985a) and is sufficiently large to influence the stability limits of albite-bearing mineral assemblages. By way of contrast, $|G_{\text{elastic}}|$ for the $P6/mcc \rightleftharpoons Cccm$ transition in cordierite is a very small fraction of $|G_{\text{excess}}|$ (Carpenter, 1988), and its influence in determining the stability limits of cordierite-bearing assemblages is probably negligible. Secondly, these elastic constants are by definition the second derivatives of free energy with respect to strain, $\partial^2 G/\partial e_i \partial e_k$. As such they should be particularly sensitive to the shape of the free-energy potential which governs the overall transition behaviour. While several different formulations of G_{excess} might give minima corresponding approximately to observed equilibrium

structural states from *first* derivatives, such as $\partial G/\partial Q$ where Q is the order parameter, the correct formulation must be close to physical reality if it is also to predict the observed elastic constants from the *second* derivatives. This means that the closeness of fit between predicted and observed elastic constants can be a stringent criterion for testing the validity of any thermodynamic mechanism proposed for a phase transition.

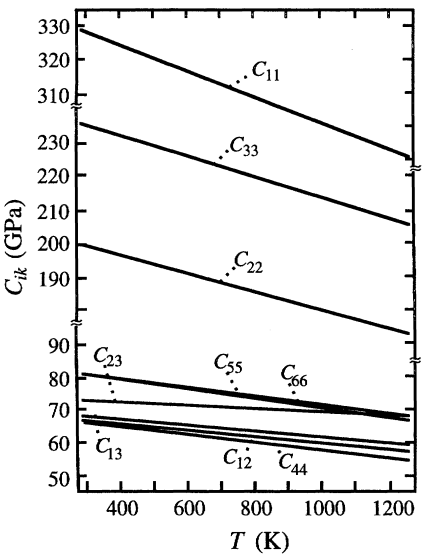

Fig. 1. Variations of the elastic constants of forsterite as a function of temperature (after Suzuki *et al.*, 1983). The smooth decline with increasing T is characteristic of materials at temperatures and pressures far removed from any structural phase transition.

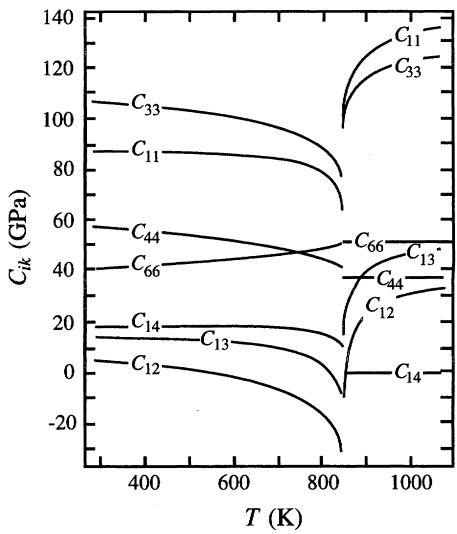

Fig. 2. Variations of the elastic constants of quartz as a function of temperature showing the marked anomalies associated with the $\beta \rightleftharpoons \alpha$ transition at ~846 K (after Höchli, 1972, and Yamamoto, 1974).

As discussed at some length in the physics literature, phase transitions which involve significant lattice distortions should tend to conform closely to the predictions of Landau-type theories (Cowley, 1976; Folk *et al.*, 1976a and b, 1979; Als-Nielsen & Birgeneau, 1977; Schwabl, 1980; Bruce & Cowley, 1981; Wadhawan, 1982; Cummins, 1983; David, 1984; Ginzburg *et al.*, 1987; and see also Carpenter & Salje, 1989; Salje, 1992, 1993; Schwabl & Täuber, 1996). Indeed, it is the comparative rarity of systems which do not that now attracts attention (Folk *et al.*, 1979; Mayer & Cowley, 1988; Harris *et al.*, 1993, 1995; Harris & Dove, 1995). There is a high expectation that the elastic properties of most natural materials can be described from the same macroscopic point of view, and a selection of phase transitions for which the overall approach should be directly relevant is given in Table 1.

An illustration of the link between elastic behaviour and other properties is provided by a simple example. For a transition in which a spontaneous strain, e_k, arises by coupling with a driving order parameter, Q, the excess energy of the low-symmetry phase with respect to the high-symmetry phase (at the same conditions of pressure, temperature, *etc.*) may be expressed as:

$$G_{\text{excess}} = G_{\text{Q}} + G_{\text{coupling}} + G_{\text{elastic}} \qquad (1).$$

Table 1. Phase transitions in minerals for which elastic-constant variations should conform to solutions of a Landau free-energy expansion. The basis of the classification is set out in section 7. There is also a reversible transition at high pressures in gillespite ($BaFeSi_4O_{10}$), but the symmetry change, $P4/ncc \rightarrow P2_12_12$, does not follow the normal group → subgroup relations, and does not fit conveniently into this scheme (Hazen & Finger, 1983; Redfern *et al.*, 1993).

Selected phase transitions in minerals	
Proper ferroelastic behaviour	Co-elastic behaviour
albite: $C2/m \rightleftharpoons C\bar{1}$ ($Q_{od} = 0$)	quartz: $P6_422$ or $P6_222 \rightleftharpoons P3_12$ or $P3_22$
Sr-anorthite: $I2/c \rightleftharpoons I\bar{1}$	leucite: $I4_1/acd \rightleftharpoons I4_1/a$
leucite: $Ia3d \rightleftharpoons I4_1/acd$	pigeonite: $C2/c \rightleftharpoons P2_1/c$
Pseudo-proper ferroelastic behaviour	anorthite: $I\bar{1} \rightleftharpoons P\bar{1}$
tridymite: $P6_322 \rightleftharpoons C222_1$	calcite: $R\bar{3}m \rightleftharpoons R\bar{3}c$
vesuvianite: $P4/nnc \rightleftharpoons P2/n$ (?)	tridymite: $P6_3/mmc \rightleftharpoons P6_322$
Improper ferroelastic behaviour	kaliophilite: $P6_322 \rightleftharpoons P6_3$
$(Mg,Fe)SiO_3$ perovskite: cubic ⇌ tetragonal (?)	kalsilite: $P6_3mc \rightleftharpoons P6_3$
tetragonal ⇌ orthorhombic (?)	$P6_3mc \rightleftharpoons P6_3mc$ (superlattices)
neighborite: $Pm3m \rightleftharpoons Pbnm$	$P6_3 \rightleftharpoons P6_3$ (superlattices)
$CaTiO_3$ perovskite: $Pm3m \rightleftharpoons I4/mcm \rightleftharpoons Pbnm$	cummingtonite: $C2/m \rightleftharpoons P2_1/m$
cristobalite: $Fd3m \rightleftharpoons P4_32_12$ or $P4_12_12$	lawsonite: $Cmcm \rightleftharpoons Pmcn \rightleftharpoons P2_1cn$
calcite: $R\bar{3}c \rightleftharpoons P2_1/c$	titanite: $A2/a \rightleftharpoons P2_1/a$

Here G_Q signifies the change in energy due to the effect of Q alone and $G_{coupling}$ is the energy due to interactions between Q and e_k; both are usually negative. $G_{elastic}$ is invariably a positive quantity because of the condition that the elastic-constant matrix must be positive definite for a crystal to be in an elastically stable state (Born & Huang, 1954). These energies are shown schematically in Fig. 3. If the crystal is subjected to an external stress, $\sigma_{i,ext}$, it will deform by an amount $e_{k,ext}$ that should depend on the bare elastic constants, C^o_{ik}, according to Hooke's law:

$$\sigma_{i,ext} = \sum_{i,k} C^o_{ik} e_{k,ext} \qquad (2).$$

However, a change in the strain state of the crystal from e_k to $(e_k + e_{k,ext})$ will result in a change of the equilibrium value of Q, via the Q/e_k coupling term. The crystal will therefore respond to the external stress by adjusting its structural state to the new equilibrium condition. Such a relaxation implies a reduction in energy. In fact, the act of deforming the crystal will have been made slightly easier so that it will appear to be softer than an identical crystal which was not susceptible to undergoing a phase transition. The effective, or "renormalised" elastic constants, C_{ik}, will be smaller than C^o_{ik}, with the magnitude of the effect depending on the form of G_Q. The most important conclusion here is that the effective elastic constants depend not only on the coupling terms but also on the shape of the free-energy potential for Q. This "shape" is formally the susceptibility, χ, of Q where $\chi^{-1} = \partial^2 G/\partial Q^2$; χ^{-1} is generally referred to in this context as the inverse susceptibility of the crystal with respect to Q.

If the driving order parameter is itself a symmetry-breaking spontaneous strain, G_{excess} would be entirely elastic in origin. The susceptibility of a crystal with respect to this strain is the

"critical" elastic constant. Quite characteristic C_{ik} variations are observed, but such behaviour appears to be relatively uncommon in both minerals and man-made materials. Coupling of the symmetry-breaking strain with other strains is still possible and causes changes in some of the non-critical elastic constants which may be revealing of more subtle details of the transition.

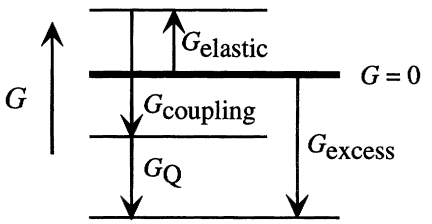

Fig. 3. Schematic illustration of the contributions from different excess energies to the total excess free energy due to a phase transition. The relative size of each contribution varies greatly between transitions. (It can easily be shown that $G_{\text{elastic}} = -\frac{1}{2}G_{\text{coupling}}$).

Since the elastic constants relate directly to the order-parameter susceptibility, their variations are quite different from those shown by excess properties such as spontaneous strain. Most significantly, the susceptibility varies in both the high-symmetry phase and the low-symmetry phase of a crystal. Consequently, evidence of an impending phase transition is often clearly displayed by an anomalous decrease in one or more elastic constants as the transition point is approached either from above or from below the transition point. Precursor behaviour is shown by quartz (Fig. 2), for example, although, as will be discussed later, the $\beta \rightleftharpoons \alpha$ transition in quartz is not as straightforward in this context as some other phase transitions. The excess free energy, enthalpy, entropy, *etc.*, on the other hand, are by definition zero in the high-symmetry phase (ignoring short-range ordering and fluctuations) and only vary as a direct function of Q in the low-symmetry phase.

From these preliminary remarks it should be clear that the elastic constants associated with phase transitions are expected to show diverse variations, and that their evolution will be quite specifically dependent on transition mechanism. Some possible patterns of elastic behaviour are illustrated in Fig. 4 for cubic $\rightleftharpoons$ tetragonal ($m3m \rightleftharpoons 4/mmm$) transitions, for example. The key issues and equations which underpin the prediction and interpretation of these variations form the subject of this review. The intention is: (a) to describe, from a purely macroscopic point of view, the physical processes that are responsible for the dramatic variations in elastic constants observed in minerals such as quartz, (b) to present a coherent framework of theory which might allow quantitative analysis of such variations in other minerals, and (c) to provide illustrative examples from a range of different materials. As in the accompanying review on spontaneous strain (Carpenter *et al.*, 1998a), the format adopted is largely pedagogical. Section 2 is designed to explain why strain effects lead to changes in the evolution of individual elastic constants. Section 3 gives essential background information concerning the role of symmetry in defining formal criteria for elastic instabilities. Section 4 deals with the relationship between acoustic velocities and elastic constants. This is included because certain acoustic phonons can determine the manner in which a

Fig. 4. (Facing page) Schematic variations of elastic constants at second-order transitions involving the point-group change $m3m \rightleftharpoons 4/mmm$, based on expressions given later in this review (Table 8); e_a is the non-symmetry-breaking strain. For the proper and pseudo-proper cases, it has been assumed that the third-order term is negligibly small. In the improper case ($Pm3m \rightleftharpoons I4/mcm$), this term is strictly zero by symmetry. Note: $(\overline{C}_{11} - \overline{C}_{12}) = \frac{1}{3}(C_{11} + C_{12} + 2C_{33} - 4C_{13})$, $\frac{1}{3}(\overline{C}_{11} + 2\overline{C}_{12}) = \frac{1}{9}(2C_{11} + C_{33} + 2C_{12} + 4C_{13})$. The causes of these variations in elastic constants for different categories of phase transitions are discussed in detail in section 6.

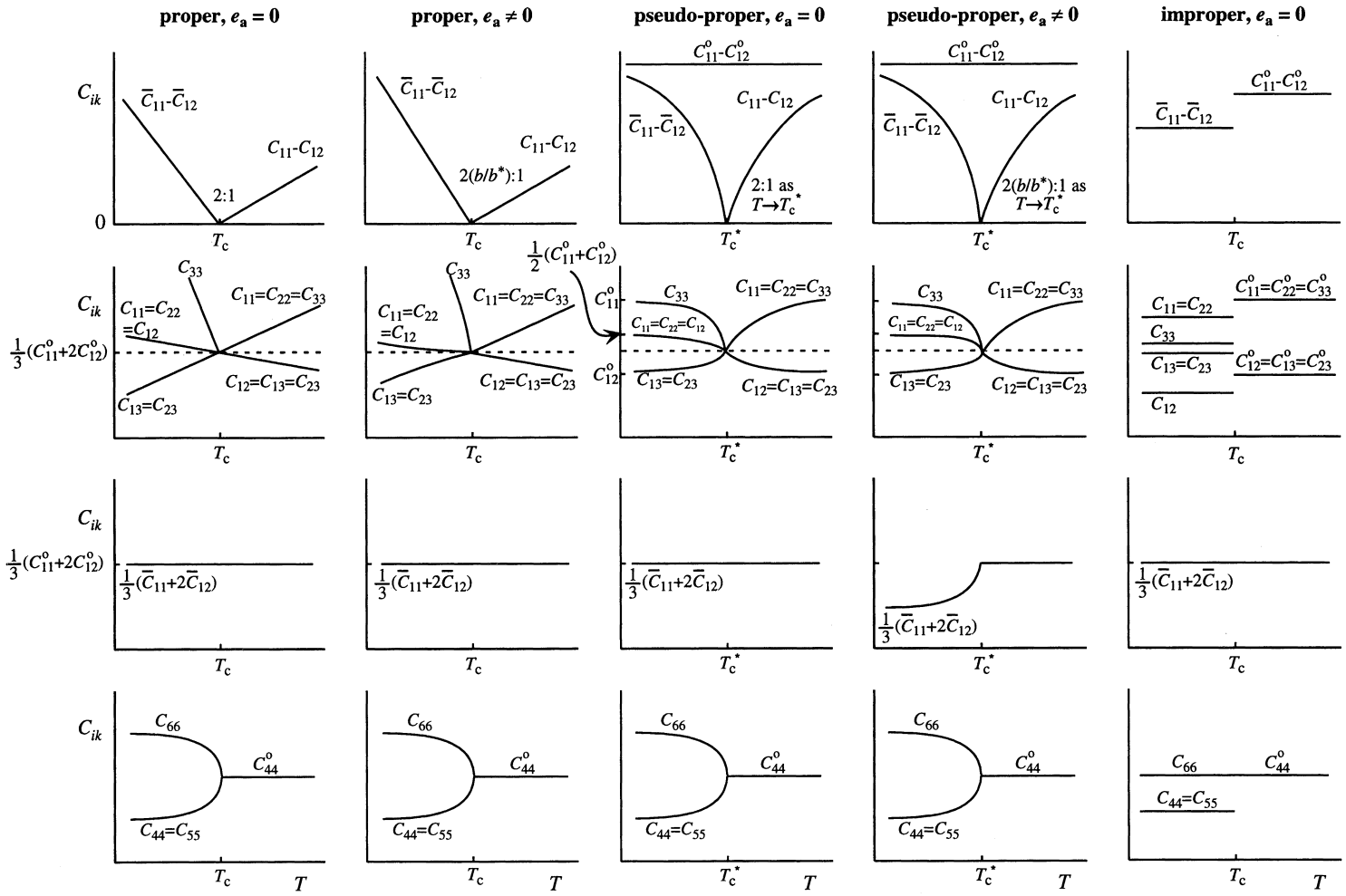

symmetry-breaking distortion occurs when an elastic constant tends to zero, and because dynamical effects can cause additional elastic softening in the vicinity of the transition point. In section 5 experimental methods for determining elastic constants are briefly described in order to highlight differences between data obtained by dynamic, as opposed to static techniques. Sections 6 and 7 represent the main substance of the paper. Section 6 is devoted to the ideal behaviour expected at second-order phase transitions driven by small atomic displacements. Worked examples cover almost all the aspects of symmetry and order-parameter coupling which are likely to arise in practice. In section 7 ideal behaviour predicted using the appropriate Landau expansions is compared with actual behaviour observed in a variety of materials. Because existing data for minerals are sparse, phase transitions in a number of synthetic materials are used to illustrate the likely properties of natural systems.

Different aspects of both theory and experimental practice relating to ferroelastic properties are dealt with in previous review articles, including: Rehwald (1973), Lüthi & Rehwald (1981), Fleury & Lyons (1981), Wadhawan (1982), Liakos & Saunders (1982), Cummins (1983), Tolédano *et al.* (1983), Schwabl (1985), Bulou *et al.* (1992) and Schwabl & Täuber (1996). For readers who are not at all familiar with Landau theory, basic background information will be found in Carpenter (1988, 1992), Salje (1992, 1993) and Dove (1997). Some familiarity with irreducible representations in crystallographic point groups is also helpful, but not essential. A gentle introduction to this topic is given by Wooster (1973). Readers of the present review who are already familiar with the overall approach may wish to proceed directly to sections 6 and 7, in which predicted and observed elastic-constant variations are compared.

2. Renormalisation of elastic constants: the formal basis

Phase transitions in real materials are governed by a diversity of mechanisms. In order to understand how each mechanism can yield a distinctive pattern of elastic-constant variations, it is instructive to consider the form of the elastic energy, G_{elastic}, first.

In the limit of small elastic strains in a crystal, the relationship between an applied stress, σ_i, and the resultant strain, e_k, is given by the tensor relationship (in Voigt notation):

$$\sigma_i = C_{ik} e_k \qquad (3).$$

The elastic energy stored in the crystal is equal to the work done on the crystal and, from Nye (1985), is:

$$G_{\text{elastic}} = \frac{1}{2} \sum_{i,k} C_{ik} e_i e_k \qquad (4).$$

In most situations of stresses applied externally to a crystal, the linear relationship between stress and strain given by Hooke's law provides an adequate description of the energy changes. This is not necessarily the case when the elastic constants become very small, however. If some C_{ik}'s in equation 4 became zero, a crystal might become infinitely soft – it would continue to deform without a change in energy even at infinite strain. Clearly, higher-order terms are needed to

describe the effective restoring forces beyond the equilibrium state of strain, and equation 3 should be given more fully as:

$$\sigma_i = C_{ik}e_k + C_{ikl}e_k e_l + C_{iklm}e_k e_l e_m + \ \ldots \qquad (5).$$

Here C_{ik}, C_{ikl} and C_{iklm} are second-order, third-order and fourth-order elastic constants. The elastic energy is then:

$$G_{\text{elastic}} = \frac{1}{2}\sum_{i,k} C_{ik}e_i e_k + \frac{1}{3!}\sum_{i,k,l} C_{ikl}e_i e_k e_l + \frac{1}{4!}\sum_{i,k,l,m} C_{iklm}e_i e_k e_l e_m + \ \ldots \qquad (6)$$

where the prefactors are necessary to avoid counting equivalent terms (due to $C_{ikl} = C_{ilk} = C_{lik}$, *etc.*) more than once.

Equation 6 has the form of a Landau expansion in which $G_{\text{excess}} = G_{\text{elastic}}$. It should describe transitions in systems for which strain is the driving order parameter and the only excess energy is elastic. On the basis that such systems are expected to behave in a Landau-like manner, the coefficient for the second-order term (in $e_i e_k$) might be expected to show a linear temperature dependence, while the coefficients for higher-order terms are expected to be weakly temperature dependent or constant. This contrasts with systems in which G_Q and G_{coupling} contribute significantly to G_{excess}. A classical Landau expansion forms the starting point for the thermodynamic description of the latter case, and might be given as (see Carpenter *et al.*, 1998a, for example):

$$G = \frac{1}{2}a(T - T_c)Q^2 + \frac{1}{4}bQ^4 + \sum_{i,m,n}\lambda_{i,m,n}e_i^m Q^n + \frac{1}{2}\sum_{i,k} C_{ik}^{o}e_i e_k \qquad (7).$$

In writing out the expansion in Q but truncating the elastic energy after a second-order term, it is implied not only that the structural feature represented by Q drives the transition, but also that restoring forces which prevent the crystal from becoming infinitely soft are due to the higher-order terms in Q and not to those in e. Different coupling mechanisms require different values for the exponents m and n. (Note that the subscripts for λ are only labels and do not signify tensor properties for the coupling constants).

The manner in which alternative patterns of elastic-constant variations emerge from the different transition mechanisms represented by equations 6 and 7 may be illustrated using a simple example. In the following sections, an orthorhombic $\rightleftharpoons$ monoclinic ($mmm \rightleftharpoons 2/m$) transition with e_5 as the symmetry-breaking strain is used. Only a single elastic constant, C_{55}, need be considered at first and odd-order terms are excluded by symmetry from the Landau expansions, which greatly simplifies the algebra. The weak temperature dependence of the bare elastic constants has been ignored.

2.1 Strain as order parameter

Taking e_5 as the order parameter for an orthorhombic $\rightleftharpoons$ monoclinic transition with second-order character, the elastic energy may be written in the form of a Landau expansion ($G_{excess} = G_{elastic}$) as:

$$G = \frac{1}{2}a(T - T_c)e_5^2 + \frac{1}{4}be_5^4 \quad (8)$$

where T_c is the equilibrium transition temperature. The equilibrium variation of e_5 is obtained in the usual way from:

$$\frac{\partial G}{\partial e_5} = 0 = a(T - T_c)e_5 + be_5^3 \quad (9)$$

giving $e_5 = 0$, or:

$$e_5^2 = \frac{a}{b}(T_c - T) \quad (10).$$

The elastic constant C_{55} is the inverse susceptibility of the crystal with respect to e_5, *i.e.*:

$$C_{55} = \frac{\partial^2 G}{\partial e_5^2} = a(T - T_c) + 3be_5^2 \quad (11).$$

At $T > T_c$, $e_5 = 0$ and $C_{55} = a(T - T_c)$, while at $T < T_c$, e_5 is given by equation 10 and $C_{55} = 2a(T_c - T)$. On this basis, C_{55} is expected to go linearly to zero at $T = T_c$ with slopes below and above T_c in the ratio 2:1 (Fig. 5a). By comparing equations 6 and 8 the fourth-order coefficient, b, is seen to be equivalent to $\frac{1}{6}C_{5555}$, where C_{5555} is a fourth-order elastic constant of the crystal (Tolédano *et al.*, 1983).

The variation of C_{55} with temperature for tricritical and first-order transitions can also be derived quite simply from the relevant form of the Landau expansion in e_5, and is shown schematically in Fig. 5b and 5c. In the case of tricritical behaviour, C_{5555} is zero and the ratio of the slopes of C_{55} below and above T_c should be 4:1. A first-order transition (C_{5555} negative and a positive sixth-order term) would be marked by a discontinuity in C_{55} at an equilibrium transition temperature, T_{tr}, higher than T_c.

Fig. 5. (Facing page) Schematic variations of selected elastic constants at phase transitions involving the change in point-group symmetry $mmm \rightleftharpoons 2/m$, with e_5 as the symmetry-breaking strain. The three columns are for second-order (left), tricritical (centre) and first-order (right) character. (a–c) Proper ferroelastic, no non-symmetry-breaking strain. (d–f) Pseudo-proper ferroelastic, no non-symmetry-breaking strain. (g–i) Improper ferroelastic transition ($Pmma \rightleftharpoons P2/c$). (j–l) e_5 as the driving order parameter with coupling to the non-symmetry-breaking strain component e_1, as $\lambda_1 e_1 e_5^2$. (m–o) Pseudo-proper ferroelastic with coupling terms $\lambda_5 e_5 Q$ and $\lambda_1 e_1 Q^2$. (p–r) Variations due to coupling of the form $\lambda_4 e_4^2 Q^2$ (or $\lambda_4 e_4^2 e_5^2$). (s–u) Variations due to coupling of the form $\lambda_7 e_4 e_6 Q$ (or $\lambda_7 e_4 e_6 e_5$).

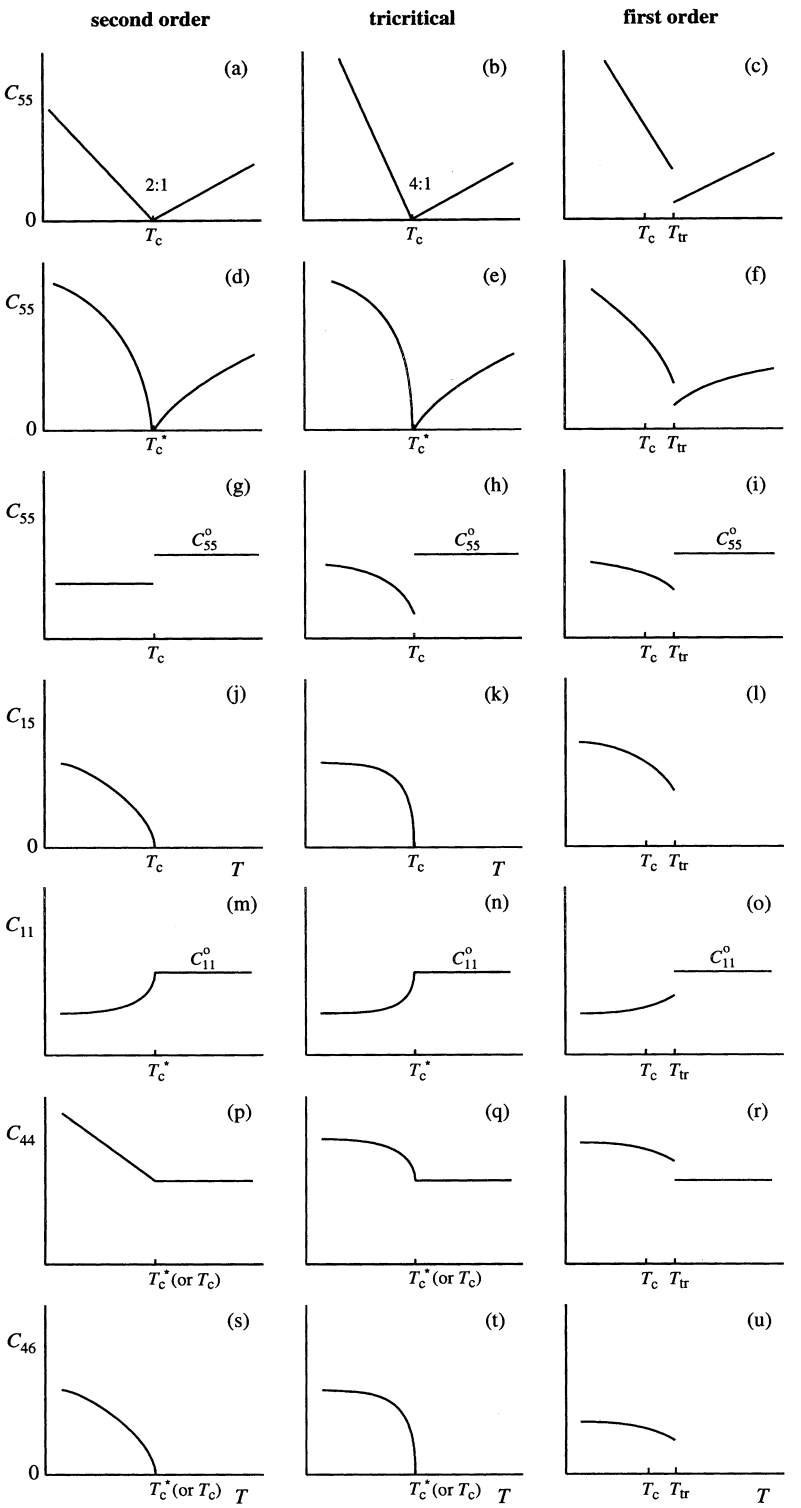

The underlying thermodynamic mechanism represented by equation 8 might be described formally as softening of the elastic constant C_{55} at a proper ferroelastic transition (Wadhawan, 1982; Salje, 1993). Wadhawan actually uses the term "true" proper, but this terminology can be controversial. The essential points are that the driving order parameter is a strain, the excess energy is purely elastic, and that this represents one limiting type of behaviour.

2.2 Linear coupling between strain and a different driving order parameter

If the driving mechanism for the transition comes from some structural feature other than a purely elastic effect, the strain arises from coupling with the driving order parameter, Q. For the case of Q and e_5 being associated with the same irreducible representation of the space group of the high-symmetry phase, the coupling between e_5 and Q is bilinear, and, again considering second-order behaviour for Q, the excess free energy is given by:

$$G = \frac{1}{2}a(T - T_c)Q^2 + \frac{1}{4}bQ^4 + \lambda_5 e_5 Q + \frac{1}{2}C_{55}^o e_5^2 \qquad (12).$$

C_{55}^o refers to the bare elastic constant. As in equation 7 it is assumed that the elastic energy may be truncated after the second-order term and, for the time being, it is also assumed that λ_5 is constant.

Under equilibrium conditions, the crystal relaxes to a stress-free state such that:

$$\frac{\partial G}{\partial e_5} = 0 = \lambda_5 Q + C_{55}^o e_5 \qquad (13)$$

$$\Rightarrow e_5 = -\frac{\lambda_5}{C_{55}^o} Q \qquad (14).$$

Substituting equation 14 into equation 12 gives the usual renormalisation of T_c to a higher transition temperature, T_c^*, in:

$$G = \frac{1}{2}a\left(T - T_c^*\right)Q^2 + \frac{1}{4}bQ^4 \qquad (15)$$

where:

$$T_c^* = T_c + \frac{\lambda_5^2}{aC_{55}^o} \qquad (16).$$

One way of deriving the temperature dependence of C_{55} to take into account the coupling between e_5 and Q, as discussed qualitatively in the introduction, is to first express the free energy in terms of e_5 alone. A simplifying step in this is to make use of the order-parameter susceptibility. Taking that part of the free energy due to the terms in Q alone as:

$$L = \frac{1}{2}a(T - T_c)Q^2 + \frac{1}{4}bQ^4 \tag{17}$$

the inverse susceptibility of Q alone (unmodified by coupling with the strain) is given by:

$$\chi^{-1} = \frac{\partial^2 L}{\partial Q^2} = a(T - T_c) + 3bQ^2 \tag{18}.$$

To a good approximation for small deviations of Q from its equilibrium value, equation 17 can be simplified to:

$$L = \frac{1}{2}\chi^{-1}Q^2 \tag{19}.$$

Equation 12 may then be rewritten as:

$$G = \frac{1}{2}\chi^{-1}Q^2 + \lambda_5 e_5 Q + \frac{1}{2}C_{55}^{o}e_5^2 \tag{20}.$$

The condition of Q being at equilibrium is expressed as:

$$\frac{\partial G}{\partial Q} = 0 = \chi^{-1}Q + \lambda_5 e_5 \tag{21}$$

$$\Rightarrow Q = -\frac{\lambda_5 e_5}{\chi^{-1}} \tag{22}.$$

Substituting equation 22 into equation 20 gives G as a function of e_5 alone, as required:

$$G = \frac{1}{2}\left(C_{55}^{o} - \frac{\lambda_5^2}{\chi^{-1}}\right)e_5^2 \tag{23}.$$

The variation of C_{55} for a crystal which is free to undergo the transition is then given simply by:

$$C_{55} = \frac{\partial^2 G}{\partial e_5^2} = C_{55}^{o} - \lambda_5^2\chi \tag{24}$$

and it is only necessary to explore the behaviour of χ. At $T > T_c^*$, the equilibrium value of Q is zero so that equation 18 becomes:

$$\chi^{-1} = a(T - T_c) \tag{25}$$

and, hence:

$$C_{55} = C_{55}^{o} - \frac{\lambda_5^2}{a(T - T_c)} \quad (26).$$

At $T = T_c^*$, the renormalised elastic constant falls to:

$$C_{55} = C_{55}^{o} - \frac{\lambda_5^2}{a\left(T_c + \frac{\lambda_5^2}{aC_{55}^{o}} - T_c\right)} = 0 \quad (27).$$

Below T_c^*, the equilibrium value of Q is obtained by applying the equilibrium condition, $\partial G/\partial Q = 0$, to equation 15, giving:

$$Q^2 = \frac{a}{b}\left(T_c^* - T\right) \quad (28).$$

Equation 18 can then be written in the form:

$$\begin{aligned} \chi^{-1} &= a(T - T_c) + 3a\left(T_c^* - T\right) \\ &= 2a\left(T_c^* - T\right) + a\left(T_c^* - T_c\right) \end{aligned} \quad (29)$$

and the renormalised elastic constant becomes:

$$C_{55} = C_{55}^{o} - \frac{\lambda_5^2}{2a\left(T_c^* - T\right) + a\left(T_c^* - T_c\right)} \quad (30).$$

The slopes, $\partial C_{55}/\partial T$, below and above T_c^* at small $\left|T_c^* - T\right|$ are respectively $-2a\left(C_{55}^{o}\right)^2/\lambda_5^2$ and $a\left(C_{55}^{o}\right)^2/\lambda_5^2$. As for the case of the driving order parameter being e_5, the measured value of C_{55} should go smoothly to zero as the equilibrium transition temperature is approached, with the ratio of the slopes tending to 2:1. In this case the transition occurs at T_c^* rather than at T_c, however, and the form of the variation of C_{55} given by equations 26 and 30 (illustrated in Fig. 5d) is quite different from that given by equation 11 (illustrated in Fig. 5a). As an aside, it is worth pointing out that, while C_{55} is no longer identical to χ^{-1}, it can still be thought of instructively as a probe for the susceptibility of Q since it is linearly dependent on χ (equation 24). The variations of C_{55} for tricritical (zero fourth-order term) and first-order transitions (negative fourth-order term) may be derived by following the same lines of argument; they are shown schematically in Fig. 5e and 5f.

Bearing in mind that T_c represents the transition temperature for a transition driven by Q with no strain coupling, a useful relationship between C_{ik}, C_{55}^{o}, T_c and T_c^* is obtained by

combining equations 16 and 26 to eliminate λ_5^2/a (Feile *et al.*, 1982; Knorr *et al.*, 1986). In the present example this yields (for $T > T_c$):

$$C_{55} = C_{55}^o\left(\frac{T - T_c^*}{T - T_c}\right) \qquad (31).$$

From one set of measurements of C_{55} over a range of temperatures above T_c and an experimental value of T_c^* it is therefore possible (in principle) to extract values of C_{55}^o and T_c. This expression also provides a test of whether strain is the driving order parameter or a driven order parameter, in the sense that has been used here, since $\left|T_c^* - T_c\right|$ is a measure of the strength of the coupling coefficient (equation 16).

Implicit in this treatment is the assumption that the response time of Q to some external stimulus is small relative to the response time of the strain, e_5. There are actually two important time scales involved, the first depending on the rate of structural relaxation with respect to Q and e, and the second on the rate of thermal equilibration. When local regions of a crystal are deformed during the passage of an acoustic wave in an ultrasonic experiment, for example, it is assumed that there is time for internal atomic adjustments to occur according to relationships predicted from the *equilibrium* dependence of Q on e_5. If Q involves only small atomic displacements in a soft optic mode, this assumption is not unreasonable. Under these conditions there might not be time for thermal equilibration on a local scale, however, so that, while the theory describes isothermal behaviour, the experiment would give adiabatic behaviour. Under most circumstances the difference between isothermal and adiabatic limits is small (see section 5 below), and this is not a serious issue. On the other hand, if the relaxation with respect to Q involves a relatively slow process with some significant activation energy, the assumption of structural equilibration will be invalid, and equations 26, 30 and 31 will not provide an adequate description of the elastic properties. Strictly speaking, the predicted (isothermal) elastic-constant variations will only be matched by data from static or very-low-frequency experiments (*e.g.* Schranz & Havlik, 1994).

Behaviour of this overall type, involving bilinear strain/order-parameter coupling, falls into the category of pseudo-proper ferroelastic phase transitions according to Wadhawan (1982). Clearly it represents a wide range of possibilities controlled by the strength of the coupling.

2.3 Quadratic coupling between strain and the driving order parameter

If a strain component and the driving order parameter have different symmetries, *i.e.* they are associated with different irreducible representations of the space group of the high-symmetry phase, the coupling between them will usually be linear in the strain and quadratic in the order parameter. For the illustrative orthorhombic $\rightleftharpoons$ monoclinic transition being considered here, two situations can be envisaged. Since all macroscopic strains are associated with the Brillouin zone centre, any driving order parameter associated with some other point in the Brillouin zone, to give a doubling of the unit cell, for example, must have different symmetry. Coupling with the symmetry-breaking strain, e_5, would then be of the form $\lambda e_5 Q^2$, and, in relation to the categories of Wadhawan (1982), this would be described as improper ferroelastic behaviour. Alternatively,

when the driving order parameter is e_5, coupling to a non-symmetry-breaking strain, e_{nsb}, will be of the form $\lambda e_{nsb} e_5^2$ since the two strains are associated with different representations.

For the case of a zone-boundary transition, an additional consideration is that the degeneracy of the order parameter may increase relative to that of a related zone-centre transition. If such a degeneracy arises, the specific terms allowed by symmetry depend on the exact change in space group. The usual symmetry rule still applies, namely that each term in the expansion must be invariant with respect to all symmetry operations of the space group of the high-symmetry phase. However, the formal group-theoretical manipulations are not straightforward. Illustrations of the necessary steps are provided by Dvorak (1971), Torres (1975) and Hatch (1981). A useful starting point for any system of interest is provided by the tables of Stokes & Hatch (1988), though a compilation of all allowed coupling terms is not yet available.

As an example of a zone-boundary transition, the symmetry change $Pmma \rightleftharpoons P2/c$ has been chosen, somewhat arbitrarily. From the tables of Stokes & Hatch (1988), this symmetry change is seen to be associated with the X point of the Brillouin zone, giving a doubling of the unit-cell dimension in the direction of the x-axis of the orthorhombic lattice. The order parameter is two-dimensional and the free-energy expansion must be written in terms of components q_1 and q_2 in place of Q. Considering only one strain, e_5, the excess free energy may be written as (from Stokes & Hatch, 1988, and Hatch, pers. comm.):

$$G = \frac{1}{2}a(T - T_c)\left(q_1^2 + q_2^2\right) + \frac{1}{4}b'\left(q_1^2 + q_2^2\right)^2 + \frac{1}{4}b''\left(q_1^4 + q_2^4\right) + \lambda_5 e_5\left(q_1^2 - q_2^2\right) + \frac{1}{2}C_{55}^{o} e_5^2 \qquad (32).$$

In this case, the problem is simplified by the fact that one component of the order parameter remains zero in the monoclinic phase. The final form of the predicted elastic constants is not compromised if $q_2 = 0$ is assumed from the start. Equation 32 can then be reduced to:

$$G = \frac{1}{2}a(T - T_c)Q^2 + \frac{1}{4}bQ^4 + \lambda_5 e_5 Q^2 + \frac{1}{2}C_{55}^{o} e_5^2 \qquad (33)$$

where $b = b' + b''$, $Q^2 = \left(q_1^2 + q_2^2\right)$, and $q_2 = 0$.

At equilibrium the value of Q under the influence of the strain coupling is given by:

$$\frac{\partial G}{\partial Q} = 0 = a(T - T_c)Q + bQ^3 + 2\lambda_5 e_5 Q \qquad (34).$$

Hence, $Q = 0$, or:

$$Q^2 = \left(\frac{a(T_c - T) - 2\lambda_5 e_5}{b}\right) \qquad (35).$$

Expressing the excess free energy in terms of e_5 alone gives, for $T < T_c$:

$$G = \frac{1}{2}a(T - T_c)\left[\frac{a(T_c - T) - 2\lambda_5 e_5}{b}\right] + \frac{1}{4}b\left[\frac{a(T_c - T) - 2\lambda_5 e_5}{b}\right]^2 + \lambda_5 e_5\left[\frac{a(T_c - T) - 2\lambda_5 e_5}{b}\right] + \frac{1}{2}C_{55}^o e_5^2 \quad (36).$$

For transitions in which changes in Q are rapid relative to changes in e_5, C_{55} is given by the second derivative of G (equation 36) with respect to e_5:

$$C_{55} = \frac{\partial^2 G}{\partial e_5^2} = C_{55}^o - \frac{2\lambda_5^2}{b} \qquad (\text{at } T < T_c) \quad (37).$$

Since $Q = 0$ at $T > T_c$, the excess free energy would simply become:

$$G = \frac{1}{2}C_{55}^o e_5^2 \quad (38)$$

and the second derivative with respect to e_5 is:

$$C_{55} = \frac{\partial^2 G}{\partial e_5^2} = C_{55}^o \quad (39).$$

At $T = T_c$, therefore, there should be a step in the elastic constant C_{55} with no softening in anticipation of the transition as T_c is approached from either the high-temperature or the low-temperature side (Fig. 5g).

The algebra becomes more complicated for a tricritical transition, but the general solution discussed in a later section (equation 79) yields an expected temperature dependence for C_{55} of the form (at $T < T_c$):

$$C_{55} = C_{55}^o - \frac{2\lambda^2}{b + 2cQ^2} \quad (40)$$

as illustrated in Fig. 5h. Here c is the coefficient of the sixth-order term in Q, and the fourth-order coefficient, b^*, as renormalised by the coupling between Q^2 and e_5 ($b^* = b - 2\lambda^2/C_{55}^o$), is zero. A schematic representation of the possible behaviour of C_{55} at a first-order transition is illustrated in Fig. 5i.

The non-symmetry-breaking strains e_1, e_2 and e_3 can be added to equation 32. Because they couple with $q_1^2 + q_2^2$, it follows that C_{11}, C_{22}, C_{33}, C_{12}, C_{13}, C_{23} would also show a step at $T = T_c$ for a second-order transition. C_{15}, C_{25} and C_{35} are constrained by symmetry to be zero in the orthorhombic phase but may be non-zero in the monoclinic phase, when they should show variations that are qualitatively similar to those of C_{55}. In all cases, of course, the precise values of the elastic constants in the monoclinic phase would depend on the signs and magnitudes of the relevant coefficients.

The alternative situation in which quadratic coupling arises is when e_5 is the driving order parameter for the transition and there is also a non-symmetry-breaking strain, such as e_1. In this case, the excess free energy becomes:

$$G = \frac{1}{2}a(T - T_c)e_5^2 + \frac{1}{4}be_5^4 + \lambda_1 e_1 e_5^2 + \frac{1}{2}C_{11}^o e_1^2 \qquad (41).$$

Here the coupling coefficient λ_1 is also proportional to the third-order elastic constant C_{155}^o (Tolédano *et al.*, 1983).

The elastic constant C_{55} remains the inverse susceptibility of the crystal with respect to e_5 but is now:

$$C_{55} = \frac{\partial^2 G}{\partial e_5^2} = a(T - T_c) = a(T - T_c) + 3be_5^2 + 2\lambda_1 e_1 \qquad (42).$$

Under equilibrium conditions the crystal is stress free and the condition $\partial G/\partial e_1 = 0$ yields:

$$e_1 = -\frac{\lambda_1}{C_{11}^o}e_5^2 \qquad (43).$$

Substituting this into equation 41 and manipulating terms in e_5^4 gives, for the renormalised fourth-order coefficient:

$$b^* = b - \frac{2\lambda_1^2}{C_{11}^o} \qquad (44)$$

and, for the equilibrium variation of e_5 at $T < T_c$ in a second-order transition:

$$e_5^2 = \frac{a}{b^*}(T_c - T) \qquad (45).$$

The temperature dependence of C_{55} derived from equation 42 is then:

$$C_{55} = a(T - T_c) \qquad (\text{at } T > T_c) \qquad (46)$$

$$C_{55} = 2a\frac{b}{b^*}(T_c - T) \qquad (\text{at } T < T_c) \qquad (47).$$

Thus, due to the non-symmetry-breaking strain e_1, the ratio of slopes for C_{55} below and above T_c in Fig. 4a becomes $2\left(b/b^*\right)$:1 instead of 2:1.

At a tricritical transition a sixth-order term, $\frac{1}{6}ce_5^6$, is needed in equation 41 and $b^* = 0$, $e_5^4 = (a/c)(T_c - T)$. Above T_c, C_{55} behaves as in equation 46, but for $T < T_c$, it can easily be shown that:

$$C_{55} = 4ce_5^4 + 2be_5^2$$
$$= 4a(T_c - T) + \frac{4\lambda_1^2}{C_{11}^o}\left[\frac{a}{c}(T_c - T)\right]^{1/2} \quad (48).$$

The behaviour illustrated in Fig. 5b is therefore modified by a non-linearity in the stability field of the monoclinic phase, the magnitude of which depends on λ_1.

Whatever the thermodynamic character of the transition, the variation of C_{11} is given simply by:

$$C_{11} = \frac{\partial^2 G}{\partial e_1^2} = C_{11}^o \quad (49)$$

with no anomaly predicted. Other elastic constants can be derived as easily, with C_{15}, for example being given by:

$$C_{15} = \frac{\partial^2 G}{\partial e_1 \partial e_5} = 2\lambda_1 e_5 \quad (50).$$

This produces variations of the form illustrated in Fig. 5j, k, l for second-order, tricritical and first-order transitions, respectively. C_{15} is strictly zero in an orthorhombic crystal.

2.4 Simultaneous linear and quadratic coupling of strain components to the driving order parameter

For an orthorhombic $\rightleftharpoons$ monoclinic transition driven by Q in a real crystal there would almost certainly be both a symmetry-breaking strain, e_5, and non-symmetry-breaking strains, e_1, e_2 and e_3. Again using only e_5 and e_1 for simplicity, the free-energy expansion for a second-order transition is:

$$G = \frac{1}{2}a(T - T_c)Q^2 + \frac{1}{4}bQ^4 + \lambda_1 e_1 Q^2 + \lambda_5 e_5 Q + \frac{1}{2}C_{11}^o e_1^2 + \frac{1}{2}C_{55}^o e_5^2 \quad (51)$$

where e_5 and Q are both associated with the active representation.

From all the preceding examples, the physical origin of the elastic-constant renormalisation should be apparent. Rather than follow the same approach, which becomes increasingly more laborious as strain terms are added, a general mathematical solution given towards the end of this section is anticipated and the behaviour of C_{55}, C_{11} and C_{15} are merely quoted here without derivation. For the free-energy expansion in equation 51 the renormalised elastic constants are expected to behave as:

$$C_{55} = C_{55}^{o} - \lambda_5^2 \chi \qquad (52) \qquad C_{11} = C_{11}^{o} - 4\lambda_1^2 Q^2 \chi \qquad (53)$$

$$C_{15} = -2\lambda_1 \lambda_5 Q \chi \qquad (54).$$

Here the order-parameter susceptibility is itself renormalised by the coupling between e_1 and Q^2 such that, from equation 51:

$$\chi^{-1} = \frac{\partial^2 G}{\partial Q^2} = a(T - T_c) + 3bQ^2 + 2\lambda_1 e_1 \qquad (55)$$

which, after the usual substitutions, yields for a second-order transition:

$$\chi^{-1} = a(T - T_c) \qquad \left(\text{at } T > T_c^*\right) \qquad (56)$$

$$\chi^{-1} = 2a\frac{b}{b^*}\left(T_c^* - T\right) + a\left(T_c^* - T_c\right) \qquad \left(\text{at } T < T_c^*\right) \qquad (57).$$

This gives, for $T > T_c^*$:

$$C_{55} = C_{55}^{o} - \frac{\lambda_5^2}{a(T - T_c)} \qquad (58) \qquad C_{11} = C_{11}^{o} \qquad (59)$$

$$C_{15} = 0 \qquad (60).$$

At $T < T_c^*$, the equilibrium value of Q depends on the renormalised values of T_c and the renormalised value of b as $Q^2 = \left(a/b^*\right)\left(T_c^* - T\right)$, which may be substituted into equations 52 – 54, together with the susceptibility given in equation 57, to obtain C_{55}, C_{11} and C_{15}. C_{55} behaves as shown in Fig. 5d except that the ratio of the slopes as $T \rightarrow T_c^*$ is $2(b/b^*)$:1 rather than 2:1. C_{11} does not have a step of the form shown in Fig. 5g, but varies continuously through T_c^* as in Fig. 5m. C_{15} decreases continuously to zero at $T = T_c^*$, though more steeply than shown in Fig. 5j.

At a tricritical transition, $b^* = 0$, $Q^4 = (a/c)\left(T_c^* - T\right)$ and $\chi^{-1} = 4a\left(T_c^* - T\right) + \left(4\lambda_1^2/C_{11}^{o}\right)\left[(a/c)\left(T_c^* - T\right)\right]^{1/2} + a\left(T_c^* - T_c\right)$, which can be substituted into equations 52 – 54 to predict the variations of C_{55}, C_{11} and C_{15}. Schematic representations of C_{11} at tricritical and first-order transitions are shown in Fig. 5n and 5o, respectively.

2.5 Other couplings

In principle, the correct free-energy expansion to describe a phase transition should always contain all six of the possible strain components. Usually these are incorporated in the lowest-order form allowed by symmetry, and higher-order terms are assumed to be negligibly small in comparison. As discussed above, in the case of an orthorhombic $\rightleftharpoons$ monoclinic transition where the active representation is associated with the Brillouin zone centre, the symmetry-breaking strain, e_5, couples with Q. The non-symmetry-breaking strains, e_1, e_2 and e_3, which are associated with the identity representation, each couple with Q^2. To show how the remaining two strain components, e_4 and e_6, contribute to the transition it is necessary first to examine the irreducible representations of the point group of the high-symmetry phase.

The condition for any term appearing in the Landau expansion is that it must be invariant with respect to all symmetry operations of the high-symmetry space group, or, in other words, the product of the related irreducible representations must contain the identity representation. For a zone-centre transition involving the symmetry change $mmm \rightleftharpoons 2/m$, the active representation is B_{2g} when the retained diad is parallel to the crystallographic y-axis (Table 2). Thus the symmetry of a term in e_5Q is $B_{2g} \otimes B_{2g}$ which necessarily contains the identity representation A_g. Similarly, the symmetry of terms in e_1Q^2, e_2Q^2 and e_3Q^2 is $A_g \otimes B_{2g} \otimes B_{2g}$ which, again, necessarily contains the identity representation. The remaining strain components, e_4 and e_6, are associated with B_{3g} and B_{1g} respectively (Table 2), and the lowest-order coupling terms in e_4 or e_6 allowed by symmetry have the form $e_4^2Q^2$ and $e_6^2Q^2$. [$B_{3g} \otimes B_{3g} \otimes B_{2g} \otimes B_{2g}$ and $B_{1g} \otimes B_{1g} \otimes B_{2g} \otimes B_{2g}$ obviously contain A_g]. It is always necessary to check other possibilities, however, and in this case $B_{1g} \otimes B_{3g} = B_{2g}$. Thus a term in e_4e_6Q is also invariant and is allowed in the free-energy expansion. The full free-energy expansion of the transition with Q as the driving order parameter should therefore be:

$$G = \frac{1}{2}a(T-T_c)Q^2 + \frac{1}{4}bQ^4 + \lambda_1 e_1 Q^2 + \lambda_2 e_2 Q^2 + \lambda_3 e_3 Q^2 + \lambda_5 e_5 Q + \lambda_4 e_4^2 Q^2 + \lambda_6 e_6^2 Q^2 + \lambda_7 e_4 e_6 Q + \frac{1}{2}\sum_{i,k=1-3} C_{ik}^{o} e_i e_k + \frac{1}{2}\sum_{i=4-6} C_{ii}^{o} e_i^2 \qquad (61).$$

Table 2. Irreducible representations and basis functions for point group *mmm*. Only basis functions up to second order are shown. Individual strain components are related to the basis functions as: $x^2 \rightarrow e_1$, $y^2 \rightarrow e_2$, $z^2 \rightarrow e_3$, $yz \rightarrow e_4$, $xz \rightarrow e_5$, $xy \rightarrow e_6$. R_x, R_y and R_z relate to properties which involve rotations about the principle axes, such as optical activity; x, y and z become polar properties.

	E	C_2 [001]	C_2 [010]	C_2 [100]	i	σ (001)	σ (010)	σ (100)	Basis functions
A_g	1	1	1	1	1	1	1	1	x^2, y^2, z^2
B_{1g}	1	1	–1	–1	1	1	–1	–1	R_z, xy
B_{2g}	1	–1	1	–1	1	–1	1	–1	R_y, xz
B_{3g}	1	–1	–1	1	1	–1	–1	1	R_x, yz
A_u	1	1	1	1	–1	–1	–1	–1	
B_{1u}	1	1	–1	–1	–1	–1	1	1	z
B_{2u}	1	–1	1	–1	–1	1	–1	1	y
B_{3u}	1	–1	–1	1	–1	1	1	–1	x

The terms in e^2Q^2 are frequently not specified because they are expected to be small. They are significant in some materials, however, including, for example, K_2SeO_4 (Cho & Yagi, 1981; Cummins, 1983) and quartz (Lüthi & Rehwald, 1981).

Under equilibrium conditions the crystal must be at a free-energy minimum with respect to e_4 and e_6, giving:

$$\frac{\partial G}{\partial e_4} = 0 = 2\lambda_4 e_4 Q^2 + \lambda_7 e_6 Q + C^o_{44} e_4 \qquad (62)$$

and

$$\frac{\partial G}{\partial e_6} = 0 = 2\lambda_6 e_6 Q^2 + \lambda_7 e_4 Q + C^o_{66} e_6 \qquad (63)$$

for which the only solution is, as expected for a monoclinic crystal, $e_4 = e_6 = 0$. The second derivatives are:

$$\frac{\partial^2 G}{\partial e_4^2} = 2\lambda_4 Q^2 + C^o_{44} \qquad (64) \qquad \frac{\partial^2 G}{\partial e_6^2} = 2\lambda_6 Q^2 + C^o_{66} \qquad (65)$$

$$\frac{\partial^2 G}{\partial e_4 \partial e_6} = \lambda_7 Q \qquad (66).$$

These are independent of e_4 and e_6 and are not constrained to be zero. By inspection of equation 61 it is in fact evident that the renormalised elastic constants C_{44}, C_{66} and C_{46} could have been given directly as:

$$C_{44} = C^o_{44} + 2\lambda_4 Q^2 \qquad (67) \qquad C_{66} = C^o_{66} + 2\lambda_6 Q^2 \qquad (68)$$

$$C_{46} = \lambda_7 Q \qquad (69).$$

Such variations of C_{44}, C_{66} and C_{46} are illustrated for second-order, tricritical and first-order transitions in Fig. 5p-u. Again the precise values of the elastic constants depend on the signs and magnitudes of the coupling coefficients λ_4, λ_6 and λ_7.

These coupling terms clearly do not have any influence on the minima of the free-energy expansion describing a transition, and need not be considered in an analysis either of the equilibrium free energy or of the equilibrium values of Q, e_1, e_2, e_3 or e_5, therefore. Their influence is only in modifying the shape of the free-energy function away from the equilibrium point and, hence, in renormalising some of the elastic constants.

2.6 Temperature-dependent coupling coefficients

In Landau theory the excess entropy due to a phase transition driven by some order parameter Q is taken as being proportional to Q^2, and the coefficient of the second-order term in the free-energy

expansion is made explicitly temperature dependent as $\frac{1}{2}a(T-T_c)Q^2$. If the transition is driven by a symmetry-breaking strain, such as e_5 in the preceding discussions, the equivalent term is $\frac{1}{2}a(T-T_c)e_5^2$ and it is the elastic constants which are explicitly temperature dependent. These two cases correspond to two extremes – either Q or e_5 drives the transition. The coupling term $\lambda_5 e_5 Q$ also has the same form, however, and might be temperature dependent in the same manner, *i.e.* with $\lambda_5 = \lambda_5'(T-T_c)$, where λ_5' is a constant. The driving mechanism would be ascribed to the temperature dependence of the coupling coefficient and not to either of Q^2 or e_5^2. Equation 24 can be adapted to give C_{55} as:

$$C_{55} = C_{55}^{o} - \left[\lambda_5'(T-T_c)\right]^2 \chi \qquad (70)$$

where χ may or may not be explicitly temperature dependent. The behaviour of C_{55} would be quite different from the previous examples and, although this point is not considered further in this paper, equations of the form of equation 70 provide a basis for predicting the elastic behaviour of such systems.

Following the same line of reasoning, it is not expected that the coefficients of coupling terms with the form $\lambda e Q^2$ would be strongly temperature dependent since they contribute only to the fourth-order Landau terms.

2.7 General solutions

In summary, it is evident that the elastic constants of a material vary at a phase transition in a manner that is highly sensitive to the transition mechanism. Three mechanisms, in particular, have been considered: (i) strain as the driving order parameter at a purely elastic instability, (ii) some structural feature other than strain acting as the driving parameter, and (iii) a temperature dependence of the coupling between strain and some other structural feature. In each case, a full set of elastic-constant measurements through a transition would show some pattern characteristic of mechanism and thermodynamic character. While the underlying causes of this sensitivity can be understood by following the step by step approach adopted up to this point, it is fortunately not necessary to follow every step for every material of interest. A general solution can be used to predict the same effects more economically.

By definition a second-order elastic constant is given by:

$$C_{ik} = \frac{\partial^2 G}{\partial e_i \partial e_k} \qquad (71).$$

When G is expressed purely in terms of strains, this double differentiation gives the elastic constants directly. All relaxations of the crystal, when a stress is applied, are accounted for explicitly. For example, if the excess free energy is written in terms of elastic energies and a coupling energy, equation 41 can be written as:

$$G = \frac{1}{2}C_{55}e_5^2 + \lambda_1 e_1 e_5^2 + \frac{1}{2}C_{11}^{o}e_1^2 + C_{15}^{o}e_1 e_5 \qquad (72).$$

The bare elastic constant C_{15}^{o} has been added for completeness, although it is strictly zero by symmetry. A stress, σ_5, produces strains according to:

$$\sigma_5 = \frac{\partial G}{\partial e_5} = C_{55}e_5 + 2\lambda_1 e_1 e_5 + C_{15}^{o} e_1 \qquad (73).$$

C_{55} is the constant of proportionality for e_5 and the additional relaxation, e_1, is accounted for by the elastic constant C_{15} (which is given by $C_{15}^{o} + 2\lambda_1 e_5 = 2\lambda_1 e_5$; equation 50). When the same stress is applied to a crystal with e_5 coupled to Q, the relaxation of Q is not accounted for in the same way. The inverse susceptibility of the crystal with respect to e_5, *i.e.* C_{55}, now also involves the susceptibility of the crystal with respect to Q.

To find a general solution for systems driven by Q, it is convenient to take a general expression for the excess free energy as a function of Q and a strain e, $G(Q,e)$. The first derivative of this with respect to e is:

$$\frac{dG}{de} = \frac{\partial G}{\partial e} + \frac{\partial G}{\partial Q}\cdot\frac{\partial Q}{\partial e} \qquad (74).$$

Here the second term on the right-hand side is zero under equilibrium conditions because $\partial G/\partial Q = 0$, though $\partial Q/\partial e$ is not zero. Any elastic constant is then:

$$C = \frac{d^2G}{de^2} = \frac{d}{de}\left(\frac{dG}{de}\right) = \frac{\partial^2 G}{\partial e^2} + \frac{\partial^2 G}{\partial e \partial Q}\cdot\frac{\partial Q}{\partial e} \qquad (75).$$

$\partial Q/\partial e$ is found by considering the derivative:

$$\frac{d}{de}\left(\frac{\partial G}{\partial Q}\right) = \frac{\partial^2 G}{\partial e \partial Q} + \frac{\partial^2 G}{\partial Q^2}\cdot\frac{\partial Q}{\partial e} \qquad (76)$$

which, taking $\partial G/\partial Q = 0$, is also equal to zero. Thus:

$$\frac{\partial Q}{\partial e} = -\frac{\partial^2 G}{\partial e \partial Q}\cdot\left(\frac{\partial^2 G}{\partial Q^2}\right)^{-1} \qquad (77).$$

Substituting for $\partial Q/\partial e$ in equation 75 then gives:

$$C = \frac{\partial^2 G}{\partial e^2} - \frac{\partial^2 G}{\partial e \partial Q}\cdot\left(\frac{\partial^2 G}{\partial Q^2}\right)^{-1}\cdot\frac{\partial^2 G}{\partial Q \partial e} \qquad (78).$$

This is the general result for a transition with a driving order parameter which is not a strain, as first obtained by Slonczewski & Thomas (1970). $\partial^2 G/\partial e^2$ is the inverse susceptibility of the crystal with respect to strain alone, *i.e.* the unrenormalised or bare elastic constant C_{ik}^{o}. The terms

in $\partial^2 G/\partial e \partial Q$ incorporate the coupling between e and Q, while $\left(\partial^2 G/\partial Q^2\right)^{-1}$ is the order-parameter susceptibility, χ.

For standard applications, equation 78 is usually written in a form such as:

$$C_{ik} = C_{ik}^{o} - \sum_{m,n} \frac{\partial^2 G}{\partial e_i \partial Q_m} \cdot \left(\frac{\partial^2 G}{\partial Q_m \partial Q_n} \right)^{-1} \cdot \frac{\partial^2 G}{\partial e_k \partial Q_n} \tag{79}$$

where, for $m = n$, Q_m and Q_n are the same order parameter, and, for $m \neq n$, Q_m and Q_n might be two discrete order parameters or two components of a single order parameter. This equation yields elastic-constant variations in a quite straightforward manner. Some useful expressions for χ^{-1} at second-order transitions are listed in Table 3.

Table 3. Order-parameter susceptibilities for second-order transitions with a single, one-component order parameter. e_{sb} is the symmetry-breaking strain, e_{nsb} is a non-symmetry-breaking strain.

Role of e_{sb}	Value of e_{nsb}	χ^{-1}
driving order parameter	0	$\begin{cases} a(T - T_c) & \text{at } T > T_c \\ 2a(T_c - T) = 2be_{sb}^2 & \text{at } T < T_c \end{cases}$
" " "	$\neq 0$	$\begin{cases} a(T - T_c) & \text{at } T > T_c \\ 2a\frac{b}{b^*}(T_c - T) = 2be_{sb}^2 & \text{at } T < T_c \end{cases}$
bilinearly coupled to Q ($\lambda e_{sb} Q$)	0	$\begin{cases} a(T - T_c) & \text{at } T > T_c^* \\ 2a(T_c^* - T) + a(T_c^* - T_c) & \text{at } T < T_c^* \end{cases}$
" " " " "	$\neq 0$	$\begin{cases} a(T - T_c) & \text{at } T > T_c^* \\ 2a\frac{b}{b^*}(T_c^* - T) + a(T_c^* - T_c) & \text{at } T < T_c^* \end{cases}$
quadratically coupled to Q ($\lambda e_{sb} Q^2$)	$\neq 0$	$\begin{cases} a(T - T_c) & \text{at } T > T_c \\ 2a\frac{b}{b^*}(T_c - T) = 2bQ^2 & \text{at } T < T_c \end{cases}$

3. Criteria for stability with respect to elastic lattice distortions

For a crystal to be in an equilibrium state, its free energy must be at a minimum with respect to any distortion. In other words, the elastic energy, $\frac{1}{2}\sum_{i,k} C_{ik} e_i e_k$, must be positive for all strains e_i, e_k. This requires, formally, that the elastic-constant matrix is positive definite (Born & Huang, 1954). An identical expression of the stability condition is that all the eigenvalues of the elastic-constant matrix must be positive. Should one (or more) of the eigenvalues go to zero the crystal will

become unstable with respect to some spontaneous lattice distortion (Boccara, 1968; Cowley, 1976; McLellan, 1980; Liakos & Saunders, 1982). The resulting strains have the symmetry of the corresponding eigenvector(s). A simple set of stability criteria based on the properties of the C_{ik} matrix may therefore be derived. For this, the diagonalised form of the elastic-constant matrix is of more practical use than its conventional form. In the following sections, a brief outline of the symmetry properties of the elastic constants is given, before returning to the criteria for stability. It can also be convenient, when writing out Landau expansions, to express strains and elastic energies in their symmetry-adapted forms.

3.1 Symmetry properties of the elastic-constant matrix

Elastic properties are centrosymmetric since they do not depend on whether the stress in a given direction is positive or negative (compressional or tensile). Rather than having to deal with different sets of elastic constants for all thirty-two crystallographic point groups, it is therefore necessary only to consider the eleven Laue classes. The second-order elastic constants allowed by symmetry for Laue classes *m*3 and *m*3*m* are the same, however, as are those for Laue classes 6/*m* and 6/*mmm*, which reduces the number of distinct matrices to nine. These are given in many standard texts (*e.g.* Nye, 1985), and each is a real, symmetric 6 x 6 matrix with six eigenvalues that are also real. Associated with each eigenvalue is at least one eigenvector. The eigenvectors are, or can be chosen to be, orthogonal to each other. They have six components which may be understood most easily in terms of their relationship to the six components of the strain tensor. Each eigenvector has a symmetry which is specified by reference to the irreducible representations of the thirty-two crystallographic point groups. In the present context of trying to understand elastic anomalies at structural phase transitions, it is not necessary to be able to derive all the eigenvalues and eigenvectors. They are tabulated and discussed in detail elsewhere (*e.g.* Boccara, 1968; McLellan, 1980; Liakos & Saunders, 1982; David, 1983a; Nye, 1985; Terhune *et al.*, 1985; Bulou, 1992; Bulou *et al.*, 1992).

The most significant aspects of the symmetry constraints may be illustrated with two examples, *m*3*m* and 422, as the point-group symmetry of a parent crystal. For a cubic crystal the conventional form of the second-order elastic-constant matrix is:

$$\begin{pmatrix} C_{11} & C_{12} & C_{12} & 0 & 0 & 0 \\ C_{12} & C_{11} & C_{12} & 0 & 0 & 0 \\ C_{12} & C_{12} & C_{11} & 0 & 0 & 0 \\ 0 & 0 & 0 & C_{44} & 0 & 0 \\ 0 & 0 & 0 & 0 & C_{44} & 0 \\ 0 & 0 & 0 & 0 & 0 & C_{44} \end{pmatrix}$$

Diagonalisation yields:

$$\begin{pmatrix} C_{11}+2C_{12} & 0 & 0 & 0 & 0 & 0 \\ 0 & C_{11}-C_{12} & 0 & 0 & 0 & 0 \\ 0 & 0 & C_{11}-C_{12} & 0 & 0 & 0 \\ 0 & 0 & 0 & C_{44} & 0 & 0 \\ 0 & 0 & 0 & 0 & C_{44} & 0 \\ 0 & 0 & 0 & 0 & 0 & C_{44} \end{pmatrix}$$

The eigenvectors and their corresponding irreducible representation labels are given in Table 4. The eigenvalue $(C_{11}+2C_{12})$ is associated with the eigenvector $\left(\frac{1}{\sqrt{3}},\frac{1}{\sqrt{3}},\frac{1}{\sqrt{3}},0,0,0\right)$, which has the symmetry of the identity representation, A_{1g}. The six components of the eigenvector scale as the six strains, $e_1 - e_6$, so that the equivalent spontaneous strain becomes $e_a = \frac{1}{\sqrt{3}}(e_1+e_2+e_3)$ in its symmetry-adapted form. This is a pure volume strain. There are two degenerate eigenvalues associated with eigenvectors with E_g symmetry and three degenerate eigenvalues associated with T_{2g} eigenvectors. The symmetry-adapted spontaneous strains describe orthorhombic distortions, $e_o = \frac{1}{\sqrt{2}}(e_1 - e_2)$, or tetragonal distortions, $e_t = \frac{1}{\sqrt{6}}(2e_3 - e_1 - e_2)$, for the former, and trigonal ($D = E = F$, $e_4 = e_5 = e_6$), monoclinic ($D = E \neq F$, $e_4 = e_5 \neq e_6$) or triclinic distortions ($D \neq E \neq F$, $e_4 \neq e_5 \neq e_6$) for the latter. The coefficients D, E and F (introduced in Table 4) are related by $D^2 + E^2 + F^2 = 1$, and are needed to ensure that the eigenvectors have unit length.

Table 4. Symmetry-adapted elastic constants (eigenvalues) and strains (from the eigenvectors) of the elastic constant matrix for point group $m3m$. Note: $A^2 + B^2 = D^2 + E^2 + F^2 = 1$.

Irreducible representation	Eigenvalue	Eigenvector	Symmetry-adapted spontaneous strain
A_{1g}	$C_{11} + 2C_{12}$	$\left(\frac{1}{\sqrt{3}},\frac{1}{\sqrt{3}},\frac{1}{\sqrt{3}},0,0,0\right)$	$e_a = \frac{1}{\sqrt{3}}(e_1+e_2+e_3)$
E_g	$C_{11} - C_{12}$	$A\left(\frac{1}{\sqrt{2}},-\frac{1}{\sqrt{2}},0,0,0,0\right)$	$e_o = \frac{1}{\sqrt{2}}(e_1 - e_2)$
	$C_{11} - C_{12}$	$B\left(-\frac{1}{\sqrt{6}},-\frac{1}{\sqrt{6}},\frac{2}{\sqrt{6}},0,0,0\right)$	$e_t = \frac{1}{\sqrt{6}}(2e_3 - e_1 - e_2)$
T_{2g}	C_{44}	$D(0,0,0,1,0,0)$	e_4
	C_{44}	$E(0,0,0,0,1,0)$	e_5
	C_{44}	$F(0,0,0,0,0,1)$	e_6

The most obvious difference for a parent crystal with symmetry less than $m3m$ is that some of the eigenvalues are not such simple functions of the standard elastic constants. For a tetragonal crystal with point group 422 (Laue class $4/mmm$), the eigenvalues of the elastic-constant matrix are $(C_{11} - C_{12})$, C_{66}, C_{44}, C_{44} and the eigenvalues of a submatrix:

$$\begin{pmatrix} C_{11}+C_{12} & \sqrt{2}C_{13} \\ \sqrt{2}C_{13} & C_{33} \end{pmatrix}$$

which are:

$$\tfrac{1}{2}\left\{(C_{11}+C_{12}+C_{33})+\left[(C_{11}+C_{12}-C_{33})^2+8C_{13}^2\right]^{1/2}\right\}$$

and

$$\tfrac{1}{2}\left\{(C_{11}+C_{12}+C_{33})-\left[(C_{11}+C_{12}-C_{33})^2+8C_{13}^2\right]^{1/2}\right\}$$

(Table 5). The coefficients α, α', β and β' in Table 5 describe the eigenvectors. They are constrained by $2\alpha^2+\beta^2=2\alpha'^2+\beta'^2=1$ to ensure, again, that the eigenvectors have unit length. An additional constraint, $2\alpha\alpha'+\beta\beta'=0$, ensures that the two A_1 eigenvectors are orthogonal.

Table 5. Symmetry-adapted elastic constants (eigenvalues) and strains (from the eigenvectors) of the elastic constant matrix for point group 422 (Laue class 4/*mmm*). Note: $2\alpha^2+\beta^2=2\alpha'^2+\beta'^2=1$, $2\alpha\alpha'+\beta\beta'=0$, $A^2+B^2=1$. A semi-colon is placed between two strains to signify that, although they have the same symmetry, they would develop in different proportions according to the values of the coefficients α, β, α' and β'.

Irreducible representation	Eigenvalue	Eigenvector	Symmetry-adapted spontaneous strain
A_1	$\frac{1}{2}\left\{(C_{11}+C_{12}+C_{33})-\left[(C_{11}+C_{12}-C_{33})^2+8C_{13}^2\right]^{1/2}\right\}$	$(\alpha,\alpha,\beta,0,0,0)$	$(e_1+e_2);\ e_3$
A_1	$\frac{1}{2}\left\{(C_{11}+C_{12}+C_{33})+\left[(C_{11}+C_{12}-C_{33})^2+8C_{13}^2\right]^{1/2}\right\}$	$(\alpha',\alpha',\beta',0,0,0)$	$(e_1+e_2);\ e_3$
B_1	$C_{11}-C_{12}$	$\left(\frac{1}{\sqrt{2}},-\frac{1}{\sqrt{2}},0,0,0,0\right)$	$e_o=\frac{1}{\sqrt{2}}(e_1-e_2)$
B_2	C_{66}	$(0,0,0,0,0,1)$	e_6
E	C_{44}	$A(0,0,0,1,0,0)$	e_4
	C_{44}	$B(0,0,0,0,1,0)$	e_5

For parent crystals with still lower symmetry, some of the eigenvalues and eigenvectors become algebraically more complex in a similar manner, but the essential features remain the same. The eigenvectors are of less practical use than the symmetry-adapted strains which are derived from them. Note, however, that the parameters A, B..., α, β ..., refer to real properties of a material. The values of coefficients specified here by capital letters determine the symmetry of the product structure at the instability due to a degenerate eigenvector. They determine, for example, whether a crystal becomes orthorhombic or tetragonal at an E_g instability in a cubic crystal. Values of the coefficients specified by greek letters characterise the relative magnitudes of two (or more) strains with the same symmetry belonging to non-degenerate representations.

3.2 Stability criteria

Stability with respect to spontaneous elastic distortions can be assessed by inspection of the eigenvalues of the relevant elastic-constant matrix. Thus, if $(C_{11} - C_{12})$ became zero with pressure or temperature, a cubic crystal would be expected to deform spontaneously to an orthorhombic or tetragonal form (Table 4). In this case the active representation for the transition is E_g. If C_{44} became zero the crystal would become unstable with respect to shearing, leading to trigonal, monoclinic or triclinic states, with T_{2g} as the active representation. Similarly, a spontaneous volume change, in excess of the normal effects of thermal expansion, would occur if $(C_{11} + 2C_{12})$ became zero, though this would not involve a change in symmetry. For a tetragonal crystal with point group 422 (Table 5) the condition $(C_{11} - C_{12}) \rightarrow 0$ would lead to the development of an orthorhombic form (B_1 or B_2 active), and $C_{44} \rightarrow 0$ would yield a monoclinic form for $A \neq 0$, $B = 0$ ($e_4 \neq 0$, $e_5 = 0$), or $A = 0$, $B \neq 0$ ($e_4 = 0$, $e_5 \neq 0$), or $A = -B \neq 0$ ($e_4 = -e_5 \neq 0$), and a triclinic form for $A \neq B \neq 0$ ($e_4 \neq e_5 \neq 0$). Rather than using the eigenvalues to predict elastic stability limits with respect to A_1 strains, however, it is simpler to refer to the determinant of the submatrix (the determinant of a matrix equals the product of its eigenvalues). Thus, considering the submatrix given in the previous section, if $(C_{11} + C_{12})C_{33} - 2C_{13}^2$ tended to zero, a tetragonal crystal would become unstable with respect to an A_1 (non-symmetry-breaking) strain. This is the same limiting condition as for the full A_1 eigenvalue. It is unlikely that two or more eigenvalues of the elastic-constant matrix which are not related by symmetry would tend to zero simultaneously in a real material.

These elastic stability criteria are summarised for all possible symmetry changes in Table 6 (after: Boccara, 1968; Cowley, 1976; Liakos & Saunders, 1982; Terhune *et al.*, 1985; Bulou, 1992). Note that, more often than not, it is a combination of elastic constants and not the value of an individual elastic constant that determines whether an elastic instability develops. Also, while the diagonal elements, C_{ii}, of the conventional elastic-constant matrix must be positive for stability, the off-diagonal elements, C_{ik} ($i \neq k$) need not be. In the limiting case of a triclinic crystal, the general stability condition with respect to any elastic distortion reduces to the requirement that the determinant of the full elastic-constant matrix remains positive. If an elastic instability point of this type is reached, the low-symmetry form of the crystal remains triclinic, but has a different unit cell.

Instabilities determined by elastic effects of this type are approached both when the spontaneous strain acts as the driving order parameter and when it is linearly coupled to a different driving order parameter. The symmetry-adapted elastic constant might go to zero (or at least become very small) at the equilibrium transition temperature if the transition is thermodynamically continuous. For first-order transitions, the symmetry change certainly occurs before the eigenvalue reaches zero, though the relevant elastic constants would be expected to show significant softening as the transition is approached. On the other hand, as will be seen, if the transition is driven by an order parameter which couples with strain as $\lambda e Q^2$, the nature of the primary elastic anomaly is rather different.

Table 6. Elastic stability limits for proper and pseudo-proper ferroelastic phase transitions: symmetry, strain, soft-acoustic-mode orientations and velocities (modified after Cowley, 1976, and Terhune *et al.*, 1985; see, also, Liakos & Saunders, 1982).

Representation	Spontaneous strains[1]	Stability limit[2] ($C_{ik} \rightarrow 0$)	Transition type[3]	Orientation of soft acoustic mode[4]	ρv^2 for soft acoustic mode[5]
Cubic classes					
A_1	$e_1 = e_2 = e_3$	$C_{11} + 2C_{12}$	0	–	–
E	$e_1 = -e_2$, $e_3 = -2e_1 = -2e_2$	$C_{11} - C_{12}$	I	$\vec{q}$//[110], $\vec{u}$//[1 $\bar{1}$ 0]	$\frac{1}{2}(C_{11} - C_{12})$
T_2	e_4, e_5, e_6	C_{44}	II	$\vec{q} \perp$[100], $\vec{u}$//[100]	C_{44}
Hexagonal classes					
$2A_1$	$e_1 = e_2$; e_3	$(C_{11} + C_{12})C_{33} - 2C_{13}^2$	0	–	–
E_2	$e_1 = -e_2$, e_6	$C_{11} - C_{12}$	II	$\vec{q} \perp$[001], $\vec{u} \perp$[001] & $\vec{q}$	$\frac{1}{2}(C_{11} - C_{12})$
E_1	e_4, e_5	C_{44}	II	$\vec{q} \perp$[001], $\vec{u}$//[001]	C_{44}
Trigonal classes 32, $\bar{3}m$, $3m$					
$2A_1$	$e_1 = e_2$; e_3	$(C_{11} + C_{12})C_{33} - 2C_{13}^2$	0	–	–
2E	$e_1 = -e_2$, e_6; e_4, e_5	$(C_{11} - C_{12})C_{44} - 2C_{14}^2$	I	$\vec{q} \perp$[001], $\vec{u} \perp \vec{q}$	$\frac{1}{4}\left\{(C_{11} - C_{12} + 2C_{44}) - \left[(C_{11} - C_{12} - 2C_{44})^2 + 16C_{14}^2\right]^{1/2}\right\}$
Trigonal classes 3, $\bar{3}$					
2A	$e_1 = e_2$; e_3	$(C_{11} + C_{12})C_{33} - 2C_{13}^2$	0	–	–
2E	$e_1 = -e_2$, e_6; e_4, e_5	$(C_{11} - C_{12})C_{44} - 2C_{14}^2 - 2C_{15}^2$	I	$\vec{q} \perp$[001], $\vec{u} \perp \vec{q}$	$\frac{1}{4}\left\{(C_{11} - C_{12} + 2C_{44}) - \left[(C_{11} - C_{12} - 2C_{44})^2 + 16(C_{14}^2 + C_{15}^2)\right]^{1/2}\right\}$
Tetragonal classes $4mm$, $\bar{4}2m$, 422, $4/mmm$					
$2A_1$	$e_1 = e_2$; e_3	$(C_{11} + C_{12})C_{33} - 2C_{13}^2$	0	–	–
B_1	$e_1 = -e_2$	$C_{11} - C_{12}$	I	$\vec{q}$//[110], $\vec{u}$//[1 $\bar{1}$ 0]	$\frac{1}{2}(C_{11} - C_{12})$
B_2	e_6	C_{66}	I	$\vec{q}$//[100], $\vec{u}$//[010]	C_{66}
E	e_4, e_5	C_{44}	II	$\vec{q} \perp$[001], $\vec{u}$//[001]	C_{44}

Tetragonal classes 4, $\bar{4}$, 4/*m*					
2A	$e_1 = e_2$; e_3	$(C_{11}+C_{12})C_{33}-2C_{13}^2$	0	–	–
2B	$e_1 = -e_2$; e_6	$(C_{11}-C_{12})C_{66}-2C_{16}^2$	I	$\vec{q}\perp[001]$, $\vec{u}\perp[001]$ & $\vec{q}$	$\frac{1}{4}\left\{(C_{11}-C_{12}+2C_{66}) - \left[(C_{11}-C_{12}-2C_{66})^2+16C_{16}^2\right]^{1/2}\right\}$
E	e_4, e_5	C_{44}	II	$\vec{q}\perp[001]$, $\vec{u}//[001]$	C_{44}
Orthorhombic classes					
$3A_1$	e_1; e_2; e_3	K_1	0	–	–
B_1	e_6	C_{66}	I	$\vec{q}//[010]$, $\vec{u}//[100]$	C_{66}
B_2	e_5	C_{55}	I	$\vec{q}//[100]$, $\vec{u}//[001]$	C_{55}
B_3	e_4	C_{44}	I	$\vec{q}//[001]$, $\vec{u}//[010]$	C_{44}
Monoclinic classes					
4A	e_1; e_2; e_3; e_5	K_2	0	–	–
2B	e_4; e_6	$C_{44}C_{66}-C_{46}^2$	I	$\vec{q}//[010]$, $\vec{u}\perp[010]$ & $\vec{q}$	$\frac{1}{2}\left\{(C_{44}+C_{66})-\left[(C_{44}-C_{66})^2+4C_{46}^2\right]^{1/2}\right\}$
Triclinic classes					
6A	e_1; e_2; e_3; e_4; e_5; e_6	K_3	0	–	–

$K_1 = \det|C_{ik}|$, $i,k \le 3$; $K_2 = \det|C_{ik}|$, $i,k \le 3$ or 5; $K_3 = \det|C_{ik}|$, $i,k \le 6$

Notes:

1. Degenerate strains in each class are separated by a comma; non-degenerate strains which have the same symmetry as each other are separated by a semi-colon.
2. Under "stability limit" is the combination of elastic constants, derived from the relevant eigenvalue of the elastic constant matrix, which tends to zero at the transition point.
3. "Transition type" refers to the classification scheme of Cowley (1976): 0, no acoustic mode can give the required strain; I, $\vec{q}$ and $\vec{u}$ of the soft acoustic mode are restricted to specific directions; II, $\vec{q}$ of the soft acoustic mode is restricted to a specific direction but $\vec{u}$ is unrestricted within a specific plane (or *vice-versa*).
4. Only one orientation of the soft mode is specified; others may be derived by interchanging $\vec{q}$ and $\vec{u}$, and by considering all symmetry-related directions. For trigonal (2E), tetragonal (2B) and monoclinic (2B) classes, the angles between $\vec{q}$ or $\vec{u}$ and a prominent crystallographic direction are functions of the elastic constants and are listed by Terhune *et al.* (1985).
5. The set of soft-mode velocities has been derived from Table III of Bulou (1992).

3.3 Symmetry-adapted elastic constants and elastic energies

When writing out a Landau free-energy expansion in full, use of symmetry-adapted strains can simplify the task of specifying coupling terms in their invariant forms, and use of symmetry-adapted elastic constants can lead to similar simplification of the elastic energy. In the case of a transition $m3m \rightarrow 4/mmm$, for example, the elastic energy is:

$$\frac{1}{2}\sum_{i,k} C_{ik}e_i e_k = \frac{1}{2}C_a e_a^2 + \frac{1}{2}C_t e_t^2$$

$$= \frac{1}{2}(C_{11}+2C_{12})\left[\frac{1}{\sqrt{3}}(e_1+e_2+e_3)\right]^2 + \frac{1}{2}(C_{11}-C_{12})\left[\frac{1}{\sqrt{6}}(2e_3-e_1-e_2)\right]^2 \quad (80).$$

C_a represents the A_{1g} eigenvalue, the symmetry-adapted elastic constant for the A_{1g} strain, and C_t is the E_g eigenvalue corresponding to the symmetry-breaking strain e_t (*i.e.* for $A = 0$, $B = 1$ in Table 4). These strains are often quoted as $e_a = e_1 + e_2 + e_3$ and $e_t = \frac{1}{\sqrt{3}}(2e_3 - e_1 - e_2)$, as in Carpenter *et al.* (1998a), for example, with the corresponding elastic constants then given as $\frac{1}{2}(C_{11}+2C_{12})$ and $\frac{1}{2}(C_{11}-C_{12})$. Placing of the scale factor either in expressions for the elastic constants or for the strains is a matter of arbitrary choice.

Symmetry-adapted strains and elastic constants can be obtained by inspection of the eigenvalues and eigenvectors for the elastic-constant matrix of the high-symmetry phase. For a symmetry change $422 \rightarrow 222$, the active representation is B_1 and the symmetry-adapted elastic energy due to the B_1 strain would be $\frac{1}{2}(C_{11}-C_{12})\left[\frac{1}{\sqrt{2}}(e_1-e_2)\right]^2$. An equivalent simplification is not achieved for the A_1 (non-symmetry breaking) elastic energy because of the algebraic complexity of the eigenvalues and eigenvectors. In this case there might be some advantage in making use of the submatrix to express the energy as:

$$\frac{1}{2}\left(\frac{e_1+e_2}{\sqrt{2}}, e_3\right)\begin{pmatrix} C_{11}+C_{12} & \sqrt{2}C_{13} \\ \sqrt{2}C_{13} & C_{33} \end{pmatrix}\begin{pmatrix} \frac{e_1+e_2}{\sqrt{2}} \\ e_3 \end{pmatrix}.$$

For lower-symmetry systems it may be more convenient simply to take the sum of individual contributions, $\frac{1}{2}C_{11}e_1^2 + \frac{1}{2}C_{12}e_1e_2$, *etc.*

4. Elastic instabilities and acoustic phonons

In the preceding sections, only macroscopic stresses and strains have been considered. The velocities of acoustic waves in a crystal are also functions of the elastic constants, which means that anomalous variations in the elastic properties are necessarily accompanied by anomalies in the behaviour of the acoustic phonons. If an elastic constant, or symmetry-adapted combination of elastic-constants, decreases (softens) to zero as the equilibrium transition point is approached from above or below, the velocity of a related acoustic phonon, the soft acoustic mode, will also tend to

zero. The mechanism of a ferroelastic transition may be thought of, on a mesoscopic length scale (~10 – 1000 unit cells), as the freezing in of lattice distortions due to certain critical acoustic waves, therefore. An additional consideration is that elastic constants are not usually determined directly, but are often obtained by measuring the velocities of acoustic waves in a crystal of interest.

In order to be more specific about the role played by acoustic phonons in phase transitions, it is necessary to start with the relationship between acoustic-wave velocities and elastic constants. Formal treatments of this relationship are given in a number of standard texts (see, for example, Landau & Lifshitz, 1986, or Dove, 1993). A summary is presented here primarily to emphasise that, although the criteria for predicting an elastic instability, based on the properties of the 6 x 6 elastic-constant matrix, are quite different from those used to predict the velocity, polarisation and propagation direction of soft acoustic modes, based on the properties of a 3 x 3 dynamical matrix, the mesoscopic and macroscopic pictures of a phase transition must be mutually consistent. On the other hand, if some understanding of additional anomalous softening due to dynamical effects is also sought, it is essential to consider processes at the mesoscopic or microscopic (atomistic) length scale.

4.1 Orientation, polarisation and velocity of acoustic waves

Following Landau & Lifshitz (1986), the general equation of motion for elastic waves in a crystal is given by:

$$\rho \frac{\partial^2 u_i(x_j)}{\partial t^2} = \frac{\partial \sigma_{ij}(x_j)}{\partial x_j} \tag{81}$$

where ρ is density and u_i is the displacement which would be observed at a distance x_j from the origin in the direction of propagation of the wave, and t is time. Summation over repeated indices, 1 – 3, is implied both here and in the following equations, and four-figure suffix notation is used for maximum clarity. A stress σ_{ij} is related to the strain e_{kl} by Hooke's law which, for present purposes, is written as:

$$\sigma_{ij}(x_j) = C_{ijkl} e_{kl}(x_j) \tag{82}.$$

The strain e_{kl} is defined by:

$$e_{kl} = \frac{\partial u_k(x_j)}{\partial x_l} \tag{83}$$

so that equation 81 becomes:

$$\rho \frac{\partial^2 u_i(x_j)}{\partial t^2} = C_{ijkl} \frac{\partial^2 u_k(x_j)}{\partial x_j \partial x_l} \tag{84}.$$

One solution is:

$$u_i(x_j) = u_{oi} \exp\left[i(q_j x_j - \omega t)\right] \tag{85}$$

where u_{oi} is the amplitude and ω the frequency of the elastic wave, and q_j is a component of its wavevector, $\vec{q}$. The normal usage of q_i for a component of the order parameter and $\vec{q}_i$ as the component of a wavevector can, unfortunately, lead to some confusion. In this review, the distinction is almost always clear from the context but is expressly stated wherever there might be some doubt. Differentiation of equation 85 gives equation 84 in the form:

$$\rho\omega^2 u_i(x_j) = C_{ijkl} q_j q_l u_k(x_j) \tag{86}$$

which is the equation of motion of acoustic waves in a crystal for wavelengths that are large relative to the unit-cell dimensions. The 3 x 3 matrix, $\sum_{j,l} C_{ijkl} q_j q_l$, represents the dynamical matrix of Brillouin-zone-centre ($\vec{q} \rightarrow 0$) acoustic phonons, and therefore governs the behaviour of soft acoustic modes at proper or pseudoproper ferroelastic transitions. Note in passing that the elastic constants, C_{ijkl}, considered here usually refer to adiabatic conditions. When motion occurs in a deformed crystal, small temperature variations occur as functions of time and distance in the crystal and it is generally assumed that the time scale of acoustic vibrations is short in comparison with the time required for heat transfer and local thermal re-equilibration.

The equation of motion may be expressed in terms of acoustic-mode velocities, v, by substituting $v = \omega/|q|$ in equation 86 and normalising the wavevector, $\vec{q}$, through the use of direction cosines, n_j ($n_j = q_j/|q|$, *etc.*). This yields, in its conventional form:

$$\left(C_{ijkl} n_j n_l - \rho v^2 \delta_{ik}\right) u_k = 0 \tag{87}$$

or, in the form due to Christoffel (see Musgrave, 1970):

$$\left|\Gamma_{ik} - \rho v^2 \delta_{ik}\right| u_k = 0 \tag{88}.$$

Here δ is the Kroneker symbol, $\delta_{ik} = 1$ for $i = k$ and $\delta_{ik} = 0$ for $i \neq k$, and Γ_{ik} are quadratic functions of the direction cosines, n_j, with coefficients as specified in Table 7 (from Musgrave, 1970).

Equations 87 and 88 represent a set of three equations for the displacements u_1, u_2 and u_3. This is more easily visualised if the equations are written out in full as:

$$\begin{pmatrix} A_1 - \rho v^2 & \alpha_1\alpha_2 & \alpha_1\alpha_3 \\ \alpha_1\alpha_2 & A_2 - \rho v^2 & \alpha_2\alpha_3 \\ \alpha_1\alpha_3 & \alpha_2\alpha_3 & A_3 - \rho v^2 \end{pmatrix} \begin{pmatrix} u_1 \\ u_2 \\ u_3 \end{pmatrix} = 0 \tag{89}$$

where each of the new terms is defined in Table 7. The only non-zero solutions occur if the determinant of the coefficients is zero, *i.e.*:

$$\mathrm{Det}\left|\Gamma_{ik} - \rho v^2 \delta_{ik}\right| = 0 \qquad (90)$$

in the Christoffel form. The three solutions for ρv^2 are the three eigenvalues of the matrix Γ_{ik}. Associated with these eigenvalues are three mutually perpendicular eigenvectors which determine the displacement vectors, $\vec{u}$. For any given direction in the crystal, as specified by a set of direction cosines, n_1, n_2 and n_3, therefore, three velocities and three polarisation vectors are obtained and these are the three modes of vibration for the chosen wave-propagation direction. In high-symmetry directions, *i.e.* for waves propagating parallel to rotation or inversion-rotation axes, the modes are purely longitudinal or purely transverse in character. For propagation directions within a mirror plane one mode is purely transverse, with its displacement vector perpendicular to the mirror plane; the other two modes are of mixed longitudinal/transverse character. For arbitrary directions all three modes will generally be of mixed character, though pure modes can occur in orientations which depend on the numerical values of the elastic constants (Brugger, 1965; Vacher & Boyer, 1972).

Table 7. Coefficients for Equation 88 (from Musgrave, 1970).

	n_1^2	n_2^2	n_3^2	$2n_2n_3$	$2n_3n_1$	$2n_1n_2$
$\Gamma_{11} = A_1$	C_{11}	C_{66}	C_{55}	C_{56}	C_{15}	C_{16}
$\Gamma_{22} = A_2$	C_{66}	C_{22}	C_{44}	C_{24}	C_{46}	C_{26}
$\Gamma_{33} = A_3$	C_{55}	C_{44}	C_{33}	C_{34}	C_{35}	C_{45}
$\Gamma_{23} = \alpha_2\alpha_3$	C_{56}	C_{24}	C_{34}	$\frac{1}{2}(C_{23}+C_{44})$	$\frac{1}{2}(C_{36}+C_{45})$	$\frac{1}{2}(C_{25}+C_{46})$
$\Gamma_{13} = \alpha_1\alpha_3$	C_{15}	C_{46}	C_{35}	$\frac{1}{2}(C_{36}+C_{45})$	$\frac{1}{2}(C_{13}+C_{55})$	$\frac{1}{2}(C_{14}+C_{56})$
$\Gamma_{12} = \alpha_1\alpha_2$	C_{16}	C_{26}	C_{45}	$\frac{1}{2}(C_{25}+C_{46})$	$\frac{1}{2}(C_{14}+C_{56})$	$\frac{1}{2}(C_{12}+C_{66})$

In piezoelectric crystals, the analysis of acoustic-wave velocities derived from equation 90 has to include electrostriction because the lattice distortions due to the acoustic waves would give rise to varying electric polarisation and, hence, to electric fields (David, 1983b).

4.2 Soft acoustic modes

The formal problem of identifying which acoustic mode might be expected to soften as an elastic instability point is approached has now been reduced to finding the eigenvalue of the dynamical matrix for a chosen direction of $\vec{q}$ which goes to zero simultaneously with the relevant eigenvalue of the elastic-constant matrix. Aubry & Pick (1971) and David (1983b) proved that there is always at least one purely transverse, zone-centre acoustic mode which should have zero velocity at any elastic stability limit governed by the elastic-constant matrix, with the exception of the eigenvalue associated with the identity representation. Three categories of behaviour can be illustrated using the example of a cubic parent crystal, and making use of the eigenvalues quoted in Table 4 (see, also, David, 1983b).

For a phase transition giving a symmetry change $m3m \rightarrow 4/mmm$ the elastic stability limit is given by $(C_{11} - C_{12}) \rightarrow 0$ (E_g symmetry, Table 4). From equation 88 it can easily be shown that the velocity of the transverse acoustic mode with $\vec{q}$ // [110] and $\vec{u}$ // [1$\bar{1}$0] is $\sqrt{(1/2\rho)(C_{11} - C_{12})}$. This mode would clearly go to zero velocity at the elastic stability limit. A solution with $\vec{q}$ // [1$\bar{1}$0] and $\vec{u}$ // [110] is equally valid, however, which means that the soft mode consists of two mutually perpendicular transverse acoustic waves which possess identical velocities and frequencies. By symmetry in a cubic crystal, equivalent pairs of modes must also exist in each of the *yz* and *xz* planes. The strain at a cubic → tetragonal transition is produced by two sets of these soft modes (4-fold axis retained), and the strain at a cubic → orthorhombic transition is produced by all three. This is illustrated for one plane in Fig. 6. The spontaneous strain is, of course, given by the E_g eigenvector of the elastic-constant matrix, as discussed above.

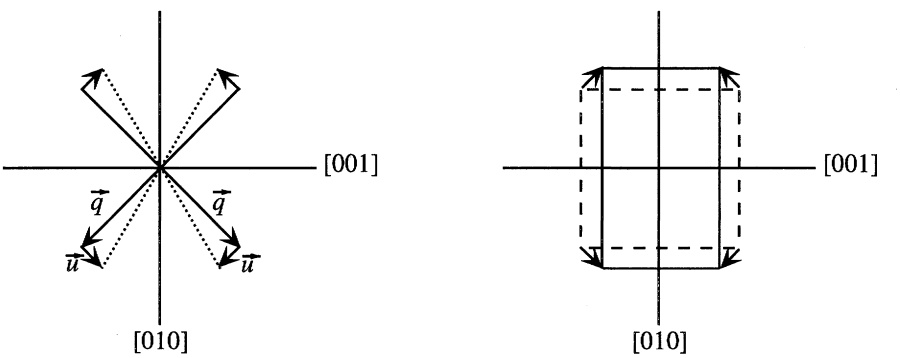

Fig. 6. A soft transverse acoustic mode acts as two mutually perpendicular waves to produce distortions which, when frozen in, result in a loss of macroscopic symmetry. In this plane a square becomes a rectangle (after David, 1983b). The same form of distortion occurs simultaneously in two perpendicular planes at a transition $m3m \rightarrow 4/mmm$ or in three planes at a transition $m3m \rightarrow mmm$.

For cubic → trigonal, cubic → monoclinic or cubic → triclinic transitions, the elastic stability limit is given by $C_{44} \rightarrow 0$ (active representation T_{2g}, Table 4). The corresponding soft acoustic mode, with velocity $\sqrt{C_{44}/\rho}$, has $\vec{q}$ // [100] and $\vec{u}$ in the plane perpendicular to [100]. Again, each soft mode operates as a mutually perpendicular pair of modes, and there are symmetry-related modes in other planes. The spontaneous strains develop in an analogous manner to the case illustrated in Fig. 6 (see David, 1983b).

Finally, the eigenvalue of the $m3m$ elastic-constant matrix corresponding to A_{1g} symmetry (identity representation) is $(C_{11} + 2C_{12})$. There are, of course, no individual acoustic modes which would go to zero as $(C_{11} + 2C_{12}) \rightarrow 0$. The spontaneous strain at such an elastic instability would be a pure volume, non-symmetry-breaking strain and could not be directly responsible for any change of symmetry.

The direction and polarisation of the soft acoustic mode associated with an elastic instability is not always so simply related to the crystallographic axes. For a transition involving a symmetry change $4/m \rightarrow 2/m$, for example, the relevant elastic-constant eigenvalue is $\frac{1}{2}\left\{(C_{11} - C_{12} + C_{66}) - \left[(C_{11} - C_{12} - C_{66})^2 + 8C_{16}^2\right]^{1/2}\right\}$ (active representation B_g, Table 6). This

goes to zero simultaneously with a transverse acoustic mode that has $\rho v^2 = \frac{1}{4}\left\{(C_{11} - C_{12} + 2C_{66}) - \left[(C_{11} - C_{12} - 2C_{66})^2 + 16C_{16}^2\right]^{1/2}\right\}$ and both $\vec{q}$ and $\vec{u}$ in the (001) plane but not otherwise constrained by symmetry (Benyuan *et al.*, 1981; David, 1983c; Cummins, 1983; Tokumoto & Unoki, 1983). The actual orientation of $\vec{q}$ is characterised by the angle θ between $\vec{q}$ and the x-axis, [100]. Its numerical value depends explicitly on the elastic constants as (Benyuan *et al.*, 1981; David, 1983c; Cummins, 1983):

$$\tan 4\theta = \frac{4C_{16}}{C_{11} - C_{12} - 2C_{66}} \qquad (91).$$

Note that if the ratio between C_{16} and $(C_{11} - C_{12} - 2C_{66})$ changes as a function of pressure, temperature or chemical composition, the direction of the soft mode rotates in the (001) plane. A mechanism for inducing this transition can again be thought of as the freezing in of displacements due to two mutually perpendicular transverse acoustic waves (Fig. 7). Expressions equivalent to equation 91 for the angles between soft-mode directions and prominent crystallographic directions are listed by Terhune *et al.* (1985).

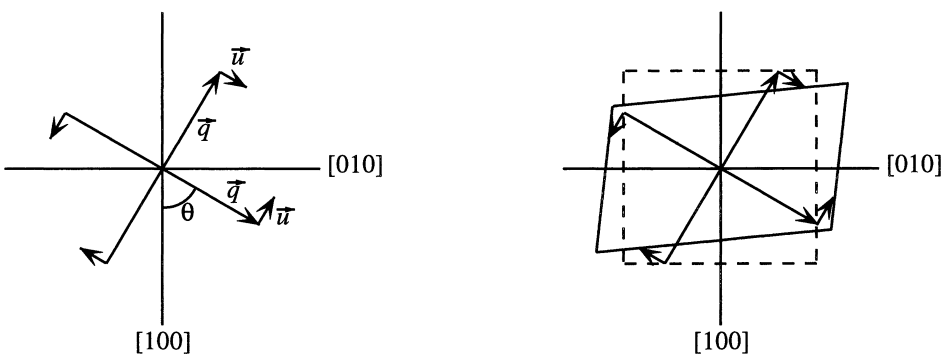

Fig. 7. A mutually perpendicular pair of transverse acoustic waves produces the distortion arising at a transition $4/m \rightarrow 2/m$ (after David, 1983c).

Although derived in different ways, the expressions for ρv^2 and the critical elastic-constant eigenvalue should have the same form. That they do not in the example used here and in some trigonal systems, is a consequence of the convention used to reduce nine strains of the form e_{ij} ($i, j = 1 - 3$) to six of the form e_i ($i = 1 - 6$) and changing C_{ijkl} to C_{ik} notation (Cummins, 1983; Terhune *et al.*, 1985). Bulou (1992) has shown how the apparent discrepancy can be resolved using an alternative convention. The value of ρv^2 for a soft acoustic mode (involving pure shear strains) should be half the value of the critical elastic-constant eigenvalue (Cummins, 1983), though the comparison must be made using eigenvalues derived via the formal conventions of Bulou (1992). This highlights the need to use the Voigt notation with care. A complete set of expressions for ρv^2 of the critical soft acoustic modes, using the normal conventions, is given in Table 6.

One general and important conclusion which results from this type of discussion is that those zone-centre acoustic modes which could (theoretically) have zero velocity at a second-order

phase transition inevitably occur as *pairs of mutually perpendicular modes even when the two propagation directions are not related by crystallographic symmetry*. The propagation and displacement directions of one wave are respectively the displacement and propagation directions of the other (Aubry & Pick, 1971; David, 1983c, 1984; Terhune *et al.*, 1985). The orientations of transformation twins which arise at ferroelastic transitions are controlled by the same physical effects, as may be understood from the following argument (from David, 1983c). Energy minimisation requires that there should be no mismatch in lattice dimensions across the boundary between two transformation twins. In the direction of propagation of a purely transverse distortion there is also no change in the lattice dimension. As a result, the propagation direction of the soft acoustic mode lies within the transformation twin plane. There are, however, two equally soft (orthogonal) directions in the crystal as the transition point is approached and there must therefore also be two mutually perpendicular twin planes. The soft-mode propagation directions lie at right angles to the line of intersection of these twins, therefore. A useful corollary of this, pointed out by David (1983c) and Cummins (1983), is that the orientation of the critical soft acoustic mode for a ferroelastic transition in a crystal can always be found simply by locating the transformation twin boundaries in that crystal.

The propagation directions and polarisation of all possible soft acoustic modes for phase transitions associated with the Brillouin zone centre are given in Table 6 (after Cowley, 1976; David, 1984; Terhune *et al.*, 1985; Bulou, 1992). The classification scheme of Cowley (1976) has also been used to distinguish between transitions in which the soft acoustic mode has different dimensionality. Type I behaviour refers to transitions in which the wave vector, $\vec{q}$, and the displacement vector, $\vec{u}$, of the soft acoustic mode are restricted to specific directions (a one-dimensional soft mode). Type II behaviour refers to situations where $\vec{q}$ is restricted to specific directions but $\vec{u}$ can be anywhere within the plane perpendicular to $\vec{q}$ (or vice versa). In this case the soft acoustic mode is two-dimensional. One example of the former is $4/m \rightarrow 2/m$, and one example of the latter is $m3m \rightarrow 2/m$ with T_{2g} as the active representation. Most natural ferroelastic materials appear to be of type I, but a few examples of type II behaviour are known, the best characterised of which occurs in Na_2CO_3 (Harris *et al.*, 1993, 1995; Harris & Dove, 1995). Type 0 behaviour refers to the cases of eigenvalues associated with the identity representation going to zero, when the resulting (non-symmetry-breaking) strains cannot be described in terms of any acoustic phonons.

As with the analysis of elastic instabilities, this discussion is relevant only for transitions involving symmetry changes associated with the Γ point of the Brillouin zone (zone centre). The velocities of acoustic modes with wavevectors other than close to the zone centre do not depend on the elastic constants in the same way. Critical softening of an acoustic branch at the Brillouin zone boundary might be accompanied by a slight softening of the same branch at the zone centre, but this would be a property of specific materials and need not be a general phenomenon. The Landau potentials used so far do not predict this type of softening unless, for example, the effects of fluctuations are included. Schematic dispersion curves are shown in Fig. 8 to illustrate some alternative situations.

4.3 Soft acoustic modes and the Landau free-energy expansion

If the driving mechanism for a phase transition is the softening of an acoustic mode, the excess entropy is purely phononic with no further contributions from configurational effects. The

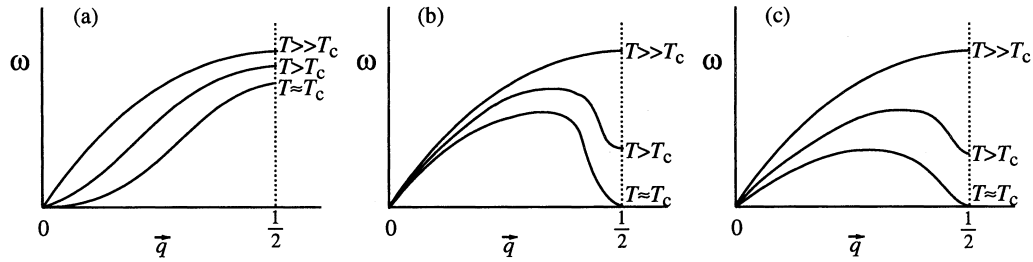

Fig. 8. Schematic dispersion curves illustrating possible softenings of a transverse acoustic mode for: (a) a zone-centre transition, (b) a zone-boundary transition, (c) a zone-boundary transition with some softening at the zone centre. The slope of the dispersion curve as $\vec{q} \rightarrow 0$ is $\sqrt{C_{ik}/\rho}$. (ω = frequency, $\vec{q}$ = wavevector).

transition would be described in the physics literature as being "ideally" displacive. In this case, the function describing the energetics of the elastic deformation in terms of atomic displacements, the effective Hamiltonian (H_{eff}), has the same form as the Landau-type Gibbs free energy (Salje *et al.*, 1991). Additional heterogeneities which are thermal in origin can be described by the Ginzburg energy, $\frac{1}{2}g(\nabla e)^2$, so that the energy on an atomistic level becomes:

$$H_{\text{eff}} = \frac{1}{2}C_{55}e^2 + \frac{1}{4}be^4 + \ \ldots\ + \frac{1}{2}g(\nabla e)^2 \qquad (92).$$

Two types of heterogeneities due to thermal effects are possible. At $T < T_c$, small variations of e locally in a structure will occur about the equilibrium value, but will not be large enough in amplitude to exceed the central barrier in the double potential well of H_{eff}. The first two terms in equation 92 can therefore be replaced by the susceptibility, giving:

$$H_{\text{eff}} \approx \frac{1}{2}\chi^{-1}e^2 + \frac{1}{2}g(\nabla e)^2 \qquad (93).$$

This is a wave equation equivalent to equation 90, with the excitation of a harmonic phonon for which $\rho v^2 = \chi^{-1}$. For the limiting case of proper ferroelastic behaviour, it was shown earlier that $\chi^{-1} = C_{55}$ at an orthorhombic $\rightleftharpoons$ monoclinic transition, so that the low-amplitude excitation is, indeed, the soft acoustic mode with $\rho v^2 = C_{55}$.

The second type of thermally induced heterogeneity involves the transfer of the local strain state from one minimum of H_{eff} to another. This means that the spontaneous strain does not oscillate around its stable equilibrium position but changes sign. On a macroscopic level, such a change of sign is equivalent to transferring from one side of a twin wall to the other. The thermal excitation is then a kink-soliton, with the solution for the simplest case (Salje, 1993) being:

$$e = e_0 \tanh\left(\frac{X}{W}\right) \qquad (94)$$

where e_0 is the equilibrium value of e, X is distance in the crystal measured perpendicular to the solitary wave, and $W \approx \sqrt{g/(a|T - T_c|)}$ is the wall thickness. W increases when T_c is approached from below and incorporates the whole crystal at $T = T_c$ in a second-order phase transition. At this point, the notion that an acoustic wave with $\omega \rightarrow 0$ and a soliton with $W \rightarrow \infty$ coexist becomes meaningless, and theories beyond the scope of this paper are necessary to describe the situation. Nevertheless, if the limiting case close to T_c is excluded, it is apparent that the acoustic softening and the elastic instability describe the same physical mechanism in the case of a proper ferroelastic phase transition.

Another aspect of the relationship between acoustic modes and macroscopic effects also leads to some questioning of the validity of the analysis close to T_c for a second-order transition. Elastic constants in the Landau expansion refer to equilibrium, *i.e.* isothermal, conditions. The macroscopic crystal should become soft with respect to a particular stress orientation at the transition point. In describing the acoustic modes, however, it has been assumed that, as a wave propagates through a crystal, the time scale of local distortions is too short for any thermal reequilibration to occur. At temperatures and pressures well removed from any equilibrium transition point the difference between the adiabatic and isothermal values of an elastic constant is less than 1%. For many practical purposes, such a small difference can be ignored, but a divergence can occur when the transition is approached. This is most easily illustrated for the difference between the adiabatic compliance, S_{ik}^{S}, and the isothermal compliance, S_{ik}^{T} (from Nye, 1985):

$$S_{ik}^{S} - S_{ik}^{T} = -\alpha_i \alpha_k \frac{T}{C_\sigma} \qquad (95).$$

(The elastic compliance is obtained by writing Hooke's law as $e_i = S_{ik}\sigma_k$ instead of $\sigma_i = C_{ik}e_k$). C_σ is the heat capacity at constant stress, and α_i, α_k are thermal expansion coefficients. The equivalent expression for elastic constants is (from Rehwald, 1973):

$$C_{mn}^{S} - C_{mn}^{T} = \frac{T}{C_e} \sum_{i,k} \alpha_i \alpha_k C_{mi} C_{nk} \qquad (96)$$

where C_e is the heat capacity at constant strain (for a clamped crystal). The divergence near a phase transition is due to the increase in α_i and α_k as $T \rightarrow T_c$, and the effect can become large. As discussed by Coe & Patterson (1969) and Dolino & Bachheimer (1982), for example, the difference between the adiabatic and isothermal elastic constants of quartz in theory amounts to ~10 – 20% at ~3 K below the $\beta \rightleftharpoons \alpha$ transition. Within 1K of the transition in KDP the difference may be 50% or more (Brody & Cummins, 1974; Cummins, 1979). Thus the data from acoustic-mode velocities in the close vicinity of the transition point do not necessarily represent the equilibrium variations in elastic constants quantitatively. In the same context, measured acoustic-wave velocities are the principal source of elastic-constant data. The equations used for ρv^2 are themselves derived on the basis of adiabatic conditions. When the acoustic-mode velocity tends to zero, this assumption becomes increasingly tenuous and the elastic constant governing the soft acoustic mode may become neither truly adiabatic nor truly isothermal.

4.4 Elastic softening due to dynamical effects

In its conventional form, as used so far in this review, the Landau free-energy expansion describes the consequences of static phenomena. The order parameter is treated as having a fixed value which is uniform throughout a crystal under equilibrium conditions. In real crystals there are fluctuations which may be understood in terms of local variations in the value of the order parameter and of the effects of normal phonons. These may contribute an additional variation to the elastic properties in the vicinity of a phase transition when their amplitudes become large. Their influence will be most clearly identifiable as variations of those elastic constants of the high-symmetry phase (above the transition temperature) which, according to the static predictions, are expected to be unaffected by the approaching phase transition. In β-quartz, such softening is observed over a temperature interval of at least 100 K (Kammer *et al.*, 1948), and comparable effects are observed in the high-symmetry forms of gadolinium molybdate (GMO) (Höchli, 1972), terbium molybdate (Yao *et al.*, 1981) and $KMnF_3$ perovskite (Cao & Barsch, 1988). If the temperature interval over which the softening occurred was restricted to only a few degrees, it might be attributed solely to the effects of critical fluctutations. That this is not the case implies that normal (non-critical) fluctuations are important.

Following the theoretical analysis of Pytte (1970, 1971) and Axe & Shirane (1970), fluctuation contributions to elastic softening have usually been considered in terms of the effects of coupling betwen different vibrational modes (Höchli, 1972; Rehwald, 1973; Cummins, 1979; Lüthi & Rehwald, 1981; Yao *et al.*, 1981; Fossum, 1985). The underlying physical picture is that, associated with a soft mode at some specific point in reciprocal space, there will be a set of branches which also soften to some extent. Along with the soft mode itself, when the frequencies of modes along the soft branches decrease so their amplitudes become larger. They can combine to produce stress fluctuations and, hence, also, strain fluctuations. The summation of all such combinations will yield a net softening of some specific acoustic modes and, therefore, of some specific elastic constants. The total effect should increase as the amplitudes of the modes increase, reaching a maximum at the transition point. The temperature dependence of the softening can be described conveniently by:

$$C_{ik} - C_{ik}^{o} = \Delta C_{ik} = A_{ik}|T - T_c|^K \qquad (97).$$

A_{ik} and K are properties of the material of interest; K is sensitive both to the degree of anisotropy of dispersion curves about the reciprocal lattice vector of the soft mode, and to the extent of softening along each branch (Axe & Shirane, 1970; Pytte, 1970, 1971; Höchli, 1972). An approach going back to the original atomistic approach of Born & Huang (1954), also following the analysis of Axe & Shirane (1970) and Pytte (1970), has been adopted here. The treatment is set out formally in an appendix, while the main conclusions are summarised in this section.

If a crystal is deformed elastically by some external stress, the atoms in it can move in two ways: a uniform change in all interatomic distances may be induced, or atoms may move relative to each other in some non-uniform manner. The latter would be caused by rotations of relatively rigid polyhedra, for example. The non-uniform motions can be thought of as creating internal strain and might, by chance, mimic the atomic motions of certain phonons. If they matched the motions due to a soft optic mode, there would be a much reduced restoring force on the atoms in the vicinity of

a transition point associated with that soft mode. As a result, the crystal would appear to be unexpectedly soft. This softening is exactly that described by bilinear coupling in a Landau expansion, since motions due to the soft mode and due to the elastic deformation would have the same symmetry – that of the active representation for the transition.

If, on the other hand, the internal strains due to non-uniform atomic motions do not match the symmetry of the soft mode, there can still be interactions which lead to the elastic deformation becoming easier. Anomalous softening not anticipated from the static Landau expansion is then expected. In this case, optic phonons with opposite wave vectors $+\vec{q}$ and $-\vec{q}$ combine to produce a fluctuating stress field. The average value for the amplitude of this stress field is zero but the average value of the square of the amplitude is not, and an energy reduction, as specified by an interaction term of the form $e_{\text{local}} < Q_\lambda^2 >$, is possible. Here e_{local} is the internal strain and $< Q_\lambda^2 >$ is the mean square amplitude of the optic phonon. The total effect is given by the summation over all optic phonons, but the greatest contribution will clearly be due to phonons with the largest amplitudes, *i.e.* those which also reduce in frequency with the soft mode itself as the transition point is approached. The analytical treatment in the appendix leads to the following conclusions concerning this anomalous softening.

(a) There are symmetry constraints dictating which elastic constants can soften by this mechanism. The effect should be observed only for those elastic constants which transform as the identity representation. The influence on other elastic constants is expected to be zero under the approximations made in the appendix. As a consequence of the constraints of symmetry on which phonons may interact, variations in different individual elastic constants may also be related. For all crystal systems $\left(\Delta C_{12}\right)^2 = \Delta C_{11}\Delta C_{22}$, $\left(\Delta C_{13}\right)^2 = \Delta C_{11}\Delta C_{33}$ and $\left(\Delta C_{23}\right)^2 = \Delta C_{22}\Delta C_{33}$ should apply, implying that there are only three independent variables. For elastically uniaxial systems these reduce to $\Delta C_{12} = \Delta C_{11}$ and $\left(\Delta C_{13}\right)^2 = \left(\Delta C_{23}\right)^2 = \Delta C_{11}\Delta C_{33}$ (2 independent variables). For cubic or elastically isotropic systems there is only one independent value since $\Delta C_{11} = \Delta C_{22} = \Delta C_{33} = \Delta C_{12} = \Delta C_{13} = \Delta C_{23}$ is expected. These relations may not hold in systems with significant thermal expansion, which contributes an additional effect to the diagonal terms of the elastic-constant matrix, ΔC_{ii}, but not to the off-diagonal terms, ΔC_{12}, ΔC_{13} and ΔC_{23}.

(b) The value of K in equation 97 depends on the anisotropy of soft branches around the critical point in the Brillouin zone. Four situations, illustrated schematically in Fig. A.1 (see appendix), have been considered. For the limiting case of weak dispersion in three orthogonal directions and more or less uniform softening of each branch with the soft mode itself, $K = -2$ is obtained. For strong dispersion, different results are obtained depending on the anisotropy of the branch softening. If a single branch flattens significantly as the soft mode decreases in frequency, the result is $K = -3/2$. If two branches flatten while the third remains relatively steep, the result is $K = -1$. If the dispersion of all three branches reduces with the softening of the soft mode, then $K = -1/2$ is obtained. A constant value of K may not describe the variations of ΔC_{ii} in systems with significant thermal expansion.

(c) A large value of A_{ik} and, hence, a large softening effect might be anticipated for materials which display large mode Gruneisen parameters, indicative of strong acoustic mode – optic mode coupling. If the softening is observed in the high-symmetry phase it must also occur in the low-symmetry phase, where it would be superimposed on static effects predicted in the normal manner. Its magnitude need not be the same in both phases.

(d) The approach outlined in the appendix is quite general for systems in which the soft optic mode shows a classical temperature dependence. Thermal fluctuations or critical fluctuations can be treated in the same manner. Similarly, the soft mode might be associated either with the zone centre or some zone-boundary point without loss of generality.

A great deal more effort has been expended in attempts to understand the role of the critical fluctuations. These are highly correlated local regions of a crystal in which the amplitude of fluctuations of an order parameter becomes greater than its mean value, and occur in the so-called Ginzburg interval around the transition point. For type I proper and pseudo-proper ferroelastic transitions this interval is strictly zero (Folk *et al.*, 1976a and b, 1979; Cowley, 1976; Als-Nielsen & Birgeneau, 1977; and see: Wadhawan, 1982; Cummins, 1983; David, 1984). For type II ferroelastics and improper ferroelastic or co-elastic transitions, there is no general criterion for the size of the Ginzburg interval. Fluctuation corrections may be large in isotropic systems and may lead to significant corrections both for the spontaneous strain and the elastic constants (Levanyuk *et al.*, 1993). Salje & Vallade (1994) have shown that these corrections are irrelevant in sufficiently anisotropic materials (*e.g.* with two rather than three elastically soft directions). Only the latter cases are considered in this review.

5. Measurement of elastic properties

In principle, it should be possible to find the elastic stability limit of a crystal with respect to some phase transition by applying an external stress, adjusting temperature or pressure and measuring the resultant strain. With the appropriate selection of stress and strain orientations a complete set of elastic constants might be determined. The isothermal values of C_{ik} obtained in this way could then be used directly in thermodynamic descriptions of equilibrium behaviour. A dynamical mechanical technique with a frequency range (~0.1 – 50 Hz) which approaches the static limit has been applied to phase transitions in a small number of systems (*e.g.* Schranz *et al.*, 1993; Schranz & Havlik, 1994; Kityk *et al.*, 1996), but most experimental studies have depended on high-frequency measurements of the velocities of acoustic waves. These make use of the general relationship:

$$C_s = \rho v_s^2 \qquad (98)$$

where v_s is the propagation velocity of a long-wavelength acoustic wave in a given direction and C_s is the related second-order elastic constant (or combination of elastic constants). Acoustic vibrations are fast relative to thermal diffusion, so the values of C_s obtained refer to adiabatic conditions.

There have been many investigations of the elastic anomalies accompanying phase transitions using ultrasonic interferometry (reviewed by: Rewald, 1973; Lüthi & Rehwald, 1981; Berger, 1989). The essence of this technique is that a piezoelectric transducer is used to generate sound waves in a crystal at an operating frequency of ~10 – 100 MHz. Values of v_s are determined in different directions within crystals which have dimensions, typically, of a few mm. Equally effective has been the use of Brillouin scattering (Cummins, 1979, 1983; Fleury & Lyons, 1981). Smaller crystals are used and the frequency range is higher, at ~10 – 60 GHz. The basis of this

technique is that light scattered by thermally-activated acoustic phonons present in a crystal suffers a frequency shift, $\Delta\omega$, with respect to the frequency, ω, of the incident beam. Because energy is conserved, the Brillouin shift is the frequency of the acoustic mode responsible for the scattering. The velocity of this acoustic mode is given by:

$$v_s = \frac{\Delta\omega}{\omega}\left(\frac{c}{\sqrt{n_i^2 + n_s^2 - 2n_i n_s \cos\theta}}\right) \qquad (99)$$

where c is the velocity of light in a vacuum, n_i and n_s are the refractive indices of the crystal in the directions of the incident and scattered beams, respectively, and θ is the angle between these two directions (typically chosen to be 90°).

Experimental difficulties have certainly restricted the use of elastic constant observations for characterising the mechanisms of phase transitions in minerals. In the case of conventional ultrasonic measurements, crystals of natural materials are not necessarily available with the size and perfection required. There can also be problems in devising a coherent and stress-free interface, between the buffer rod (to which the transducer is usually attached) and the sample, which retains its integrity to high temperatures (or high pressures). For Brillouin scattering, comparable difficulties might arise with identification of peaks in complex spectra from low symmetry crystals, or the loss of intensity as acoustic modes become progressively depopulated with increasing temperature. Fortunately, there has been significant progress with experimental techniques during the last few years and the prospects for immediate advances in this field seem auspicious. By moving to GHz frequency, the thicknesses of crystals required for ultrasonic interferometry has been reduced to ~100 μm (Chen *et al.*, 1993; Spetzler *et al.*, 1996; Shen *et al.*, 1998). In an alternative approach, resonance ultrasound spectroscopy (RUS), the acoustic resonance frequencies (~0.5 – 2.0 MHz) of crystals cut to convenient shapes are used to derive values for individual elastic constants (Migliori *et al.*, 1993; Isaak & Masuda, 1995; Ohno, 1995; Maynard, 1996; and references therein). Crystals with dimensions down to a few hundred microns can be used (Maynard, 1996), and the method has a distinct advantage of only requiring minimal contact between sample and buffer rods for transmitting the sound waves to the crystal. Impulsive stimulated scattering (ISS) is a new optical technique operating at ~1 GHz which makes use of light scattered from acoustic phonons which are excited from outside the crystal (Brown *et al.*, 1989; Zaug *et al.*, 1992, 1993; Chai *et al*, 1997). It does not yet seem to have been applied to phase transitions, however.

Among mineralogical systems, elastic-constant data for $MgAl_2O_4$ spinel, calcite, corundum, olivine, wadsleyite, garnet, orthopyroxene and wüstite have been collected at temperatures of up to ~1800 K and pressures of up to ~200 kbar (Suzuki *et al.*, 1983; Vo Thanh & Lacam, 1984; Isaak *et al.*, 1989; Webb, 1989; Goto *et al.*, 1989; Jackson *et al.*, 1990; Rigden *et al.*, 1992; Zaug *et al.*, 1993; Webb & Jackson, 1993; Askarpour *et al.*, 1993; Zha *et al.*, 1996, 1998; Chai et al., 1997; and see Sumino & Anderson, 1984, for a compilation of results published prior to 1980). Data for quartz at high temperatures have been available since the 1940's (Atanasoff & Hart, 1941; Atanasoff & Kammer, 1941; Kammer *et al.*, 1948; Zubov & Firsova, 1962; Shapiro & Cummins, 1968; Höchli, 1970; Höchli & Scott, 1971; Pelous & Vacher, 1976; Unoki *et al.*, 1984; Ohno, 1995).

All these techniques can give results which are modified by the influence of domain walls within the sample. The effects may be most serious in the vicinity of a ferroelastic transition because of the development of transformation twins (*e.g.* $SrTiO_3$, Rehwald, 1973). Light scattering techniques are the least susceptible to this problem since the volume sampled at each scattering event is only on the order of the wavelength of the phonons (~2,000 – 5,000 Å). If the size of twin domains present in the crystal is larger than this, the influence of domain walls on the total signal may be small.

Brillouin scattering and ultrasonic methods both give the propagation velocities of acoustic waves which have wave vectors, $\vec{q}$, that are small with respect to the dimensions of the Brillouin zone, $\vec{q}_{max}$, for most crystals. In a typical ultrasonic interferometry experiment at ~10 – 100 MHz, the range of wavelengths of sound waves with propagation velocities of ~5×10^6 – 10^7 mm.s^{-1} is ~0.05 – 1 mm. If the unit-cell dimension is ~10 Å this gives a $|q|/|q_{max}|$ value of ~10^{-5} – 10^{-6}. In Brillouin scattering experiments, the wavevector of the acoustic mode sampled varies with θ and the wavevector, $\vec{k}$, of the incident laser beam according to (Fleury & Lyons, 1981; Berger, 1989):

$$q = 2k \sin \frac{\theta}{2} \qquad (100).$$

For a 5,000 Å light source and a 90° scattering angle, $|q|/|q_{max}|$ is ~10^{-3} in a crystal with a 10 Å unit-cell repeat. Under normal conditions, the propagation velocities of acoustic waves are effectively constant over these ranges of $|q|/|q_{max}|$ and both techniques should give a good estimate of the static elastic constants (for $\vec{q} \rightarrow 0$). In other words, the dispersion curves for acoustic modes are usually very close to being linear functions of q in this part of the Brillouin zone. The dispersion curves of selected acoustic modes might change radically in the vicinity of a second-order transition, however. One form of variation is illustrated in Fig. 8a; the slope at $\vec{q} \rightarrow 0$ can go to zero, in theory at least, with a recovery in frequency at $q \neq 0$. If there is a soft optic mode which couples with the acoustic mode when their frequencies converge, more complex dispersion relations can result (*e.g.* Fig. 2 of Cummins, 1979). The ultrasonic interferometry and Brillouin experiments should then give different acoustic-mode velocities because they would effectively be sampling different parts of a non-linear acoustic branch. For a thorough investigation of the temperature evolution of the full dispersion curve in the soft direction, inelastic neutron scattering data are required (*e.g.* Dorner, 1981; Dove, 1993), but this technique does not resolve details of the evolution close to the zone centre.

An alternative, and more likely cause of discrepancies between ultrasound and optical scattering data for a given phase transition relates to the response time of the order parameter to an applied stress. It has been emphasised at several points earlier in this review that elastic softening due to coupling of a strain with a driving order parameter, Q, will only be observed if the time scale for changes in Q is short with respect to the time scale of the lattice distortions in the acoustic wave for which v_s is measured. If the frequency of the acoustic wave is too high relative to the frequency of the response of Q, then the experimental value of C_{ik} will not represent equilibrium behaviour. A clear example of this is provided by the orthorhombic (*Pmnb*) $\rightleftharpoons$ orthorhombic ($P2_1nb$) transition in NH_4LiSO_4, for which ultrasonic and Brillouin scattering experiments yield quite different patterns of evolution of C_{55} (Schranz *et al.*, 1987; Schranz, 1993). Such a discrepancy yields insights into the microscopic processes responsible for a transition, but also

serves to emphasise the need for caution in interpreting all elastic-constant data in the close vicinity of the transition point. Another possible example is the frequency dependence of C_{11} in $KBr_{1-x}KCN_x$ observed by Feile *et al.* (1982) over a temperature interval of ~4 K.

Considerable effort has also been put into measurements of the attenuation of acoustic waves near phase transitions since, in principle, these carry information about dynamical aspects of the transitions (*e.g.* Rehwald, 1973; Lüthi & Rehwald, 1981; Fossheim & Fossum, 1984; Fossum & Fossheim, 1985; Fossum, 1985; Deorani *et al.*, 1990; and references therein). The loss of energy by a transmitted acoustic wave due to absorption or scattering is observed in an ultrasonic experiment as a decrease in signal intensity and in Brillouin scattering experiments as spectral line broadening. Critical fluctuations in the Ginzburg interval might cause attenuation with some characteristic temperature dependence, but the presence of inhomogeneities, impurities and domain walls can also cause similar effects near the transition point (Lüthi & Rehwald, 1981). Response time effects can also result in line broadening of Brillouin peaks (Schranz *et al.*, 1987). The observation of attenuation cannot be taken as unambiguous evidence for the existence of critical fluctuations in a given system, therefore.

6. Renormalisation of second-order elastic constants at phase transitions: some examples of ideal behaviour

Having established the criteria which determine the evolution of individual elastic constants at a phase transition, it is possible to derive expressions for the variations of all the elastic constants of a crystal when it undergoes a given change in symmetry. This is illustrated here using four selected examples, which, in terms of the point groups involved, are $m3m \rightleftharpoons 4/mmm$, $422 \rightleftharpoons 222$, $mmm \rightleftharpoons 2/m$ and $622 \rightleftharpoons 32$. Between them, these examples display many of the features likely to be encountered in the analysis of elastic properties of materials undergoing phase transitions. They are also relevant for some of the real systems discussed in the following section.

For the first three examples, the macroscopic mechanisms considered involve either strain as the driving order parameter (proper ferroelastic behaviour) or a different structural effect, associated first with the centre of the Brillouin zone (pseudo-proper) and then with a special point on the zone boundary (improper), acting as the driving order parameter. In the fourth example, $622 \rightleftharpoons 32$, there are no symmetry-breaking strains. Any spontaneous strain which does arise is associated only with the identity representation (co-elastic behaviour) and is due to coupling with the square of the driving order parameter. The possibility of temperature-dependent coupling coefficients providing the driving mechanism is not considered. Also, no attempt is made to explain the group-theory manipulations required to determine which coupling terms are allowed by symmetry. As pointed out in section 2.3 these can be complicated, particularly for transitions associated with points away from the centre of the Brillouin zone.

For reasons of space, the illustrations are restricted to second-order transitions, but their extension to tricritical or first-order character should be quite straightforward, as discussed for individual elastic constants in earlier sections. For a similar reason, the possible effects of fluctuations are not included. Use is made of the symmetry-adapted strains and symmetry-adapted elastic constants, as appropriate. Only coupling between the driving order parameter and the individual strain components is considered, and only the lowest-order coupling terms allowed by

symmetry are included. Some of the coefficients have a physical meaning related to high-order elastic constants (Tolédano *et al.*, 1983) but these are not set out explicitly here.

For geological problems, bulk and shear moduli may be of more practical use than individual elastic constants. These can be derived from the equations given here using an appropriate averaging procedure, as required. Different approaches to this averaging are summarised by Sumino & Anderson (1984).

6.1 $m3m \rightleftharpoons 4/mmm$

Proper. The active representation for an equitranslational (Brillouin zone centre) phase transition involving the symmetry change $m3m \rightleftharpoons 4/mmm$ is the two-dimensional representation E_g. The order parameter therefore contains two components which, in terms of strains, correspond to the orthorhombic strain, $e_o = \frac{1}{\sqrt{2}}(e_1 - e_2)$, and the tetragonal strain, $e_t = \frac{1}{\sqrt{6}}(2e_3 - e_1 - e_2)$ (Table 4). The remaining strains are associated with the identity representation, $e_a = \frac{1}{\sqrt{3}}(e_1 + e_2 + e_3)$, and with the three-dimensional representation T_{2g} (e_4, e_5, e_6). Treating the transition as being driven by the symmetry-breaking spontaneous strain, the relevant Landau free-energy expansion can be given (after Tolédano *et al.*, 1983) as:

$$G = \frac{1}{2}a(T - T_c)\left(e_o^2 + e_t^2\right) + \frac{1}{3}u\left(e_t^3 - 3e_t e_o^2\right) + \frac{1}{4}b\left(e_o^2 + e_t^2\right)^2 + \lambda_a e_a\left(e_o^2 + e_t^2\right)$$
$$+\lambda_4\left[\sqrt{3}e_o\left(e_4^2 - e_5^2\right) + e_t\left(2e_6^2 - e_4^2 - e_5^2\right)\right] + \frac{1}{2}C_a^o e_a^2 + \frac{1}{2}C_{44}^o\left(e_4^2 + e_5^2 + e_6^2\right) \qquad (101).$$

The third-order term in e_t and e_o with the coefficient u ensures that the phase transition is first order in character. The term with the coefficient λ_a corresponds to the normal coupling of non-symmetry-breaking strains with the square of the driving order parameter. The term with λ_4 as the coefficient (from Lüthi & Rehwald, 1981) represents the lowest-order coupling allowed by symmetry between strains with E_g symmetry and strains with T_{2g} symmetry. It contains elements of the form $e_t e_4^2$ because $T_{2g} \otimes T_{2g}$ contains the active representation, E_g, and, hence, $E_g \otimes T_{2g} \otimes T_{2g}$ must contain the identity representation (see character table for $m3m$ in Wooster, 1973, or Cotton, 1990). (Determination of the precise form of this term requires an analysis of the symmetric square of the T_{2g} representation and its associated eigenvectors). The remaining contributions to the excess free energy are Hooke's law elastic energies (note: $C_a^o = C_{11}^o + 2C_{12}^o$, from Table 4). Tolédano *et al.* (1983) also included a term describing coupling between strains with A_{1g} symmetry and strains with T_{2g} symmetry but, because it does not involve direct coupling with the driving order parameter, this contribution has been omitted here.

Variations of the elastic constants can be obtained by differentiating equation 101. Thus, for example, in the absence of non-symmetry-breaking strain ($\lambda_a = 0$), C_{11} is obtained from $\partial^2 G/\partial e_1^2$ quite simply. Ignoring the terms in e_4, e_5 and e_6 which do not influence C_{11}, the first derivative is:

$$\frac{\partial G}{\partial e_1} = a(T - T_c)\left(\frac{e_o}{\sqrt{2}} - \frac{e_t}{\sqrt{6}}\right) + u\left(\frac{e_o^2}{\sqrt{6}} - \frac{e_t^2}{\sqrt{6}} - \sqrt{2}e_o e_t\right) + b\left(e_o^2 + e_t^2\right)\left(\frac{e_o}{\sqrt{2}} - \frac{e_t}{\sqrt{6}}\right) + \frac{1}{\sqrt{3}}C_a^o e_a \quad (102)$$

and the second derivative is:

$$\frac{\partial^2 G}{\partial e_1^2} = \frac{2}{3}a(T - T_c) + u\left(e_o - \frac{2e_t}{3}\right) + b\left(\frac{5e_o^2}{3} - \frac{2e_o e_t}{\sqrt{3}} + e_t^2\right) + \frac{1}{3}C_a^o \quad (103).$$

Now, $e_o = 0$ in a tetragonal crystal so that equation 103 becomes:

$$C_{11} = \frac{2}{3}a(T - T_c) + be_t^2 + \frac{1}{3}C_a^o \quad (104).$$

For $T > T_c$, it follows that:

$$C_{11} = \frac{2}{3}a(T - T_c) + \frac{1}{3}\left(C_{11}^o + 2C_{12}^o\right) \quad (105).$$

Expressions for the remaining elastic constants can easily be obtained in a similar manner. For example, the variation of C_{44} is given by $\partial^2 G/\partial e_4^2$, so that, for $e_o = 0$:

$$C_{44} = C_{44}^o \qquad (\text{at } T > T_c) \quad (106)$$

and

$$C_{44} = C_{44}^o - 2\lambda_4 e_t \qquad (\text{at } T < T_c) \quad (107).$$

From the equilibrium condition, $\partial G/\partial e_t = 0$, it is straightforward to derive the variation of e_t with T:

$$e_t = \frac{3}{4}e_{t,o}\left\{1 + \left[1 - \frac{8}{9}\left(\frac{T - T_c}{T_{tr} - T_c}\right)\right]^{1/2}\right\} \quad (108)$$

where $e_{t,o}$ is the value of e_t at the transition temperature, T_{tr}. The latter is given by:

$$T_{tr} = T_c + \frac{2u^2}{9ab} \quad (109).$$

At $T > T_{tr}$, the E_g eigenvector of the $m3m$ elastic-constant matrix varies linearly with T as:

$$(C_{11} - C_{12}) = a(T - T_c) \quad (110).$$

At $T < T_{tr}$, the equivalent combination of elastic constants is $\frac{1}{3}(C_{11} + C_{12} + 2C_{33} - 4C_{13})$, from the form of the symmetry-breaking strain tensor and the relationships between elastic constants under 4/*mmm* symmetry (see Table 1 of Tolédano *et al.*, 1983). For the case of $\lambda_a = 0$ (*i.e.* $e_a = 0$), this recovers as:

$$\begin{aligned}(\overline{C}_{11} - \overline{C}_{12}) &= \tfrac{1}{3}(C_{11} + C_{12} + 2C_{33} - 4C_{13}) \\ &= a(T - T_c) + 2ue_t + 3be_t^2 \end{aligned} \quad (111).$$

It is interesting to note, however, that the symmetry-adapted combination $(C_{11} - C_{12})$ of the tetragonal phase only recovers below T_{tr} as (for $e_a = 0$):

$$(C_{11} - C_{12}) = a(T - T_c) - 2ue_t + be_t^2 \quad (112).$$

Thus, as pointed out by Tolédano *et al.* (1983), a crystal will be close to the instability point for an orthorhombic distortion if equation 101 represents an adequate description of the excess energy.

Comparison with the effects of other symmetry changes is most easily achieved by setting $u \approx 0$, to produce a second-order transition at $T = T_c$ with (for $e_a = 0$):

$$e_t^2 = \frac{a(T_c - T)}{b} \quad (113).$$

A complete list of expressions for the elastic constants then obtained is given in Table 8, and their evolution through the transition point is illustrated schematically in Fig. 4. Note that $(C_{11} - C_{12})$ (tetragonal) and $(C_{11} - C_{12})$ (cubic) have slopes in the ratio 2:1 below and above T_c. First-order behaviour ($u > 0$) would give a similar pattern of evolution, except that $(C_{11} - C_{12})$ would not reach zero and there would be discontinuities at $T = T_{tr}$.

The soft acoustic mode for the transition has $\vec{q} \,//\, [110]_{cubic}$ and $\vec{u} \,//\, [1\bar{1}0]_{cubic}$, plus all symmetry-related directions, with $\rho v^2 = \frac{1}{2}(C_{11} - C_{12})$ in the cubic phase (Table 6). For $u \approx 0$, $(C_{11} - C_{12})$ remains zero in the 4/*mmm* phase, which would imply that a crystal should remain at the stability limit with respect to an orthorhombic distortion, *i.e.* acoustic modes with $\vec{q} \,//\, [110]_{tet}$ and $\vec{u} \,//\, [1\bar{1}0]_{tet}$ would not recover below T_c.

Equation 101 yields the variations of the elastic constants for $\lambda_a \neq 0$ by the same sequence of steps. The resulting temperature dependences of the second-order elastic constants are also given in Table 8 and shown schematically in Fig. 4, again for the simplified case of $u \approx 0$. Significant differences can arise as a consequence of coupling between the driving strain and non-symmetry-breaking strain, depending on the magnitude of the coupling coefficient, λ_a. In particular, the ratio of the slopes of critical elastic constants below and above T_c, $\frac{1}{3}(C_{11} + C_{12} + 2C_{33} - 4C_{13})_{tet}$ and $(C_{11} - C_{12})_{cubic}$, becomes $2\left(b/b^*\right) : 1$ instead of 2:1, where b^* is the renormalised fourth-order coefficient $\left(= b - \left[2\lambda_a^2/\left(C_{11}^o + 2C_{12}^o\right)\right]\right)$. The individual elastic constants C_{11}, C_{33}, C_{12}, C_{13} will be expected to show some deviation from linearity. Note that no

Pseudo-proper ferroelastic transition (assuming third order term ≈ 0)

*m*3*m* phase	4/*mmm* phase, $e_a = 0$	4/*mmm* phase, $e_a \neq 0$
$q_t = 0$	$q_t^2 = \frac{a}{b}\left(T_c^* - T\right), \quad T_c^* = T_c + \left[\frac{\lambda_t^2}{a\left(C_{11}^o - C_{12}^o\right)}\right]$	$q_t^2 = \frac{a}{b^*}\left(T_c^* - T\right), \quad T_c^* = T_c + \left[\frac{\lambda_t^2}{a\left(C_{11}^o - C_{12}^o\right)}\right]$ $b^* = b - \left[\frac{2\lambda_a^2}{\left(C_{11}^o + 2C_{12}^o\right)}\right]$
$C_{11} = C_{22} = C_{33}$ $= C_{11}^o - \frac{2}{3}\left[\frac{\lambda_t^2}{a(T - T_c)}\right]$	$C_{11} = C_{22}$ $= C_{11}^o - \left[\frac{\frac{1}{6}\lambda_t^2}{2a\left(T_c^* - T\right) + a\left(T_c^* - T_c\right)}\right] - \frac{1}{2}\left(C_{11}^o - C_{12}^o\right)$ $C_{33} = C_{11}^o - \left[\frac{\frac{2}{3}\lambda_t^2}{2a\left(T_c^* - T\right) + a\left(T_c^* - T_c\right)}\right]$	$C_{11} = C_{22}$ $= C_{11}^o - \left[\frac{\frac{1}{6}\lambda_t^2 + \frac{4}{3}\lambda_a^2 q_t^2 - \frac{2\sqrt{2}}{\sqrt{9}}\lambda_t\lambda_a q_t}{2a\frac{b}{b^*}\left(T_c^* - T\right) + a\left(T_c^* - T_c\right)}\right] - \frac{1}{2}\left(C_{11}^o - C_{12}^o\right)$ $C_{33} = C_{11}^o - \left[\frac{\frac{2}{3}\lambda_t^2 + \frac{4}{3}\lambda_a^2 q_t^2 + \frac{4\sqrt{2}}{\sqrt{9}}\lambda_t\lambda_a q_t}{2a\frac{b}{b^*}\left(T_c^* - T\right) + a\left(T_c^* - T_c\right)}\right]$
$C_{12} = C_{13} = C_{23}$ $= C_{12}^o + \frac{1}{3}\left[\frac{\lambda_t^2}{a(T - T_c)}\right]$	$C_{12} = C_{12}^o - \left[\frac{\frac{1}{6}\lambda_t^2}{2a\left(T_c^* - T\right) + a\left(T_c^* - T_c\right)}\right] + \frac{1}{2}\left(C_{11}^o - C_{12}^o\right)$ $C_{13} = C_{23} = C_{12}^o - \left[\frac{-\frac{1}{3}\lambda_t^2}{2a\left(T_c^* - T\right) + a\left(T_c^* - T_c\right)}\right]$	$C_{12} = C_{12}^o - \left[\frac{\frac{1}{6}\lambda_t^2 + \frac{4}{3}\lambda_a^2 q_t^2 - \frac{2\sqrt{2}}{\sqrt{9}}\lambda_t\lambda_a q_t}{2a\frac{b}{b^*}\left(T_c^* - T\right) + a\left(T_c^* - T_c\right)}\right] + \frac{1}{2}\left(C_{11}^o - C_{12}^o\right)$ $C_{13} = C_{23} = C_{12}^o - \left[\frac{-\frac{1}{3}\lambda_t^2 + \frac{4}{3}\lambda_a^2 q_t^2 + \frac{\sqrt{2}}{\sqrt{9}}\lambda_t\lambda_a q_t}{2a\frac{b}{b^*}\left(T_c^* - T\right) + a\left(T_c^* - T_c\right)}\right]$
$C_{11} - C_{12}$ $= \left(C_{11}^o - C_{12}^o\right) - \left[\frac{\lambda_t^2}{a(T - T_c)}\right]$	$C_{11} - C_{12} = 0$	$C_{11} - C_{12} = 0$
	$\overline{C}_{11} - \overline{C}_{12} = \frac{1}{3}\left(C_{11} + C_{12} + 2C_{33} - 4C_{13}\right)$ $= \left(C_{11}^o - C_{12}^o\right) - \left[\frac{\lambda_t^2}{2a\left(T_c^* - T\right) + a\left(T_c^* - T_c\right)}\right]$	$\overline{C}_{11} - \overline{C}_{12} = \frac{1}{3}\left(C_{11} + C_{12} + 2C_{33} - 4C_{13}\right)$ $= \left(C_{11}^o - C_{12}^o\right) - \left[\frac{\lambda_t^2}{2a\frac{b}{b^*}\left(T_c - T\right) + a\left(T_c^* - T_c\right)}\right]$

$C_{11}+2C_{12}=C_{11}^{o}+2C_{12}^{o}$	$\overline{C}_{11}+2\overline{C}_{12}=\frac{1}{3}(C_{33}+2C_{11}+2C_{12}+4C_{13})$	$\overline{C}_{11}+2\overline{C}_{12}=\frac{1}{3}(C_{33}+2C_{11}+2C_{12}+4C_{13})$
	$=C_{11}^{o}+2C_{12}^{o}$	$=\left(C_{11}^{o}+2C_{12}^{o}\right)-\left[\frac{4\lambda_a^2 q_t^2}{2a\frac{b}{b^*}\left(T_c^*-T\right)+a\left(T_c^*-T_c\right)}\right]$
$C_{44}=C_{55}=C_{66}=C_{44}^{o}$	$C_{44}=C_{55}=C_{44}^{o}-2\lambda_4 q_t$	$C_{44}=C_{55}=C_{44}^{o}-2\lambda_4 q_t$
	$C_{66}=C_{44}^{o}+2\lambda_4 q_t$	$C_{66}=C_{44}^{o}+2\lambda_4 q_t$

Proper ferroelastic transition (assuming third-order term ≈ 0)		
*m*3*m* phase	4/*mmm* phase, $e_a=0$	4/*mmm* phase, $e_a\neq 0$
$e_t=0$	$e_t^2=\frac{a}{b}(T_c-T)$	$e_t^2=\frac{a}{b^*}(T_c-T),\quad b^*=b-\left[\frac{2\lambda_a^2}{\left(C_{11}^{o}+2C_{12}^{o}\right)}\right]$
$C_{11}=C_{22}=C_{33}=\frac{1}{3}\left(C_{11}^{o}+2C_{12}^{o}\right)+\frac{2}{3}a(T-T_c)$	$C_{11}=C_{22}=\frac{1}{3}\left(C_{11}^{o}+2C_{12}^{o}\right)+\frac{1}{3}a(T_c-T)$	$C_{11}=C_{22}=\frac{1}{3}\left(C_{11}^{o}+2C_{12}^{o}\right)+\frac{1}{3}a\frac{b}{b^*}(T_c-T)-\frac{2\sqrt{2}}{\sqrt{9}}\lambda_a e_t$
	$C_{33}=\frac{1}{3}\left(C_{11}^{o}+2C_{12}^{o}\right)+\frac{4}{3}a(T_c-T)$	$C_{33}=\frac{1}{3}\left(C_{11}^{o}+2C_{12}^{o}\right)+\frac{4}{3}a\frac{b}{b^*}(T_c-T)+\frac{4\sqrt{2}}{\sqrt{9}}\lambda_a e_t$
$C_{12}=C_{13}=C_{23}=\frac{1}{3}\left(C_{11}^{o}+2C_{12}^{o}\right)-\frac{1}{3}a(T-T_c)$	$C_{12}=\frac{1}{3}\left(C_{11}^{o}+2C_{12}^{o}\right)+\frac{1}{3}a(T_c-T)$	$C_{12}=\frac{1}{3}\left(C_{11}^{o}+2C_{12}^{o}\right)+\frac{1}{3}a\frac{b}{b^*}(T_c-T)-\frac{2\sqrt{2}}{\sqrt{9}}\lambda_a e_t$
	$C_{13}=C_{23}=\frac{1}{3}\left(C_{11}^{o}+2C_{12}^{o}\right)-\frac{2}{3}a(T_c-T)$	$C_{13}=C_{23}=\frac{1}{3}\left(C_{11}^{o}+2C_{12}^{o}\right)-\frac{2}{3}a\frac{b}{b^*}(T_c-T)+\frac{\sqrt{2}}{\sqrt{9}}\lambda_a e_t$
$C_{11}-C_{12}=a(T-T_c)$	$C_{11}-C_{12}=0$	$C_{11}-C_{12}=0$
	$\overline{C}_{11}-\overline{C}_{12}=\frac{1}{3}(C_{11}+C_{12}+2C_{33}-4C_{13})$	$\overline{C}_{11}-\overline{C}_{12}=\frac{1}{3}(C_{11}+C_{12}+2C_{33}-4C_{13})$
	$=2a(T_c-T)$	$=2a\frac{b}{b^*}(T_c-T)$
$C_{11}+2C_{12}=C_{11}^{o}+2C_{12}^{o}$	$\overline{C}_{11}+2\overline{C}_{12}=\frac{1}{3}(C_{33}+2C_{11}+2C_{12}+4C_{13})$	$\overline{C}_{11}+2\overline{C}_{12}=\frac{1}{3}(C_{33}+2C_{11}+2C_{12}+4C_{13})$
	$=C_{11}^{o}+2C_{12}^{o}$	$=C_{11}^{o}+2C_{12}^{o}$
$C_{44}=C_{55}=C_{66}=C_{44}^{o}$	$C_{44}=C_{55}=C_{44}^{o}-2\lambda_4 e_t$	$C_{44}=C_{55}=C_{44}^{o}-2\lambda_4 e_t$
	$C_{66}=C_{44}^{o}+2\lambda_4 e_t$	$C_{66}=C_{44}^{o}+2\lambda_4 e_t$

Table 8. (Previous two pages and below) Predicted variations for elastic constants of a material subject to a phase transition involving the symmetry change $m3m \rightleftharpoons 4/mmm$. The expressions for individual C_{ik}'s have been derived for second-order transitions.

Improper ferroelastic transition	
Pm3m phase	*I4/mcm* phase, $e_a = 0$
$q_1 = q_2 = q_3 = 0$	$q_1 = q_2 = 0,\quad q_3^2 = \frac{a}{b^*}(T_c - T)$ $b^* = b + b' - \left[\frac{8\lambda_2^2}{C_{11}^o - C_{12}^o}\right]$
$C_{11} = C_{22} = C_{33} = C_{11}^o$	$C_{11} = C_{22} = C_{11}^o - \left[\frac{4\lambda_2^2}{3(b+b')}\right]$ $C_{33} = C_{11}^o - \left[\frac{16\lambda_2^2}{3(b+b')}\right]$
$C_{12} = C_{13} = C_{23} = C_{12}^o$	$C_{12} = C_{12}^o - \left[\frac{4\lambda_2^2}{3(b+b')}\right]$ $C_{13} = C_{23} = C_{12}^o + \left[\frac{8\lambda_2^2}{3(b+b')}\right]$
$C_{11} - C_{12} = C_{11}^o - C_{12}^o$	$C_{11} - C_{12} = C_{11}^o - C_{12}^o$ $\overline{C}_{11} - \overline{C}_{12} = \frac{1}{3}(C_{11} + C_{12} + 2C_{33} - 4C_{13})$ $= (C_{11}^o - C_{12}^o) - \left[\frac{24\lambda_2^2}{3(b+b')}\right]$
$C_{11} + 2C_{12} = C_{11}^o + 2C_{12}^o$	$\overline{C}_{11} + 2\overline{C}_{12} = \frac{1}{3}(C_{33} + 2C_{11} + 2C_{12} + 4C_{13})$ $= C_{11}^o + 2C_{12}^o$
$C_{44} = C_{55} = C_{66} = C_{44}^o$	$C_{44} = C_{55} = C_{44}^o - \left[\frac{\lambda_3^2}{\left[12\lambda_2^2/(C_{11}^o - C_{12}^o)\right] - b'}\right]$ $C_{66} = C_{44}^o$

anomaly is expected for C_a^o, in spite of there being coupling of e_a with the square of the driving order parameter.

Pseudo-proper. Should the strains arise by coupling with a different driving order parameter with E_g symmetry, the relevant free-energy expansion becomes:

$$G = \frac{1}{2}a(T - T_c)(q_o^2 + q_t^2) + \frac{1}{3}u(q_t^3 - 3q_t q_o^2) + \frac{1}{4}b(q_o^2 + q_t^2)^2 + \lambda_t(q_o e_o + q_t e_t) + \lambda_a e_a(q_o^2 + q_t^2) + \lambda_4\left[\sqrt{3}q_o(e_4^2 - e_5^2) + q_t(2e_6^2 - e_4^2 - e_5^2)\right] + \frac{1}{2}(C_{11}^o - C_{12}^o)(e_o^2 + e_t^2) + \frac{1}{2}C_a^o e_a^2 + \frac{1}{2}C_{44}^o(e_4^2 + e_5^2 + e_6^2) \qquad (114).$$

The two components of the driving order parameter Q have been specified as q_t and q_o here to correspond with the tetragonal and orthorhombic distortions, and the equation is derived from equation 101 by replacing e_t with q_t and e_o with q_o. If terms in $(q_o^2 + q_t^2)$ and $(e_o^2 + e_t^2)$ are

allowed by symmetry, then so is the bilinear coupling term $(q_o e_o + q_t e_t)$. Because the strains e_t and e_o are now being treated as "driven" rather than "driving", the series expansion representing their contributions to the free energy is truncated after this second-order term. The remaining terms represent $E_g \otimes T_{2g} \otimes T_{2g}$ type coupling energies, as in equation 101, and elastic energies.

Variations of the individual elastic constants may be predicted from equation 114 by making use of the general solution given earlier (equation 79). As an example, the variation of C_{11} for a material with $u \approx 0$, $\lambda_a \approx 0$, is given by:

$$C_{11} = C_{11}^o - \left[\frac{\partial^2 G}{\partial e_1 \partial q_t} \cdot \left(\frac{\partial^2 G}{\partial q_t^2} \right)^{-1} \cdot \frac{\partial^2 G}{\partial e_1 \partial q_t} + \frac{\partial^2 G}{\partial e_1 \partial q_o} \cdot \left(\frac{\partial^2 G}{\partial q_o^2} \right)^{-1} \cdot \frac{\partial^2 G}{\partial e_1 \partial q_o} + \frac{\partial^2 G}{\partial e_1 \partial q_t} \cdot \left(\frac{\partial^2 G}{\partial q_t \partial q_o} \right)^{-1} \cdot \frac{\partial^2 G}{\partial e_1 \partial q_o} \right] \quad (115).$$

Under equilibrium conditions $q_o = 0$ at all temperatures and $q_t^2 = (a/b)\left(T_c^* - T\right)$ at $T < T_c^*$ for a second-order transition. The renormalised transition temperature, T_c^*, is given by:

$$T_c^* = T_c + \frac{\lambda_t^2}{a\left(C_{11}^o - C_{12}^o\right)} \quad (116).$$

Thus equation 115 becomes:

$$C_{11} = C_{11}^o - \frac{2}{3}\left(\frac{\lambda_t^2}{a\left(T - T_c\right)} \right) \qquad (\text{at } T > T_c^*) \quad (117)$$

and:

$$C_{11} = C_{11}^o - \frac{1}{6}\left(\frac{\lambda_t^2}{2a\left(T_c^* - T\right) + a\left(T_c^* - T_c\right)} \right) - \frac{1}{2}\left(C_{11}^o - C_{12}^o\right) \quad (\text{at } T < T_c^*) \quad (118).$$

Solutions for all the elastic constants are given in Table 8, and their predicted elastic-constant temperature-dependences are illustrated schematically in Fig. 4. As discussed for the simple case in section 2.2, the critical combinations of elastic constants, $(C_{11} - C_{12})_{cubic}$ and $\frac{1}{3}(C_{11} + C_{12} + 2C_{33} - 4C_{13})_{tet}$, now show a marked curvature, though the ratio of the slopes below and above T_c^* still tends toward 2:1 as $T \rightarrow T_c^*$; $(C_{11} - C_{12})_{tet}$ remains zero below T_c^* as a consequence of choosing $u \approx 0$. The bulk modulus is not affected by the transition.

Elastic-constant variations for the same driving order parameter with $u \approx 0$, but $\lambda_a \neq 0$, are also given in Table 8 and Fig. 4. The general form of their variations is rather similar to the case of

$\lambda_a = 0$, but, significantly, there is now expected to be an anomaly in the bulk modulus, and the ratio of the slopes for the critical elastic-constant variations is expected to tend to $2\left(b/b^*\right)$:1 instead of 2:1 as $T \rightarrow T_c^*$.

Improper. Finally, if the active representation for the transition is not E_g, the lowest-order coupling allowed by symmetry is between strain and the square of the order parameter. This might occur for a cubic $\rightleftharpoons$ tetragonal transition in which a unit-cell dimension is doubled, for example. The order parameter becomes triply degenerate and, as discussed in section 2.3, the group-theoretical derivation of terms allowed in the Landau expansion depends on the precise change in space group. A well known example is *Pm3m* $\rightleftharpoons$ *I4/mcm*, associated with the R point $(\frac{1}{2},\frac{1}{2},\frac{1}{2})$ of the Brillouin zone, for which the excess free energy can be expressed to fourth-order terms in q_i (after Slonczewski & Thomas, 1970; Ridou *et al.*, 1980) as:

$$\begin{aligned} G = &\frac{1}{2}a(T-T_c)\left(q_1^2+q_2^2+q_3^2\right)+\frac{1}{4}b\left(q_1^2+q_2^2+q_3^2\right)^2+\frac{1}{4}b'\left(q_1^4+q_2^4+q_3^4\right) \\ &+\lambda_1 e_a\left(q_1^2+q_2^2+q_3^2\right)+\lambda_2\left[\sqrt{3}e_o\left(q_1^2-q_2^2\right)+e_t\left(2q_3^2-q_1^2-q_2^2\right)\right] \\ &+\lambda_3\left(e_6q_1q_2+e_5q_1q_3+e_4q_2q_3\right)+\frac{1}{2}\left(C_{11}^o-C_{12}^o\right)\left(e_o^2+e_t^2\right) \\ &+\frac{1}{2}C_a^o e_a^2+\frac{1}{2}C_{44}^o\left(e_4^2+e_5^2+e_6^2\right) \end{aligned} \qquad (119).$$

The third-order term in equation 114 (with coefficient u), which makes a *Pm3m* $\rightleftharpoons$ *P4/mmm* transition first order, is constrained by symmetry to be strictly zero in this case. The form of allowed terms arises from group-theoretical considerations discussed by Rehwald (1973): the order parameter is an axial vector belonging to T_{1g}, the symmetric square of which contains all the strain representations ($T_{1g} \otimes T_{1g} = A_{1g} \oplus E_g \oplus T_{2g}$).

Variations of the individual elastic constants may now be derived in the usual way. The algebra becomes complicated for the general case, so the expressions given in Table 8 and illustrated in Fig. 4 are for $\lambda_1 = 0$, *i.e.* for no non-symmetry-breaking strain. The equilibrium evolution of the order parameter at $T < T_c$ for a second-order transition is given by $q_1 = q_2 = 0$, and $q_3^2 = \left(a/b^*\right)(T_c - T)$, with $b^* = b + b' - \left[8\lambda_2^2/\left(C_{11}^o - C_{12}^o\right)\right]$. Taking C_{11} as an example, equation 79 gives:

$$C_{11} = C_{11}^o - \sum_{m,n}\frac{\partial^2 G}{\partial e_1 \partial q_m}\left(\frac{\partial^2 G}{\partial q_m \partial q_n}\right)^{-1}\cdot\frac{\partial^2 G}{\partial e_1 \partial q_n} \qquad (120)$$

which yields, from equation 119:

$$C_{11} = C_{11}^o - \frac{4\lambda_2^2}{3(b+b')} \qquad (121).$$

There is expected to be a step in C_{11} at $T = T_c$, but it should not show any strong temperature dependence in either of the cubic or tetragonal phases. C_{12}, C_{33} and C_{13} are also expected to show steplike features at T_c (Fig. 4). The bulk modulus is expected to remain constant if $\lambda_1 = 0$, but will display a step similar to the other elastic constants if there is any non-symmetry-breaking strain accompanying the transition. C_{44} (=C_{55}) will show a step at T_c, derived from the term in $\lambda_3(e_6q_1q_2 + ...)$, but C_{66} should be unaffected. The next higher-order coupling term for e_6 would be $\lambda_6 e_6 q_3^2$, which would give the variation $C_{66}^o = C_{44}^o + 2\lambda_6 q_3^2$.

6.2 422 ⇌ 222

Proper. For a transition giving the symmetry change 422 ⇌ 222, but with no change in translational symmetry, the active representation is B_1. From Table 5 the symmetry-breaking strain is $\left[(e_1 - e_2)/\sqrt{2}\right]$, for which the associated elastic constant is $(C_{11} - C_{12})$; the non-symmetry-breaking strains are $(e_1 + e_2)$ and e_3. The remaining strain components are e_4 and e_5, associated with the E representation, and e_6, which belongs to the B_2 representation. When the driving order parameter for the transition is the symmetry-breaking strain, the relevant free-energy expansion may be written as:

$$G = \frac{1}{2}a(T - T_c)\left(\frac{e_1 - e_2}{\sqrt{2}}\right)^2 + \frac{1}{4}b\left(\frac{e_1 - e_2}{\sqrt{2}}\right)^4 + \lambda_1\left(\frac{e_1 + e_2}{\sqrt{2}}\right)\left(\frac{e_1 - e_2}{\sqrt{2}}\right)^2$$
$$+\lambda_3 e_3\left(\frac{e_1 - e_2}{\sqrt{2}}\right)^2 + \lambda_4\left(e_4^2 - e_5^2\right)\left(\frac{e_1 - e_2}{\sqrt{2}}\right) + \lambda_6 e_6^2\left(\frac{e_1 - e_2}{\sqrt{2}}\right)^2$$
$$+\frac{1}{2}\left(C_{11}^o + C_{12}^o\right)\left(\frac{e_1 + e_2}{\sqrt{2}}\right)^2 + C_{13}^o(e_1 + e_2)e_3$$
$$+\frac{1}{2}C_{33}^o e_3^2 + \frac{1}{2}C_{44}^o\left(e_4^2 + e_5^2\right) + \frac{1}{2}C_{66}^o e_6^2 \qquad (122).$$

From group theory (Stokes & Hatch, 1988; Hatch, pers. comm.), $(e_1 + e_2)$ and e_3 each couple with $\left[(e_1 - e_2)/\sqrt{2}\right]^2$ in the normal way, e_4^2 and $-e_5^2$ couple with $\left[(e_1 - e_2)/\sqrt{2}\right]$ ($E \otimes E = A_1 \oplus B_1 \oplus B_2$, which contains B_1), and e_6^2 couples with $\left[(e_1 - e_2)/\sqrt{2}\right]^2$. The symmetry-adapted elastic constant for A_1 strains is analytically complex, but a convenient simplification is achieved by taking $\frac{1}{2}\left(C_{11}^o + C_{12}^o\right)$ and C_{33}^o as separate elastic constants for (e_1 + e_2) and e_3, respectively. In this case the scaling factor has been transferred to give $\left(C_{11}^o + C_{12}^o\right)$ and $\left[(e_1 + e_2)/\sqrt{2}\right]$.

Variations in the elastic constants may be predicted from the second derivatives of equation 122, as for the proper ferroelastic examples already discussed. Expressions for these variations are given in Table 9 and they are shown schematically in Fig. 9. The transition occurs when C_{11} = C_{12}, and the related soft acoustic mode has $\vec{q}$ // [110] and $\vec{u}$ // [1$\bar{1}$0] (or *vice versa*) in the tetragonal phase, with $\rho v^2 = \frac{1}{2}(C_{11} - C_{12})$ (Table 6). The values of $\frac{1}{2}(C_{11} + C_{22} - 2C_{12})_{ortho}$ and $(C_{11} - C_{12})_{tet}$ give slopes in the ratio 2:1 if there is no non-symmetry-breaking strain (e_1 + e_2 = e_3

= 0), or $2\left(b/b^*\right)$:1 otherwise ($e_1 + e_2 \neq 0$, $e_3 \neq 0$). The negative sign of $-e_5^2$ in the coupling term $\lambda_4\left(e_4^2 - e_5^2\right)\left[(e_1 - e_2)/\sqrt{2}\right]$ arises in the group-theoretical analysis and ensures that C_{44} and C_{55} diverge in the stability field of the orthorhombic phase.

Pseudo-proper. If the driving order parameter is not the symmetry-breaking strain, the excess free energy may be written as:

$$G = \frac{1}{2}a(T - T_c)Q^2 + \frac{1}{4}bQ^4 + \lambda_1(e_1 + e_2)Q^2 + \lambda_2(e_1 - e_2)Q + \lambda_3 e_3 Q^2$$
$$+\lambda_4\left(e_4^2 - e_5^2\right)Q + \lambda_6 e_6^2 Q^2 + \frac{1}{4}\left(C_{11}^o + C_{12}^o\right)(e_1 + e_2)^2$$
$$+\frac{1}{4}\left(C_{11}^o - C_{12}^o\right)(e_1 - e_2)^2 + C_{13}^o(e_1 + e_2)e_3$$
$$+\frac{1}{2}C_{33}^o e_3^2 + \frac{1}{2}C_{44}^o\left(e_4^2 + e_5^2\right) + \frac{1}{2}C_{66}^o e_6^2 \qquad (123).$$

Here the factor of $\frac{1}{\sqrt{2}}$ in the strains has been incorporated into the coupling coefficients. The elastic-constant variations may again be predicted using the general solution for the case of order-parameter/strain coupling (equation 79). Analytical expressions are given in Table 9 for the cases of zero and non-zero values of the non-symmetry-breaking strain parameters $(e_1 + e_2)$ and e_3, while schematic variations are illustrated in Fig. 9.

Improper. Finally, an example of improper ferroelastic behaviour is provided by the symmetry change $P422 \rightleftharpoons C222$, where the driving order parameter is associated with the R_1 representation and the special point $\left(\frac{1}{2}, 0, \frac{1}{2}\right)$ of the Brillouin zone. The order parameter is doubly degenerate in this case. Making use of the tables of Stokes & Hatch (1988) and group-theoretical analysis of allowed coupling terms (Hatch, pers. comm.), the excess free energy due to the transition can be written as:

$$G = \frac{1}{2}a(T - T_c)\left(q_1^2 + q_2^2\right) + \frac{1}{4}b\left(q_1^2 + q_2^2\right)^2 + \frac{1}{4}b'\left(q_1^4 + q_2^4\right) + \lambda_1(e_1 + e_2)\left(q_1^2 + q_2^2\right)$$
$$+\lambda_2(e_1 - e_2)q_1q_2 + \lambda_3 e_3\left(q_1^2 + q_2^2\right) + \lambda_4\left(e_4^2 - e_5^2\right)q_1q_2 + \lambda_5\left(e_4^2 + e_5^2\right)\left(q_1^2 + q_2^2\right)$$
$$+\lambda_6 e_6^2\left(q_1^2 + q_2^2\right) + \frac{1}{4}\left(C_{11}^o + C_{12}^o\right)(e_1 + e_2)^2 + \frac{1}{4}\left(C_{11}^o - C_{12}^o\right)(e_1 - e_2)^2$$
$$+C_{13}^o(e_1 + e_2)e_3 + \frac{1}{2}C_{33}^o e_3^2 + \frac{1}{2}C_{44}^o\left(e_4^2 + e_5^2\right) + \frac{1}{2}C_{66}^o e_6^2 \qquad (124).$$

Fig. 9. (Facing page) Schematic variation of elastic constants at second-order transitions involving the point-group change 422 $\rightleftharpoons$ 222, based on expressions given in Table 9. Note: $\left(\overline{C}_{11} - \overline{C}_{12}\right) = \frac{1}{2}(C_{11} + C_{22} - 2C_{12})$, $\left(\overline{C}_{11} + \overline{C}_{12}\right) = \frac{1}{2}(C_{11} + C_{22} + 2C_{12})$. The improper example is $P422 \rightleftharpoons C222$.

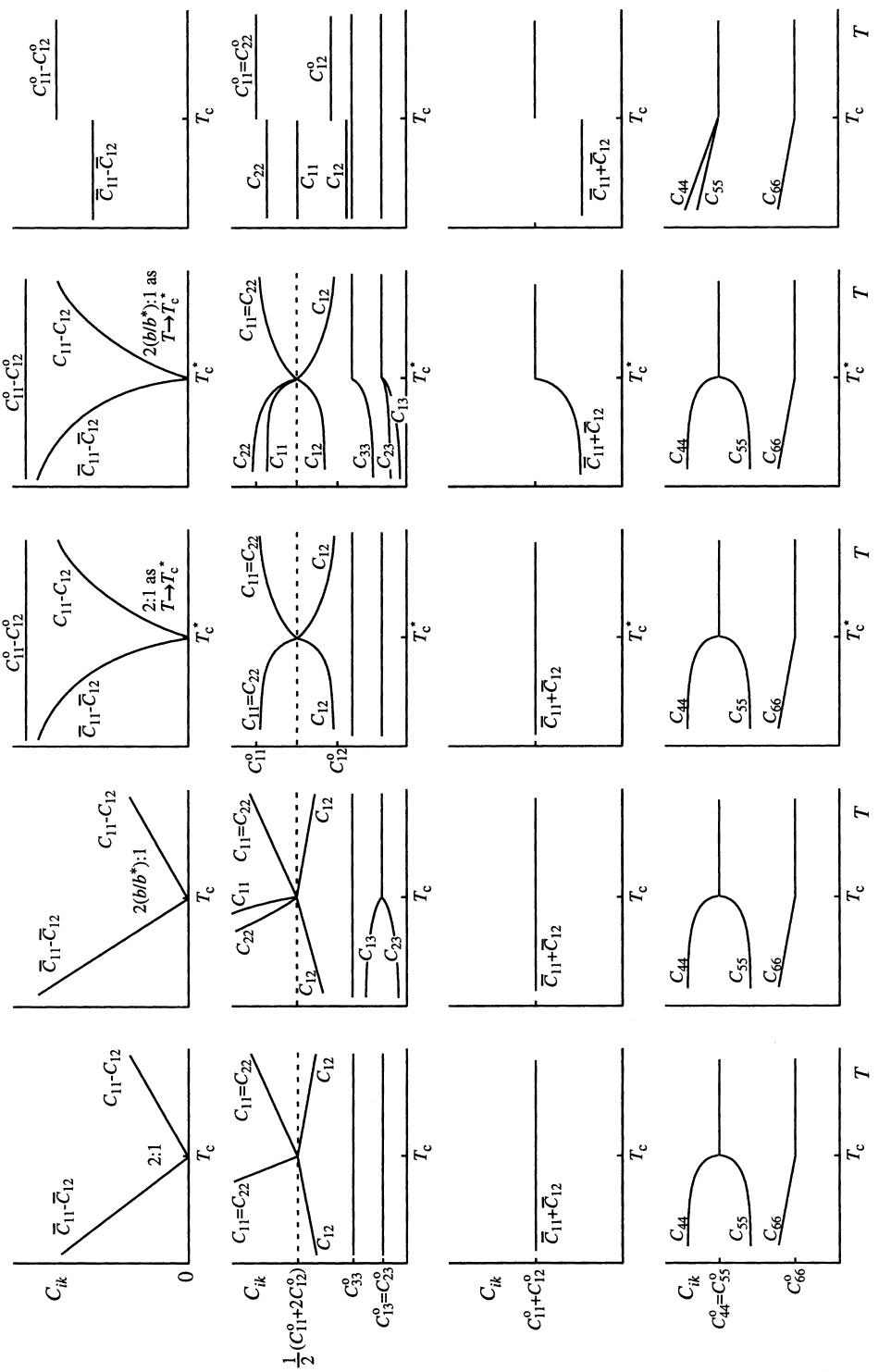

Proper ferroelastic transition		
422 phase	222 phase, $e_{nsb} = 0$	222 phase, $e_{nsb} \neq 0$
$\left(\frac{e_1 - e_2}{\sqrt{2}}\right) = 0$	$\left(\frac{e_1 - e_2}{\sqrt{2}}\right)^2 = \frac{a}{b}(T_c - T)$	$\left(\frac{e_1 - e_2}{\sqrt{2}}\right)^2 = \frac{a}{b^*}(T_c - T)$ $b^* = b - 2\left[\frac{\lambda_3^2\left(C_{11}^o + C_{12}^o\right) + \lambda_1^2 C_{33}^o - 2\sqrt{2}\lambda_1\lambda_3 C_{13}^o}{\left(C_{11}^o + C_{12}^o\right)C_{33}^o - 2C_{13}^{o\,2}}\right]$
$C_{11} = C_{22} = \frac{1}{2}\left(C_{11}^o + C_{12}^o\right) + \frac{1}{2}a(T - T_c)$	$C_{11} = C_{22} = \frac{1}{2}\left(C_{11}^o + C_{12}^o\right) + a(T_c - T)$	$C_{11} = \frac{1}{2}\left(C_{11}^o + C_{12}^o\right) + a\frac{b}{b^*}(T_c - T) + \sqrt{2}\lambda_1(e_1 - e_2)$ $C_{22} = \frac{1}{2}\left(C_{11}^o + C_{12}^o\right) + a\frac{b}{b^*}(T_c - T) - \sqrt{2}\lambda_1(e_1 - e_2)$
$C_{33} = C_{33}^o$	$C_{33} = C_{33}^o$	$C_{33} = C_{33}^o$
$C_{12} = \frac{1}{2}\left(C_{11}^o + C_{12}^o\right) - \frac{1}{2}a(T - T_c)$	$C_{12} = \frac{1}{2}\left(C_{11}^o + C_{12}^o\right) - \frac{1}{2}a(T - T_c)$	$C_{12} = \frac{1}{2}\left(C_{11}^o + C_{12}^o\right) - a\frac{b}{b^*}(T_c - T)$
$C_{13} = C_{23} = C_{13}^o$	$C_{13} = C_{23} = C_{13}^o$	$C_{13} = C_{13}^o + \lambda_3(e_1 - e_2)$ $C_{23} = C_{13}^o - \lambda_3(e_1 - e_2)$
$C_{11} - C_{12} = a(T - T_c)$	$C_{11} - C_{12} = 2a(T_c - T)$	$C_{11} - C_{12} = 2a\frac{b}{b^*}(T_c - T) + \sqrt{2}\lambda_1(e_1 - e_2)$
	$\overline{C}_{11} - \overline{C}_{12} = \frac{1}{2}(C_{11} + C_{22} - 2C_{12})$ $= 2a(T_c - T)$	$\overline{C}_{11} - \overline{C}_{12} = \frac{1}{2}(C_{11} + C_{22} - 2C_{12})$ $= 2a\frac{b}{b^*}(T_c - T)$
$C_{11} + C_{12} = C_{11}^o + C_{12}^o$	$\overline{C}_{11} + \overline{C}_{12} = \frac{1}{2}(C_{11} + C_{22} + 2C_{12})$ $= C_{11}^o + C_{12}^o$	$\overline{C}_{11} + \overline{C}_{12} = \frac{1}{2}(C_{11} + C_{22} + 2C_{12})$ $= C_{11}^o + C_{12}^o$
$C_{44} = C_{55} = C_{44}^o$	$C_{44} = C_{44}^o + \sqrt{2}\lambda_4(e_1 - e_2)$ $C_{55} = C_{44}^o - \sqrt{2}\lambda_4(e_1 - e_2)$	$C_{44} = C_{44}^o + \sqrt{2}\lambda_4(e_1 - e_2)$ $C_{55} = C_{44}^o - \sqrt{2}\lambda_4(e_1 - e_2)$
$C_{66} = C_{66}^o$	$C_{66} = C_{66}^o + \lambda_6(e_1 - e_2)^2$	$C_{66} = C_{66}^o + \lambda_6(e_1 - e_2)^2$

$$E = \frac{1}{2} C^{o} e^{2} \tag{A.19}$$

and the energy for the coupling between the optic and acoustic mode is:

$$E_{\text{coupling}} = \phi < Q^{2} > e = \lambda e \tag{A.20}$$

where λ plays the role of a stress produced by the phonons. The change of the elastic constant in Equation A.18 can now be rewritten as:

$$\Delta C = \frac{\lambda^{2}}{2\omega_{E}^{2} < Q^{2} >} \tag{A.21}.$$

The denominator is twice the optical phonon energy. Expressing λ^2 via the elastic strain-stress relation $\lambda = C^{o} e$ yields:

$$\frac{\Delta C}{C^{o}} = \frac{\frac{1}{2} C^{o} e^{2}}{\omega^{2} < Q^{2} >} = \frac{\Delta E_{\text{elastic}}}{E_{\text{optic}}} \tag{A.22}.$$

Thus, the relative change of the elastic constant is equal to the ratio of the elastic energy (with the bare elastic constants C^{o} and the thermal strain e at $T > T_c$) to the total energy of the Einstein oscillator. In crystals without phase transitions the thermal expansion is typically on the order of $e \approx 10^{-4}$ per $\Delta T \approx 1$ K. The phonon energy is much larger than the resulting elastic energy and, consequently, the ratio $\left(\Delta C / C^{o}\right)$ is small enough to be ignored for all practical purposes. In the case of displacive phase transitions, on the other hand, the energy of the soft mode is of the same order of magnitude as the elastic energy. A typical example is quartz where the soft optical phonon at $T > T_c$ approaches the acoustic branch near $q \approx (1/10a)$ where a is the lattice parameter. Then, taking $C^{o} = \left(\omega_{\text{acoustic}}^{2} / q_{\text{acoustic}}^{2}\right)$ equation A.22 can be rewritten as:

$$\frac{\Delta C}{C^{o}} \approx \frac{1}{2} \frac{\omega_{\text{acoustic}}^{2}}{\omega_{\text{optic}}^{2}} \frac{1}{q_{\text{acoustic}}^{2}} \frac{1}{< Q^{2} >} e^{2} \tag{A.23}$$

and, if $\omega_{\text{acoustic}} \approx \omega_{\text{optic}}$, $< Q^{2} > \approx 10^{-4} a^{2}$, which leads to $\left(\Delta C / C^{o}\right) \approx 10^{6} e^{2}$. This rough estimate gives a value of $\left(\Delta C / C^{o}\right) \approx 1$ for $e \approx 10^{-3}$. Thus the elastic constants soften completely due to the interaction between the optic and acoustic phonons. In three dimensions the summation is for all $\vec{q}$, and the coupling can occur between the strain and any phonon. There is, however, the symmetry constraint that terms of the form $e_{\alpha\beta} < Q_{\lambda}^{2} >$ must transform as the identity representation, so that any strain, $e_{\alpha\beta}$, which transforms as the identity representation can be involved. As a consequence, those elastic constants which themselves transform as the identity representation should always soften in the high-symmetry form of a crystal as the transition point is approached. In addition, those strains which transform as the active representation may couple

derivative ϕ in the direction of λ). It is important to recognise that in this approach it is not necessary to identify the actual physical mechanism by which large values of $<Q_\lambda^2>$ are generated. Typical causes might be fluctuations of the order parameter ($<Q_\lambda^2> \approx <Q^2>$), or phononic vibrations with large amplitudes (*i.e.* phonons with low frequencies) which are not the driving soft modes, for example.

The second term represents bi-quadratic coupling between the strain and the phonon coordinate:

$$\Delta C_{\alpha\gamma,\beta\lambda} = \int dq^3 \left\{ \sum_{\vec{l}\vec{k}} \sum_{\vec{l}'\vec{k}'} \sum_{k\mu} \sum_{l'k'\nu} \phi_{\alpha\gamma\mu\nu}\begin{pmatrix} \vec{l} & \vec{l}' & o & l' \\ \vec{k} & \vec{k}' & k & k' \end{pmatrix} x_\beta\begin{pmatrix}\vec{l}\\ \vec{k}\end{pmatrix} x_\lambda\begin{pmatrix}\vec{l}'\\ \vec{k}'\end{pmatrix} \cdot \frac{1}{\sqrt{m_k m_{k'}}} e_\mu^q e_\nu^{-q} \exp\left(-2\pi i \vec{k}\vec{x}\right) <Q^2\begin{pmatrix} q \\ j \end{pmatrix}> \right\} \qquad \text{(A.17).}$$

In this equation, the fourth derivative, $\phi_{\alpha\gamma\mu\nu}$, is only relevant if the crystal is anharmonic with respect to both the elastic deformation and the phonon movement. It is generally assumed that this is rarely the case although there is little experimental evidence in favour of such an assumption. The normal situation is that the phonons are not those of the active representation and have $<Q^2> \propto T$ at high temperatures. The renormalisation due to this term leads to a linear temperature evolution of the elastic constants at $T > T_c$ without any anomaly at T_c. Such an effect appears as a general background in the T-dependence of elastic constants and is not significant in relation to the analysis of elastic softening associated with a phase transition.

The third term in Equation A.10 is dominant in determining those elastic anomalies which are not generated by direct bilinear coupling between the strain and the order parameter. The coupling is now described by $\phi_{\alpha\beta}\begin{pmatrix} -q & q \\ j & j \end{pmatrix}$, the coefficient of a third-order anharmonic interaction between phonons and strain. Here j is the phonon branch, and coupling involves optic phonons with wave vectors $+\vec{q}$ and $-\vec{q}$ along the same branch.

Before describing this interaction in more detail, it is instructive to illustrate its relevance using, again, the simple example of a one-dimensional crystal. Consider a system that has an acoustic mode and an optic branch of an Einstein oscillator with frequency ω_E. The renormalisation of the elastic constant C^o is due to the interaction between the acoustic and optic phonon via:

$$\Delta C = \sum \frac{1}{2\omega_E^2} \phi^2 \begin{pmatrix} -k & k \\ l & l \end{pmatrix} <Q^2\begin{pmatrix} k \\ l \end{pmatrix}> = N \frac{1}{2\omega_E^2} \phi^2 <Q^2> \qquad \text{(A.18)}$$

where the omission of (k, l) indicates that the summation over N atoms has been carried out. The unrenormalised elastic energy is:

atoms inside the unit cell, and can be understood as an "internal" strain which compensates the uniform strain. Such a compensation leads to a reduction of the elastic constants – an effective softening of the crystal.

The essence of the physical effect is easily illustrated by a one-dimensional example. In this case the indices can be dropped and only the momentum, P, and phonon amplitude, Q, need be considered. The harmonic phonon then has the simple Hamiltonian:

$$H = \frac{1}{2}\Sigma\left(P^2 + \omega^2 Q^2\right) - hQ \qquad \text{(A.12)}$$

where h is the field that is generated by the macroscopic strain:

$$h = ge \qquad \text{(A.13)}$$

with g as a proportionality constant. The phonon energy follows from the transformation $Q' = \left[Q + \left(h^2/\omega^2\right)\right]$ with:

$$H' = \frac{1}{2}\Sigma\left(P^2 + \omega^2 Q'^2\right) - \frac{1}{2}\frac{h^2}{\omega^2} \qquad \text{(A.14).}$$

The oscillator is again harmonic with the same frequency. The energy:

$$E_n = \sum \hbar\omega\left(n + \frac{1}{2}\right) - \frac{1}{2}\frac{h^2}{\omega^2} \qquad \text{(A.15)}$$

is that of the phonon without a field, minus the self energy. This self energy depends on e^2 as:

$$\Delta E = -\frac{1}{2}\frac{g^2}{\omega^2}e^2 = -\frac{1}{2}\Delta C e^2 \qquad \text{(A.16).}$$

The elastic constant of the system is reduced by $(g/\omega)^2$, therefore.

Now consider the dimension of the first term in equation A.10. The elastic softening in the stability field of the high-symmetry phase here is due to the existence of the soft phonon, but is independent of its amplitude, Q. This result is identical with the earlier prediction in equation A.11, as becomes clear when ω^2 is identified with χ^{-1} in a displacive phase transition, with $\Delta C \propto \chi^{-1} \propto \left(1/\omega^2\right)$. The symmetry constraints are that $\left[Q\left(\begin{smallmatrix}o\\j\end{smallmatrix}\right)e_{\alpha\beta}\right]$ has to transform as the identity representation. This is always the case if $Q\left(\begin{smallmatrix}o\\j\end{smallmatrix}\right)$ and $e_{\alpha\beta}$ belong to the same representation, *e.g.* the active representation of the transition. Only the elastic constants transforming as the representation of $e_{\alpha\beta}$ will show this anomaly, and the result is the same as derived from a standard Landau expansion with bilinear coupling between the macroscopic order parameter and strain.

All other terms in equation A.10 are proportional to $< Q_\lambda^2 >$ and can hence be called "dynamic" renormalisations. (The index λ is added to indicate that this amplitude stems from a

$$C^{\text{uniform}}_{\alpha\gamma,\beta\lambda} = C^{\text{o}}_{\alpha\gamma,\beta\lambda} + \frac{1}{2}\sum_{q}\sum_{jj'}\phi_{(\alpha\beta)(\gamma\lambda)}\begin{pmatrix} q & -q \\ j & j' \end{pmatrix} Q\begin{pmatrix} q \\ j \end{pmatrix} Q\begin{pmatrix} -q \\ j' \end{pmatrix} \tag{A.8}$$

leaving out terms linear in the phonon amplitude for symmetry reasons. The thermodynamic expectation value of $< Q^2 >$, which is the average value of the square of the amplitude (averaged over the whole crystal) for a given phonon, depends simply on the number of excited phonons via:

$$< Q^2 >= \left[\frac{\hbar}{2\omega\begin{pmatrix} q \\ j \end{pmatrix}}\right] \coth\left[\frac{\hbar\omega\begin{pmatrix} q \\ j \end{pmatrix}}{2kT}\right] \tag{A.9}.$$

For $2kT >> \hbar\omega$, $< Q^2 >$ increases linearly with temperature. Adding all contributions to the elastic constants gives, for temperatures above the equilibrium transition point, a renormalisation per phonon branch ($j = j'$) of:

$$C_{\alpha\beta\gamma\lambda} - C^{\text{o}}_{\alpha\beta\gamma\lambda} = -\frac{1}{V}\sum_{j}\left[\frac{1}{\omega^2\begin{pmatrix} o \\ j \end{pmatrix}}\right]\phi_{\alpha\beta}\begin{pmatrix} o \\ j \end{pmatrix}\phi_{\gamma\lambda}\begin{pmatrix} o \\ j \end{pmatrix} + \sum_{j}\int dq^3\,\phi_{(\alpha\beta)(\gamma\lambda)}\begin{pmatrix} q & -q \\ j & j \end{pmatrix} < Q^2 >$$

$$-\sum_{j}\int dq^3\left[\frac{1}{2\omega^2\begin{pmatrix} q \\ j \end{pmatrix}}\right]\phi_{\alpha\beta}\begin{pmatrix} -q & q \\ j & j \end{pmatrix}\phi_{\gamma\lambda}\begin{pmatrix} q & -q \\ j & j \end{pmatrix} < Q^2 > -\delta_{\alpha\beta}\int dq^3\,\phi_{\beta\lambda}\begin{pmatrix} q & -q \\ j & j \end{pmatrix} < Q^2 > \tag{A.10}.$$

The four terms in this expression represent four separate contributions which are now discussed in turn.

The first term is due to a static response and does not depend on the amplitude of the phonon movement. Rewriting $\phi_{\alpha\beta}\begin{pmatrix} o \\ j \end{pmatrix}$ in real space leads to:

$$\phi_{\alpha\beta}\begin{pmatrix} o \\ j \end{pmatrix} = \sum_{lk}\sum_{k'\mu}\phi_{\alpha\mu}\begin{pmatrix} l & o \\ k & k' \end{pmatrix} x_{\beta}\begin{pmatrix} l \\ k \end{pmatrix}\frac{1}{\sqrt{m_{k'}}} e_{\mu}(k') \tag{A.11}$$

where $\phi_{\alpha\beta}\begin{pmatrix} l & o \\ k & k' \end{pmatrix}$ is the derivative of the force constant for the movement of atom (k, l) against atom (k', o), and $x_{\beta}\begin{pmatrix} l \\ k \end{pmatrix}$ is the projection of the position vector of atom (k, l) along the β-axis. The normal coordinate of the phonon movement is $e_{\mu}(k')$ (atom k' along the μ-axis). The physical meaning of this is that a phononic movement leads to shifts of atoms that do not correspond to a simple uniform compression or dilation of the sample. These movements involve relative shifts of

where H_0 describes the phonon:

$$H_0 = \frac{1}{2}\sum_q \sum_j \sum_\lambda \left[P_\lambda^2 \begin{pmatrix} q \\ j \end{pmatrix} + \omega^2 Q_\lambda^2 \begin{pmatrix} q \\ j \end{pmatrix} \right] \quad \text{(A.2).}$$

Strain is measured with respect to the actual time and space averaged structure as $e_{\alpha\beta}^{\text{local}}$, with

$$H_1 = \sum_{\alpha\beta} h^{(\alpha\beta)} . e_{\alpha\beta}^{\text{local}} \quad \text{(A.3)}$$

where $h^{(\alpha\beta)}$ is the field conjugated to $e_{\alpha\beta}^{\text{local}}$; $h^{(\alpha\beta)}$ is allowed to depend on the normal coordinate of the phonon, *i.e.* it depends on the pattern generated by the phononic lattice distortion. Finally, the elastic energy is:

$$H_2 = \frac{1}{2NV}\sum_{\alpha\beta} \sum_{\gamma\lambda} C_{\alpha\gamma,\beta\lambda}^{\text{uniform}} e_{\alpha\beta}^{\text{local}} e_{\gamma\lambda}^{\text{local}} \quad \text{(A.4)}$$

where N is the number of atoms, V is the volume per unit cell and $C_{\alpha\gamma,\beta\lambda}^{\text{uniform}}$ is the elastic constant that describes a uniform deformation. By uniform, what is meant is a deformation which only causes distances between all atoms in a structure to change by the same fraction.

Interactions between phonons and strain are due to the Q_λ-dependence of $h^{(\alpha\beta)}$. These are expressed formally as:

$$h^{(\alpha\beta)}(Q) = h_{\text{external}}^{(\alpha\beta)} + \sum_j h_j^{(\alpha\beta)} Q \begin{pmatrix} o \\ j \end{pmatrix} + \sum_{q,jj'} h_{\alpha\beta} \begin{pmatrix} q & -q \\ j & j' \end{pmatrix} Q \begin{pmatrix} q \\ j \end{pmatrix} Q \begin{pmatrix} -q \\ j' \end{pmatrix} + \ldots \quad \text{(A.5)}$$

where $h_{\text{external}}^{(\alpha\beta)} = 0$ when there is no external stress. Writing the other field coefficients as force constants, one finds:

$$h_j^{(\alpha\beta)} = \sqrt{N}\phi_{\alpha\beta} \begin{pmatrix} o \\ j \end{pmatrix} \quad \text{(A.6)}$$

and

$$h^{(\alpha\beta)} \begin{pmatrix} q & -q \\ j & j' \end{pmatrix} = \phi_{\alpha\beta} \begin{pmatrix} q & -q \\ j & j' \end{pmatrix} \quad \text{(A.7).}$$

The two field parameters correspond directly to the first and second derivatives of the force constant $\phi_{\alpha\beta}$. For convenience they can be written in reciprocal space rather than real space, where the connection is made by standard Fourier transformation. Direct coupling between the elastic constants and optical phonons is also introduced:

Landau theory then highlight more subtle details of a transition, such as the role of fluctuations or coupling between other phonons, which are specific to a material. The symmetry constraints on the elastic behaviour also define general categories of behaviour such that the general form of elastic-constant variations may be predicted successfully with very little prior information concerning either the detailed crystal structure or the transition mechanism.

Many mineral systems could be examined in the context of the overall philosophy set out here, and a summary list of some of these was given in Table 1. The theoretical background is well established and the weak link is now a paucity of experimental data. With improved techniques for determining the elastic constants of small and low-symmetry crystals at ranges of P and T it should become possible to advance our understanding of the behaviour of geological materials under stress to a far higher level of sophistication than has so far been achieved.

Acknowledgements: We are grateful to D. Hatch for his substantial assistance in providing the invariant forms of many of the free-energy expansions given in this review, Prof. A. Bulou for advice on the symmetrical forms of elastic-constant matrices and A. Shen for advice on experimental matters. The work was undertaken while MAC and EKHS were in receipt of a research grant from the Natural Environment Research Council of Great Britain (no. GR3/8220), and MAC was in receipt of a Royal Society Leverhulme Trust Senior Reseach Fellowship, both of which are gratefully acknowledged. W. Schranz and an anonymous reviewer are thanked for their helpful comments on the manuscript. Finally, the care and consideration of R.J. Angel and C. Chopin in their editorial handling is particularly appreciated.

Appendix: Anomalous softening due to dynamical effects

A conventional Landau expansion can be used quite effectively to predict variations of elastic constants at phase transitions. It only gives the variations due to static effects, however, and does not account for changes due to thermal fluctuations. One way of accounting for the dynamical effects is to adopt a more atomistic approach and consider a simple "ball and spoke" model of a crystal. Atoms may be treated as balls on lattice points (k, l; k-th atom in l-th unit cell) with mass m_k. These atoms are connected by springs with a spring constant, $\phi_{\alpha\beta}\begin{pmatrix} k & k' \\ l & l' \end{pmatrix}$, describing the movement of (k, l) along the α-axis and (k', l') along the β-axis. Details of this approach go back to the illuminating book of Born & Huang (1954) and many subsequent studies. In order to allow anharmonicity to enter into this model, an optical phonon is introduced. It has kinetic energy $\sum P_\lambda^2\begin{pmatrix} q \\ j \end{pmatrix}$ and potential energy $\sum \omega^2\begin{pmatrix} q \\ j \end{pmatrix} Q_\lambda^2\begin{pmatrix} q \\ j \end{pmatrix}$, where P_λ is the momentum, Q_λ is the normal coordinate, λ is a Cartesian coordinate, q is the wavevector and j is the number of the phonon branch. The basic idea is to allow the phonon to be the soft mode $\left(\omega^2 = \chi^{-1} \propto A|T - T_c|\right)$ which drives a displacive phase transition. It is the anharmonic interactions between Q_λ and strain coordinates which then give rise to the elastic anomalies.

The atomistic picture is described by a model Hamiltonian:

$$H = H_0 + H_1 + H_2 \qquad \text{(A.1)}$$

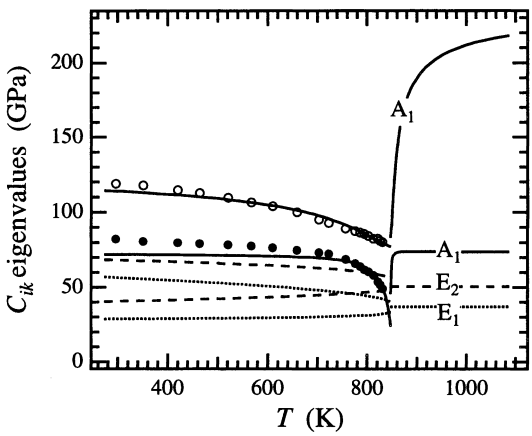

Fig. 27. Variations of the eigenvalues of the elastic-constant matrix for crystals with point group 622 ($T > T_{tr}$) and point group 32 ($T < T_{tr}$) (from Carpenter *et al.*, 1998b). Expressions for the eigenvalues of 622 crystals are given in Table 12. E_1 is plotted as C_{44} and E_2 as C_{66}. A_1 eigenvalues of crystals with 32 symmetry have the same form as those of crystals with 622 symmetry. The smooth curves were determined from the calculated variations shown in Fig. 25 (solutions derived from assuming $\Delta C_{11} = \Delta C_{12}$ and $\Delta C_{13}^2 = \Delta C_{11}\Delta C_{33}$ in β-quartz). Solid lines represent the A_1 eigenvalues; broken and dotted lines represent the other eigenvalues. Each of the E_1 and E_2 eigenvalues of β-quartz splits into two in α-quartz. Experimental data points for A_1 eigenvalues are shown below T_{tr} (data from Ohno, 1995). There is reasonable agreement between calculated and experimental data over the complete temperature range for one of the A_1 eigenvalues and close agreement between T_{tr} and ~700 K for the other. Neither of the A_1 eigenvalues reaches zero at the transition point.

Other minerals. Co-elastic transitions are particularly common amongst minerals and yet appear not to have been examined from this overall point of view. Some examples of transitions which may display co-elastic features are: $I4_1/acd \rightleftharpoons I4_1/a$ leucite (Boysen, 1990; Palmer, 1990a; Palmer *et al.*, 1990, 1997; Palmer & Salje, 1990; Hatch *et al.*, 1990a; Heaney & Veblen, 1990; Ito *et al.*, 1991), $C2/c \rightleftharpoons P2_1/c$ pigeonite (Cameron & Papike, 1980; Shimobayashi & Kitamura, 1991; Shimobayashi, 1992), $I\bar{1} \rightleftharpoons P\bar{1}$ anorthite (Salje, 1987; Redfern & Salje, 1987, 1992; Redfern *et al.*, 1988; Angel *et al.*, 1989; Hatch & Ghose, 1989; Angel, 1992; Redfern, 1992), $R\bar{3}m \rightleftharpoons R\bar{3}c$ calcite (Redfern *et al.*, 1989; Dove & Powell, 1989), $P6_3/mmc \rightleftharpoons P6_322$ tridymite (de Dombal & Carpenter, 1993; Cellai *et al.*, 1994), $C2/m \rightleftharpoons P2_1/m$ cummingtonite (Prewitt *et al.*, 1970), $P6_322 \rightleftharpoons P6_3$ kaliophilite (Cellai *et al.*, 1992), $P6_3mc \rightleftharpoons P6_3$, $P6_3mc \rightleftharpoons P6_3mc$ with multiple superlattices, and $P6_3 \rightleftharpoons P6_3$ with $\sqrt{3}A$ superlattice in kalsilite (Carpenter & Cellai, 1996; Xu & Veblen, 1996), $A2/a \rightleftharpoons P2_1/a$ titanite (Taylor & Brown, 1976; Ghose *et al.*, 1991; Van Heurck *et al.*, 1991; Bismayer *et al.*, 1992; Salje *et al.*, 1993; Zhang *et al.*, 1995; Meyer *et al.*, 1996; Kunz *et al.*, 1996; Chrosch *et al.*, 1997) and $Cmcm \rightleftharpoons Pmcn \rightleftharpoons P2_1cn$ lawsonite (Libowitzky & Armbruster, 1995).

8. Conclusion

Landau theory provides a straightforward framework for generating quantitative descriptions of the elastic-constant variations that accompany phase transitions in many materials. The elastic-constant variations themselves also provide unique insights into the mechanisms of these phase transitions. Matching observed and predicted variations provides a test of any proposed mechanism that is far more stringent than simply matching the variation of the order parameter alone. In particular, it is necessary to account correctly for contributions due to both symmetry-breaking and non-symmetry-breaking strains. Anomalies in the elastic properties not anticipated by

(Scott, 1974; Yamamoto, 1974; Dolino, 1988, 1990, and references therein). It can now clearly be seen that most of the energy reduction associated with the transition is actually due to the coupling of Q with strain. For example, at $T = \frac{1}{2}T_{tr} = 424$ K, separate contributions to the total excess energy due to the transition (–1085 J.mole^{-1}) are $G_Q = 358$ J.mole^{-1}, $G_{coupling} = -2885$ J.mole^{-1}, $G_{elastic} = 1442$ J.mole^{-1} (Carpenter *et al.*, 1998b). Substantial renormalisation of the fourth-order coefficient from $b \approx +4900$ J.mole^{-1} to $b^* = -1931$ J.mole^{-1} (equation 163) due to this coupling also drives the transition from second order to first order in character. In addition, the renormalisation causes the value of χ^{-1} (equation 162) to increase much more steeply than would be anticipated for a classical soft-mode transition and accounts, at least semi-quantitatively, for the steep recovery of the soft-mode frequency in α-quartz (Fig. 26; ω^2 data for the soft mode from Tezuka *et al.*, 1991, and Höchli & Scott, 1971).

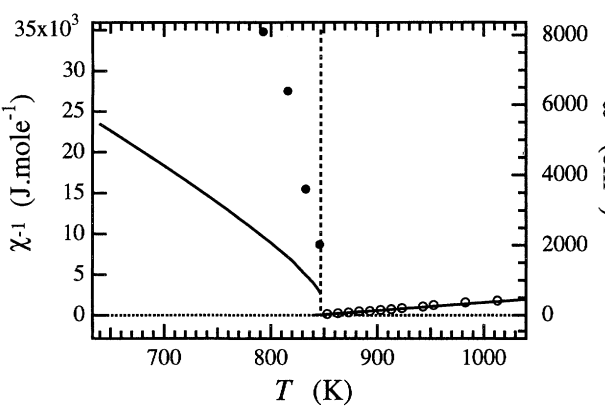

Fig. 26. Comparison between experimental data for the frequency of the soft mode of quartz and the calculated susceptibility from a Landau free-energy expansion (from Carpenter *et al.*, 1998b). A relationship of the form $\omega^2 \propto \chi^{-1}$ is expected. The axes for ω^2 (right) and χ^{-1} (left) have been adjusted so that, above T_{tr}, the experimental data for ω^2 (open circles, from Tezuka *et al.*, 1991) are superimposed on the calculated variation of $\chi^{-1} = a(T - T_c)$ (solid line). Below T_{tr}, experimental data for ω^2 are shown as filled circles (from Höchli & Scott, 1971), and the solid line is χ^{-1} calculated using equation 162. (Note that the mismatch below T_{tr} could be reduced by choosing an alternative scaling between ω^2 and χ^{-1} at $T > T_{tr}$).

While the B_1 soft mode provides the symmetry-breaking mechanism, the spontaneous strains and the largest elastic anomalies are associated with the A_1 (identity) representation of point group 622. McLellan (1973) suggested that one of the A_1 eigenvalues might extrapolate to zero at the transition point in much the same way that the eigenvalues associated with the active representation can evolve at a proper ferroelastic transition. The individual elastic constants have therefore been used to calculate variations of the relevant eigenvalues, as shown in Fig. 27. The A_1 eigenvalues show large variations but do not go to zero. In this regard, the elastic behaviour is consistent with the classical behaviour of a co-elastic material. An unexplained curiosity remains, however, in that C_{13} extrapolates to zero at 847 ± 1 K (Fig. 25). By itself, this cannot lead to an elastic instability, but it corresponds to a limiting point beyond which the elastic energy $\frac{1}{2}C_{13}e_1e_3$ for e_1 and e_3 with the same sign becomes negative, *i.e.* starting to favour simultaneous contraction parallel and perpendicular to the z-axis. Thus, while the overall elastic variations may not be regarded as being primarily responsible for the $\beta \rightleftharpoons \alpha$ transition, they are certainly associated with most of the energy change and could also be involved in some aspect of the triggering mechanism.

(1948) and Zubov & Firsova (1962) under this cubic constraint yields $K = -0.65$. Including the hexagonal symmetry constraints in the fitting gives values of $K_{11} = -0.63$, $K_{13} = -0.60$ and $K_{33} = -0.60$. A value of $K = -0.5$ would be expected if the branches of the soft mode all soften uniformly in three dimensions, while softening in two directions would be described by $K = -1$ (section 4.4). The implication of the fit values of ~–0.6 is again that β-quartz softens more or less isotropically. These fits reproduce the observed softening quite well, as shown in Fig. 25, and also yield values for the bare elastic constants, C_{11}^{o}, C_{12}^{o}, C_{13}^{o}, C_{33}^{o}.

Expressions derived from equation 161 for the variations of the elastic constants of α-quartz are listed in Table 15. They were used to extract values for the coupling coefficients λ_4, λ_5, λ_6 and λ_9, using values of Q given by equation 157 and experimental data for C_{14}, C_{44} and C_{66}. A reasonable description of the observed variations results (Fig. 25) but is, of course, not a real test of the model. On the other hand, the predicted variations of C_{11}, C_{12}, C_{13} and C_{33} depend on values of the coefficients extracted from independent measurements of strain or heat capacity, and on values of the bare elastic constants extracted from the data for β-quartz. Close agreement between the observed and calculated values of C_{11} and C_{12} therefore implies that equation 161 provides a good description of the strain and elastic behaviour of quartz in the (001) plane. The agreement for C_{33} within ~100 K of T_{tr} and for C_{13} is not as close, but the correct form is reproduced. Below ~700 K, C_{33} increases more steeply than predicted, and it seems likely that the description of strain parallel to [001] is incomplete. Finally, there is no evidence for a divergence between the calculated elastic constants, which represent isothermal conditions, and the experimental values, which are adiabatic, immediately below the transition point. This is perhaps because the transition is just first order and occurs at a temperature which is sufficiently far from T_c that the thermal expansion coefficients do not become large enough to cause a measurable difference between isothermal and adiabatic values (equations 95 and 96).

Table 15. Equations for calculating the elastic constants of α-quartz, as derived from equation 161 which includes higher-order strain/order parameter coupling terms.

α-quartz (32)	
$C_{11} = C_{22} = C_{11}^{o} + 2\lambda_6 Q^2 - \left[2\lambda_1 Q + 4\lambda_7 Q^3\right]^2 \chi$	$C_{11} - C_{12} = \left(C_{11}^{o} - C_{12}^{o}\right) + 4\lambda_6 Q^2$
$C_{33} = C_{33}^{o} - \left[2\lambda_3 Q + 4\lambda_8 Q^3\right]^2 \chi$	$C_{11} + C_{12} = \left(C_{11}^{o} + C_{12}^{o}\right) - 2\left[2\lambda_1 Q + 4\lambda_7 Q^3\right]^2 \chi$
$C_{12} = C_{12}^{o} - 2\lambda_6 Q^2 - \left[2\lambda_1 Q + 4\lambda_7 Q^3\right]^2 \chi$	$C_{14} = -C_{24} = C_{56} = \lambda_5 Q + \lambda_9 Q^3$
$C_{13} = C_{23} = C_{13}^{o} - \left[2\lambda_1 Q + 4\lambda_7 Q^3\right] . \left[2\lambda_3 Q + 4\lambda_8 Q^3\right] \chi$	$C_{44} = C_{55} = C_{44}^{o} + 2\lambda_4 Q^2$
	$C_{66} = C_{66}^{o} + 2\lambda_6 Q^2 = \frac{1}{2}(C_{11} - C_{12})$

Having demonstrated that an appropriate Landau expansion can account quantitatively for most of the elastic variations of α-quartz and that the softening in β-quartz is consistent with a dynamical origin (though not involving critical fluctuations), what can be concluded about the nature of the $\beta \rightleftharpoons \alpha$ transition? The soft zone-centre (B_1) optic mode observed by Axe & Shirane (1970), Tezuka *et al.* (1991) and Dolino *et al.* (1992) follows the $\omega^2 \propto |T - T_c|$ behaviour of a classical soft mode and is generally accepted as providing the driving mechanism for the transition

A general expression for the order-parameter susceptibility derived from equation 161 is:

$$\chi^{-1} = a(T - T_c) + \left(2b + b^*\right)Q^2 + \frac{1}{3}\left(8c + 7c^*\right)Q^4 + \left(4d + 3d^*\right)Q^6 \qquad (162)$$

where b, c and d are unrenormalised coefficients for the fourth-, sixth- and eighth-order terms in the standard Landau expansion; d^* is the renormalised eighth-order coefficient and is assumed to be zero in equation 158. The renormalised and unrenormalised coefficients are related by:

$$b^* = b - 2\left[\frac{\lambda_3^2\left(C_{11}^o + C_{12}^o\right) + 2\lambda_1^2 C_{33}^o - 4\lambda_1\lambda_3 C_{13}^o}{\left(C_{11}^o + C_{12}^o\right)C_{33}^o - 2{C_{13}^o}^2}\right] \qquad (163)$$

$$c^* = c - 6\left[\frac{\lambda_3\lambda_8\left(C_{11}^o + C_{12}^o\right) + 2\lambda_1\lambda_7 C_{33}^o - 2\lambda_1\lambda_8 C_{13}^o - 2\lambda_3\lambda_7 C_{13}^o}{\left(C_{11}^o + C_{12}^o\right)C_{33}^o - 2{C_{13}^o}^2}\right] \qquad (164)$$

$$d^* = d - 4\left[\frac{2\lambda_7^2 C_{33}^o - 4\lambda_7\lambda_8 C_{13}^o + \lambda_8^2\left(C_{11}^o + C_{12}^o\right)}{\left(C_{11}^o + C_{12}^o\right)C_{33}^o - 2{C_{13}^o}^2}\right] \qquad (165).$$

Numerical values for all the coefficients in these equations have been extracted from strain and heat-capacity data. For calculating variations of the individual elastic constants, the only additional information required is a set of values of the bare elastic constants, which may be extracted from the C_{ik} data for β-quartz.

Pronounced softening shown by C_{11}, C_{12}, C_{13} and C_{33} in β-quartz as $T \rightarrow T_{tr}$ has been accounted for successfully by dynamical effects of the type described in section 4.4 (Axe & Shirane, 1970; Pytte, 1971; Höchli, 1972; Yamamoto, 1974). Höchli (1972) used the experimental data to fit the coefficients in equation 97 and obtained values of $K = -0.60 \pm 0.06$ for C_{11} and $K = -0.64 \pm 0.06$ for C_{33}, with $T_c = 838 \pm 5$ K. Axe & Shirane (1970) fit the same data with $K = -1$ and a lower value of T_c. The observed variations of the four elastic constants are almost parallel, and the simplest explanation for this is that the bare elastic constants, C_{11}^o, C_{12}^o, C_{13}^o and C_{33}^o, are effectively constant, with a dynamical softening, ΔC_{ik}, which is the same for each. C_{66} is almost constant in β-quartz, which, since $C_{66} = \frac{1}{2}(C_{11} - C_{12})$, is consistent with C_{11}^o and C_{12}^o being effectively constant as well. C_{44} hardly varies with temperature either. The very small thermal expansion of β-quartz (Kihara, 1990; Carpenter *et al.*, 1998b; and references therein) is a further indication that the bare elastic constants might not vary strongly with temperature.

The symmetry constraints for a hexagonal system require $\Delta C_{11} = \Delta C_{12}$ and $(\Delta C_{13})^2 = \Delta C_{11}\Delta C_{33}$ (section 4.4), but quartz appears to conform to the constraints $\Delta C_{11} = \Delta C_{12} = \Delta C_{13} = \Delta C_{33}$ that apply in a cubic system. In other words, as far as local fluctuations in the order parameter are concerned, the material behaves as if it is an isotropic medium. Obtaining the coefficients in equation 97 by fitting them to the data of Kammer *et al.*

$$Q^2 = \frac{2}{3}Q_o^2\left\{1+\left[1-\frac{3}{4}\left(\frac{T-T_c}{T_{tr}-T_c}\right)\right]^{1/2}\right\} \quad (157).$$

This is derived from the standard Landau expansion to sixth order:

$$G = \frac{1}{2}a(T-T_c)Q^2 + \frac{1}{4}b^*Q^4 + \frac{1}{6}c^*Q^6 \quad (158)$$

where b^* is the fourth-order coefficient, as renormalised by strain coupling, and is negative in this case; c^* is the sixth-order coefficient as renormalised by higher-order strain-coupling terms. The jump in Q at the transition temperature, T_{tr}, from $Q = 0$ to $Q = Q_o$ is given by:

$$Q_o^2 = -\frac{4a}{b^*}(T_{tr}-T_c) \quad (159).$$

The difference $(T_{tr}-T_c)$ may be expressed as:

$$(T_{tr}-T_c) = \frac{3(b^*)^2}{16ac^*} \quad (160)$$

which provides a measure of how close the transition is to being tricritical ($b^* = 0$).

At this level, the most important parameters are T_{tr} and T_c. Carpenter *et al.* (1998b) adopted T_{tr} = 847 K and T_c = 840 K for internal consistency, on the basis of T_{tr} falling between hysteresis limits of $\alpha \rightarrow \beta$ on heating, $\beta \rightarrow$ IC on cooling, T_c = 841 from spectroscopic investigation of the soft mode in β-quartz (Tezuka *et al.*, 1991), a best fit value of $(T_{tr}-T_c) = 7.2$ K from second-harmonic generation of light data (Bachheimer & Dolino, 1975), and an analysis of heat capacity through the transition.

A new set of lattice-parameter measurements suggests that there is higher-order strain/order-parameter coupling in α-quartz, which means that terms in λeQ^4 must be added to equation 129 if the elastic behaviour is to be described correctly. A higher-order coupling term can also be included to describe the non-linear behaviour of C_{14}. The full Landau expansion is then (from Carpenter *et al.*, 1998b):

$$\begin{aligned} G = {} & \frac{1}{2}a(T-T_c)Q^2 + \frac{1}{4}bQ^4 + \frac{1}{6}cQ^6 + \frac{1}{8}dQ^8 + \lambda_1(e_1+e_2)Q^2 + \lambda_3e_3Q^2 \\ & + \lambda_4\left(e_4^2+e_5^2\right)Q^2 + \lambda_5(e_1e_4 - e_2e_4 + e_5e_6)Q + \lambda_6\left[e_6^2 + (e_1-e_2)^2\right]Q^2 \\ & + \lambda_7(e_1+e_2)Q^4 + \lambda_8e_3Q^4 + \lambda_9(e_1e_4 - e_2e_4 + e_5e_6)Q^3 \\ & + \frac{1}{4}\left(C_{11}^o + C_{12}^o\right)(e_1+e_2)^2 + \frac{1}{4}\left(C_{11}^o - C_{12}^o\right)(e_1-e_2)^2 + C_{13}^o(e_1+e_2)e_3 \\ & + \frac{1}{2}C_{33}^o e_3^2 + \frac{1}{2}C_{44}^o\left(e_4^2+e_5^2\right) + \frac{1}{2}C_{66}^o e_6^2 \end{aligned} \quad (161).$$

7.4 Co-elastic behaviour

Quartz. The zone-centre $\beta \rightleftharpoons \alpha$ ($622 \rightleftharpoons 32$) transition in quartz has been investigated intensively over many years. Its most characteristic features are reviewed by Dolino (1988, 1990), Heaney (1994) and Dolino & Vallade (1994). Early studies of lattice dynamics and elastic properties are summarised by Scott (1974) and Höchli (1972), respectively. Data from the literature for the variations of the elastic constants are shown in Fig. 25. The incommensurate phase (IC) is stable only over a temperature interval of < 2 K above the transition point (Dolino *et al.*, 1992; Vallade *et al.*, 1992; and references therein) and probably does not have a direct bearing on the elastic-constant variations over the much wider interval considered here. As pointed out by Salje *et al.* (1992), the transition is co-elastic, with a large non-symmetry-breaking spontaneous strain. Critical fluctuations are unlikely to occur over any easily measurable interval on either side of the equilibrium transition point and, contrary to views expressed in the 1970's (*e.g.* discussion in Scott, 1974), classical critical exponents are expected to provide a good description of the thermodynamic evolution. A full analysis of the elastic behaviour has recently been completed (Carpenter *et al.*, 1998b) and the main results are summarised here.

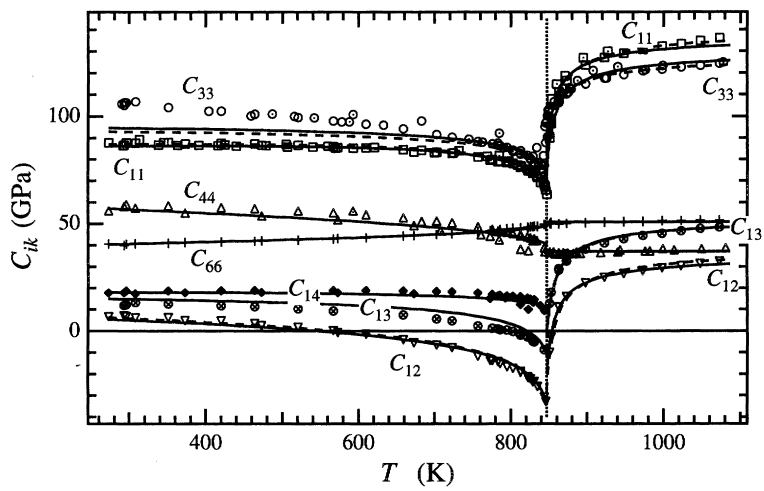

Fig. 25. Comparison between observed and calculated elastic-constant variations of quartz (from Carpenter *et al.*, 1998b). Data from: Atanasoff & Hart (1941), Atanasoff & Kammer (1948); Kammer *et al.* (1941), Zubov & Firsova (1962), Shapiro & Cummins (1968), Höchli (1970), Pelous & Vacher (1976), Unoki *et al.* (1984), Ohno (1995). For C_{11}, C_{33} and C_{44} a distinction has been made between data from ultrasonic experiments (open symbols) and data from Brillouin scattering (open symbols containing a dot). Two sets of calculated variations are shown for C_{11}, C_{12}, C_{13} and C_{33}, depending on how the bare elastic constants, C°_{ik}, were determined. For one set $\Delta C_{11} = \Delta C_{12}$ and $(\Delta C_{13})^2 = \Delta C_{11}\Delta C_{33}$ were assumed (solid lines); for the second set $\Delta C_{11} = \Delta C_{12} = \Delta C_{13} = \Delta C_{33}$ was assumed (broken lines). In the case of C_{13} the two curves are almost superimposed. Fits to the data for C_{14}, C_{44} and C_{66} in α-quartz, using equations listed in Table 15, are shown as solid lines; C°_{44} and C°_{66} were assumed to be constant.

Among others, Grimm & Dorner (1975), Bachheimer & Dolino (1975), Banda *et al.* (1975) and Dolino & Bachheimer (1982) have shown that the $\beta \rightleftharpoons \alpha$ transition is first order in character and that the evolution of the order parameter in α-quartz follows, to a good approximation:

attributed the discrepancy to heterogeneous stresses in the polycrystalline sample. Wide variations in published values of the equilibrium transition pressure and temperature reflect a high degree of sensitivity of the transition to non-hydrostatic stresses (Decker & Zhao, 1989).

(Mg,Fe)SiO_3 perovskite. Without the appropriate experimental data, what predictions can be made in relation to the possible elastic behaviour at a phase transition in natural (Mg,Fe)SiO_3? Firstly, the proximity of a tricritical point to the cubic $\rightleftharpoons$ tetragonal transition in perovskite may be typical, allowing a first approximation of the likely evolution of the order parameter. The $Pm3m \rightleftharpoons Pbnm$ (cubic $\rightleftharpoons$ orthorhombic) transition in the natural perovskite neighborite ($NaMgF_3$) is also close to being tricritical, for example, based on the strain data given by Zhao *et al.* (1993a and b) (and see Carpenter *et al.*, 1998a). Secondly, both the fluoride and oxides perovskites can show anomalous softening due to fluctuations in the cubic phase as the transition point is approached. In a polycrystalline sample, the bulk modulus would be expected to show a more or less sharp discontinuity at the transition point, depending on the strength of coupling between the driving order parameter and the volume strain. The shear modulus of such a sample would also show a discontinuity if coupling described by the terms with λ_2 and λ_3 as the coupling constants in equations 119 and 154 was significant. Natural (Mg,Fe)SiO_3 perovskite appears to be orthorhombic (*Pbnm*) under most of the relevant range of mantle conditions (Mao *et al.*, 1991; Hemley & Cohen, 1992; Stixrude & Cohen, 1993; Funamori & Yagi, 1993; and references therein) but a tetragonal $\rightleftharpoons$ orthorhombic transition has been suggested (Wolf & Bukowinski, 1987; Bukowinski & Wolf, 1988; Wang *et al.*, 1990, 1991; Kapusta & Guillopé, 1993; Warren & Ackland, 1996). The equivalent transition, as a function of temperature alone, in $CaTiO_3$ certainly appears to give rise to a stability field for the tetragonal phase between those of the cubic and orthorhombic phases (Redfern, 1996, and references therein). A $Pm3m \rightleftharpoons I4/mcm$ transition in $CaSiO_3$ could occur at P, T conditions appropriate for the lower mantle (Stixrude *et al.*, 1996). Suitable Landau free-energy expansions could be derived quite simply for any proposed symmetry change, allowing at least the form of likely variations in elastic properties associated with the transition to be predicted.

Other systems. Other systems that show improper ferroelastic behaviour and provide useful illustrative examples of the ways in which the influence of a phase transition on elastic properties can be understood include $Pb_3(PO_4)_2$ and $Gd_2(MoO_4)_3$. The former is reviewed in Bulou *et al.* (1992) and Salje (1993), and the latter in Fleury & Lyons (1981), Lüthi & Rehwald (1981), Cummins (1983) and Bulou *et al.* (1992). One example of improper ferroelastic behaviour among minerals is the cubic $\rightleftharpoons$ tetragonal transition in cristobalite, though this is strongly first order in character (Hatch & Ghose, 1991; Hatch *et al.*, 1994; Schmahl *et al*, 1992; Finnie *et al.*, 1994; Dove *et al.*, 1997; and references therein). An example of improper ferroelastic behaviour with pressure as the external driving force is the $R\bar{3}c \rightleftharpoons P2_1/c$ transition in calcite, $CaCO_3$, (Merrill & Bassett, 1975; Hatch & Merrill, 1981; Vo Thanh & Lacam, 1984; Vo Thanh & Diep-The-Hung, 1985; Biellmann *et al.*, 1993). The elastic constants appear to vary through the transition in a manner that conforms closely to the predictions from a standard Landau free-energy expansion (Vo Thanh & Diep-The-Hung, 1985).

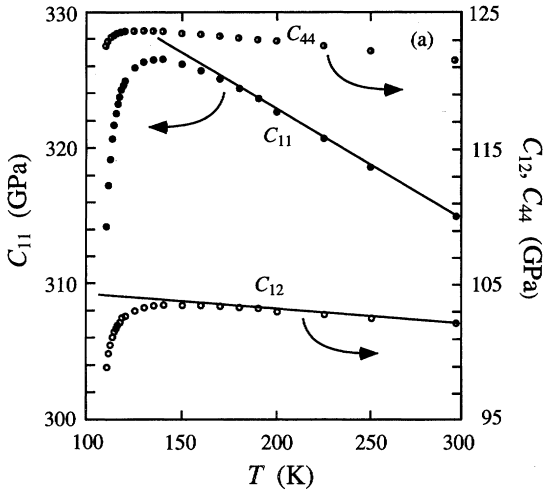

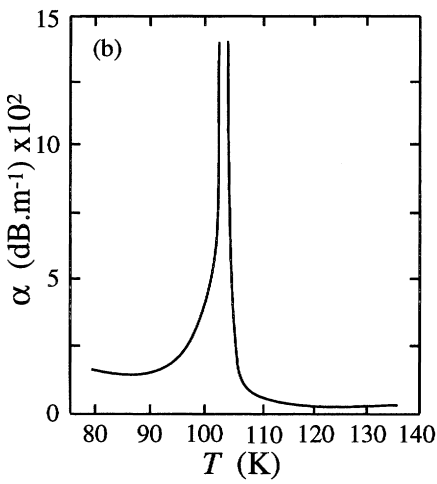

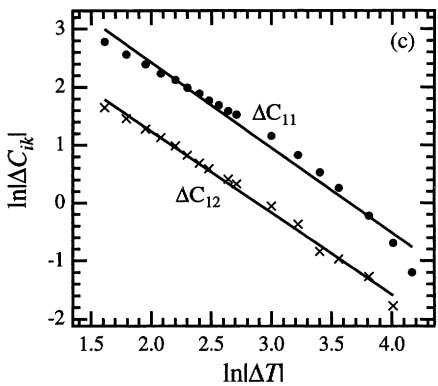

Fig. 24. Elastic properties of $SrTiO_3$ at the cubic $\rightleftarrows$ tetragonal transition in $SrTiO_3$ (second order, T_c = 105 K). (a) Data from Migliori *et al.* (1993) showing the pronounced softening of C_{11} and C_{12} in the cubic phase. C_{44} softens only within ~15 K of the transition point. Straight lines show the extrapolations used to estimate C_{11}^o and C_{12}^o. (b) Attenuation of a longitudinal ultrasonic wave propagating in the [100] direction (after Deorani *et al.*, 1990). Note that strong attenuation occurs only in a narrow temperature interval around T_c. (c) The data of Migliori *et al.* replotted to show a linear variation of $\ln|\Delta C_{12}|$ and a less obviously linear variation of $\ln|\Delta C_{11}|$ with $\ln|T-105|$. The linear least squares fits shown yield K = −1.41, A = 57.3 GPa for C_{12} and K = −1.47, A = 211.1 GPa for C_{11}. Within ~15 K of T_c, the effects of defects and, perhaps, critical fluctuations contribute to the softening.

al, 1986; Ramirez *et al.*, 1990). The most recent location of the tricritical point is ~35 kbar, ~233 K (Decker & Zhao, 1989). The A_{1g} and T_{2g} elastic constants, $(C_{11}+2C_{12})$ and C_{44}, show little softening in single crystals of the cubic phase in anticipation of the equilibrium transition pressure at room temperature (Ishidate & Sasaki, 1989). On the other hand, the E_g elastic constant, $(C_{11}-C_{12})$, does soften (Fischer & Polian, 1987; Ishidate & Sasaki, 1989), implying $\Delta C_{11} \neq \Delta C_{12}$ in the thermal fluctuation regime. The transition pressure is marked by discontinuities in some of the C_{ik} variations, but a full set of elastic constants for the tetragonal phase is not yet available. A polycrystalline sample, in the form of a hot-pressed pellet, gives a discontinuity in the bulk modulus ($\frac{1}{3}(C_{11}+2C_{12})$ for the cubic phase), with no softening ahead of the transition pressure (Fischer *et al.*, 1993). The shear modulus ($\frac{1}{5}[(C_{11}-C_{12})+3C_{44}]$ in the Voigt approximation for an aggregate of cubic crystals, Hill, 1952) shows a break in slope. These anomalies are not entirely consistent with the single-crystal data, however, and Fischer *et al.*

Rousseau *et al.*, 1975; Berger *et al.*, 1978). The same transition in $RbCaF_3$ occurs close to a tricritical point (Buzaré *et al.*, 1979), for example.

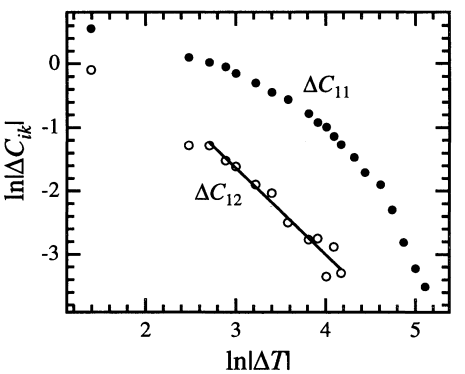

Fig. 23. Variation of ΔC_{ik} with ΔT (= T – 185 K) for $KMnF_3$, as extracted from data of Cao & Barsch (1988). The logarithm of ΔC_{11} is clearly a non-linear function of $\ln\Delta T$. Over a range of $\ln\Delta T$, $\ln\Delta C_{12}$ is approximately linear, with a slope of $K = -1.37$ for the line shown here; the intercept yields A_{12} = 12.0 GPa. At small ΔT and small ΔC_{ik}, the log values are subject to large uncertainties because T_c and C_{ik}^o are not known precisely. T_c = 185 K has been chosen somewhat arbitrarily; $T_{tr} - T_c$ is at least known to be small. The expected value of K is ~–3/2 for a system with softening along one branch of the soft mode.

$SrTiO_3$ perovskite. The same transition in $SrTiO_3$ is second order in character, though with a small deviation from $\beta = 1/2$ over a few degrees below T_c (Müller & Berlinger, 1971; Franke & Hegenbarth, 1974; Sato *et al.*, 1985; Cowley, 1996). The region of C_{11} and C_{12} softening is within ~70 K of T_c (Fig. 24a, after Migliori *et al.*, 1993), and again extends well beyond the interval of strong acoustic attenuation (Fig. 24b, after Deorani *et al.*, 1990), (see also: Bell & Ruprecht, 1963; Rehwald, 1970a and b; Lüthi & Moran, 1970; Fossheim & Berre, 1972; Okai & Yoshimoto, 1975; Rehwald, 1977; Fossum & Fossheim, 1985). Both ΔC_{12} and ΔC_{11}, extracted from the data of Migliori *et al.* (1993), vary in a manner consistent with K = ~–3/2, though $\ln\Delta C_{11}$ is less obviously a linear function of $\ln\Delta T$ than $\ln\Delta C_{12}$ (Fig. 24c). C_{44} softening coincides more nearly (though not exactly) with the range of observed attenuation (Fig. 24). Measurements of the elastic properties of the tetragonal phase are complicated by the presence of transformation twins, but, under a non-hydrostatic stress applied to suppress these twins, C_{11} tends towards the variation expected for a second-order improper ferroelastic transition – a simple step at $T = T_c$ (Fossheim & Berre, 1972; Rehwald, 1977). Details of the transition behaviour again appear to be highly sensitive to the influence of defects (Andrews, 1986; Nelmes *et al.*, 1988; McMorrow *et al.*, 1990; Cowley, 1996).

$BaTiO_3$ perovskite. One example of a zone-centre improper ferroelastic transition is the cubic ⇌ tetragonal transition in $BaTiO_3$, which occurs by the displacement of the Ti atoms rather than rotations of the TiO_6 octahedra. The symmetry change is $Pm3m \rightleftharpoons P4mm$, and the active representation is T_{1u}. There are no strains associated with this representation and the lowest-order coupling allowed between the symmetry-breaking strain and the driving order parameter is linear in strain and quadratic in Q. The Landau free-energy expansion has the same form as for the cubic ⇌ tetragonal transition in $KMnF_3$ and $SrTiO_3$ because the point symmetry at the R point of the Brillouin zone is identical to the point symmetry at the zone centre (Rehwald, 1973). The transition is first order as a function of temperature at one atmosphere pressure (Clarke, 1976; Irie *et al.*, 1987; Kovaleva *et al.*, 1988; Tomonaga *et al.*, 1990; Darlington *et al.*, 1994), and also first order, but close to tricritical, as a function of pressure at room temperature (Samara, 1971; Malinowski *et*

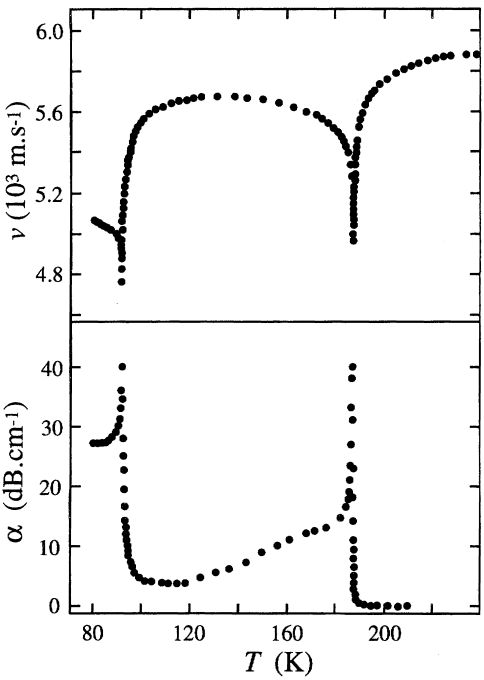

Fig. 22. Attenuation, α, and velocity, v, for a longitudinal wave travelling parallel to [100] in $KMnF_3$ (after Fossheim *et al.*, 1974, and Fossheim & Fossum, 1984). Note that the large anomaly in the attenuation at the 186 K transition occurs over a very limited temperature interval relative to the anomaly in the velocity.

As discussed in section 4.4, the influence of dynamical effects on the elastic constants above T_c is not included in a simple Landau expansion, but can be described using a power law of the form given as equation 97 (for elastic constants associated with the identity representation). In $KMnF_3$ there is marked softening along the whole branch between the R $\left(\frac{1}{2},\frac{1}{2},\frac{1}{2}\right)$ and M $\left(\frac{1}{2},\frac{1}{2},0\right)$ points of the Brillouin zone (Minkiewicz *et al.*, 1970; Shirane *et al.*, 1970; Shapiro *et al.*, 1972; Gesi *et al.*, 1972; Hidaka *et al.*, 1986; Nicholls & Cowley, 1987). According to the arguments presented in the appendix, this might correspond to the situation illustrated as (b) in Fig. A.1, for which $K = -3/2$ is predicted. The results of Cao & Barsch (1988) have been used to estimate C_{11}^{o} and C_{12}^{o} as linear functions of T, extrapolated from the highest-temperature data points. ΔC_{12} varies in a manner consistent with $K = -1.4$ for a value of T_c assumed to be 185 K, but a single value of K does not describe the variation of ΔC_{11} (Fig. 23). A large deviation from the expected symmetry relation $\Delta C_{11} = \Delta C_{12}$ is due to the effects of thermal expansion contributing to C_{11} (Appendix A.1). Off-diagonal terms in the elastic-constant matrix are not expected to be modified in the same way and the observed ΔC_{12} variation represents good agreement between experiment and theory.

The overall picture that emerges for the cubic $\rightleftharpoons$ tetragonal transition in $KMnF_3$ is of improper ferroelastic properties and tricritical thermodynamic character. The transition is accompanied by elastic softening over a wide temperature interval as $T \rightarrow T_{tr}$ from above, in a manner not predicted by the Landau free-energy expansion. The influence of defects and any critical fluctuations appears to be restricted to a small temperature range near T_{tr}, and the rest of the softening in the cubic phase can be accounted for by thermal fluctuations. This pattern of elastic-constant variations and ultrasonic attenuation is repeated in other fluoride perovskites (*e.g.*

tetragonal phase are sparse and of uncertain quality due to the problem of accounting for the influence of domain boundaries (Holt & Fossheim, 1981), but they are broadly consistent with the predicted variations. C_{11} shows a marked curvature as T_{tr} is approached from below, comparable with the predicted form for an average of the C_{11}, C_{22} and C_{33} variations shown in Fig. 20. C_{44} shows a step at T_{tr} but little obvious curvature in the stability field of the tetragonal phase, again with the expected general form. C_{12} shows a curvature in the tetragonal field which is similar in form to the average of predicted variations for C_{12}, C_{13} and C_{23}. In the cubic stability field, all three elastic constants show a marked curvature as T_{tr} is approached over a temperature interval of ~50 – 100 K for C_{11} and C_{12}, and over an interval of ~10 – 20 K for C_{44}. This anomaly is not predicted by the normal static Landau expansions and has been attributed to the influence of fluctuations of the order parameter (Pytte, 1971; Rehwald, 1971; Cao & Barsch, 1988). Strong attenuation of ultrasonic waves has been observed within ~5 – 10 K of T_{tr} (Fig. 22, from Fossheim *et al.*, 1974; Reshchikova *et al.*, 1970; Fossheim & Holt, 1980; Holt & Fossheim, 1981; Fossheim & Fossum, 1984), suggesting an outer limit on the temperature interval of any critical fluctuations. Details of the structural evolution in this narrow temperature range also appear to be sensitive to the influence of defects (*e.g.* Stokka & Fossheim, 1982; Nicholls & Cowley, 1987; Cox *et al.*, 1988; Cox & Cussen, 1989; Scott, 1989a and b; Gibaud *et al.*, 1989, 1991). Such defects and any critical fluctuations could account for the weakly first-order character of the transition, a small difference between T_{tr} and T_c, and the steep variation in C_{44} close to T_{tr}, but do not account for the much broader elastic anomalies in C_{11} and C_{12}.

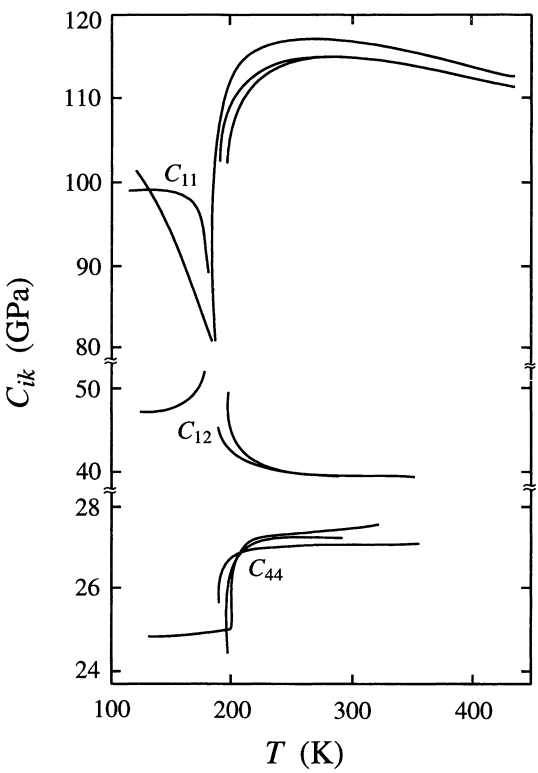

Fig. 21. Summary of elastic-constant data for $KMnF_3$ in the vicinity of the cubic $\rightleftharpoons$ tetragonal transition (from Aleksandrov *et al.*, 1966; Reshchikova *et al.*, 1970; Melcher & Plovnik, 1971; Cao & Barsch, 1988).

Table 14. Predicted variations for elastic constants of a material subject to a phase transition involving the symmetry change $Pm3m \rightleftharpoons I4/mcm$ when the transition is tricritical in character.

Improper ferroelastic transition	
Pm3m phase	*I4/mcm* phase, $e_a = 0$
$q_1 = q_2 = q_3 = 0$	$q_1 = q_2 = 0, \quad q_3^4 = \left[\frac{a(T_c - T)}{(c + c'')}\right]$ $A = 3\left[(b + b') + 2(c + c'')q_3^2\right]$
$C_{11} = C_{22} = C_{33} = C_{11}^o$	$C_{11} = C_{22} = C_{11}^o - \left(\frac{4\lambda_2^2}{A}\right)$ $C_{33} = C_{11}^o - \left(\frac{16\lambda_2^2}{A}\right)$
$C_{12} = C_{13} = C_{23} = C_{12}^o$	$C_{12} = C_{12}^o - \left(\frac{4\lambda_2^2}{A}\right)$ $C_{13} = C_{23} = C_{12}^o + \left(\frac{8\lambda_2^2}{A}\right)$
$C_{11} - C_{12} = C_{11}^o - C_{12}^o$	$C_{11} - C_{12} = C_{11}^o - C_{12}^o$ $\overline{C}_{11} - \overline{C}_{12} = \frac{1}{3}(C_{11} + C_{12} + 2C_{33} - 4C_{13})$ $= (C_{11}^o - C_{12}^o) - \left(\frac{24\lambda_2^2}{A}\right)$
$C_{11} + 2C_{12} = C_{11}^o + 2C_{12}^o$	$\overline{C}_{11} + 2\overline{C}_{12} = \frac{1}{3}(C_{33} + 2C_{11} + 2C_{12} + 4C_{13})$ $= C_{11}^o + 2C_{12}^o$
$C_{44} = C_{55} = C_{66} = C_{44}^o$	$C_{44} = C_{55} = C_{44}^o - \left[\frac{6\lambda_3^2}{3(3b + b') - 4c''q_3^2}\right]$ $C_{66} = C_{44}^o$

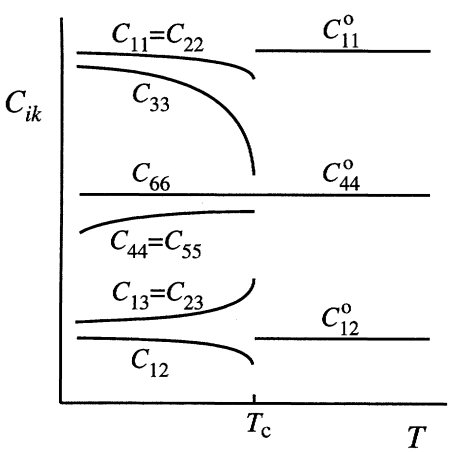

Fig. 20. Schematic variation of the elastic constants at a tricritical transition involving the symmetry change $Pm3m \rightleftharpoons I4/mcm$, based on the expressions given in Table 14. (The normal weak temperature dependence of the bare elastic constants has been ignored).

Experimental data for the elastic constants of $KMnF_3$ are shown in Fig. 21 (Aleksandrov *et al.*, 1966; Reshchikova *et al.*, 1970; Melcher & Plovnik, 1971; Cao & Barsch, 1988). Data for the

carried out with externally applied non-hydrostatic pressure confirm the proximity to a tricritical point (Stokka *et al.*, 1981; Stokka & Fossheim, 1982). The same transition can be induced by the application of hydrostatic pressure at room temperature, when it displays second-order character (Åsbrink *et al.*, 1993).

The order parameter for the transition is three-dimensional and the relevant Landau free-energy expansion has the form given in equation 119. In order to describe a transition which is close to being tricritical it is necessary to extend the expansion to sixth-order terms (as given in Appendix Table 1b of Salje, 1993). The full equation then becomes (after Slonczewski & Thomas, 1970; Rehwald, 1973; Ridou *et al.*, 1980; Lüthi & Rehwald, 1981; Fleury & Lyons, 1981; Cao & Barsch, 1990; Bulou *et al.*, 1992):

$$G = \frac{1}{2}a(T-T_c)\left(q_1^2+q_2^2+q_3^2\right)+\frac{1}{4}b\left(q_1^2+q_2^2+q_3^2\right)^2+\frac{1}{4}b'\left(q_1^4+q_2^4+q_3^4\right)$$
$$+\frac{1}{6}c\left(q_1^2+q_2^2+q_3^2\right)^3+\frac{1}{6}c'\left(q_1q_2q_3\right)^2+\frac{1}{6}c''\left(q_1^2+q_2^2+q_3^2\right)\left(q_1^4+q_2^4+q_3^4\right)$$
$$+\lambda_1 e_a\left(q_1^2+q_2^2+q_3^2\right)+\lambda_2\left[\sqrt{3}e_o\left(q_1^2-q_2^2\right)+e_t\left(2q_3^2-q_1^2-q_2^2\right)\right]$$
$$+\lambda_3\left(e_6q_1q_2+e_5q_1q_3+e_4q_2q_3\right)+\frac{1}{2}\left(C_{11}^o+2C_{12}^o\right)e_a^2+\frac{1}{2}\left(C_{11}^o-C_{12}^o\right)\left(e_o^2+e_t^2\right)$$
$$+\frac{1}{2}C_{44}^o\left(e_4^2+e_5^2+e_6^2\right) \qquad (154).$$

Variations of the elastic constants can be predicted from this free-energy expansion in the usual way. The simplification that the volume strain is treated as being negligible ($\lambda_1 = 0$) has been incorporated because the algebra becomes overly cumbersome otherwise.

Under equilibrium conditions, $q_1 = q_2 = e_o = 0$ and $e_t \neq 0$, $q_3 \neq 0$ at $T < T_c$. It can easily be shown that the coupling between e_t and q_i^2 terms leads to a renormalisation of the fourth-order coefficient such that:

$$b^* = b + b' - \frac{8\lambda_2^2}{\left(C_{11}^o - C_{12}^o\right)} \qquad (155)$$

which is zero for tricritical behaviour. The susceptibility with respect to q_3 is given by:

$$\left(\frac{\partial^2 G}{\partial {q_3}^2}\right)^{-1} = \left[2(b+b')+4(c+c'')q_3^4\right]^{-1} \qquad (156)$$

and expressions for the individual elastic constants are listed in Table 14. A schematic representation of the temperature dependence of these parameters is shown in Fig. 20. Note that the lowest-order coupling term which can influence the evolution of C_{66} is not given in Equation 154 but would be $\lambda_4 e_6^2 q_3^2$. This gives $C_{66} = C_{44}^o + 2\lambda_4 q_3^2$ as a possible dependence on q.

The data of Gibaud *et al.* (1991) have been used here to calculate symmetry-breaking $\left[e_t = \frac{1}{\sqrt{6}}(2e_3 - e_1 - e_2)\right]$ and non-symmetry-breaking $\left[e_a = \frac{1}{\sqrt{3}}(e_1 + e_2 + e_3)\right]$ strains, using reference values of a_o extrapolated from the cubic phase at high temperatures. As already mentioned, e_a for the transition is small, but the variation of e_a^2 with T shows little scatter and is remarkably close to being linear (Fig. 19a). e_a^2 extrapolates to zero at 187.7 K, which is barely distinguishable from the transition temperature of 186.5 K given by Gibaud *et al.* This suggests transition behaviour which is very close to tricritical (β = 0.25, $e_a^2 \propto Q^4 \propto T$). A non-linearity between the symmetry-breaking and non-symmetry-breaking strains (Fig. 19b) could be accounted for by a higher-order coupling term, $e_t Q^4$, becoming influential at large values of e_t. This would in turn account for the deviation from a linear variation of e_t^2 with temperature (Fig. 19c). In any case, the transition at one atmosphere is evidently close to being tricritical in character (Sakashita *et al.*, 1981, 1990; Nicholls & Cowley, 1987).

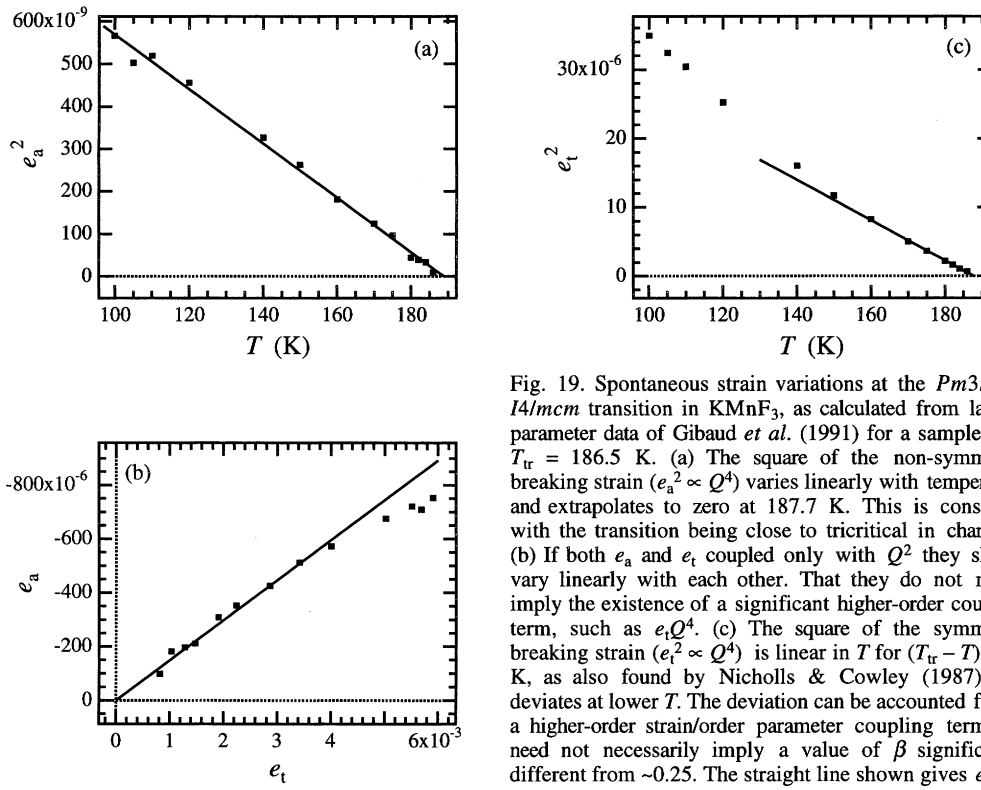

Fig. 19. Spontaneous strain variations at the $Pm3m \rightleftharpoons I4/mcm$ transition in $KMnF_3$, as calculated from lattice-parameter data of Gibaud *et al.* (1991) for a sample with T_{tr} = 186.5 K. (a) The square of the non-symmetry-breaking strain ($e_a^2 \propto Q^4$) varies linearly with temperature and extrapolates to zero at 187.7 K. This is consistent with the transition being close to tricritical in character. (b) If both e_a and e_t coupled only with Q^2 they should vary linearly with each other. That they do not might imply the existence of a significant higher-order coupling term, such as $e_t Q^4$. (c) The square of the symmetry-breaking strain ($e_t^2 \propto Q^4$) is linear in T for $(T_{tr} - T) \leq 40$ K, as also found by Nicholls & Cowley (1987), but deviates at lower T. The deviation can be accounted for by a higher-order strain/order parameter coupling term and need not necessarily imply a value of β significantly different from ~0.25. The straight line shown gives $e_t^2 \rightarrow 0$ at 188.9 K.

Data of Aleksandrov & Flerov (1978), Stokka *et al.* (1981) and Stokka & Fossheim (1982) for the excess specific heat of $KMnF_3$ over an interval of $(T_{tr} - T)$ up to ~7 K are consistent with $\Delta Cp \propto (T_c - T)^{-\alpha}$, with α = 1/2, as expected for a tricritical transition. Only in the range $(T_{tr} - T)$ < ~0.3 K do the data appear to deviate from this relationship. Measurements

7.3 Improper ferroelastic behaviour

In a geological context, perhaps the material for which elastic properties have provoked the most interest is perovskite. The lower mantle is believed to consist predominantly of perovskite with composition ~$(Mg,Fe)SiO_3$, and there has been a debate as to whether it undergoes a phase transition from an orthorhombic form to some higher-symmetry form with increasing depth (Navrotsky & Weidner, 1989; Mao *et al*, 1991; Wang *et al.*, 1990, 1991, 1992; Hemley & Cohen, 1992; Stixrude & Cohen, 1993; Funamori & Yagi, 1993; Kapusta & Guillopé, 1993; Warren & Ackland, 1996; and references therein). If such a transition occurs, it could give rise to an anomaly in the bulk elastic constants of the lower mantle (Bukowinski & Wolf, 1988; Yeganeh-Haeri *et al.*, 1989a and b), perhaps over a rather narrow depth interval. This issue is discussed also by Stixrude *et al.* (1996) for $CaSiO_3$. Data for the natural material are sparse but the likely form of elastic-constant variations can be anticipated with some confidence from studies of synthetic analogues.

$KMnF_3$ perovskite. Structural phase transitions in perovskites are frequently improper ferroelastic in character. The order parameter is associated with a special point on the Brillouin zone boundary and couples with symmetry-breaking strains as eQ^2. A useful illustrative example for which extensive experimental data are available is the *Pm3m* $\rightleftharpoons$ *I4/mcm* (cubic $\rightleftharpoons$ tetragonal) transition in $KMnF_3$. The transition mechanism involves a soft mode at the R point $\left(\frac{1}{2},\frac{1}{2},\frac{1}{2}\right)$ of the Brillouin zone (Minkiewicz *et al.*, 1970; Shirane *et al.*, 1970; Shapiro *et al.*, 1972; Gesi *et al.*, 1972). A small discontinuity has been observed in properties such as birefringence, spontaneous strain and superlattice reflection intensities at the equilibrium transition temperature (T_{tr}) of ~186 K (one atmosphere pressure), and the transition has therefore been referred to as being weakly first order (*e.g.* see Furukawa *et al.*, 1970; Shirane *et al.*, 1970; Gesi *et al.*, 1972; Hirotsu & Sawada, 1973; Benard & Walker, 1976; Kleeman *et al.*, 1979).

Values of the critical exponents for the transition are controversial, largely because of problems associated with making measurements on finely twinned crystals in the tetragonal stability field. The proportions of different twin components vary with temperature (Tietze *et al.*, 1983), and, as a consequence, measurements of superlattice reflection intensities are an unreliable quantitative measure of the order-parameter behaviour (Nicholls & Cowley, 1987; Cox, 1989). Birefringence measurements have also produced inconsistent results (Aleksandrov & Reshchikova, 1970; Hirotsu & Sawada, 1973; Benard & Walker, 1976; Kleeman *et al.*, 1979). The spontaneous strain and excess heat capacity should be influenced by the twinning to a much lesser extent and indeed reveal a more self-consistent pattern. The volume strain is sufficiently small that the symmetry-breaking strain can be expressed as $\left[(c-a)/a\right]$, rather than as its correct form $\left[(c-a_o)/a_o\right]$, without introducing significant error. Values of $\beta = 0.26 \pm 0.02$ (Nicholls & Cowley, 1987; Cox, 1989) and $\beta = 0.316 \pm 0.005$ (Gibaud *et al.*, 1991) have been obtained from data collected over temperature intervals, $(T_{tr} - T)$, of ~40 and 90 K respectively, using the relationship $\left[(c-a)/a\right] \propto (T_c - T)^{2\beta}$. The temperature at which $\left[(c-a)/a\right]$ extrapolates to zero is greater than T_{tr}, the actual transition temperature, by only a few degrees at most. (For observations in the vicinity of T_{tr}, see also Ratuszna *et al.*, 1979; Sakashita *et al.*, 1981, 1990; Sakashita & Ohama, 1982).

Minerals. Comparable studies of ferroelastic transitions in minerals have not yet been undertaken, but there are some possible candidates for pseudo-proper behaviour. The cubic $\rightleftharpoons$ tetragonal transition in leucite discussed in the previous section might belong to this category. Similarly, the hexagonal $\rightleftharpoons$ orthorhombic ($P6_222 \rightleftharpoons C222_1$) transition in tridymite, SiO_2, is in principle a proper ferroelastic transition, but several other structural changes occur over a temperature interval of ~200 – 300 K (references to recent work include Wennemer & Thompson, 1984a and b; Kihara *et al.*, 1986a and b; Smelik & Reeber, 1990; Graetsch & Flörke, 1991; de Dombal & Carpenter, 1993; Xiao *et al.*, 1993, 1994, 1995; Cellai *et al.*, 1994; Xiao & Kirkpatrick, 1995; Kitchin *et al.*, 1996). Coupling between several lattice modes almost certainly occurs. Variations in the elastic constants would probably be diagnostic of the underlying driving mechanisms in these phases. The tetragonal $\rightleftharpoons$ monoclinic ($P4/nnc \rightleftharpoons P2/n$?) transition in vesuvianite described by Groat *et al.* (1995) has tentatively been placed in this category on the basis of its change in space group and its very small spontaneous strain, but rather little is known about the underlying mechanism.

In addition to the standard determination of the temperature dependence of the symmetry-breaking strain and the corresponding symmetry-adapted elastic constant, key features to be examined in detail are the exact relationships between the strain and the proposed order parameter, and the behaviour of all the other elastic constants. For real materials with an order parameter different from the strain but bilinearly coupled to it, we should expect conformity to a Landau free-energy expansion of the form:

$$G = \frac{1}{2}C'e^2 + \frac{1}{4}C''e^4 + \ \ldots\ + \lambda_1 Qe + \lambda_2 Q^3 e + \ \ldots\ + \frac{1}{2}AQ^2 + \frac{1}{4}BQ^4 + \ \ldots \qquad (153)$$

where C' and C'' are second- and fourth-order elastic constants; e is the symmetry-breaking strain and the non-symmetry-breaking strain has been ignored. For LaP_5O_{14} and $BiVO_4$, it is believed that the soft optic mode drives the transition, implying that the A coefficient is temperature dependent. The elastic-constant softening then occurs purely as a consequence of the coupling between Q and e such that C' is the bare elastic constant and is not by itself strongly temperature dependent. The fourth-order term in e and the high-order coupling terms can be neglected. If, on the other hand, the driving order parameter was e, it would be the temperature dependence of C' (and the higher-order terms in e) which would account for the transition. The A coefficient would not be expected to be temperature dependent and the Q^4 term could be neglected. In this case the optic-mode softening would be a consequence only of the bilinear coupling with e. The third possibility is that the coupling coefficient, λ_1, is the temperature-dependent property giving rise to the transition, though this at present appears to be only a theoretical possibility and has not been considered in the case of real materials. Between these three extremes are cases where both C' and A (and λ_1) might have an explicit temperature dependence, implying that both soft acoustic and soft optic modes contribute to the driving mechanism for the transition. In each case, the relationship between e and Q and the variations of elastic constants can be predicted using the manipulations discussed in detail in the body of this review. Comparison of the real behaviour of a pseudo-proper ferroelastic material with the predicted variations should then indicate whether details of an initial model are in fact physically correct. Such details might be of less importance relative to, say, predicting the grosser characteristics of the elastic-constant behaviour at some phase transition in a geological material for which little or no data were available, however.

$K_2Cd_2(SO_4)_3$. Another instructive transition is the first-order $P2_13 \rightleftharpoons P2_12_12_1$ transition in langbeinite, $K_2Cd_2(SO_4)_3$ (Abrahams *et al.*, 1978; Lissalde *et al.*, 1979; Devarajan & Salje, 1984, 1986; Percival *et al.*, 1989; Percival & Salje, 1989; Percival, 1990; Hatch *et al.*, 1990b; Kaminsky, 1996; Guelylah *et al.*, 1996). The evolution of the symmetry-breaking strains is at least consistent with linear coupling of e_o and e_t with a two-component order parameter (Carpenter *et al.*, 1998a), and the symmetry-adapted elastic constant $(C_{11} - C_{12})$ of the cubic phase shows the characteristic curvature of a pseudo-proper ferroelastic transition (Fig. 18, after Antonenko *et al.*, 1983). Antonenko *et al.* (1983) extracted a value of $\left(T_c^* - T_c\right)$ = 16 K from their data, using an equation of the form of equation 31 (replacing C_{55} by $(C_{11} - C_{12})$ and C_{55}^o by $\left(C_{11}^o - C_{12}^o\right)$), suggesting relatively weak strain/order-parameter coupling. A soft optic mode has not yet been found (Moiseenko *et al.*, 1983; Devarajan & Salje, 1986). Speer & Salje (1986) and Devarajan & Salje (1986) suggested that the transition is triggered by a local distortion of the CdO_6 octahedra. This is supported by optical spectroscopy data, though in detail the nature of the distortion may be slightly different from that originally envisaged (Percival & Salje, 1989; Hatch *et al.*, 1990b).

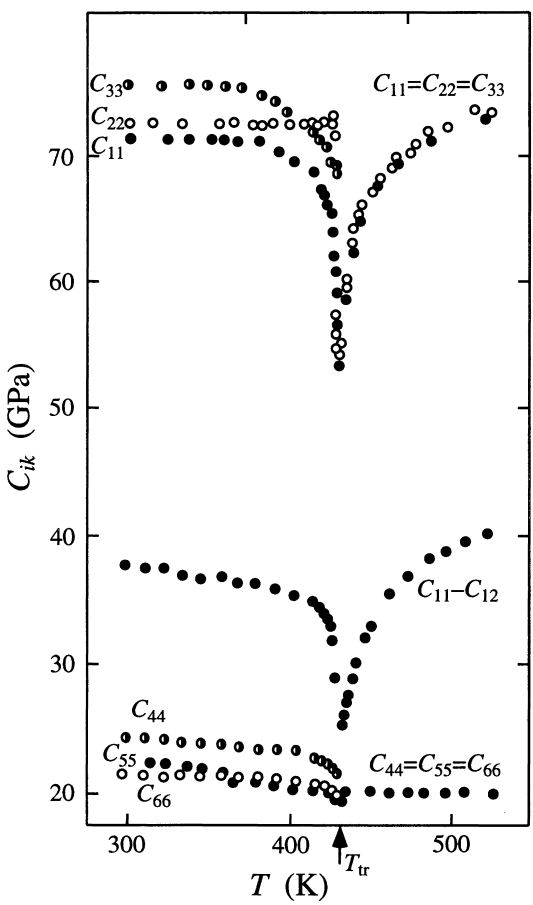

Fig. 18. Elastic anomalies at the first-order cubic $\rightleftharpoons$ orthorhombic transition in $K_2Cd_2(SO_4)_3$ langbeinite (after Antonenko *et al.*, 1983). The strong curvature of C_{11} and $(C_{11} - C_{12})$ above T_{tr} is characteristic of a transition in which the symmetry-breaking strain develops by bilinear coupling with some other driving order parameter.

A straightforward measure of the strength of coupling between soft optic and soft acoustic modes, the magnitude of the coefficient λ_5 in equation 127, is given by the difference between T_c and the renormalised transition temperature T_c^*. T_c is the temperature at which the transition would occur in the absence of coupling of Q to the strain, and is given by the linear extrapolation of ω^2 to zero in Fig. 15 (where ω is the frequency of the soft optic mode in the orthorhombic phase). T_c^* is the observed transition temperature and the difference, $\left(T_c^* - T_c\right)$, is proportional to λ_5^2 (equation 16). For LaP_5O_{14} the observed value of $\left(T_c^* - T_c\right)$ is 161 ± 11 K (Errandonea, 1980; Errandonea & Savary, 1981) and the value calculated by Errandonea is 170 K, implying strong bilinear coupling. Errandonea was also able to derive the observed pressure dependence of the transition temperature from the Landau expansion and the numerical values of the coefficients.

Other examples of pseudo-proper ferroelastic behaviour are reviewed by Rehwald (1973), Lüthi & Rehwald (1981), Cummins (1983), Tolédano *et al.* (1983) and Bulou *et al.* (1992). An interesting comparison can be made between $BiVO_4$ and $LaNbO_4$, for example. Both materials have the same structure and undergo a transition which involves the symmetry change $I4_1/a \rightleftharpoons I2/a$. However, there is a soft optic mode in $BiVO_4$ which is believed to drive the transition and to which the strain is linearly coupled. The value of $\left(T_c^* - T_c\right)$ is ~163 K (Pinczuk *et al.*, 1979) indicating that the coupling is quite strong (Pinczuk *et al.*, 1977, 1979; David, 1983a; Tokumoto & Unoki, 1983). In $LaNbO_4$ no equivalent soft mode is observed and the transition appears to have strain as the driving order parameter (Wada *et al.*, 1979; Hara *et al.*, 1989). The soft acoustic modes in each case clearly display this difference in mechanism. In $LaNbO_4$, the square of the frequency of the soft acoustic mode goes linearly to zero as $T \rightarrow T_c$, while in $BiVO_4$ the same acoustic mode shows a marked curvature (Fig. 17, after Ishibashi *et al.*, 1988; and see Benyuan *et al.*, 1981; Tokumoto & Unoki, 1983).

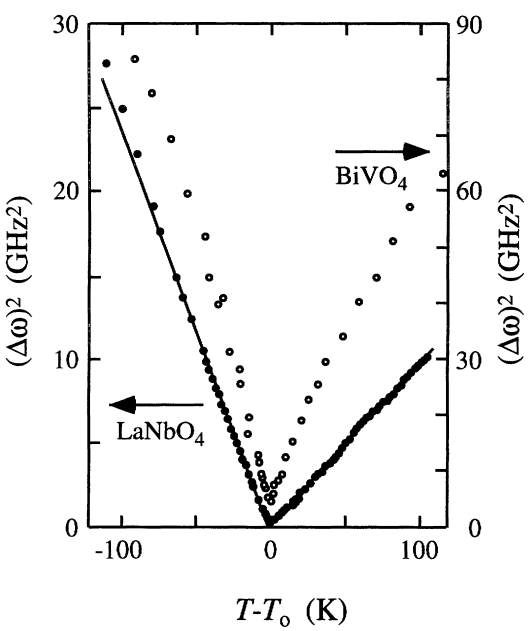

Fig. 17. Variation of the square of the Brillouin frequency shift of the soft acoustic mode $\left[\propto \left(C_{11} - C_{12}\right)\right]$ in $BiVO_4$ and $LaNbO_4$ (after Ishibashi *et al.*, 1988), with respect to the transition temperature T_o (= T_c for $LaNbO_4$; = T_c^* for $BiVO_4$). The linear variations for $LaNbO_4$ are characteristic of proper ferroelastic behaviour. The distinctly non-linear variations for $BiVO_4$ are characteristic of pseudo-proper ferroelastic behaviour.

constant (C_{55}) shows the distinctly non-linear approach to zero characteristic of a pseudo-proper transition. The ratio of slopes in the vicinity of the transition point is 2.9:1 instead of 2:1 due to the renormalisation of the fourth-order coefficient by non-symmetry-breaking strains. Errandonea (1980) determined values for all the Landau coefficients and then calculated values of C_{ik} from the free-energy expansion. These calculated values match the observed values closely, suggesting that the mechanism proposed for the transition is broadly correct. Not every detail is reproduced by the chosen Landau expansion, however. For example, C_{44} shows an anomaly which is not predicted. As suggested by Errandonea, this deviation could arise by coupling of e_4 with the B_{3g} optic mode which softens in a manner that could be unrelated to the $mmm \rightleftharpoons 2/m$ transition. Similarly, deviations from $e_5^2 \propto T$ observed at low temperatures can be explained by the contribution of higher-order terms in Q (Fousek *et al.*, 1979; Errandonea, 1980) or by the contribution of a higher-order strain/order parameter coupling term. The detailed variations of strains and elastic constants again expose subtelties of the transition mechanism specific to the material.

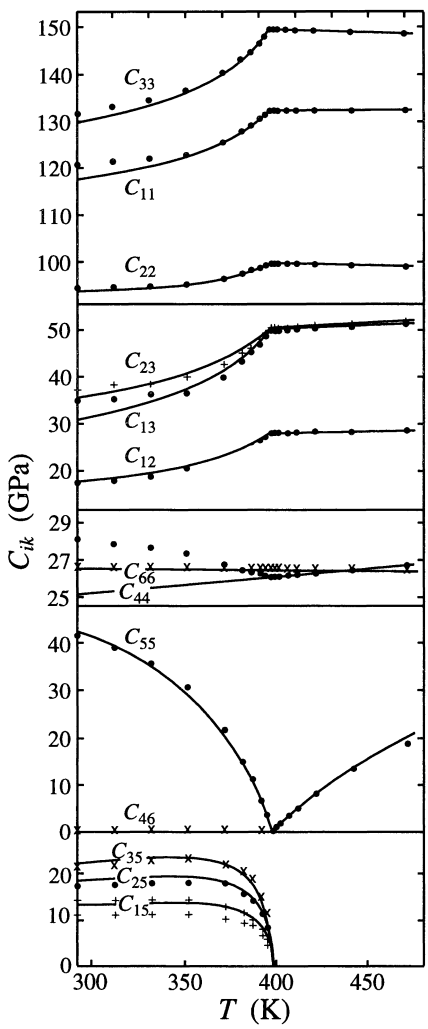

Fig.16. Variations with temperature of the complete set of elastic constants for LaP_5O_{14} at the $mmm \rightleftharpoons 2/m$ transition (after Errandonea, 1980). Solid curves are solutions of the form listed in Table 11, from equation 127, for a pseudo-proper ferroelastic transition with values determined for all the coefficients. Only C_{44} deviates substantially from its calculated trend. C_{46} remains zero in the monoclinic phase for structural rather than symmetry reasons ($\lambda_7 \approx 0$ in equation 127).

phase. The square of the symmetry-breaking strain (e_5^2) varies approximately linearly with temperature as $T \rightarrow T_c$, indicating a classical second-order transition (Errandonea & Bastie, 1978; Errandonea, 1980). Small deviations from linearity can be accounted for by the addition of a sixth-order term in the Landau expansion (Errandonea, 1980).

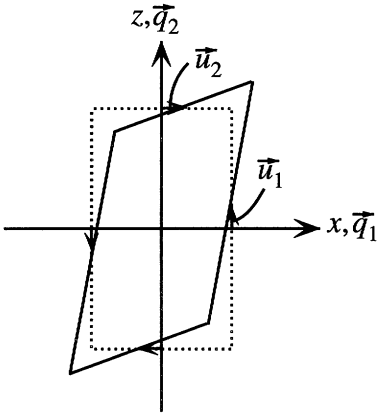

Fig. 14. Two orthogonal acoustic modes, $\vec{q}_1$, $\vec{u}_1$ and $\vec{q}_2$, $\vec{u}_2$, parallel to the crystallographic x- and z-axes generate a monoclinic distortion (solid lines) from an orthorhombic unit cell (dotted lines), as shown schematically here.

Raman spectroscopic studies have shown that two zone-centre optic modes also soften as the orthorhombic $\rightleftharpoons$ monoclinic transition is approached (Fig. 15, after Errandonea & Sapriel, 1979; Errandonea & Savary, 1981; Chen & Scott, 1989). The softer of the two has B_{2g} symmetry and is regarded as providing the driving mechanism for the transition (Errandonea, 1980). Significant non-symmetry-breaking strains have also been observed (Errandonea, 1980), and the appropriate form of Landau expansion to describe the transition is thus the same as equation 127. The expected form of elastic-constant variations is that illustrated in Fig. 10 for a pseudo-proper transition with $e_{nsb} \neq 0$.

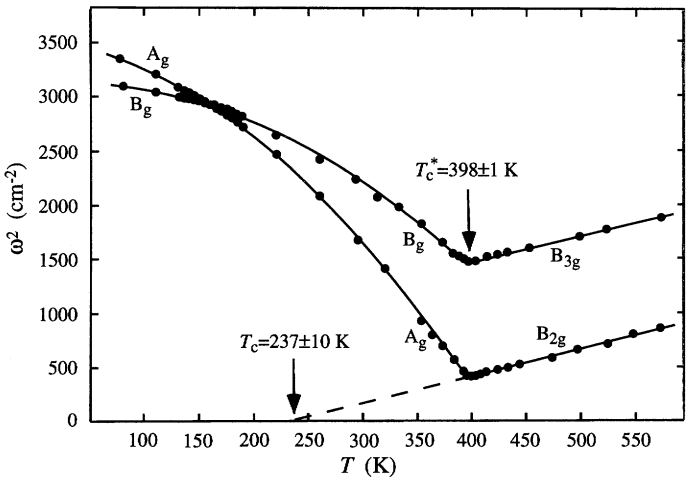

Fig. 15. Temperature dependence of ω^2 for the two soft modes in LaP_5O_{14} (after Errandonea & Sapriel, 1979). In the absence of coupling with strain there would be an $mmm \rightleftharpoons 2/m$ transition at the temperature determined by $\omega^2 \rightarrow 0$ for the B_{2g} mode. Coupling of the strain e_5 causes renormalisation of the transition temperature to T_c^*, where C_{55} tends to zero instead.

All the elastic constants and their variation with temperature through the transition have been measured by Brillouin spectroscopy (Fig. 16, after Errandonea, 1980). The soft elastic

There is an analogous transition in the $(Ca,Sr,Ba)Al_2Si_2O_8$ system where crystals develop high degrees of Al/Si order under equilibrium conditions and the symmetry change is $I2/c \rightleftharpoons I\bar{1}$ (Nager *et al.*, 1970; Bambauer & Nager, 1981; Tribaudino *et al.*, 1993; McGuinn & Redfern, 1994a and b, 1997; Redfern *et al.*, 1997). These materials have not been investigated in as much detail, but the transition mechanism would be expected to be rather similar, and should be amenable to the same analysis.

The mineral leucite ($KAlSi_2O_6$) undergoes a cubic $\rightleftharpoons$ tetragonal transition at ~938 K followed by a tetragonal $\rightleftharpoons$ tetragonal transition at ~918 K (Peacor, 1968; Sadanaga & Ozawa, 1968; Grögel *et al.*, 1984; Lange *et al.*, 1986; Rüscher *et al.*, 1987; Palmer *et al.*, 1988, 1989, 1990, 1997; Palmer, 1990a; Palmer & Salje, 1990; Heaney & Veblen, 1990; Hatch *et al.*, 1990a; Boysen, 1990; Ito *et al.*, 1991). Both transitions are associated with the Brillouin zone centre and the sequence of changes in point group is $m3m \rightarrow 4/mmm \rightarrow 4/m$. The high-temperature transition is ferroelastic, but the transition mechanism is not yet understood. Although no zone-centre soft optic mode with the symmetry of the active representation (E_g) has yet been observed (Palmer *et al.*, 1990), there appear to be changes in structure involving the K^+ ions which influence the transition (Palmer & Salje, 1990; Boysen, 1990), and which might imply a pseudo-proper mechanism. On the other hand, analysis of possible rigid unit modes (those involving only relative motions of rigid SiO_4 and AlO_4 tetrahedra) suggests that an appropriate soft acoustic mode does exist to provide the driving mechanism (M.T.Dove, pers. comm.). Observations of the temperature dependence of $(C_{11} - C_{12})$ would resolve this question. Interestingly, the transition appears to be not far from second order in character (Palmer *et al.*, 1989, 1990; Palmer, 1990b), implying that energy contributions from odd-order terms in the driving order parameter are small. The elastic behaviour might therefore have the general form illustrated in Fig. 4, though with additional superimposed anomalies from the second transition at ~918 K.

7.2 Pseudo-proper ferroelastic behaviour

A more common circumstance among ferroelastic materials is that the symmetry-breaking strain is not the driving order parameter for the phase transition. Changes in some other physical property may be responsible for the transition and the symmetry-breaking strain arises only as a consequence of linear coupling to it. Softening of a zone-centre optic mode might be implicated, for example, as in $BiVO_4$ (Pinczuk *et al.*, 1979) and LaP_5O_{14} (Errandonea & Sapriel, 1979).

LaP_5O_{14}. The most thoroughly characterised transition showing the effects of pseudo-proper behaviour on a complete set of elastic constants is the $Pncm \rightleftharpoons P2_1/c$ ($mmm \rightleftharpoons 2/m$) transition in LaP_5O_{14} at ~398 K (Tolédano *et al.*, 1976; Errandonea & Bastie, 1978; Errandonea & Sapriel, 1979; Fousek *et al.*, 1979; Errandonea, 1980; Errandonea & Savary, 1981; Chen & Scott, 1989; Cai *et al.*, 1990; Scott & Chen, 1991; and see reviews by: Tolédano *et al.*, 1983; Bulou *et al.*, 1992). It serves as a perfect model for minerals. The soft acoustic mode has B_{2g} symmetry and its velocity in the orthorhombic phase is given by $\rho v^2 = C_{55}$, which should tend to zero at the elastic stability limit (Errandonea, 1980). The transition can be described in terms of the softening of two mutually perpendicular transverse acoustic waves with direction and amplitude vectors along the crystallographic x- and z-axes of the orthorhombic phase (Fig. 14). Transformation twins in the monoclinic phase will lie perpendicular to the [001] and [100] directions of the orthorhombic

using substitutions from equations 142 and 143, and by incorporating the equilibrium variation of e_4^2 given below in equation 151. This shows that C_{44} does not go to zero at $T = T_c^*$ but reaches a minimum value, $\left(C_{46}^o\right)^2 / C_{66}^o$, and then recovers in the triclinic stability field.

There are sufficient experimental data available to estimate values for all the coefficients in equation 138, and hence predict numerical values for C_{44} and C_{46}. The data for e_4 ($\approx -\cos\alpha^*$) and e_6 ($\approx \cos\gamma$) give (from Carpenter *et al.*, 1998a):

$$e_6 = 0.0251 e_4 + 7.78 e_4^3 \qquad (150).$$

Best estimates for C_{46}^o and C_{66}^o in monoclinic albite are provided by the ultrasonic data of Haussühl (1993) for sanidine, –0.8 and 39.3 GPa respectively. These give the first coefficient in equation 140 as $-C_{46}^o / C_{66}^o = 0.020$, which is in reasonable agreement with the equivalent coefficient in equation 150. Treating the other coefficients of equations 140 and 150 as also being equivalent gives λ = –39.3 x 7.78 = –306 GPa (= –306 x 10^5 J.mole^{-1}, using a molar volume of 100.1 cm^3 for $NaAlSi_3O_8$). The sixth-order term in equation 141 turns out to be small and the renormalised equilibrium temperature dependence of e_4 becomes:

$$e_4^2 = \frac{a}{b^*}\left(T_c^* - T\right) \qquad (151).$$

Taking the estimate of a = 5.48 J.mole^{-1}.K^{-1} from Salje *et al.* (1985b) gives b^* = 6801 J.mole^{-1} for T_c^* = 1241 K (using the transition temperature from Fig. 9a of Carpenter *et al.*, 1998a). Rescaling the coefficients so as to replace Q by e_4 gives a = 835 J.mole^{-1}.K^{-1} and b^* = 1.58 x 10^8 J.mole^{-1} (using $-e_4 \approx \cos\alpha^* = 0.081Q$ from Carpenter *et al.*, 1998a). Equations 142 and 143 then give $\left(T_c^* - T_c\right)$ = 2.0 K and $\left(b^* - b\right)$ = –2 x 10^6 J.mole^{-1}. Thus, also to a good approximation, equation 149 reduces to:

$$C_{44} = \frac{\left(C_{46}^o\right)^2}{C_{66}^o} + 2a\left(T_c^* - T\right) \qquad (\text{at } T < T_c^*) \qquad (152).$$

Finally, variations of C_{44}, C_{46} and C_{66} due to the $C2/m \rightleftharpoons C\bar{1}$ transition may be calculated using the estimated coefficients and the data of Haussühl (1993) for C_{46}^o and C_{66}^o. These are shown in Fig. 13b, ignoring the normal weak temperature dependence of the bare elastic constants. According to this model, the transition occurs because C_{44} softens almost to zero. The softening is a linear function of temperature in the stability fields of both polymorphs, but the transition point is at T_c^*, when C_{44} = 0.016 GPa, rather than 2 K lower, when it would extrapolate (from $T > T_c^*$) to zero. The ratio of slopes for C_{44} below and above T_c^* should be close to 2:1. The strain component e_6 remains small and is a distinctly non-linear function of e_4 because, in both monoclinic and triclinic feldspars, C_{46} is already close to zero (Ryzhova, 1964; Ryzhova & Alexandrov, 1965; Haussühl, 1993).

Substituting for e_6 in equation 138 then gives:

$$G = \frac{1}{2}a\left(T - T_c^*\right)e_4^2 + \frac{1}{4}b^* e_4^4 - \frac{\lambda^2}{2C_{66}^o}e_4^6 \qquad (141)$$

where:

$$T_c^* = T_c + \frac{\left(C_{46}^o\right)^2}{aC_{66}^o} \qquad (142) \qquad b^* = b - \frac{4\lambda C_{46}^o}{C_{66}^o} \qquad (143).$$

The elastic constants C_{44}, C_{46} and C_{66} may be derived from equation 138 in the usual way:

$$C_{66} = \frac{\partial^2 G}{\partial e_6^2} = C_{66}^o \qquad (144) \qquad C_{46} = \frac{\partial^2 G}{\partial e_4 \partial e_6} = C_{46}^o + 3\lambda e_4^2 \qquad (145)$$

$$C_{44} = \frac{\partial^2 G}{\partial e_4^2} = a\left(T - T_c\right) + \left(3b - \frac{6\lambda C_{46}^o}{C_{66}^o}\right)e_4^2 - \frac{6\lambda^2}{C_{66}^o}e_4^4 \qquad (146).$$

Thus C_{66} is not expected to be influenced by the transition, C_{46} should show a linear deviation from C_{46}^o for $e_4^2 \propto \left(T_c^* - T\right)$, and C_{44} behaves almost as the critical elastic constant for a classical proper ferroelastic transition, with $C_{44} = a\left(T - T_c\right)$ at $T > T_c^*$. At the transition point $T = T_c^*$ and $e_4 = 0$, giving:

$$C_{44} = a\left(T_c^* - T_c\right) = \frac{\left(C_{46}^o\right)^2}{C_{66}^o} \qquad (147)$$

or:

$$C_{44}C_{66}^o = \left(C_{46}^o\right)^2 \qquad (148)$$

in accordance with the predicted elastic stability limit (equation 135). (Note that the elastic constants must in reality behave as $\left(C_{44}C_{66} - C_{46}^2\right) \to 0$ with $T \to T_c$, but in this model C_{66} is taken to be effectively constant and equal to C_{66}^o). For $T < T_c^*$, equation 146 can be reformulated as:

$$C_{44} = \frac{\left(C_{46}^o\right)^2}{C_{66}^o} + 2\left(b - \frac{\lambda C_{46}^o}{C_{66}^o}\right)e_4^2 - \frac{6\lambda^2}{C_{66}^o}e_4^4 \qquad (149)$$

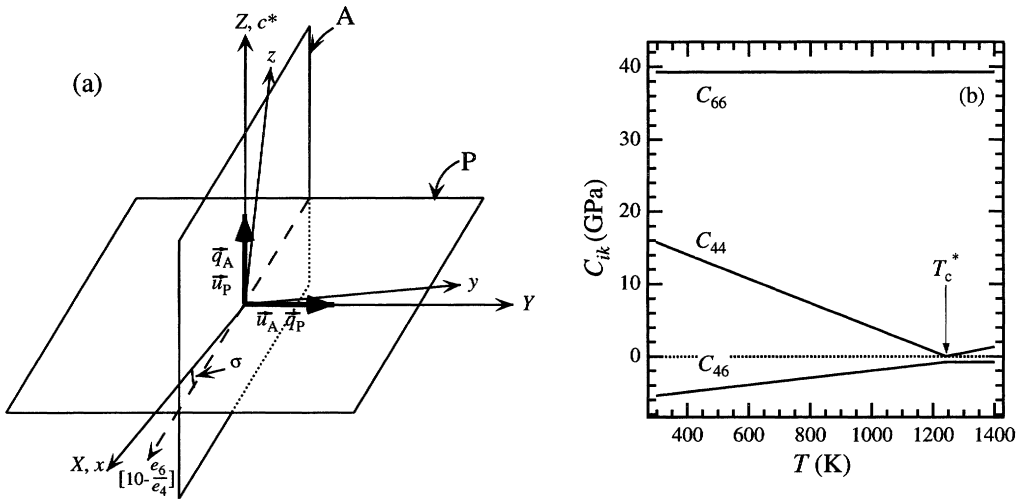

Fig. 13. Proper ferroelastic behaviour at the $C2/m \rightleftharpoons C\bar{1}$ transition in albite with no long-range Al/Si order. (a) Schematic illustration of the relationship between soft acoustic mode propagation directions ($\vec{q}_A$, $\vec{q}_P$) and displacement directions ($\vec{u}_A$, $\vec{u}_P$), twin-plane orientations (A = albite, P = pericline), and crystallographic axes (x, y, z; c^* is a reciprocal lattice direction) for the triclinic phase. X, Y and Z are the Cartesian reference axes. (b) Calculated variation of the elastic constants C_{44}, C_{66}, C_{46} (ignoring their normal background temperature dependence) through the transition point. The calculated value of C_{44} at $T = T_c^*$ is 0.016 GPa, assuming that C_{66}^o and C_{46}^o are constant.

the most significant for $e_6 << e_4$. For a second-order transition, a suitable expansion therefore has the form, :

$$G = \frac{1}{2}a(T - T_c)e_4^2 + \frac{1}{4}be_4^4 + \lambda e_4^3 e_6 + \frac{1}{2}C_{66}^o e_6^2 + C_{46}^o e_4 e_6 \qquad (138).$$

The non-symmetry-breaking strains, e_1, e_2, e_3, e_5, which would couple as $e_i e_4^2$, are a factor of at least ~5 smaller than e_4 (Harrison & Salje, 1994). For the present, and in the absence of any suitable experimental data, the associated elastic constants, C_{11}^o, C_{22}^o, C_{12}^o, *etc.*, have not been considered further.

Under equilibrium conditions, a crystal must be stress free, giving:

$$\frac{\partial G}{\partial e_6} = 0 = \lambda e_4^3 + C_{66}^o e_6 + C_{46}^o e_4 \qquad (139)$$

and, hence:

$$e_6 = -\frac{C_{46}^o}{C_{66}^o}e_4 - \frac{\lambda}{C_{66}^o}e_4^3 \qquad (140).$$

in a monoclinic crystal, but is less constrained in a triclinic crystal. A straightforward method for determining the orientation relationships is to first identify the composition planes of the transformation twins that arise as a consequence of the transition, since the amplitude and direction vectors of the soft mode must lie within them (see section 4.2). With respect to a right-handed Cartesian coordinate system having X parallel to the crystallographic x-axis, Z parallel to c^*, and Y perpendicular to X and Z, the spontaneous strain for one twin is given by $(0\ 0\ 0\ 2e_{23}\ 0\ 2e_{12})$ and for the second by $(0\ 0\ 0\ -2e_{23}\ 0\ -2e_{12})$. The twin composition plane is a plane within which the two twins have identical strain. From the description of the strain representation surfaces, this implies (Sapriel, 1975; Wadhawan, 1982):

$$\sum_{i,k}\left[(0,0,0,2e_{23},0,2e_{12})-(0,0,0,-2e_{23},0,-2e_{12})\right]x_i x_k = 0 \qquad (136)$$

where x_i and x_k (i, k = 1 – 3) are coordinates of the reference system (Salje, 1985, 1993). This yields:

$$e_{23}x_2x_3 + e_{12}x_1x_2 = 0 \qquad (137)$$

and, hence, $x_2 = 0$ for the albite twin composition plane or $x_1 = -(e_{23}/e_{12})x_3 = -(e_4/e_6)x_3$ for the pericline twin plane (assuming only small volume changes accompanying the transition), (Salje, 1993). The soft-mode propagation directions lie within these planes and are perpendicular to their intersection. In terms of the Cartesian reference system, the line of intersection of the two planes is parallel to $[1\ 0\ -\frac{e_6}{e_4}]$; the orientation relationships are illustrated in Fig. 13a. The pericline twin plane is also the rhombic section and the angle between the crystallographic x-axis and its intersection with (010) is usually specified as σ (Smith & Brown, 1988). It is found experimentally that e_4 and e_6 do not vary linearly with each other (Carpenter *et al.*, 1998a), implying that the pericline twin plane orientation in albite changes with temperature. Close to the monoclinic $\rightleftharpoons$ triclinic transition $\sigma \approx 2^\circ$, and at room temperature $\sigma \approx 4^\circ$, from $\tan\sigma = e_6/e_4$ and using the $\cos\alpha^*$, $\cos\gamma$ data of Kroll *et al.* (1980) and A. Graeme-Barber (unpublished) to calculate e_4 and e_6. In monoclinic crystals the soft acoustic mode has direction and amplitude vectors oriented along the crystallographic y and c^* directions ($\sigma \equiv 0$).

There is no experimental evidence for the softening of an optic mode with B_g symmetry (Raman active) at the centre of the Brillouin zone and the frequencies of the hard modes show little temperature dependence (Salje, 1986). Thus the driving mechanism for the transition could indeed be due to the acoustic-mode softening alone, with the symmetry-breaking strain as the driving order parameter. The excess free energy for the transition should be an expansion in both e_4 and e_6 since both these strains have the symmetry of the active representation. However, e_6 is found to be small relative to e_4, and, as a simplification, the latter can be treated as the driving order parameter. Variations in e_6 are then accounted for by coupling with e_4 (in a manner that is analogous to the treatment by Wada *et al.*, 1979, of the proper ferroelastic transition in $LaNbO_4$). The bilinear coupling term in e_4e_6 has C_{46}^o as the coupling coeficient, but this, on its own, would give a linear relationship between e_4 and e_6. The observed non-linear relationship requires higher-order coupling and the next terms with correct symmetry are $e_4^3e_6$, $e_4^2e_6^2$, $e_4e_6^3$. Of these the first may be

order coupling term, $\lambda_4'\left(e_4^2+e_5^2\right)\left[\left(e_1-e_2\right)/\sqrt{2}\right]^2$, in equation 122 (see also Tolédano *et al.*, 1983) gives:

$$C_{44}=C_{44}^{o}+2\lambda_4\left(\frac{e_1-e_2}{\sqrt{2}}\right)+2\lambda_4'\left(\frac{e_1-e_2}{\sqrt{2}}\right)^2 \tag{132}$$

$$C_{55}=C_{44}^{o}-2\lambda_4\left(\frac{e_1-e_2}{\sqrt{2}}\right)+2\lambda_4'\left(\frac{e_1-e_2}{\sqrt{2}}\right)^2 \tag{133}$$

as the approximate form of the expected variations. Assuming equal volume proportions of the two twin components, an average value would be:

$$\frac{C_{44}+C_{55}}{2}=C_{44}^{o}+2\lambda_4'\left(\frac{e_1-e_2}{\sqrt{2}}\right)^2 \tag{134}$$

again giving a linear deviation due to the transition.

This type of formalism provides a description of the observed elastic anomalies, but does not necessarily account for their physical origin. In the case of paratellurite, the soft-acoustic-mode model of the transition explains the $\left(C_{11}-C_{12}\right)$ variation. An anomaly in the dielectric constant measured parallel to the *x*-axis has also been observed and may be responsible for, or at least be associated with, the C_{44} anomaly (Peercy & Fritz, 1974; Peercy *et al.*, 1975). Bilinear coupling between e_4 and a polar property parallel to the crystallographic *x*-axis is possible in this system because *yz* and *x* are both basis functions of the same irreducible representation (E) of point group 422. Thus, while the critical elastic constants provide evidence of the gross mechanism of a transition, the non-critical elastic constants are revealing of finer detail which may be specific to the material under investigation.

Albite. Of the many phase transitions known in minerals, the most likely to display limiting proper ferroelastic behaviour is the second-order monoclinic $\rightarrow$ triclinic transition in crystals of Na-rich feldspar with no long-range Al/Si order (Salje, 1985; Salje *et al.*, 1985a and b; Redfern *et al.*, 1997; and see Smith & Brown, 1988, for original references). The change in point group is $2/m \rightleftharpoons \bar{1}$, for which the active representation is B_g. The condition for stability with respect to this transition is given by the B_g eigenvalue of the symmetry-adapted elastic-constant matrix (Boccara, 1968) as:

$$\frac{1}{2}\left\{C_{44}+C_{66}-\left[\left(C_{44}-C_{66}\right)^2+4C_{46}^2\right]^{1/2}\right\}>0 \tag{135}$$

which reduces to $\left(C_{44}C_{66}-C_{46}^2\right)>0$ (Cowley, 1976; Table 6).

An appropriate description of the expected mechanism for the transition would be in terms of the softening of the B_g transverse acoustic mode. The orientation of this soft mode is constrained by symmetry to have direction and amplitude vectors parallel to crystallographic axes

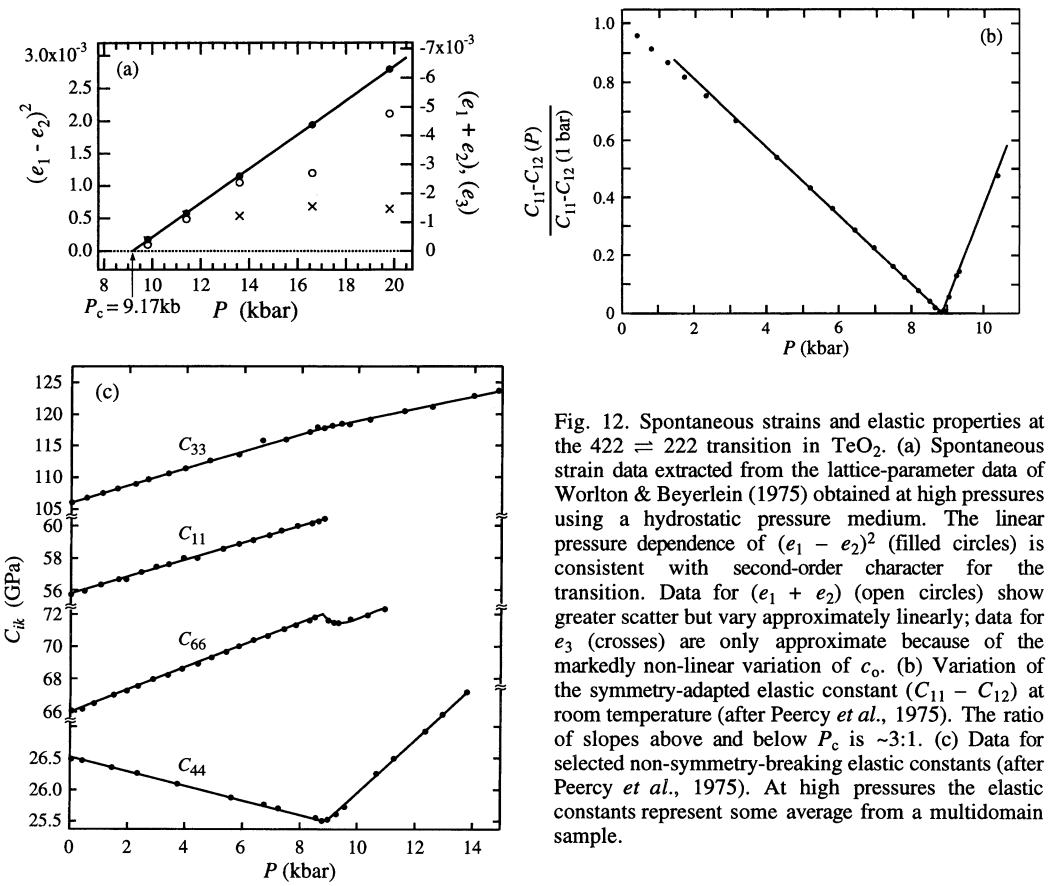

Fig. 12. Spontaneous strains and elastic properties at the 422 ⇌ 222 transition in TeO_2. (a) Spontaneous strain data extracted from the lattice-parameter data of Worlton & Beyerlein (1975) obtained at high pressures using a hydrostatic pressure medium. The linear pressure dependence of $(e_1 - e_2)^2$ (filled circles) is consistent with second-order character for the transition. Data for $(e_1 + e_2)$ (open circles) show greater scatter but vary approximately linearly; data for e_3 (crosses) are only approximate because of the markedly non-linear variation of c_o. (b) Variation of the symmetry-adapted elastic constant $(C_{11} - C_{12})$ at room temperature (after Peercy *et al.*, 1975). The ratio of slopes above and below P_c is ~3:1. (c) Data for selected non-symmetry-breaking elastic constants (after Peercy *et al.*, 1975). At high pressures the elastic constants represent some average from a multidomain sample.

shown in Fig. 12c suggests that a Landau expansion such as Equation 122 does not completely describe the energetics of the transition mechanism. C_{44} softens unexpectedly in a linear manner from both sides of P_c, and C_{33} shows a small break in slope at $P = P_c$. In the case of C_{33}, transformation twinning should not cause major problems because both twins share the same z-axis. Similarly, coupling of the form $\lambda_3 e_3\left[(e_1 - e_2)/\sqrt{2}\right]^2$, the lowest order allowed by symmetry, is not expected to lead to any renormalisation of C_{33}^o. However, the next higher-order coupling term, $\lambda_3' e_3^2\left[(e_1 - e_2)/\sqrt{2}\right]^2$, would give a variation of the form:

$$C_{33} = C_{33}^o + 2\lambda_3'\left(\frac{e_1 - e_2}{\sqrt{2}}\right)^2 \qquad (131).$$

For a second-order transition this would be a linear deviation, consistent with the observations. Measurements along the x- or y-axes of the tetragonal phase to give C_{44} (= C_{55}) would yield an approximate average of C_{44} and C_{55} along the same directions of the twinned orthorhombic derivative. (C_{44} and C_{55} are no longer equivalent and the x- and y-axes of the orthorhombic twins will be slightly misaligned because of the non-equivalence of a and b). Including the next higher-

centre optic mode with the same symmetry (B_1) shows no softening and the driving order parameter for the transition appears to be the symmetry-breaking strain alone (Peercy & Fritz, 1974; Peercy *et al.*, 1975). Inelastic neutron scattering measurements show that the active acoustic mode softens most markedly at long wavelengths and that the effect of pressure is to shift the dispersion curve for this mode more or less uniformly (McWhan *et al.*, 1975), though to a much lesser extent than shown schematically in Fig. 8a for the case of zone-centre softening.

Lattice parameters for crystals subjected to hydrostatic pressures (from Worlton & Beyerlein, 1975) have been used to calculate values for the strain components, $e_1 = \left[(a - a_o)/a_o\right]$, $e_2 = \left[(b - a_o)/a_o\right]$ and $e_3 = \left[(c - c_o)/c_o\right]$. There is a slight difficulty in extrapolating values of the tetragonal parameters a_o and c_o into the stability field of the orthorhombic structure to calculate the strains because, as in general for structures subjected to pressure rather than temperature as the external variable, the extrapolation is expected to be non-linear. A linear extrapolation of a_o is consistent with the (limited) data collected at $P < 9$ kbar, however, and should yield more precise values for the strain components than were given by Worlton & Beyerlein (1975) who used the one-atmosphere lattice parameters for a_o and c_o. A graphical non-linear extrapolation of c was used to approximate c_o at high pressures. The symmetry-breaking (B_1) strain varies as $(e_1 - e_2)^2 \propto P$, indicating that the transition may be classically second order in character (Worlton & Beyerlein, 1975; McWhan *et al.*, 1975; Skelton *et al.*, 1976; Fig. 12a). The non-symmetry-breaking strains are smaller than the B_1 strain but $(e_1 + e_2)$, which is expected to vary with $(e_1 - e_2)^2$, also varies approximately linearly with pressure (Fig. 12a). The non-linear pressure dependence shown by c_o is insufficiently constrained to allow accurate determinations of e_3, but the magnitudes of $(e_1 + e_2)$ and e_3 are comparable, giving a volume strain of ~1% at 20 kbar. This may be compared with ~5% for the value of $(e_1 - e_2)$ at the same pressure. A linear least squares fit of the square of the symmetry-breaking strain gives P_c = 9.17 kbar, with an uncertainty of ± ~0.2 kbar arising primarily from the experimental calibration of pressure.

Ultrasonic measurements of the velocity of the soft acoustic mode have shown that the B_1 symmetry-adapted elastic constant $(C_{11} - C_{12})$ goes linearly to zero both from above and below a transition pressure of ~8.86 kbar (Fig. 12b, after Peercy *et al.*, 1975). This is the classical result for a second-order proper ferroelastic transition, though a non-classical ratio of the slopes, ~3:1 instead of 2:1, was found. An appropriate Landau free-energy expansion has been given earlier (Equation 122). Because the symmetry-breaking strain is itself the driving order parameter, the Landau coefficients can be given explicitly as combinations of second-, third- and fourth-order elastic constants (see, for example, Tolédano *et al.*, 1983, or Bulou *et al.*, 1992). The effect of the $(e_1 + e_2)$ and e_3 strains is to renormalise the fourth-order Landau coefficient to yield a predicted slope ratio of $2(b/b^*)$:1 (with $b > b^*$). Tolédano *et al.* used experimental data for the third-order elastic constants (Antonenko *et al.*, 1979; Uwe & Tokumoto, 1979) to show that the calculated value of b/b^* is in close agreement with the observed ratio of slopes.

Peercy *et al.* (1975) also measured values of C_{11}, C_{33}, C_{44} and C_{66} for the tetragonal phase. They extended their measurements of C_{11}, C_{44} and C_{66} into the stability field of the orthorhombic structure (Fig. 12c, after Peercy *et al.*, 1975) but, probably because of twin domain formation due to the tetragonal → orthorhombic transition, the data for C_{11} and C_{66} were of poor quality. Comparison of the expected variation of C_{33} and C_{44} for a 422 ⇌ 222 proper ferroelastic transition that has significant non-symmetry-breaking strain (Fig. 9) with the observed variations

An example of a zone-boundary transition with the same change in point group involves the space-group change $P622 \rightleftharpoons P321$. This is associated with the K point at $\left(\frac{1}{3},\frac{1}{3},0\right)$ (for $\gamma^* = 60°$) on the surface of the Brillouin zone (or $\left(\frac{\bar{1}}{3},\frac{2}{3},0\right)$ according to the vector notation of Bradley & Cracknell, 1972); the active representation is K_2 (Stokes & Hatch, 1988). The excess free energy can be written as (Stokes & Hatch, 1988; Hatch, pers. comm.):

$$\begin{aligned} G = &\frac{1}{2}a(T-T_c)\left(q_1^2+q_2^2\right)+\frac{1}{4}b\left(q_1^2+q_2^2\right)^2+\left[\lambda_1(e_1+e_2)+\lambda_3 e_3\right]\left(q_1^2+q_2^2\right) \\ &+\lambda_4\left(e_4^2+e_5^2\right)\left(q_1^2+q_2^2\right)+\lambda_5(e_1e_4-e_2e_4+e_5e_6)\left(3q_1^2q_2+q_2^3\right) \\ &+\lambda_6\left[e_6^2+(e_1-e_2)^2\right]\left(q_1^2+q_2^2\right)+\frac{1}{4}\left(C_{11}^o+C_{12}^o\right)(e_1+e_2)^2 \\ &+\frac{1}{4}\left(C_{11}^o-C_{12}^o\right)(e_1-e_2)^2+C_{13}^o(e_1+e_2)e_3+\frac{1}{2}C_{33}^o e_3^2 \\ &+\frac{1}{2}C_{44}^o\left(e_4^2+e_5^2\right)+\frac{1}{2}C_{66}^o e_6^2 \end{aligned} \qquad (130).$$

In the trigonal phase under equilibrium conditions, $q_1 = 0$ and $q_2 \neq 0$. Variations of the elastic constants will be essentially the same as for the zone-centre case, with the exception of C_{14}, C_{24} and C_{56} which would be expected to vary linearly with q_2^3.

In summary, the form of the elastic-constant evolution with temperature (or pressure) should provide significant insights into the driving mechanism for a phase transition. The variations may be predicted by making use of the symmetry properties of the elastic constants and spontaneous strain components, writing out the appropriate form of the Landau excess free energy, and then differentiating directly (proper ferroelastic transitions), or using the general solution for order-parameter/strain coupling (pseudo-proper or improper ferroelastic transitions and co-elastic transitions). In each case the values of the coupling coefficients must be determined from experimental data.

7. Renormalisation of second-order elastic constants at phase transitions: some examples of real behaviour

7.1 Strain as driving order parameter: proper ferroelastic behaviour

TeO_2. Possibly the best example yet studied of elastic-constant variations due to proper ferroelastic behaviour is the pressure-induced tetragonal $\rightleftharpoons$ orthorhombic transition in paratellurite, TeO_2 (Peercy & Fritz, 1974; Peercy *et al.*, 1975; Worlton & Beyerlein, 1975; McWhan *et al.*, 1975; Skelton *et al.*, 1976; and see reviews by Tolédano *et al.*, 1983, Cummins, 1983, and Bulou *et al.*, 1992). At room pressure paratellurite crystals have $P4_12_12$ symmetry, while above ~9 kbar the space group becomes $P2_12_12_1$, without a change in translational symmetry. The transition mechanism can be described as the softening to zero frequency (or at least to very low frequencies) of an acoustic mode propagating in the [110] direction and polarised parallel to $[1\bar{1}0]$. The zone-

& Dolino (1975): C_{14}, C_{24} and C_{56} vary with Q, C_{44} and $(C_{11}-C_{12})$ $(=2C_{66})$ are expected to vary with Q^2, and $(C_{11}+C_{12})$, C_{33}, C_{13} and C_{23} are expected to show a simple step at $T = T_c$ if the transition is second order in character.

Table 13. Predicted variations for elastic constants of a material subject to a zone-centre phase transition involving the symmetry change 622 $\rightleftharpoons$ 32. The expressions for individual C_{ik}'s have been derived for a second-order transition.

Co-elastic transition	
622 phase	32 phase
$Q=0$	$Q^2=\frac{a}{b^*}(T_c-T)$, $\chi^{-1}=2a\frac{b}{b^*}(T_c-T)=2bQ^2$ $b^*=b-2\left[\frac{\lambda_3^2(C_{11}^o+C_{12}^o)+2\lambda_1^2C_{33}^o-4\lambda_1\lambda_3C_{13}^o}{(C_{11}^o+C_{12}^o)C_{33}^o-2C_{13}^{o\,2}}\right]$
$C_{11}=C_{22}=C_{11}^o$	$C_{11}=C_{22}=C_{11}^o+2\lambda_6Q^2-4\lambda_1^2Q^2\chi$
$C_{33}=C_{33}^o$	$C_{33}=C_{33}^o-4\lambda_3^2Q^2\chi$
$C_{12}=C_{12}^o$	$C_{12}=C_{12}^o-2\lambda_6Q^2-4\lambda_1^2Q^2\chi$
$C_{13}=C_{23}=C_{13}^o$	$C_{13}=C_{23}=C_{13}^o-4\lambda_1\lambda_3Q^2\chi$
$C_{11}-C_{12}=C_{11}^o-C_{12}^o$	$C_{11}-C_{12}=(C_{11}^o-C_{12}^o)+4\lambda_6Q^2$
$C_{11}+C_{12}=C_{11}^o+C_{12}^o$	$C_{11}+C_{12}=(C_{11}^o+C_{12}^o)-8\lambda_1^2Q^2\chi$
$C_{14}=-C_{24}=C_{56}=0$	$C_{14}=-C_{24}=C_{56}=\lambda_5Q$
$C_{44}=C_{55}=C_{44}^o$	$C_{44}=C_{55}=C_{44}^o+2\lambda_4Q^2$
$C_{66}=C_{66}^o=\frac{1}{2}(C_{11}^o-C_{12}^o)$	$C_{66}=C_{66}^o+2\lambda_6Q^2=\frac{1}{2}(C_{11}-C_{12})$

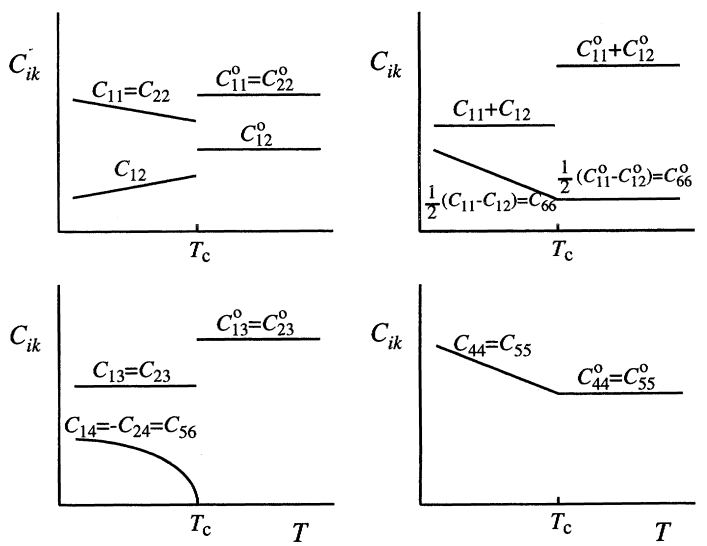

Fig.11. Schematic variations of elastic constants at a second-order transition involving the point-group change 622 $\rightleftharpoons$ 32, based on expressions given in Table 13. The form of C_{33} is the same as for C_{13}.

Table 12. Symmetry-adapted elastic constants (eigenvalues) and strains (from the eigenvectors) of the elastic-constant matrix for point group 622 (Laue class 6/*mmm*). The E_2 eigenvalues are required to be identical but, as a consequence of the convention used to reduce C_{ijkl} to C_{ik}, come out as $(C_{11}-C_{12})$ and C_{66}. Since $C_{66}=\frac{1}{2}(C_{11}-C_{12})$ in hexagonal systems, a factor of two must be applied to C_{66} and a corresponding factor of $\frac{1}{\sqrt{2}}$ to e_6 (shown in brackets) to give the correct degeneracies. Note: $2\alpha^2+\beta^2=2\alpha'^2+\beta'^2=1$, $2\alpha\alpha'+\beta\beta'=0$, $A^2+B^2=D^2+E^2=1$.

Irreducible representation	Eigenvalue	Eigenvector	Symmetry-adapted spontaneous strain
A_1	$\frac{1}{2}\left\{(C_{11}+C_{12}+C_{33}) - \left[(C_{11}+C_{12}-C_{33})^2+8C_{13}^2\right]^{1/2}\right\}$	$(\alpha,\alpha,\beta,0,0,0)$	$e_1+e_2;\ e_3$
A_1	$\frac{1}{2}\left\{(C_{11}+C_{12}+C_{33}) + \left[(C_{11}+C_{12}-C_{33})^2+8C_{13}^2\right]^{1/2}\right\}$	$(\alpha',\alpha',\beta',0,0,0)$	$e_1+e_2;\ e_3$
E_1	C_{44} C_{44}	$A(0,0,0,1,0,0)$ $B(0,0,0,0,1,0)$	e_4 e_5
E_2	$(C_{11}-C_{12})$ $(2)C_{66}$	$D\left(\frac{1}{\sqrt{2}},-\frac{1}{\sqrt{2}},0,0,0,0\right)$ $E(0,0,0,0,0,1)$	$\frac{1}{\sqrt{2}}(e_1-e_2)$ $\left(\frac{1}{\sqrt{2}}\right)e_6$

For an equitranslational phase transition giving a symmetry change $622 \rightleftharpoons 32$, the active representation is B_1. There are no basis functions with the form of a strain associated with this representation; a strain cannot be the driving order parameter and there is no single soft acoustic mode which can be responsible for the transition. The non-symmetry-breaking strains, (e_1+e_2) and e_3, are associated with the identity representation and couple with Q^2. Lowest-order coupling terms for the remaining strain components, (e_1-e_2), e_4, e_5 and e_6, have the form e^2Q^2; e_4 and e_5 are degenerate strains associated with E_1, giving a coupling term $\lambda(e_4^2+e_5^2)Q^2$, while $\frac{1}{\sqrt{2}}e_6$ and $\frac{1}{\sqrt{2}}(e_1-e_2)$ are the degenerate strains belonging to E_2 (Table 12), giving a coupling term $\lambda\left[e_6^2+(e_1-e_2)^2\right]Q^2$. Additional coupling of the form $(e_1e_4-e_2e_4+e_5e_6)Q$ is allowed because $E_1 \otimes E_2$ is equal to $B_1 \oplus B_2 \oplus E_1$ and contains the active representation (Rehwald, 1973). The degeneracy of e_1e_4, $-e_2e_4$ and e_5e_6 ensures that $C_{14}=-C_{24}=C_{56}$ in class 32.

The excess free energy due to the transition may be written as:

$$
\begin{aligned}
G=&\frac{1}{2}a(T-T_c)Q^2+\frac{1}{4}bQ^4+\lambda_1(e_1+e_2)Q^2+\lambda_3e_3Q^2+\lambda_4(e_4^2+e_5^2)Q^2\\
&+\lambda_5(e_1e_4-e_2e_4+e_5e_6)Q+\lambda_6\left[e_6^2+(e_1-e_2)^2\right]Q^2\\
&+\frac{1}{4}(C_{11}^o+C_{12}^o)(e_1+e_2)^2+\frac{1}{4}(C_{11}^o-C_{12}^o)(e_1-e_2)^2+C_{13}^o(e_1+e_2)e_3\\
&+\frac{1}{2}C_{33}^oe_3^2+\frac{1}{2}C_{44}^o(e_4^2+e_5^2)+\frac{1}{2}C_{66}^oe_6^2 \qquad (129).
\end{aligned}
$$

Predicted variations of the individual elastic constants are given in Table 13 and are illustrated in Fig. 11. Their behaviour may conveniently be separated into three groups, following Bachheimer

Table 11. (Facing page and below) Predicted variations for elastic constants of a material subject to a phase transition involving the symmetry change $mmm \rightleftharpoons 2/m$. The expressions for individual C_{ik}'s have been derived for second-order transitions.

Improper ferroelastic transition	
Pmma phase	*P2/c* phase
$q_1 = q_2 = 0$	$q_1^2 = \frac{a}{b^*}(T_c - T),\ q_2 = 0$
	$b^* = (b + b') - f(\lambda_i, i = 1,2,3,5;$
	$C_{ii}^o,\ i = 1,2,3,5;$
	$C_{ik}^o, i,k = 1,2,3, i \neq k)$
$C_{11} = C_{11}^o$	$C_{11} = C_{11}^o - \left(\frac{2\lambda_1^2}{b+b'}\right)$
$C_{22} = C_{22}^o$	$C_{22} = C_{22}^o - \left(\frac{2\lambda_2^2}{b+b'}\right)$
$C_{33} = C_{33}^o$	$C_{33} = C_{33}^o - \left(\frac{2\lambda_3^2}{b+b'}\right)$
$C_{12} = C_{12}^o$	$C_{12} = C_{12}^o - \left(\frac{2\lambda_1\lambda_2}{b+b'}\right)$
$C_{13} = C_{13}^o$	$C_{13} = C_{13}^o - \left(\frac{2\lambda_1\lambda_3}{b+b'}\right)$
$C_{23} = C_{23}^o$	$C_{23} = C_{23}^o - \left(\frac{2\lambda_2\lambda_3}{b+b'}\right)$
$C_{44} = C_{44}^o$	$C_{44} = C_{44}^o + 2\lambda_4 q_1^2$
$C_{55} = C_{55}^o$	$C_{55} = C_{55}^o - \left(\frac{2\lambda_5^2}{b+b'}\right)$
$C_{66} = C_{66}^o$	$C_{66} = C_{66}^o + 2\lambda_6 q_1^2$
$C_{15} = C_{25} = C_{35} = 0$	$C_{15} = -\left(\frac{2\lambda_1\lambda_5}{b+b'}\right)$
	$C_{25} = -\left(\frac{2\lambda_2\lambda_5}{b+b'}\right)$
	$C_{35} = -\left(\frac{2\lambda_3\lambda_5}{b+b'}\right)$
$C_{46} = 0$	$C_{46} = \lambda_7 q_1^2$

6.4 622 ⇌ 32

Co-elastic. Details of the symmetry properties of the elastic-constant matrix for a crystal with point group 622 (Laue class 6/*mmm*) are given in Table 12. If the standard elastic constants, C_{ik}, are used, the E_2 eigenvalues are $(C_{11} - C_{12})$ and C_{66}. These must be identical, and, since $C_{66} = \frac{1}{2}(C_{11} - C_{12})$ in hexagonal systems, it is necessary to apply a factor of 2 to C_{66}. In order to maintain a constant form of the elastic energy, $\frac{1}{2}C_{66}e_6^2$, it is necessary also to apply a corresponding factor of $\frac{1}{\sqrt{2}}$ to e_6 (Table 12). This anomaly arises from the conventional reduction of C_{ijkl} to C_{ik} notation, and again highlights the need to use the reduced (Voigt) terms with care. An alternative scheme can be used which yields the correct degeneracies directly (Bulou, 1992).

Proper ferroelastic transition		
mmm phase	2/*m* phase, $e_{nsb} = 0$	2/*m* phase, $e_{nsb} \neq 0$
$e_5 = 0$	$e_5^2 = \frac{a}{b}(T_c - T)$	$e_5^2 = \frac{a}{b^*}(T_c - T)$
		$b^* = b - f\left(\lambda_i, C_{ik}^o;\ i,k = 1-3\right)$
$C_{11} = C_{11}^o$	$C_{11} = C_{11}^o$	$C_{11} = C_{11}^o$
$C_{22} = C_{22}^o$	$C_{22} = C_{22}^o$	$C_{22} = C_{22}^o$
$C_{33} = C_{33}^o$	$C_{33} = C_{33}^o$	$C_{33} = C_{33}^o$
$C_{12} = C_{12}^o$	$C_{12} = C_{12}^o$	$C_{12} = C_{12}^o$
$C_{13} = C_{13}^o$	$C_{13} = C_{13}^o$	$C_{13} = C_{13}^o$
$C_{23} = C_{23}^o$	$C_{23} = C_{23}^o$	$C_{23} = C_{23}^o$
$C_{44} = C_{44}^o$	$C_{44} = C_{44}^o + 2\lambda_4 e_5^2$	$C_{44} = C_{44}^o + 2\lambda_4 e_5^2$
$C_{55} = a(T - T_c)$	$C_{55} = 2a(T_c - T)$	$C_{55} = 2a\frac{b}{b^*}(T_c - T)$
$C_{66} = C_{66}^o$	$C_{66} = C_{66}^o + 2\lambda_6 e_5^2$	$C_{66} = C_{66}^o + 2\lambda_6 e_5^2$
$C_{15} = C_{25} = C_{35} = 0$	$C_{15} = C_{25} = C_{35} = 0$	$C_{15} = 2\lambda_1 e_5$
		$C_{25} = 2\lambda_2 e_5$
		$C_{35} = 2\lambda_3 e_5$
$C_{46} = 0$	$C_{46} = \lambda_7 e_5$	$C_{46} = \lambda_7 e_5$

Pseudo-proper ferroelastic transition		
mmm phase	2/*m* phase, $e_{nsb} = 0$	2/*m* phase, $e_{nsb} \neq 0$
$Q = 0$	$Q^2 = \frac{a}{b}\left(T_c^* - T\right),\ T_c^* = T_c + \frac{\lambda_5^2}{aC_{55}^o}$	$Q^2 = \frac{a}{b^*}\left(T_c^* - T\right),\ T_c^* = T_c + \frac{\lambda_5^2}{aC_{55}^o}$
$\chi^{-1} = a(T - T_c)$	$\chi^{-1} = 2a\left(T_c^* - T\right) + a\left(T_c^* - T_c\right)$	$\chi^{-1} = 2a\frac{b}{b^*}\left(T_c^* - T\right) + a\left(T_c^* - T_c\right)$
		$b^* = b - f\left(\lambda_i, C_{ik}^o;\ i,k = 1-3\right)$
$C_{11} = C_{11}^o$	$C_{11} = C_{11}^o$	$C_{11} = C_{11}^o - 4\lambda_1^2 Q^2\chi$
$C_{22} = C_{22}^o$	$C_{22} = C_{22}^o$	$C_{22} = C_{22}^o - 4\lambda_2^2 Q^2\chi$
$C_{33} = C_{33}^o$	$C_{33} = C_{33}^o$	$C_{33} = C_{33}^o - 4\lambda_3^2 Q^2\chi$
$C_{12} = C_{12}^o$	$C_{12} = C_{12}^o$	$C_{12} = C_{12}^o - 4\lambda_1\lambda_2 Q^2\chi$
$C_{13} = C_{13}^o$	$C_{13} = C_{13}^o$	$C_{13} = C_{13}^o - 4\lambda_1\lambda_3 Q^2\chi$
$C_{23} = C_{23}^o$	$C_{23} = C_{23}^o$	$C_{23} = C_{23}^o - 4\lambda_2\lambda_3 Q^2\chi$
$C_{44} = C_{44}^o$	$C_{44} = C_{44}^o + 2\lambda_4 Q^2$	$C_{44} = C_{44}^o + 2\lambda_4 Q^2$
$C_{55} = C_{55}^o - \lambda_5^2\chi$	$C_{55} = C_{55}^o - \lambda_5^2\chi$	$C_{55} = C_{55}^o - \lambda_5^2\chi$
$C_{66} = C_{66}^o$	$C_{66} = C_{66}^o + 2\lambda_6 Q^2$	$C_{66} = C_{66}^o + 2\lambda_6 Q^2$
$C_{15} = C_{25} = C_{35} = 0$	$C_{15} = C_{25} = C_{35} = 0$	$C_{15} = -2\lambda_1\lambda_5 Q\chi$
		$C_{25} = -2\lambda_2\lambda_5 Q\chi$
		$C_{35} = -2\lambda_3\lambda_5 Q\chi$
$C_{46} = 0$	$C_{46} = \lambda_7 e_5$	$C_{46} = \lambda_7 e_5$

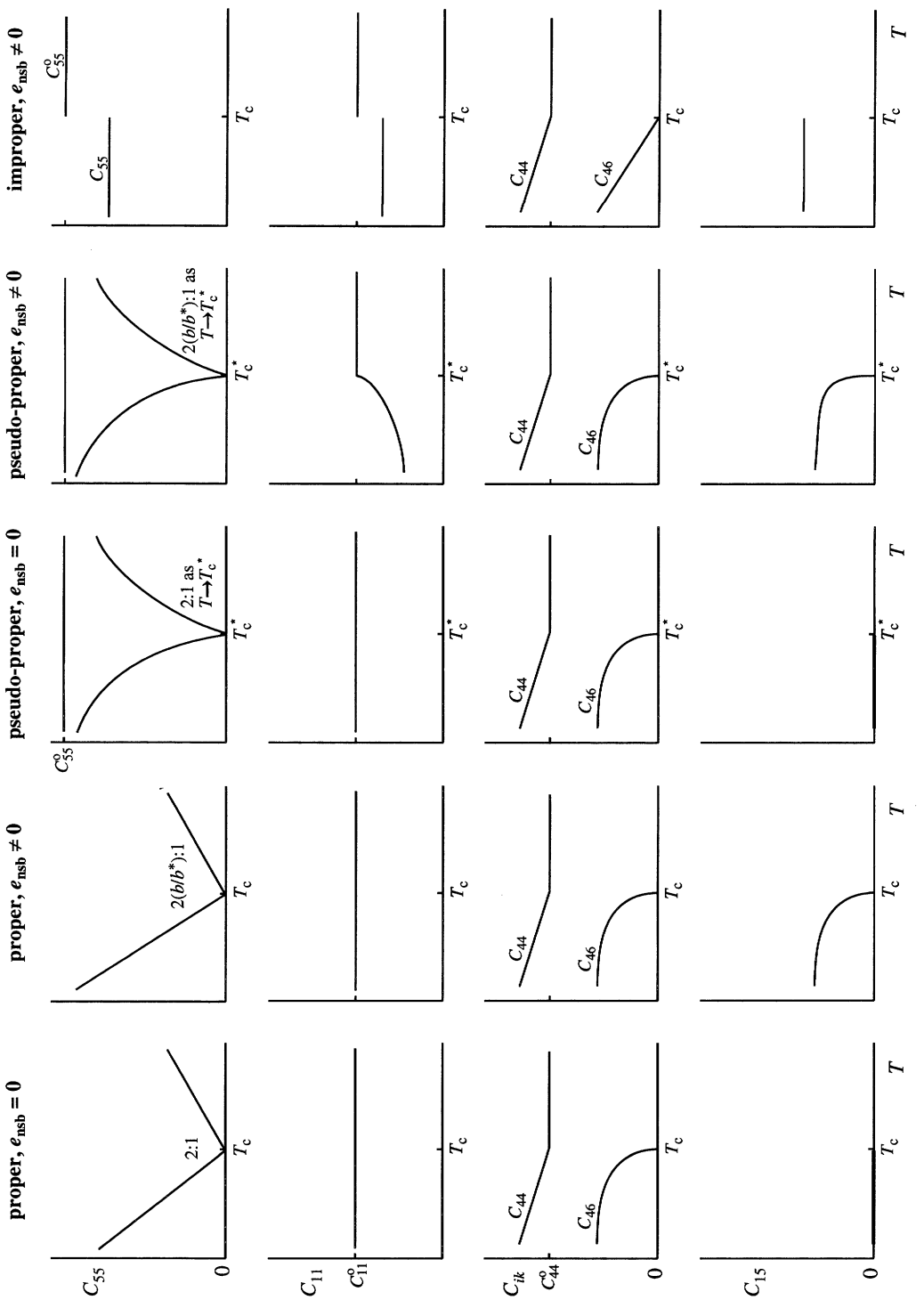

$$G = \frac{1}{2}a(T-T_c)Q^2 + \frac{1}{4}bQ^4 + (\lambda_1 e_1 + \lambda_2 e_2 + \lambda_3 e_3)Q^2 + \lambda_5 e_5 Q + (\lambda_4 e_4^2 + \lambda_6 e_6^2)Q^2$$
$$+\lambda_7 e_4 e_6 Q + \frac{1}{2}(C_{11}^o e_1^2 + C_{22}^o e_2^2 + C_{33}^o e_3^2 + C_{44}^o e_4^2 + C_{55}^o e_5^2 + C_{66}^o e_6^2)$$
$$+C_{12}^o e_1 e_2 + C_{13}^o e_1 e_3 + C_{23}^o e_2 e_3 \qquad (127).$$

Predicted variations of the individual elastic constants, making use of the general solution for strain/order-parameter coupling (equation 79), are also given in Table 11 and Fig. 10.

As with the previous examples of $m3m \rightleftharpoons 4/mmm$ and $422 \rightleftharpoons 222$ transitions, it is clear that the nature of the driving mechanism has a considerable effect on the behaviour of the elastic constants. Note, in particular, the difference in C_{55} between the cases of e_5 and Q acting as the driving order parameter. The influence of non-symmetry-breaking strains is to change the ratio of the slopes at $T \rightarrow T_c$ for the critical elastic constant, and to cause some variations in the non-critical elastic constants.

Improper. Finally, if the transition is driven by an order parameter with symmetry other than B_{2g}, *e.g.* involving a doubling of the unit-cell size, the order parameter becomes degenerate and coupling with the symmetry-breaking strain takes the form $\lambda e_5 q_i^2$. The active representation for the specific case already discussed in section 2.3, $Pmma \rightleftharpoons P2/c$, is X_2, which is associated with the special point $(\frac{1}{2},0,0)$ on the Brillouin zone boundary (or $(0,\frac{1}{2},0)$ using the vector notation of Bradley & Cracknell, 1972). The excess free energy may be written in full as (Stokes & Hatch, 1988; Hatch, pers. comm.):

$$G = \frac{1}{2}a(T-T_c)(q_1^2+q_2^2) + \frac{1}{4}b(q_1^2+q_2^2)^2 + \frac{1}{4}b'(q_1^4+q_2^4) + (\lambda_1 e_1 + \lambda_2 e_2 + \lambda_3 e_3)(q_1^2+q_2^2)$$
$$+(\lambda_4 e_4^2 + \lambda_6 e_6^2)(q_1^2+q_2^2) + (\lambda_5 e_5 + \lambda_7 e_4 e_6)(q_1^2 - q_2^2)$$
$$+\frac{1}{2}(C_{11}^o e_1^2 + C_{22}^o e_2^2 + C_{33}^o e_3^2 + C_{44}^o e_4^2 + C_{55}^o e_5^2 + C_{66}^o e_6^2) + C_{12}^o e_1 e_2 + C_{13}^o e_1 e_3 + C_{23}^o e_2 e_3$$

(128).

Under equilibrium conditions, $q_1 \neq 0$ and $q_2 = 0$ in the monoclinic structure.

Variations of the elastic constants may be predicted in the usual way using equation 79. These are given in Table 11 and illustrated in Fig. 10. Each individual elastic constant would be expected to show a step at $T = T_c$, except for C_{46}, C_{44} and C_{66}, which would be expected to show deviations from C_{46}^o (= 0), C_{44}^o and C_{66}^o proportional to q_1^2.

Fig. 10. (Facing page) Schematic variations of elastic constants at second-order transitions involving the point-group change $mmm \rightleftharpoons 2/m$, based on expressions given in Table 11. In each case the form of variation of C_{22}, C_{33}, C_{12}, C_{13} and C_{23} is the same as for C_{11}, the form of C_{66} is the same as for C_{44}, and the form of C_{25} and C_{35} is the same as for C_{15}; details vary according to the sign and magnitude of each coupling coefficient. The improper example is $Pmma \rightleftharpoons P2/c$.

$$G_{\text{elastic,A}_g} = \frac{1}{2}(e_1,e_2,e_3)\begin{pmatrix} C_{11} & C_{12} & C_{13} \\ C_{12} & C_{22} & C_{23} \\ C_{13} & C_{23} & C_{33} \end{pmatrix}\begin{pmatrix} e_1 \\ e_2 \\ e_3 \end{pmatrix} \qquad (125).$$

The remaining two strain components, e_4 and e_6, are associated with the representations B_{3g} and B_{1g} respectively. As has been discussed before, $B_{1g} \otimes B_{3g} = B_{2g}$ which means that coupling between e_4e_6 and e_5, or between e_4e_6 and some other driving order parameter with B_{2g} symmetry, can occur.

Table 10. Symmetry-adapted elastic constants (eigenvalues) and strains (from the eigenvectors) of the elastic constant matrix for point group *mmm*. Note: $\alpha^2+\beta^2+\gamma^2=\alpha'^2+\beta'^2+\gamma'^2=\alpha''^2+\beta''^2+\gamma''^2=1$, $\alpha\alpha'+\beta\beta'+\gamma\gamma'=0$, *etc.*

Irreducible representation	Eigenvalue	Eigenvector	Symmetry-adapted spontaneous strain
A_g	*	$(\alpha,\beta,\gamma,0,0,0)$	e_1; e_2; e_3
A_g	*	$(\alpha',\beta',\gamma',0,0,0)$	e_1; e_2; e_3
A_g	*	$(\alpha'',\beta'',\gamma'',0,0,0)$	e_1; e_2; e_3
B_{1g}	C_{66}	$(0,0,0,0,0,1)$	e_6
B_{2g}	C_{55}	$(0,0,0,0,1,0)$	e_5
B_{3g}	C_{44}	$(0,0,0,1,0,0)$	e_4
* eigenvalues of the submatrix $\begin{pmatrix} C_{11} & C_{12} & C_{13} \\ C_{12} & C_{22} & C_{23} \\ C_{13} & C_{23} & C_{33} \end{pmatrix}$			

This example has been used extensively in section 2 and the excess free energy for e_5 as the driving order parameter may now be written out in full to include all the possible lowest-order couplings:

$$G = \frac{1}{2}a(T-T_c)e_5^2 + \frac{1}{4}be_5^4 + (\lambda_1 e_1 + \lambda_2 e_2 + \lambda_3 e_3)e_5^2 + (\lambda_4 e_4^2 + \lambda_6 e_6^2)e_5^2 + \lambda_7 e_4 e_6 e_5$$
$$+\frac{1}{2}(C_{11}^{o}e_1^2 + C_{22}^{o}e_2^2 + C_{33}^{o}e_3^2 + C_{44}^{o}e_4^2 + C_{66}^{o}e_6^2) + C_{12}^{o}e_1e_2 + C_{13}^{o}e_1e_3 + C_{23}^{o}e_2e_3 \qquad (126).$$

Predicted variations of the individual elastic constants are given in Table 11 and shown schematically in Fig. 10. The corresponding soft acoustic mode would have $\vec{q}$ // [100] and $\vec{u}$ // [001] (or *vice versa*), with $\rho v^2 = C_{55}$.

Pseudo-proper. If the transition is driven by a different order parameter with B_{2g} symmetry, the excess free energy due to the transition may be written as:

Table 9. (Previous two pages and below) Predicted variations for elastic constants of a material subject to a phase transition involving the symmetry change 422 ⇌ 222. The expressions for individual C_{ik}'s have been derived for second-order transitions.

Improper ferroelastic transition	
*P*422 phase	*C*222 phase
$q_1 = q_2 = 0$	$q_1^2 = q_2^2 = \dfrac{a(T_c - T)}{\left(2b^* + b'^*\right)}, \quad b^* = b - \left[\dfrac{4\lambda_1^2 + 2\lambda_2^2}{C_{11}^o - C_{12}^o}\right]$
	$b'^* = b' + \dfrac{2\lambda_2^2}{\left(C_{11}^o - C_{12}^o\right)}, \quad A = \left[\dfrac{1}{\left(2b + b' + b'^*\right)} + \dfrac{1}{\left(2b + b' - b'^*\right)}\right]$
$C_{11} = C_{22} = C_{11}^o$	$C_{11} = C_{11}^o - 2(2\lambda_1 + \lambda_2)^2 A$
	$C_{22} = C_{11}^o - 2(2\lambda_1 - \lambda_2)^2 A$
$C_{33} = C_{33}^o$	$C_{33} = C_{33}^o$
$C_{12} = C_{12}^o$	$C_{12} = C_{12}^o - 2(2\lambda_1 + \lambda_2)(2\lambda_1 - \lambda_2)A$
$C_{13} = C_{23} = C_{13}^o$	$C_{13} = C_{23} = C_{13}^o$
$C_{11} - C_{12} = C_{11}^o - C_{12}^o$	$C_{11} - C_{12} = \left(C_{11}^o - C_{12}^o\right) - 4\left(\lambda_2^2 + 2\lambda_1\lambda_2\right)A$
	$\overline{C}_{11} - \overline{C}_{12} = \dfrac{1}{2}(C_{11} + C_{22} - 2C_{12}) = \left(C_{11}^o - C_{12}^o\right) - 4\lambda_2^2 A$
$C_{11} + C_{12} = C_{11}^o + C_{12}^o$	$C_{11} + C_{12} = \left(C_{11}^o + C_{12}^o\right) - 8\lambda_1(2\lambda_1 + \lambda_2)A$
	$\overline{C}_{11} + \overline{C}_{12} = \dfrac{1}{2}(C_{11} + C_{22} + 2C_{12}) = \left(C_{11}^o + C_{12}^o\right) - 16\lambda_1^2 A$
$C_{44} = C_{55} = C_{44}^o$	$C_{44} = C_{44}^o + 2(2\lambda_5 + \lambda_4)q_1^2$
	$C_{55} = C_{44}^o + 2(2\lambda_5 - \lambda_4)q_1^2$
$C_{66} = C_{66}^o$	$C_{66} = C_{66}^o + 4\lambda_6 q_1^2$

Under equilibrium conditions the degenerate components of Q are equal, *i.e.* $q_1 = q_2$ (Stokes & Hatch, 1988). Variations of the elastic constants can then be predicted from equation 79 in the usual way. The algebra becomes excessively complex if both the non-symmetry-breaking strains are included, and a set of variations has therefore been derived for the case of a second-order transition with $e_3 = 0$ ($\lambda_3 = 0$) but $(e_1 + e_2) \neq 0$ ($\lambda_1 \neq 0$). These are given in Table 9 and are illustrated in Fig. 9. Both $\left(C_{11} - C_{12}\right)$ and $\left(C_{11} + C_{12}\right)$ show a step at $T = T_c$, but only C_{44}, C_{55} and C_{66} are expected to show any marked temperature dependence at $T < T_c$.

6.3 *mmm* ⇌ *2/m*

Proper. Details of the symmetry properties of the elastic-constant matrix for a crystal with point group *mmm* are given in Table 10. For an equitranslational transition involving a symmetry change *mmm* ⇌ *2/m*, the active representation is B_{2g}, the symmetry-breaking strain is e_5 and the corresponding elastic constant is C_{55}. The non-symmetry-breaking (A_g) strains are e_1, e_2 and e_3. A_g eigenvalues and eigenvectors of the *mmm* elastic-constant matrix are analytically complex and the elastic energy is most easily handled in terms of the submatrix:

Pseudo-proper ferroelastic transition		
422 phase	222 phase, $e_{nsb} = 0$	222 phase, $e_{nsb} \neq 0$
$Q = 0$	$Q^2 = \frac{a}{b}\left(T_c^* - T\right), \quad T_c^* = T_c + \frac{2\lambda_2^2}{a\left(C_{11}^o - C_{12}^o\right)}$	$Q^2 = \frac{a}{b^*}\left(T_c^* - T\right), \quad T_c^* = T_c + \frac{2\lambda_2^2}{a\left(C_{11}^o - C_{12}^o\right)}$
		$b^* = b - 2\left[\frac{\lambda_3^2\left(C_{11}^o + C_{12}^o\right) + 2\lambda_1^2 C_{33}^o - 4\lambda_1\lambda_3 C_{13}^o}{\left(C_{11}^o + C_{12}^o\right)C_{33}^o - 2{C_{13}^o}^2}\right]$
$\chi^{-1} = a\left(T - T_c\right)$	$\chi^{-1} = 2a\left(T_c^* - T\right) + a\left(T_c^* - T_c\right)$	$\chi^{-1} = 2a\frac{b}{b^*}\left(T_c^* - T\right) + a\left(T_c^* - T_c\right)$
$C_{11} = C_{22} = C_{11}^o - \lambda_2^2\chi$	$C_{11} = C_{22} = C_{11}^o - \lambda_2^2\chi$	$C_{11} = C_{11}^o - \left(4\lambda_1^2Q^2 + \lambda_2^2 + 4\lambda_1\lambda_2 Q\right)\chi$
		$C_{22} = C_{11}^o - \left(4\lambda_1^2Q^2 + \lambda_2^2 - 4\lambda_1\lambda_2 Q\right)\chi$
$C_{33} = C_{33}^o$	$C_{33} = C_{33}^o$	$C_{33} = C_{33}^o - 4\lambda_3^2Q^2\chi$
$C_{12} = C_{12}^o + \lambda_2^2\chi$	$C_{12} = C_{12}^o + \lambda_2^2\chi$	$C_{12} = C_{12}^o - \left(4\lambda_1^2Q^2 - \lambda_2^2\right)\chi$
$C_{13} = C_{23} = C_{13}^o$	$C_{13} = C_{23} = C_{13}^o$	$C_{23} = C_{13}^o - \left(4\lambda_1\lambda_3Q^2 + 2\lambda_2\lambda_3 Q\right)\chi$
		$C_{23} = C_{13}^o - \left(4\lambda_1\lambda_3Q^2 - 2\lambda_2\lambda_3 Q\right)\chi$
$C_{11} - C_{12} = \left(C_{11}^o - C_{12}^o\right) - 2\lambda_2^2\chi$	$C_{11} - C_{12} = \left(C_{11}^o - C_{12}^o\right) - 2\lambda_2^2\chi$	$C_{11} - C_{12} = \left(C_{11}^o - C_{12}^o\right) - \left(2\lambda_2^2 + 4\lambda_1\lambda_2 Q\right)\chi$
	$\overline{C}_{11} - \overline{C}_{12} = \frac{1}{2}(C_{11} + C_{22} - 2C_{12})$	$\overline{C}_{11} - \overline{C}_{12} = \frac{1}{2}(C_{11} + C_{22} - 2C_{12})$
	$= \left(C_{11}^o - C_{12}^o\right) - 2\lambda_2^2\chi$	$= \left(C_{11}^o - C_{12}^o\right) - 2\lambda_2^2\chi$
$C_{11} + C_{12} = C_{11}^o + C_{12}^o$	$C_{11} + C_{12} = C_{11}^o + C_{12}^o$	$C_{11} + C_{12} = \left(C_{11}^o + C_{12}^o\right) - \left(8\lambda_1^2Q^2 + 4\lambda_1\lambda_2 Q\right)\chi$
	$\overline{C}_{11} + \overline{C}_{12} = \frac{1}{2}(C_{11} + C_{22} + 2C_{12})$	$\overline{C}_{11} + \overline{C}_{12} = \frac{1}{2}(C_{11} + C_{22} + 2C_{12})$
	$= C_{11}^o + C_{12}^o$	$= \left(C_{11}^o + C_{12}^o\right) - 8\lambda_1^2Q^2\chi$
$C_{44} = C_{55} = C_{44}^o$	$C_{44} = C_{44}^o + 2\lambda_4 Q$	$C_{44} = C_{44}^o + 2\lambda_4 Q$
	$C_{55} = C_{44}^o - 2\lambda_4 Q$	$C_{55} = C_{44}^o - 2\lambda_4 Q$
$C_{66} = C_{66}^o$	$C_{66} = C_{66}^o + 2\lambda_6 Q^2$	$C_{66} = C_{66}^o + 2\lambda_6 Q^2$

with phonons for which $< Q_\lambda^2 >$ also contains the active representation, but these are necessarily greatly restricted in number and any influence on the corresponding elastic constants must be relatively small. Such softening is usually not described in classical Landau theory and should not be mistaken for a sign of bilinear coupling between the order parameter and the spontaneous strain. Its magnitude depends on the force constants $\phi_{\alpha\beta}\begin{pmatrix} -q & q \\ j & j \end{pmatrix}$ and $\phi_{\gamma\lambda}\begin{pmatrix} -q & q \\ j & j \end{pmatrix}$ for a given material. Evidence that these are large would be provided by large mode Gruneisen parameters indicative of strong acoustic mode - optic mode coupling. If this type of softening is observed in the high-symmetry phase (above the transition point), it should also be expected in the low-symmetry phase below the transition point.

Having identified the significance of the interactions, it is now only necessary to give a formal description of the renormalisation involved. The coupling term $\phi_{\alpha\beta}\begin{pmatrix} -k & k \\ j & j \end{pmatrix}$ is written in real space as:

$$\phi_{\alpha\beta}\begin{pmatrix} -q & q \\ j & j \end{pmatrix} = \sum_{\bar{l}\bar{k}\bar{l}'\bar{k}'\mu\nu} \frac{8\pi^3}{NV_a}\left[\phi_{\alpha\mu\nu}\begin{pmatrix} \bar{l} & o & \bar{l}' \\ \bar{k} & k & k' \end{pmatrix} R_\beta\begin{pmatrix} \bar{l} \\ \bar{k} \end{pmatrix}\right] \cdot \frac{1}{\sqrt{m_k m_{k'}}} \xi_\mu\left(k\middle|\begin{matrix} q \\ j \end{matrix}\right)\xi_\nu\left(k'\middle|\begin{matrix} -q \\ j \end{matrix}\right)\exp\left[-2\pi i\vec{q}\vec{R}(l')\right] \qquad \text{(A.24).}$$

V_a is the volume per atomic unit, and $\phi_{\alpha\mu\nu}$ is the third-order anharmonic potential constant for the coupling between two phonon coordinates ξ and the displacement coordinate $(R.e)$. The vector $\vec{R}\begin{pmatrix} \bar{l} \\ \bar{k} \end{pmatrix}$ describes the equilibrium position of the atom $\bar{k}$ in unit cell $\bar{l}$ with mass m_k. The symmetry properties of $\phi_{\alpha\beta}\begin{pmatrix} -k & k \\ j & j \end{pmatrix}$ stem from the multiplication of $[\phi R]_{\alpha\mu\nu\beta}$ and $\xi_\mu\xi_\nu$ for each set of atoms. The matrix $[\phi R]_{\alpha\mu\nu\beta}$ has the full symmetry of the high-symmetry phase so that all symmetry constraints originate only from the product of phonon coordinates $\xi_\mu\xi_\nu$. As the tensor $\phi_{\alpha\beta}$ also describes the thermal expansion in the high-symmetry form, the symmetry of $\phi_{\alpha\beta}$ must be totally symmetric. These symmetry constraints limit the number of phonons which can interact and, hence, renormalise the elastic constants in this term: they must have opposite wavevectors and their amplitudes $\xi\left(k\middle|\begin{matrix} k \\ j \end{matrix}\right)$ and $\xi\left(k'\middle|\begin{matrix} k \\ j \end{matrix}\right)$ must form a totally symmetric tensor $\xi_\mu\left(k\middle|\begin{matrix} k \\ j \end{matrix}\right)\xi_\nu\left(k'\middle|\begin{matrix} k \\ j \end{matrix}\right)$. The tensor can be transformed into a diagonal form with the same principal axes as the tensor describing thermal expansion. It is then appropriate to rewrite the elastic constants in the same coordinate system spanned by the new principle axes. In highly symmetric systems, the standard setting of $C_{\alpha\beta\gamma\delta}$ is already in this coordinate system, while rotations are potentially necessary in monoclinic and triclinic crystals. Within the diagonal system, the relevant effective force constants are ϕ_{11}, ϕ_{22} and ϕ_{33}, with the usual identities for uniaxial systems ($\phi_{11} = \phi_{22}$) or elastically isotropic and cubic systems ($\phi_{11} = \phi_{22} = \phi_{33}$). The renormalised elastic constants are then ΔC_{11}, ΔC_{22}, ΔC_{33}, ΔC_{12}, ΔC_{13} and ΔC_{23} with possible relationships $\Delta C_{11} = \Delta C_{22}$, $\Delta C_{13} = \Delta C_{23}$ or $\Delta C_{11} = \Delta C_{22} = \Delta C_{33}$, $\Delta C_{12} = \Delta C_{13} = \Delta C_{23}$. A typical example of a uniaxial system is quartz, in which C_{11}, C_{33}, C_{12} and C_{13} soften as $T \rightarrow T_c$ but C_{44} and C_{66} do not. Further symmetry

constraints then follow trivially from matrix multiplication for quadratic corrections: $(\Delta C_{12})^2 = \Delta C_{11}\Delta C_{22}$, $(\Delta C_{13})^2 = \Delta C_{11}\Delta C_{33}$, $(\Delta C_{23})^2 = \Delta C_{22}\Delta C_{33}$. Note that these latter relationships apply to the high-symmetry phase above a transition point irrespective of which crystal system it belongs to. They refer equally to triclinic, monoclinic and orthorhombic systems, for example. For elastically uniaxial or isotropic/cubic materials they lead to: $\Delta C_{12} = \Delta C_{11}$, $(\Delta C_{23})^2 = (\Delta C_{13})^2 = \Delta C_{11}\Delta C_{33}$ or $\Delta C_{12} = \Delta C_{13} = \Delta C_{23} = \Delta C_{11} = \Delta C_{22} = \Delta C_{33}$, respectively.

Turning now to the dependence of ΔC on the frequency of the optical phonon, it becomes apparent that the form and anisotropy of its branches are important. At high temperatures ($2kT >> \hbar\omega$), the phonon amplitude may be approximated by $< Q^2 > \propto (kT/\omega)$, giving, for the j-th phonon branch:

$$\Delta C^{(jj)}_{\alpha\beta\gamma\lambda} \propto \int dq^3 \frac{kT}{\omega(q)^4} \phi_{\alpha\beta}(q)\phi_{\gamma\lambda}(q) \qquad \text{(A.25).}$$

For coupling terms which are independent of q an important relationship is obtained, namely:

$$\Delta C \propto \int dq^3 \frac{1}{\omega(q)^4} \qquad \text{(A.26).}$$

How does the temperature dependence of ΔC at $T > T_c$ now depend on the dispersion relation $\omega(q)$? Two extreme cases can be analysed rather easily using a parabolic q-dependence of ω, with the form:

$$\omega^2 = \varepsilon_o^2 \left(1 + \sum_{i=x,y,z} c_i^2 q_i^2 \right) \qquad \text{(A.27)}$$

where ε_o and c are proportionality constants. The dimensionality D of the dispersion is: $D = 1$ for $c_x << c_y, c_z$; $D = 2$ for $c_x, c_y << c_z$; $D = 3$ for $c_x \approx c_y \approx c_z$. Evaluating the relevant integral, the two most extreme assumptions for cq_{max}, namely $cq_{max} << 1$ and $cq_{max} >> 1$, are used. In the first case, for weak dispersion:

$$\int_0^{q_{max}} \frac{1}{\omega^4} dq^\delta \propto \frac{q_{max}^D}{\varepsilon_o^4} \qquad \text{(A.28).}$$

In the second case, for strong dispersion:

$$D = 1 \qquad \int_0^{q_{max}} \frac{1}{\omega^4} dq \propto \frac{1}{c\varepsilon_o^4} \qquad \text{(A.29)}$$

$$D = 2 \qquad \int_0^{q_{max}} \frac{1}{\omega^4} dq \propto \frac{1}{c^2\varepsilon_o^4} \qquad \text{(A.30)}$$

$$D=3 \qquad \int_0^{q_{max}} \frac{1}{\omega^4} dq \propto \frac{1}{c^3 \varepsilon_o^4} \qquad \text{(A.31).}$$

If a temperature dependence of ε_o similar to a soft mode, $\varepsilon_o^2 \propto \left(|T-T_c|+\varepsilon_{min}^2\right)$, is assumed, the variation of ΔC at $T >> T_c$ in the limit of weak dispersion is given by:

$$\Delta C \propto \frac{1}{|T-T_c|^2} \qquad \text{(A.32).}$$

In the case of strong dispersion, an additional temperature dependence may originate from the dispersion parameter, c. Taking $c \propto (1/\varepsilon_o)$ yields:

$$\Delta C(D=1) \propto |T-T_c|^{-3/2} \qquad \text{(A.33)}$$

$$\Delta C(D=2) \propto |T-T_c|^{-1} \qquad \text{(A.34)}$$

$$\Delta C(D=3) \propto |T-T_c|^{-1/2} \qquad \text{(A.35).}$$

The geometry of the dispersion relations giving rise to these four results for ΔC is illustrated in Fig. A.1.

This brief discussion demonstrates that the actual temperature dependence of this contribution to the elastic constant may vary considerably, depending on the dispersion of the coupled optical phonon. The strongest temperature dependence is expected for weak dispersion (independently of the dimensionality), and the weakest dependence occurs for three-dimensional systems with strong dispersion.

The fourth term in equation A.10 has the form:

$$-\delta_{\alpha\gamma} \sum_j \int dq^3 \phi_{\beta\gamma} \begin{pmatrix} q & -q \\ j & j \end{pmatrix} < Q^2 > \qquad \text{(A.36)}$$

and relates to internal strain generated by a field conjugate to the macroscopic strain. The origin of this form can be understood by noting that the macroscopic strain relates to local strain via:

$$e_{\alpha\beta}^{macroscopic} = \frac{1}{2}\left(e_{\alpha\beta} + e_{\beta\alpha} + \sum_\gamma e_{\gamma\alpha} e_{\beta\beta} \right) \qquad \text{(A.37).}$$

The strain has to be invariant with respect to small rotations of the sample:

$$e_{\alpha\beta}^{macroscopic} \rightarrow e_{\alpha\beta} + \omega_{\alpha\beta} + \sum_\sigma \omega_{\alpha\sigma} e_{\sigma\beta} \qquad \text{(A.38)}$$

where $\omega_{\alpha\beta} = -\omega_{\beta\alpha}$ is the rotatory part of the strain. Applying this transformation to elastic energies which are proportional to $e_{\alpha\beta}$ and $e_{\alpha\beta}^2$ gives, in linear order of $e_{\alpha\beta}$:

$$\delta h = \sum h^{(\alpha\beta)} e_{\alpha\beta} + \sum h^{(\alpha\beta)} \omega_{\alpha\beta} + \sum h^{(\alpha\beta)} \omega_{\alpha\gamma} e_{\gamma\beta} + \sum C_{\alpha\beta\gamma\lambda} e_{\alpha\beta} \omega_{\gamma\lambda} + \ldots \qquad \text{(A.39)}$$

where $h^{(\alpha\beta)} = h^{(\beta\alpha)}$ and $C_{\alpha\beta\gamma\lambda} = C_{\gamma\lambda\alpha\beta}$.

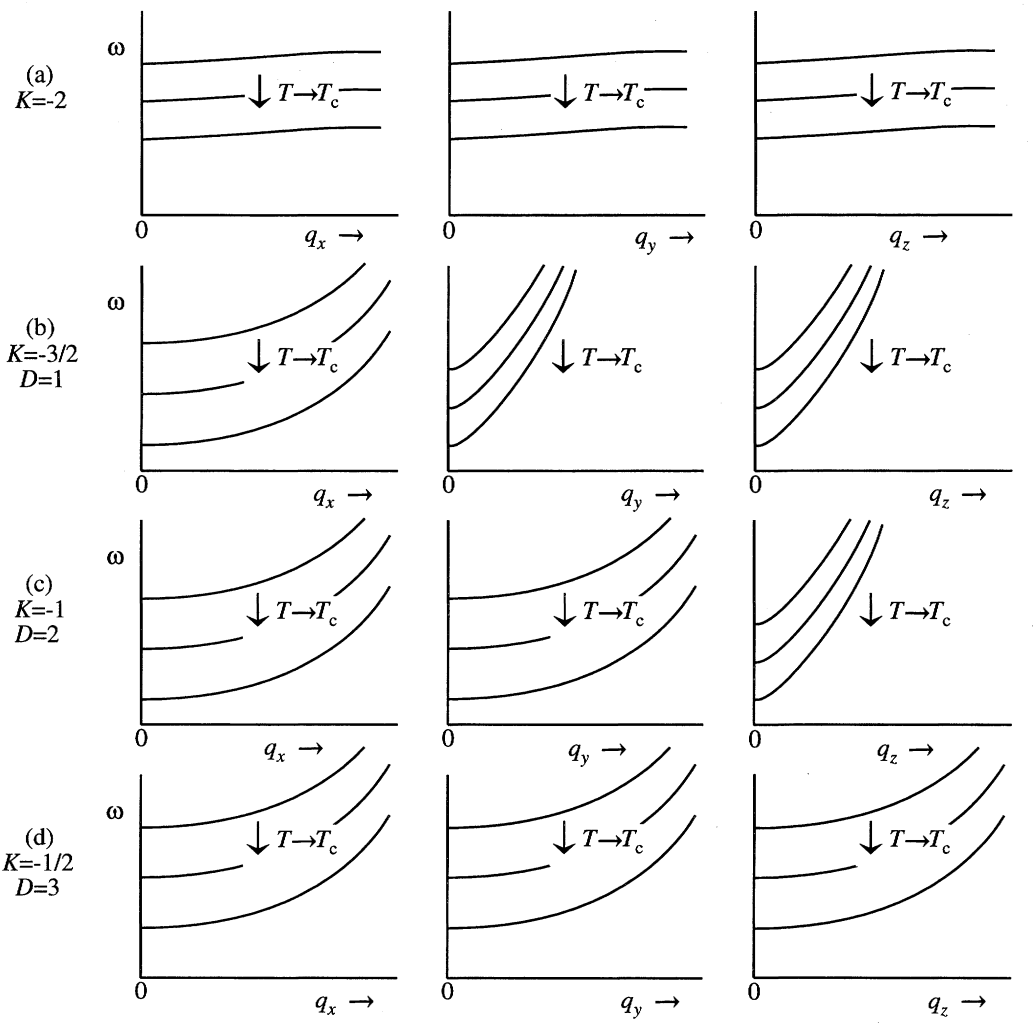

Fig. A.1. The geometry of dispersion relations giving rise to four different results for the exponent K in equation 97. This example is for a phase transition with a soft optic mode at the Brillouin zone centre, but the results apply equally well to zone-boundary soft modes. In (a) dispersion in all three orthogonal directions about the critical point is flat and softening occurs uniformly along the branches as $T \rightarrow T_c$. $K = -2$ is obtained. In (b), (c) and (d) the dispersion is steeper but occurs uniformly in one, two or three dimensions as $T \rightarrow T_c$, giving $K = -3/2$, -1 or $-1/2$, respectively.

The system is stable if $\left(\partial\delta h/\partial\omega_{\alpha\beta}\right)=0$, *i.e.* :

$$\sum_{\beta}\left(h^{(\mu\beta)}e_{\nu\beta}-h^{(\nu\beta)}e_{\mu\beta}\right)+\sum_{\alpha\beta}\left(C_{\alpha\beta\mu\nu}-C_{\alpha\beta\nu\mu}\right)e_{\alpha\beta}=0 \qquad \text{(A.40)}.$$

This condition is satisfied if:

$$h^{(\mu\lambda)}\delta_{\gamma\nu}-h^{(\nu\lambda)}\delta_{\gamma\mu}+C_{\mu\nu\gamma\lambda}-C_{\nu\mu\gamma\lambda}=0 \qquad \text{(A.41)}.$$

Rewriting the internal strain as macroscopic strain generates a quadratic term of the form $\sum_{\gamma}e_{\gamma\alpha}e_{\gamma\beta}$ in the macroscopic expression. The contribution to the elastic constants is:

$$C_{\alpha\beta\gamma\lambda}-C^{o}_{\alpha\beta\gamma\lambda}=-\delta_{\alpha\gamma}\Delta h^{(\beta\lambda)}$$
$$=-\delta_{\alpha\gamma}\left(\sum_{j}\int \mathrm{d}q^{3}\phi_{\beta\lambda}\begin{pmatrix}q & -q\\ j & j\end{pmatrix}<Q^{2}>\right) \qquad \text{(A.42)}.$$

An order of magnitude can be estimated for $\Delta h^{(\beta\lambda)}$ from the strain coordinate, $\Delta e=\left(\Delta h/C^{o}\right)\approx 10^{-3}$, which is of the same magnitude as the renormalisation of the elastic constants. Thus this effect is justifiably ignored in most applications of elastic theory.

References

Abrahams, S.C., Lissalde, F., Bernstein, J.L. (1978): Piezoelectric langbeinite-type $K_2Cd_2(SO_4)_3$ structure at four temperatures below and one above the 432°K ferroelastic-paraelastic transition. *J. Chem. Phys.*, **68**, 1926–1935.

Aleksandrov, K.S. & Flerov, I.N. (1979): Ranges of applicability of thermodynamic theory of structural phase transitions near the tricritical point. *Sov. Phys. Solid St.*, **21**, 195–200.

Aleksandrov, K.S. & Reshchikova, L.M. (1970): Twinning and birefringence in rhombic $KMnF_3$. *Sov. Phys. Crystallography*, **14**, 614–616.

Aleksandrov, K.S., Reshchikova, L.M., Beznosikov, B.V. (1966): Behaviour of the elastic constants of $KMnF_3$ single crystals near the transition of puckering. *Phys. Stat. Sol.*, **18**, K17–K20.

Als-Nielsen, J. & Birgeneau, R.J. (1977): Mean field theory, the Ginzburg criterion, and marginal dimensionality of phase transitions. *Am. J. Phys.*, **45**, 554–560.

Andrews, S.R. (1986): X-ray scattering study of the R-point instability in $SrTiO_3$. *J. Phys. C*, **19**, 3721–3743.

Angel, R.J. (1992): Order-disorder and the high-pressure $P\bar{1}-I\bar{1}$ transition in anorthite. *Am. Mineral.*, **77**, 923–929.

Angel, R.J., Redfern, S.A.T., Ross, N.L. (1989): Spontaneous strain below the $I\bar{1}-P\bar{1}$ transition in anorthite at pressure. *Phys. Chem. Minerals*, **16**, 539–544.

Antonenko, A.M., Volnyanskii, M.D., Kudzin, A.Yu. (1979): Third-order elastic constants of single crystals of paratellurite. *Sov. Phys. Crystallography*, **24**, 613–615.

Antonenko, A.M., Volnyanskii, M.D., Pozdeev, V.G. (1983): Elastic anomalies in phase transitions of $K_2Cd_2(SO_4)_3$. *Sov. Phys. Solid St.*, **25**, 1065–1066.

Åsbrink, S., Waskowska, A., Ratuszna, A. (1993): A high-pressure X-ray diffraction study of a phase transition in $KMnF_3$. *J. Phys. Chem. Solids*, **54**, 507–511.

Askarpour, V., Manghnani, M.H., Fassbender, S., Yoneda, A. (1993): Elasticity of single-crystal $MgAl_2O_4$ spinel up to 1273 K by Brillouin spectroscopy. *Phys. Chem. Minerals*, **19**, 511–519.

Atanasoff, J.V. & Hart, P.J. (1941): Dynamical determination of the elastic constants and their temperature coefficients for quartz. *Phys. Rev.*, **59**, 85–96.

Atanasoff, J.V. & Kammer, E. (1941): A determination of the C_{44} elastic constant for beta-quartz. *Phys. Rev.*, **59**, 97–99.

Aubry, S. & Pick, R. (1971): Soft-modes in displacive transitions. *J. de Physique*, **32**, 657–670.

Axe, J.D. & Shirane, G. (1970): Study of the α-β quartz phase transformation by inelastic neutron scattering. *Phys. Rev. B*, **1**, 342–348.

Bachheimer, J.P. & Dolino, G. (1975): Measurement of the order parameter of α-quartz by second-harmonic generation of light. *Phys. Rev. B*, **11**, 3195–3205.

Bambauer, H.U. & Nager, H.E. (1981): Gitterkonstanten und displazive Transformation synthetischer Erdalkalifeldspäte I. System $Ca[Al_2Si_2O_8]$-$Sr[Al_2Si_2O_8]$-$Ba[Al_2Si_2O_8]$. *N. Jb. Miner. Abh.*, **141**, 225–239.

Banda, E.J.K.B., Craven, R.A., Parks, R.D. (1975): α-β transition in quartz: classical versus critical behavior. *Solid St. Comm.*, **17**, 11–14.

Bell, R.O. & Rupprecht, G. (1963): Elastic constants of strontium titanate. *Phys. Rev.*, **129**, 90–94.

Benard, D.J. & Walker, W.C. (1976): Modulated polarization measurement of structural phase transitions in $KMnF_3$. *Rev. Sci. Instrum.*, **47**, 122–127.

Benyuan, Gu., Copic, M., Cummins, H.Z. (1981): Soft acoustic mode in ferroelastic $BiVO_4$. *Phys. Rev. B*, **24**, 4098–4100.

Berger, J.B. (1989): Elastic studies of phase transitions. *Phase Trans.*, **14**, 31–40.

Berger, J., Hauret, G., Rousseau, M. (1978): Brillouin scattering investigation of the structural phase transition of $TlCdF_3$ and $RbCaF_3$. *Solid St. Comm.*, **25**, 569–571.

Biellmann, C., Guyot, F., Gillet, P., Reynard, B. (1993): High-pressure stability of carbonates: quenching of calcite-II, high-pressure polymorph of $CaCO_3$. *Eur. J. Mineral.*, **5**, 503–510.

Bismayer, U., Schmahl, W., Schmidt, C., Groat, L.A. (1992): Linear birefringence and X-ray diffraction studies of the structural phase transition in titanite, $CaTiSiO_5$. *Phys. Chem. Minerals*, **19**, 260–266.

Boccara, N. (1968): Second-order phase transitions characterized by a deformation of the unit cell. *Annals of Physics*, **47**, 40–64.

Born, M. & Huang, K. (1954): Dynamical theory of crystal lattices. Clarendon Press, Oxford, 420 p.

Boysen, H. (1990): Neutron scattering and phase transitions in leucite. in "Phase transitions in ferroelastic and co-elastic crystals", E.K.H. Salje, ed. Cambridge University Press, Cambridge, 334–349.

Bradley, C.J. & Cracknell, A.P. (1972): The mathematical theory of symmetry in solids. Clarendon Press, Oxford, 745 p.

Brody, E.M. & Cummins, H.Z. (1974): Brillouin-scattering of the elastic anomaly in ferroelectric KH_2PO_4. *Phys. Rev. B*, **9**, 179–186.

Brown, J.M., Slutsky, L.J., Nelson, K.A., Cheng, L.-T. (1989): Single-crystal elastic constants for San Carlos peridot: an application of impulsive stimulated scattering. *J. Geophys. Res.*, **94**, 9485–9492.

Bruce, A.D. & Cowley, R.A. (1981): Structural phase transitions. Taylor and Francis, London, 326 p.

Brugger, K. (1965): Pure modes for elastic waves in crystals. *J. Appl. Phys.*, **36**, 759–768.

Bukowinski, M.S.T. & Wolf, G.H. (1988): Equation of state and possible critical phase transitions in $MgSiO_3$ perovskite at lower-mantle conditions. *in* " Structural and magnetic phase transitions in minerals", S. Ghose, J.M.D. Coey, E. Salje, eds. *Adv. Phys. Geochem.*, **7**, 91–112.

Bulou, A. (1992): On considering the elastic constant table as the matrix of an operator; consequences in ferroelasticity. *J. de Physique I*, **2**, 1445–1460.

Bulou, A., Rousseau, M., Nouet, J. (1992): Ferroelastic phase transitions and related phenomena. *Key Engineering Materials*, **68**, 133–186.

Buzaré, J.Y., Fayet, J.C., Berlinger, W., Müller, K.A. (1979): Tricritical behavior in uniaxially stressed $RbCaF_3$. *Phys. Rev. Lett.*, **42**, 465–468.

Cai, Q.R., Lan, G.X., Wang, H.F., Hong, G.Y. (1990): The effect of pressure on the ferroelastic phase transition in LnP_5O_{14}. *J. Phys. Chem. Solids*, **51**, 279–282.

Cameron, M. & Papike, J.J. (1980): Crystal chemistry of silicate pyroxenes. *Reviews in Mineralogy*, **7**, 5–92.

Cao, W. & Barsch, G.R. (1988): Elastic constants of $KMnF_3$ as functions of temperature and pressure. *Phys. Rev. B*, **38**, 7947–7958.

——, —— (1990): Landau-Ginzburg model of interphase boundaries in improper ferroelastic perovskites of D_{4h}^{18} symmetry. *Phys. Rev. B*, **41**, 4334–4348.

Carpenter, M.A. (1988): Thermochemistry of aluminium/silicon ordering in feldspar minerals. *in* "Physical properties and thermodynamic behaviour of minerals", E.K.H. Salje, ed. *NATO ASI series C*, **225**, 265–323.

—— (1992): Thermodynamics of phase transitions in minerals: a macroscopic approach. *in* "The stability of minerals", G.D. Price & N.L. Ross, eds. Chapman and Hall, London, 172–215.

Carpenter, M.A. & Cellai, D. (1996): Microstructures and high-temperature phase transitions in kalsilite. *Am. Mineral.*, **81**, 561–584.

Carpenter, M.A. & Salje, E.K.H. (1989): Time-dependent Landau theory for order/disorder processes in minerals. *Mineral. Mag.*, **53**, 483–504.

Carpenter, M.A., Salje, E.K.H., Graeme-Barber, A. (1998a): Spontaneous strain as a determinant of thermodynamic properties for phase transitions in minerals. *Eur. J. Mineral.*, **10**, 621–691.

Carpenter, M.A., Salje, E.K.H., Graeme-Barber, A., Wruck, B., Dove, M.T., Knight, K.S. (1998b): Calibration of excess thermodynamic properties and elastic constant variations due to the $\alpha \rightleftharpoons \beta$ phase transition in quartz. *Am. Mineral.*, **83**, 2–22.

Cellai, D., Carpenter, M.A., Heaney, P.J. (1992): Phase transitions and microstructures in natural kaliophilite. *Eur. J. Mineral.*, **4**, 1209–1220.

Cellai, D., Carpenter, M.A., Wruck, B., Salje, E.K.H. (1994): Characterization of high-temperature phase transitions in single crystals of Steinbach tridymite. *Am. Mineral.*, **79**, 606–614.

Chai. M., Brown, M.J., Slutsky, L.J. (1997): The elastic constants of a pyrope-grossular-almandine garnet to 20 GPa. *Geophys. Res. Lett.*, **24**, 523–526.

Chen, T. & Scott, J.F. (1989): Raman intensities near second order transitions: RP_5O_{14} ferroelastics (where R is a lanthanide). *Phys. Rev. B*, **40**, 8978–8982.

Chen, G., Spetzler, H., Getting, I.C. (1993): Elasticities and their T-derivatives of olivines with different Mg/(Fe+Mg) ratios from GHz ultrasonic interferometry. *EOS, Trans. Am. Geophys. Un.*, **74 (43)**, 676.

Cho, M. & Yagi, T. (1981): Brillouin scattering study of the successive phase transitions in K_2SeO_4. *J. Phys. Soc. Japan*, **50**, 543–550.

Chrosch, J., Bismayer, U., Salje, E.K.H. (1997): Anti-phase boundaries and phase transitions in titanite: an X-ray diffraction study. *Am. Mineral.*, **82**, 677–681.

Clarke, R. (1976): Phase transition studies of pure and flux-grown barium titanate crystals. *J. Appl. Cryst.*, **9**, 335–338.

Coe, R.S. & Paterson, M.S. (1969): The α-β inversion in quartz: a coherent phase transition under nonhydrostatic stress. *J. Geophys. Res.*, **74**, 4921–4948.

Cotton, F.A. (1990): Chemical applications of group theory (3rd edition). Wiley, New York, 461 p.

Cowley, R.A. (1976): Acoustic phonon instabilities and structural phase transitions. *Phys. Rev. B*, **13**, 4877–4885.

—— (1996): The phase transition of strontium titanate. *Phil. Trans. Roy. Soc. Lond. A*, **354**, 2799–2814.

Cox, U.J. (1989): The effect of impurities on the R-point instability in $KMnF_3$: I. An X-ray scattering study. *J. Phys. Condens. Matter*, **1**, 3365–3577.

Cox, U.J. & Cussen, L.D. (1989): The effect of impurities on the R-point instability in $KMnF_3$: II. A neutron scattering study. *J. Phys. Condens. Matter*, **1**, 3579–3589.

Cox, U.J., Gibaud, A., Cowley, R.A. (1988): Effect of impurities on the first-order phase transition of $KMnF_3$. *Phys. Rev. Lett.*, **61**, 982–985.

Cummins, H.Z. (1979): Brillouin scattering spectroscopy of ferroelectric and ferroelastic phase transitions. *Phil. Trans. Roy. Soc. Lond. A*, **293**, 393–405.

——— (1983): Brillouin scattering studies of phase transitions in crystals. *in* "Light scattering near phase transitions", H.Z. Cummins & A.P. Levanyuk, eds. North Holland Publishing Co., Amsterdam, New York, Oxford, 359–447.

Darlington, C.N.W., David, W.I.F., Knight, K.S. (1994): Structural study of barium titanate between 150 and 425 K. *Phase Trans.*, **48**, 217–236.

David, W.I.F. (1983a): Ferroelastic phase transition in $BiVO_4$: III. Thermodynamics. *J. Phys. C.*, **16**, 5093–5118.

——— (1983b): Structural relationships between spontaneous strain and acoustic properties in ferroelastics. *J. Phys. C.*, **16**, 2455–2470.

——— (1983c): Ferroelastic phase transitions in $BiVO_4$: IV. Relationships between spontaneous strain and acoustic properties. *J. Phys. C.*, **16**, 5119–5126.

——— (1984): Soft acoustic subspaces at elastic phase transitions. *J. Phys. C.*, **17**, 385–388.

Decker, D.L. & Zhao, Y.X. (1989): Dielectric and polarization measurements on $BaTiO_3$ at high pressures to the tricritical point. *Phys. Rev. B*, **39**, 2432–2438.

Deorani, S.C., Naithani, U.C., Semwal, B.S. (1990): Ultrasonic attenuation in $SrTiO_3$ perovskite above the phase transition. *J. Phys. Chem. Solids*, **51**, 1277–1280.

Devarajan, V. & Salje, E. (1984): Phase transition in $K_2Cd_2(SO_4)_3$: investigation of the non-linear dependence of spontaneous strain and morphic birefringence on order parameter as determined from excess entropy measurements. *J. Phys. C*, **17**, 5525–5537.

———, ——— (1986): Phase transitions in langbeinites II: Raman spectroscopic investigations of $K_2Cd_2(SO_4)_3$. *Phys. Chem. Minerals*, **13**, 25–30.

Dolino, G. (1988): Incommensurate phase transitions in quartz and berlinite. *in* " Structural and magnetic phase transitions in minerals", S. Ghose, J.M.D. Coey, E. Salje, eds. *Adv. Phys. Geochem.*, **7**, 17–38.

——— (1990): The α-inc-β transitions of quartz: a century of research on displacive phase transitions. *Phase Trans.*, **21**, 59–72.

Dolino, G. & Bachheimer, J.P. (1982): Effect of the α-β transition on mechanical properties of quartz. *Ferroelectrics*, **43**, 77–86.

Dolino, G. & Vallade, M. (1994): Lattice dynamical behavior of anhydrous silica. *Reviews in Mineralogy*, **29**, 403–431.

Dolino, G., Berge, B., Vallade, M., Moussa, F. (1989): Inelastic neutron scattering studies of the origin of the incommensurate phase of quartz. *Physica B.*, **156**, 15–16.

———, ———, ———, ——— (1992): Origin of the incommensurate phase of quartz: I. Inelastic neutron scattering study of the high temperature β phase of quartz. *J. de Physique I*, **2**, 1461–1480.

Dombal, R.F. de & Carpenter, M.A. (1993): High-temperature phase transitions in Steinbach tridymite. *Eur. J. Mineral.*, **5**, 607–622.

Dorner, B. (1981): Investigation of structural phase transformations by inelastic neutron scattering. *in* " Structural phase transitions I", K.A. Muller & H. Thomas, eds. Springer Verlag, Berlin, Heidelberg, New York, *Topics in Current Physics*, **23**, 93–130.

Dove, M.T. (1993): Introduction to lattice dynamics. Cambridge University Press, Cambridge, 258 p.

——— (1997): Theory of displacive phase transitions in minerals. *Am. Mineral.*, **82**, 213–244.

Dove, M.T. & Powell, B.M. (1989): Neutron diffraction study of the tricritical orientational order/disorder phase transition in calcite at 1260 K. *Phys. Chem. Minerals,* **16**, 503–507.

Dove, M.T., Keen, D.A., Hannon, A.C., Swainson, I.P. (1997): Direct measurement of the Si-O bond length and orientational disorder in the high-temperature phase of cristobalite. *Phys. Chem. Minerals*, **24**, 311–317.

Dvorak, V. (1971): The origin of the structural phase transition in $Gd_2(MoO_4)_3$. *Phys. Stat. Sol. (b)*, **45**, 147–152.

Errandonea, G. (1980): Elastic and mechanical studies of the transition in LaP_5O_{14}: a continuous ferroelastic transition with a classical Landau-type behavior. *Phys. Rev. B,* **21**, 5221–5236.

Errandonea, G. & Bastie, P. (1978): Investigation of the second order transition in lanthanum pentaphosphate. *Ferroelectrics*, **21**, 571–572.

Errandonea, G. & Sapriel, J. (1979): Polarized Raman study of the ferroelastic transition in lanthanum pentaphosphate. *Solid St. Comm.*, **32**, 391–395.

Errandonea, G. & Savary, H. (1981): Raman scattering study of the ferroelastic transition of LaP_5O_{14} under hydrostatic pressure. *Phys. Rev. B*, **24**, 1292–1297.

Feile, R., Loidl, A., Knorr, K. (1982): Elastic properties of $(KBr)_{1-x}(KCN)_x$. *Phys. Rev. B*, **26**, 6875–6880.

Finnie, K.S., Thompson, J.G., Withers, R.L. (1994): Phase transitions in cristobalite and related structures studied by variable temperature infra-red emission spectroscopy. *J. Phys. Chem. Solids*, **55**, 23–29.

Fischer, M. & Polian, A. (1987): Elastic properties of $BaTiO_3$ at high pressure. *Phase Trans.*, **9**, 205–213.

Fischer, G.J., Wang, Z, Karato, S. (1993): Elasticity of $CaTiO_3$, $SrTiO_3$ and $BaTiO_3$ perovskites up to 3.0 GPa: the effect of crystallographic structure. *Phys. Chem. Minerals*, **20**, 97–103.

Fleury, P.A. & Lyons, K. (1981): Optical studies of structural phase transitions. *in* " Structural phase transitions I", K.A. Muller & H. Thomas, eds. Springer Verlag, Berlin, Heidelberg, New York, *Topics in Current Physics*, **23**, 9–92.

Folk, R., Iro, H., Schwabl, F. (1976a): Critical statics of elastic phase transitions. *Z. Physik. B*, **25**, 69–81.

——— , ——— , ——— (1976b): Elastic phase transitions of second order. *Phys. Lett.*, **57A**, 112–114.

——— , ——— , ——— (1979): Critical dynamics of elastic phase transitions. *Phys. Rev. B*, **20**, 1229–1244.

Fossheim, K. & Berre, B. (1972): Ultrasonic propagation, stress effects, and interaction parameters at the displacive transition in $SrTiO_3$. *Phys. Rev. B*, **5**, 3292–3308.

Fossheim, K. & Fossum, J.O. (1984): Critical dynamics of sound. *in* "Multicritical phenomena", R. Pynn & A. Skjeltorp, eds. *NATO ASI Series B*, **106**, 113–128.

Fossheim, K. & Holt, R.M. (1980): Critical dynamics of sound in $KMnF_3$. *Phys. Rev. Lett.*, **45**, 730–733.

Fossheim, K., Martinsen, D., Linz, A. (1974): Critical sound velocity and attenuation in $KMnF_3$. *in* "Anharmonic lattices, structural transitions and melting", T. Riste, ed. *NATO ASI Applied Sciences*, **1**, 141–146. Noordhoff, Leiden.

Fossum, J.O. (1985): A phenomenological analysis of ultrasound near phase transitions. *J. Phys. C*, **18**, 5531–5548.

Fossum, J.O. & Fossheim, K. (1985): Measurements of ultrasonic attenuation and velocity in Verneuil-grown and flux-grown $SrTiO_3$. *J. Phys. C*, **18**, 5549–5578.

Fousek, J., Konak, C., Errandonea, G. (1979): Phase-transition-induced changes in optical properties of ferroelectric $(La,Nd)P_5O_{14}$. *J. Phys. C*, **12**, 3197–3203.

Franke, V. & Hegenbarth, E. (1974): Specific heat measurements of $SrTiO_3$ near 110 K. *Phys. Stat. Sol. (a)*, **25**, K17–K19.

Funamori, N. & Yagi, T. (1993): High pressure and high temperature in situ X-ray observation of $MgSiO_3$ perovskite under lower mantle conditions. *Geophys. Res. Lett.*, **20**, 387–390.

Furukawa, M., Fujimori, Y., Hirakawa, K. (1970): Ultrasonic attenuation near the soft mode transition point in $KMnF_3$. *J. Phys. Soc. Japan*, **29**, 1528–1532.

Gesi, K., Axe, J.D., Shirane, G., Linz, A. (1972): Dispersion and damping of soft zone-boundary phonons in $KMnF_3$. *Phys. Rev. B*, **5**, 1933–1941.

Ghose, S., Ito, Y., Hatch, D.M. (1991): Paraelectric-antiferroelectric phase transition in titanite, $CaTiSiO_5$ I. A high temperature X-ray diffraction study of the order parameter and transition mechanism. *Phys. Chem. Minerals*, **17**, 591–603.

Gibaud, A., Cowley, R.A., Nouet, J. (1989): A high-resolution X-ray scattering study of the effect of defects on the first-order transition in $KMnF_3$. *Phase Trans.*, **14**, 129–138.

Gibaud, A., Shapiro, S.M., Nouet, J., You, H. (1991): Phase diagram of $KMn_{1-x}Ca_xF_3$ ($x < 0.05$) determined by high-resolution X-ray scattering. *Phys. Rev. B*, **44**, 2437–2443.

Ginzburg, V.L., Levanyuk, A.P., Sobyanin, A.A. (1987): Comments on the region of applicability of the Landau theory for structural phase transitions. *Ferroelectrics*, **73**, 171–182.

Goto, T., Anderson, O.L., Ohno, I., Yamamoto, S. (1989): Elastic constants of corundum up to 1825 K. *J. Geophys. Res. B*, **94**, 7588–7602.

Graetsch, H. & Flörke, O.W. (1991): X-ray powder diffraction patterns and phase relationship of tridymite modifications. *Z. Krist.*, **195**, 31–48.

Grimm, H. & Dorner, B. (1975): On the mechanism of the α-β phase transformation of quartz. *J. Phys. Chem. Solids*, **36**, 407–413.

Groat, L.A., Bismayer, U., Güttler, B. (1995): A ferroelastic phase transition in vesuvianite. *Phase Trans.*, **55**, 217–227.

Grögel, T., Boysen, H., Frey, F. (1984): Phase transition and ordering in leucite. *Acta Cryst.*, **A40** (supplement), C256–C257.

Guelylah, A., Aroyo, M.I., Pérez-Mato, J.M. (1996): Microscopic distortion and order parameter in langbeinite $K_2Cd_2(SO_4)_3$. *Phase Trans.*, **59**, 155–179.

Hara, K., Sawada, A., Ishibashi, Y. (1989): High pressure Raman scattering study of $LaNbO_4$ and $NdNbO_4$. *Ferroelectrics*, **96**, 25–27.

Harris, M.J. & Dove, M.T. (1995): Lattice melting at structural phase transitions. *Modern Phys. Lett.*, **B9**, 67–85.

Harris, M.J., Cowley, R.A., Swainson, I.P., Dove, M.T. (1993): Observation of lattice melting at the ferroelastic phase transition in Na_2CO_3. *Phys. Rev. Lett.*, **71**, 2939–2942.

Harris, M.J., Dove, M.T., Godfrey, K.W. (1995): Observation of lattice melting in a single crystal: the ferroelastic phase transition in Na_2CO_3. *Phys. Rev. B*, **51**, 6758–6760.

Harrison, R.J. & Salje, E.K.H. (1994): X-ray diffraction study of the displacive phase transition in anorthoclase, grain-size effects and surface relaxations. *Phys. Chem. Minerals*, **21**, 325–329.

Hatch, D.M. (1981): Order parameter symmetry for the β-γ transition in $Pb_3(VO_4)_2$. *Phys. Stat. Sol. (b)*, **106**, 473–479.

Hatch, D.M. & Ghose, S. (1989): A dynamical model for the $I\bar{1} - P\bar{1}$ phase transition in anorthite, $CaAl_2Si_2O_8$ II. Order parameter treatment. *Phys. Chem. Minerals*, **16**, 614–620.

——, —— (1991): The α-β phase transition in cristobalite, SiO_2. Symmetry analysis, domain structure, and the dynamical nature of the β-phase. *Phys. Chem. Minerals*, **17**, 554–562.

Hatch, D.M. & Merrill, L. (1981): Landau description of the calcite-$CaCO_3$(II) phase transition. *Phys. Rev. B*, **23**, 368–374.

Hatch, D.M., Ghose, S., Stokes, H.T. (1990a): Phase transitions in leucite, $KAlSi_2O_6$ I. Symmetry analysis with order parameter treatment and the resulting microscopic distortions. *Phys. Chem. Minerals*, **17**, 220–227.

Hatch, D.M., Artman, J.I., Boerio-Goates, J. (1990b): Phase transition in $K_2Cd_2(SO_4)_3$: order parameter and microscopic distortions. *Phys. Chem. Minerals*, **17**, 334–343.

Hatch, D.M., Ghose, S., Bjorkstam, J.L. (1994): The α-β phase transition in $AlPO_4$ cristobalite: symmetry analysis, domain structure and transition dynamics. *Phys. Chem. Minerals*, **21**, 67–77.

Haussühl, S. (1993): Thermoelastic properties of beryl, topaz, diaspore, sanidine and periclase. *Z. Krist.*, **204**, 67–76.

Hazen, R.M. & Finger, L.W. (1983): High-pressure and high-temperature crystallographic study of gillespite I-II phase transition. *Am. Mineral.*, **68**, 595–603.

Heaney, P.J. (1994): Structure and chemistry of the low-pressure silica polymorphs. *Reviews in Mineralogy*, **29**, 1–40.

Heaney, P.J. & Veblen, D.R. (1990): A high-temperature study of the low-high leucite phase transition using the transmission electron microscope. *Am. Mineral.*, **75**, 464–476.

Hemley, R.J. & Cohen, R.E. (1992): Silicate perovskite. *Ann. Rev. Earth Planet. Sci.*, **20**, 553–600.

Hidaka, M., Fujii, H., Maeda, S. (1986): Structural phase transition of $KMnF_3$. *Phase Trans.*, **6**, 101–114.

Hill, R. (1952): The elastic behaviour of a crystalline aggregate. *Proc. Phys. Soc. Lond. A*, **65**, 349–354.

Hirotsu, S. & Sawada, S. (1973): Spontaneous birefringence and order parameter of $KMnF_3$ below the 186°K transition point. *Solid St. Comm.*, **12**, 1003–1005.

Höchli, U.T. (1970): Ultrasonic investigation of the first-order α-β phase transition in quartz. *Solid St. Comm.*, **8**, 1487–1490.

—— (1972): Elastic constants and soft optical modes in gadolinium molybdate. *Phys. Rev. B*, **6**, 1814–1823.

Höchli, U.T. & Scott, J.F. (1971): Displacement parameter, soft-mode frequency, and fluctuations in quartz below its α-β phase transition. *Phys. Rev. Lett.*, **26**, 1627–1629.

Holt, R.M. & Fossheim, K. (1981): Ultrasonic investigation of critical dynamics in $KMnF_3$. *Phys. Rev. B*, **24**, 2680–2692.

Irie, K., Shiono, M., Nakamura, H., Ohnishi, N., Okazaki, A. (1987): High-resolution X-ray diffraction study of the cubic-to-tetragonal transition in $BaTiO_3$. *Solid St. Comm.*, **62**, 691–693.

Isaak, D.G. & Masuda, K. (1995): Elastic and viscoelastic properties of α iron at high temperatures. *J. Geophys. Res.*, **100**, 17689–17698.

Isaak, D.G., Anderson, O.L., Goto, T. (1989): Measured elastic moduli of single-crystal MgO up to 1800 K. *Phys. Chem. Minerals*, **16**, 704–713.

Ishibashi, Y., Hara, K., Sawada, A. (1988): The ferroelastic transition in some scheelite-type crystals. *Physica B*, **150**, 258–264.

Ishidate, T. & Sasaki, S. (1989): Elastic anomaly and phase transition of $BaTiO_3$. *Phys. Rev. Lett.*, **62**, 67–70.

Ito, Y., Kuehner, S., Ghose, S. (1991): Phase transitions in leucite determined by high temperature, single crystal X-ray diffraction. *Z. Krist.*, **197**, 75–84.

Jackson, I., Khanna, S.K., Revcolevschi, A., Berthon, J. (1990): Elasticity, shear-mode softening and high-pressure polymorphism of wüstite ($Fe_{1-x}O$). *J. Geophys. Res. B*, **95**, 21671–21685.

Kammer, E.W., Pardue, T.E., Frissel, H.F. (1948): A determination of the elastic constants for beta-quartz. *J. Appl. Phys.*, **19**, 265–270.

Kaminsky, W. (1996): Reinvestigation of optical activity in the course of the ferroelastic phase transition in cadmium langbeinite, $K_2Cd_2(SO_4)_3$. *Phase Trans.*, **59**, 121–133.

Kapusta, B. & Guillopé, M. (1993): Molecular dynamics study of the perovskite $MgSiO_3$ at high temperature: structural, elastic and thermodynamical properties. *Phys. Earth Planet. Int.*, **75**, 205–224.

Kihara, K. (1990): An X-ray study of the temperature dependence of the quartz structure. *Eur. J. Mineral.*, **2**, 63–77.

Kihara, K., Matsumoto, T., Imamura, M. (1986a): Structural change of orthorhombic-I tridymite with temperature: study based on second-order thermal-vibrational parameters. *Z. Krist.*, **177**, 27–38.

——, ——, —— (1986b): High-order thermal-motion tensor analyses of tridymite. *Z. Krist.*, **177**, 39–52.

Kitchin, S.J., Kohn, S.C., Dupree, R., Henderson, C.M.B., Kihara, K. (1996): In situ ^{29}Si MAS NMR studies of structural phase transitions of tridymite. *Am. Mineral.*, **81**, 550–560.

Kityk, A.V., Sopronyuk, V.P., Fuith, A., Schranz, W., Warhanek, H. (1996): Low frequency elastic properties of the incommensurate ferroelastic $[N(CH_3)_4]_2CuCl_4$. *Phys. Rev. B*, **53**, 6337–6344.

Kleemann, W., Schäfer, F.J., Nouet, J. (1979): Linear birefringence studies on weakly discontinuous structural phase transitions in fluo-perovskites and layered copper halides. *Physica*, **97B**, 145–155.

Knorr, K., Loidl, A., Kjems, J.K. (1986): Ferroelastic transition in KBr:KCN studied by neutrons, X-rays and ultrasonics. *Physica*, **136B**, 311–314.

Kovaleva, L.A., Petrov, A.A., Anistratov, A.T. (1988): Birefringence and cubic-tetragonal phase transition in barium titanate. *Sov. Phys. Solid St.*, **30**, 1050–1052.

Kroll, H., Bambauer, H.-U., Schirmer, U. (1980): The high albite-monalbite and analbite-monalbite transitions. *Am. Mineral.*, **65**, 1192–1211.

Kunz, M., Xirouchakis, D., Lindsley, D.H., Häusermann, D. (1996): High-pressure phase transition in titanite ($CaTiOSiO_4$). *Am. Mineral.*, **81**, 1527–1530.

Landau, L.D. & Lifshitz, E.M. (1986): Theory of elasticity. *Course of theoretical physics*, **7** (3rd edition). Pergamon, Oxford, 187 p.

Lange, R.A., Carmichael, I.S.E., Stebbins, J.F. (1986): Phase transitions in leucite ($KAlSi_2O_6$), orthorhombic $KAlSiO_4$, and their iron analogues ($KFeSi_2O_6$, $KFeSiO_4$). *Am. Mineral.*, **71**, 937–945.

Levanyuk, A.P., Minyukov, S.A., Vallade, M. (1993): Fluctuation-induced first-order phase transitions near mean-field tricritical points in solids. *J. Phys. Condens. Matter*, **5**, 4419–4428.

Liakos, J.K. & Saunders, G.A. (1982): Application of the Landau theory to elastic phase transitions. *Phil. Mag. A*, **46**, 217–242.

Libowitzky, E. & Armbruster, T. (1995): Low-temperature phase transitions and the role of hydrogen bonds in lawsonite. *Am. Mineral.*, **80**, 1277–1285.

Lissalde, F., Abrahams, S.C., Bernstein, J.L., Nassau, K. (1979): X-ray diffraction and dielectric temperature dependence study of the $K_2Cd_2(SO_4)_3$ paraelastic-ferroelastic transition. *J. Appl. Phys.*, **50**, 845–851.

Lüthi, B. & Moran, T.J. (1970): Sound propagation near the structural phase transition in strontium titanate. *Phys. Rev. B*, **2**, 1211–1214.

Lüthi, B. & Rehwald, W. (1981): Ultrasonic studies near structural phase transitions. *in* " Structural phase transitions I", K.A. Muller & H. Thomas, eds. Springer Verlag, Berlin, Heidelberg, New York, *Topics in Current Physics*, **23**, 131–184.

Malinowski, M., Lukaszewicz, K., Åsbrink, S. (1986): The influence of high hydrostatic pressure on lattice parameters of a single crystal of $BaTiO_3$. *J. Appl. Cryst.*, **19**, 7–9.

Mao, H.K., Hemley, R.J., Fei, Y., Shu, J.F., Chen, L.C., Jephcoat, A.P., Wu, Y., Bassett, W.A. (1991): Effect of pressure, temperature, and composition on lattice parameters and density of $(Fe,Mg)SiO_3$-perovskites to 30 GPa. *J. Geophys. Res.*, **96**, 8069–8079.

Mayer, A.P. & Cowley, R.A. (1988): The continuous melting transition of a three-dimensional crystal at a planar elastic instability. *J. Phys. C*, **21**, 4827–4834.

Maynard, J. (1996): Resonant ultrasound spectroscopy. *Physics Today*, **49**, 26–31.

McGuinn, M.D. & Redfern, S.A.T. (1994a): Ferroelastic phase transition along the join $CaAl_2Si_2O_8$-$SrAl_2Si_2O_8$. *Am. Mineral.*, **79**, 24–30.

———, ——— (1994b): Ferroelastic phase transition in $SrAl_2Si_2O_8$ at elevated pressure. *Min. Mag.*, **58**, 21–26.

———, ——— (1997): High-temperature ferroelastic strain below the $I2/c - I\bar{1}$ transition in $Ca_{1-x}Sr_xAl_2Si_2O_8$ feldspars. *Eur J. Mineral.*, **9**, 1159–1162.

McLellan, A.G. (1973): Thermodynamic stability of the α-β quartz transition. *Phil. Mag.*, **28**, 1077–1086.

——— (1980): The classical thermodynamics of deformable materials. Cambridge University Press, Cambridge, 338 p.

McMorrow, D.F., Hamaya, N., Shimomura, S., Fujii, Y., Kishimoto, S., Iwasaki, H. (1990): On the length scales of the critical fluctuations in $SrTiO_3$. *Solid St. Comm.*, **76**, 443–448.

McWhan, D.B., Birgeneau, R.J., Bonner, W.A., Taub, H., Axe, J.D. (1975): Neutron scattering study at high pressure of the structural phase transition in paratellurite. *J. Phys. C*, **8**, L81–L85.

Melcher, R.L. & Plovnik, R.H. (1971): The anomalous elastic behavior of $KMnF_3$ near a structural phase transition. *in* "Phonons", M.A. Nusimovici, ed. Flammarion, Paris, 348–352.

Merrill, L. & Bassett, W.A. (1975): The crystal structure of $CaCO_3$ (II), a high-pressure metastable phase of calcium carbonate. *Acta Cryst.*, **B31**, 343–349.

Meyer, H.W., Zhang, M., Bismayer, U., Salje, E.K.H., Schmidt, C., Kek, S., Morgenroth, W., Bleser, T. (1996): Phase transformation of natural titanite: an infrared, Raman spectroscopic, optical birefringence and X-ray diffraction study. *Phase Trans.*, **59**, 39–60.

Migliori, A., Sarrao, J.L., Visscher, W.M., Bell, T.M., Ming Lei, Fisk, Z., Leisure, R.G. (1993): Resonant ultrasound spectroscopic techniques for measurement of the elastic moduli of solids. *Physica B*, **183**, 1–24.

Minkiewicz, V. J., Fujii, Y., Yamada, Y. (1970): X-ray scattering and the phase transition of $KMnF_3$ at 184°K. *J. Phys. Soc. Japan*, **28**, 443–450.

Moiseenko, V.N., Pozdeev, V.G., Pastukhov, V.I. (1983): Vibrational spectra of potassium cadmium langbeinite near its phase transition. *Sov. Phys. Solid State*, **25**, 1262–1263.

Müller, K.A. & Berlinger, W. (1971): Static critical exponents at structural phase transitions. *Phys. Rev. Lett.*, **26**, 13–16.

Musgrave, M.J.P. (1970): Crystal acoustics. Holden-Day, San Francisco, London, Amsterdam, 288 p.

Nager, H.E., Bambauer, H.U., Hoffmann, W. (1970): Polymorphie in der Mischreihe $(Ca,Sr)[Al_2Si_2O_6]$. *Naturwiss.*, **57**, 86–87.

Navrotsky, A. & Weidner, D.J. (1989): Perovskite: a structure of great interest to geophysics and materials science. *Geophysical Monograph Series*, **45**. American Geophysical Union, Washington D.C., 146 p.

Nelmes, R.J., Hatton, P.E., Vass, H. (1988): Observations of a very large critical length scale in $SrTiO_3$. *Phys. Rev. Lett.*, **60**, 2172–2175.

Nicholls, U.J. & Cowley, R.A. (1987): Determination of the critical exponents at the R-point instability in $KMnF_3$. *J. Phys. C*, **20**, 3417–3437.

Nye, J.F. (1985): Physical properties of crystals. Oxford University Press, Oxford, 329 p.

Ohno, I. (1995): Temperature variation of elastic properties of α-quartz up to the α-β transition. *J. Phys. Earth*, **43**, 157–169.

Okai, B. & Yoshimoto, J. (1975): Pressure dependence of the structural phase transition temperature in $SrTiO_3$ and $KMnF_3$. *J. Phys. Soc. Japan*, **39**, 162–165.

Palmer, D.C. (1990a): Volume anomaly and the impure ferroelastic phase transition in leucite. *in* "Phase transitions in ferroelastic and co-elastic crystals", E.K.H. Salje, ed. Cambridge University Press, Cambridge, 350–366.

——— (1990b): Phase transitions in leucite. Ph. D. thesis, University of Cambridge.

Palmer, D.C. & Salje, E.K.H. (1990): Phase transitions in leucite: dielectric properties and transition mechanism. *Phys. Chem. Minerals*, **17**, 444–452.

Palmer, D.C., Putnis, A., Salje, E.K.H. (1988): Twinning in tetragonal leucite. *Phys. Chem. Minerals*, **16**, 298–303.

Palmer, D.C., Salje, E.K.H., Schmahl, W.W. (1989): Phase transitions in leucite: X-ray diffraction study. *Phys. Chem. Minerals*, **16**, 714–719.

Palmer, D.C., Bismayer, U., Salje, E.K.H. (1990): Phase transitions in leucite: order parameter behaviour and the Landau potential deduced from Raman spectroscopy and birefringence studies. *Phys. Chem. Minerals*, **17**, 259–265.

Palmer, D.C., Dove, M.T., Ibberson, R.M., Powell, B.M. (1997): Structural behavior, crystal chemistry, and phase transitions in substituted leucite: high-resolution neutron diffraction studies. *Am. Mineral.*, **82**, 16–29.

Peacor, D.R. (1968): A high temperature single crystal diffractometer study of leucite, $(K,Na)AlSi_2O_6$. *Z. Krist.*, **127**, 213–224.

Peercy, P.S. & Fritz, I.J. (1974): Pressure-induced phase transition in paratellurite (TeO_2). *Phys. Rev. Lett.*, **32**, 466–469.

Peercy, P.S., Fritz, I.J., Samara, G.A. (1975): Temperature and pressure dependences of the properties and phase transition in paratellurite (TeO_2): ultrasonic, dielectric and Raman and Brillouin scattering results. *J. Phys. Chem. Solids*, **36**, 1105–1122.

Pelous, J. & Vacher, R. (1976): Thermal Brillouin scattering in crystalline and fused quartz from 20 to 1000°C. *Solid St. Comm.*, **18**, 657–661.

Percival, M.J.L. (1990): A trigger mechanism in an improper ferroelastic: the langbeinite structure. *in* "Phase transitions in ferroelastic and co-elastic crystals", E.K.H.Salje, ed. Cambridge University Press, Cambridge, 296–309.

Percival, M.J.L. & Salje, E. (1989): Optical absorption spectroscopy of the $P2_13$–$P2_12_12_1$ transformation in $K_2Co_2(SO_4)_3$ langbeinite. *Phys. Chem. Minerals*, **16**, 563–568.

Percival, M.J.L., Schmahl, W.W., Salje, E. (1989): Structure of cobalt doped $K_2Cd_2(SO_4)_3$ langbeinite at three temperatures above the $P2_13$–$P2_12_12_1$ phase transition, and a new trigger mechanism for the ferroelastic transformation. *Phys. Chem. Minerals*, **16**, 569–575.

Pinczuk, A., Burns, G., Dacol, F.H. (1977): Soft optical phonon in ferroelastic $BiVO_4$. *Solid St. Comm.*, **24**, 163–165.

Pinczuk, A., Webber, B., Dacol, F.H. (1979): Mechanisms of the ferroelastic transition in $BiVO_4$. *Solid St. Comm.*, **29**, 515–518.

Prewitt, C.T., Papike, J.J., Ross, M. (1970): Cummingtonite: a reversible, nonquenchable transition from $P2_1/m$ to $C2/m$ symmetry. *Earth Planet. Sci. Lett.*, **8**, 448–450.

Pytte, E. (1970): Soft-mode damping and ultrasonic attenuation at a structural phase transition. *Phys. Rev. B*, **1**, 924–930.

——— (1971): Acoustic anomalies at structural phase transitions. *in* "Structural phase transitions and soft modes", E.J. Samuelsen, E. Anderson, J. Feder, eds. *NATO ASI, Norway*. Scandinavian University Books, Oslo, 151–169.

Ramirez, R., Lapeña, M.F., Gonzalo, J.A. (1990): Pressure dependence of free-energy expansion coefficients in $PbTiO_3$ and $BaTiO_3$ and tricritical-point behaviour. *Phys. Rev. B*, **42**, 2604–2606.

Ratuszna, A., Pietraszko, A., Chelkowski, A., Lukaszewicz, K. (1979): The temperature dependence of lattice parameters of $KMeF_3$ and $KMn_{0.9}Me_{0.1}F_3$ compounds (Me = Mn^{2+}, Co^{2+}, and Ni^{2+}). *Phys. Stat. Sol. (a)*, **54**, 739–743.

Redfern, S.A.T. (1992): The effect of Al/Si disorder on the $I\bar{1}-P\bar{1}$ co-elastic phase transition in Ca-rich plagioclase. *Phys. Chem. Minerals*, **19**, 246–254.

——— (1996): High-temperature structural phase transitions in perovskite ($CaTiO_3$). *J. Phys. Condens. Matter*, **8**, 8267–8275.

Redfern, S.A.T. & Salje, E. (1987): Thermodynamics of plagioclase II: temperature evolution of the spontaneous strain at the $I\bar{1} \leftrightarrow P\bar{1}$ phase transition in anorthite. *Phys. Chem. Minerals*, **14**, 189–195.

——— , ——— (1992): Microscopic dynamic and macroscopic thermodynamic character of the $I\bar{1} - P\bar{1}$ phase transition in anorthite. *Phys. Chem. Minerals*, **18**, 526–533.

Redfern, S.A.T., Graeme-Barber, A., Salje, E. (1988): Thermodynamics of plagioclase III: spontaneous strain at the $I\bar{1} - P\bar{1}$ phase transition in Ca-rich plagioclase. *Phys. Chem. Minerals*, **16**, 157–163.

Redfern, S.A.T., Salje, E., Navrotsky, A. (1989): High-temperature enthalpy at the orientational order-disorder transition in calcite: implications for the calcite/aragonite phase equilibrium. *Contrib. Mineral. Petrol.*, **101**, 479–484.

Redfern, S.A.T., Clark, S.M., Henderson, C.M.B. (1993): High-pressure ferroelastic phase transition in gillespite: new evidence from energy-dispersive diffraction. *Mat. Sci. Forum*, **133-136**, 615–620.

Redfern, S.A.T., Dove, M.T., Wood, D.R.R. (1997): Static lattice simulation of feldspar solid solutions: ferroelastic instabilities and order/disorder. *Phase Trans.*, **61**, 173-194.

Rehwald, W. (1970a): Anomalous ultrasonic attenuation at the 105°K transition in strontium titanate. *Solid St. Comm.*, **8**, 607–611.

——— (1970b): Low temperature elastic moduli of strontium titanate. *Solid St. Comm.*, **8**, 1483–1485.

——— (1971): Ultrasonic properties of strontium titanate at the 105°K transition. *Phys. Condens. Matter*, **14**, 21–36.

——— (1973): The study of structural phase transitions by means of ultrasonic experiments. *Advances in Physics*, **22**, 721–755.

——— (1977): Critical behaviour of strontium titanate under stress. *Solid St. Comm.*, **21**, 667–670.

Reshchikova, L.M., Zinenko, V.I., Aleksandrov, K.S. (1970): Phase transition in $KMnF_3$. *Sov. Phys. Solid St.*, **11**, 2893–2897.

Ridou, C., Rousseau, M., Nouet, J. (1980): Phenomenological description of the first order improper ferroelastic phase transition in $RbCaF_3$ at 194 K. *Ferroelectrics*, **26**, 685–688.

Rigden, S.M., Gwanmesia, G.D., Jackson, I., Liebermann, R.C. (1992): Progress in high-pressure ultrasonic interferometry, the pressure dependence of elasticity of Mg_2SiO_4 polymorphs and constraints on the composition of the transition zone of the earth's mantle. *in* "High pressure research: application to earth and planetary sciences", Y. Syono, M.H. Manghnani, eds. American Geophysical Union, Washington D.C., 167–182.

Rousseau, M., Gesland, J.Y., Julliard, J., Nouet, J., Zarembowitch, J., Zarembowitch, A. (1975): Crystallographic, elastic, and Raman scattering investigations of structural phase transitions in $RbCdF_3$ and $TlCdF_3$. *Phys. Rev. B*, **12**, 1579–1590.

Rüscher, C., Papendick, M., Boysen, H., Putnis, A., Salje, E. (1987): Dielectric and electronmicroscopical studies on leucite $KAlSi_2O_6$. *Z. Krist.*, **178**, 195–196.

Ryzhova, T.V. (1964): Elastic properties of plagioclase. *Izv. Acad. Sci. USSR, Geophys. Ser. (English Translation)*, **7**, 633–635.

Ryzhova, T.V. & Aleksandrov, K.S. (1965): The elastic properties of potassium-sodium feldspars. *Izv. Acad. Sci. USSR, Phys. Solid Earth (English translation)*, **1965**, 53–56.

Sadanaga, R. & Ozawa, T. (1968): Thermal transition of leucite. *Mineral. J.*, **5**, 321–333.

Sakashita, H. & Ohama, N. (1982): A precursor effect in the lattice constant at the 186 K structural phase transition in $KMnF_3$. *Phase Trans.*, **2**, 263–276.

Sakashita, H., Ohama, N., Okazaki, A. (1981): Measurement of the lattice constant of $KMnF_3$ around the 186 K phase-transition: determination of the critical exponent. *J. Phys. Soc. Japan*, **50**, 4013–4021.

——— , ——— , ——— (1990): Thermal expansion and spontaneous strain of $KMnF_3$ near the 186 K-structural phase transition. *Phase Trans.*, **28**, 99–106.

Salje, E. (1985): Thermodynamics of sodium feldspar I: order parameter treatment and strain induced coupling effects. *Phys. Chem. Minerals*, **12**, 93–98.

——— (1986): Raman spectroscopic investigation of the order parameter behaviour in hypersolvus alkali feldspar: displacive phase transition and evidence for Na-K site ordering. *Phys. Chem. Minerals*, **13**, 340–346.

——— (1987): Thermodynamics of plagioclases I: theory of the $I\bar{1} - P\bar{1}$ phase transition in anorthite and Ca-rich plagioclases. *Phys. Chem. Minerals*, **14**, 181–188.

——— (1992): Applications of Landau theory for the analysis of phase transitions in minerals. *Phys. Rep.*, **215**, 49–99.

——— (1993): Phase transitions in ferroelastic and co-elastic crystals (student edition). Cambridge University Press, Cambridge, 229 p.

Salje, E.K.H. & Vallade, M. (1994): Strain-related fluctuations near tricritical points: first order transitions for anisotropic fluctuations and coupling with a tracer order parameter. *J. Phys. Condens. Matter*, **6**, 1–8.

Salje, E., Kuscholke, B., Wruck, B. (1985a): Domain wall formation in minerals: I. Theory of twin boundary shapes in Na-feldspar. *Phys. Chem. Minerals*, **12**, 132–140.

Salje, E., Kuscholke, B., Wruck, B., Kroll, H. (1985b): Thermodynamics of sodium feldspar II: experimental results and numerical calculations. *Phys. Chem. Minerals*, **12**, 99–107.

Salje, E.K.H., Wruck, B., Thomas, H. (1991): Order-parameter saturation and low-temperature extension of Landau theory. *Z. Phys. B*, **82**, 399–404.

Salje, E.K.H., Ridgewell, A., Güttler, B., Wruck, B., Dove, M.T., Dolino, G. (1992): On the displacive character of the phase transition in quartz: a hard-mode spectroscopic study. *J. Phys. Condens. Matter*, **4**, 571–577.

Salje, E., Schmidt, C., Bismayer, U. (1993): Structural phase transitions in titanite, $CaTiSiO_5$: a Raman spectroscopic study. *Phys. Chem. Minerals*, **19**, 502–506.

Samara, G.A. (1971): Pressure and temperature dependence of the dielectric properties and phase transitions of the ferroelectric perovskites: $PbTiO_3$ and $BaTiO_3$. *Ferroelectrics*, **2**, 277–289.

Sapriel, J. (1975): Domain-wall orientations in ferroelastics. *Phys. Rev. B*, **12**, 5128–5140.

Sato, M., Soejima, Y., Ohama, N., Okazaki, A., Scheel, H.J., Müller, K.A. (1985): The lattice constant vs. temperature relation around the 105 K transition of a flux-grown $SrTiO_3$ crystal. *Phase Trans.*, **5**, 207–218.

Schmahl, W.W., Swainson, I.P., Dove, M.T., Graeme-Barber, A. (1992): Landau free energy and order parameter behaviour of the α/β phase transition in cristobalite. *Z. Krist.*, **201**, 125–145.

Schranz, W.T. (1993): Acoustic methods for phase transitions investigations. *Acta Phys. Slov.*, **43**, 183–190.

Schranz, W.T. & Havlik, D. (1994): Heat-diffusion central peak in the elastic susceptibility of KSCN. *Phys. Rev. Lett.*, **73**, 2575–2578.

Schranz, W.T., Parlinski, K., Warhanek, H., Zabinska, K. (1987): Elastic constant behaviour of NH_4LiSO_4 above 460 K. *J. Phys. C*, **20**, 5045–5050.

Schranz, W., Fuith, A., Dolinar, P., Warhanek, H., Haluska, M., Kuzmany, H. (1993): Low frequency elastic properties of the structural and freezing transitions in single-crystal C_{60}. *Phys. Rev. Lett.*, **71**, 1561–1564.

Schwabl, F. (1980): Elastic phase transitions. *Ferroelectrics*, **24**, 171–178.

——— (1985): Propagation of sound at continuous structural phase transitions. *J. Stat. Phys.*, **39**, 719–737.

Schwabl, F. & Täuber, U.C. (1996): Continuous elastic phase transitions in pure and disordered crystals. *Phil. Trans. Roy. Soc. Lond. A*, **354**, 2847–2873.

Scott, J.F. (1974): Soft-mode spectroscopy: experimental studies of structural phase transitions. *Rev. Modern Phys.*, **46**, 83–128.

——— (1989a): Interpretation of the temperature dependence of the dielectric constant of $KMnF_3$ near T_o = 187.5 K. *Ferroelectrics Lett.*, **10**, 149–153.

——— (1989b): Dielectric anomalies in nonferroelectric phase transitions. *JETP Lett.*, **49**, 233–235.

Scott, J.F. & Chen, T. (1991): Evaluation of critical exponents from Raman intensities. *Phase Trans.*, **32**, 235–239.

Shapiro, S.M. & Cummins, H.Z. (1968): Critical opalescence in quartz. *Phys. Rev. Lett.*, **21**, 1578–1582.

Shapiro, S.M., Axe, J.D., Shirane, G., Riste, T. (1972): Critical neutron scattering in $SrTiO_3$ and $KMnF_3$. *Phys. Rev. B*, **6**, 4332–4341.

Shen, A.H., Reichmann, H.-J., Chen, G., Angel, R.J., Bassett, W.A., Spetzler, H. (1998): GHz ultrasonic interferometry in a diamond anvil cell: P-wave velocities in periclase to 4.4 GPa and 207 °C. *in* "Properties

of earth and planetary materials at high pressure and temperature", M.H. Manghnani & T. Yagi, eds. *Geophysical Monograph*, **101**, 71–77. American Geophysical Union.

Shimobayashi, N. (1992): Direct observation on the formation of antiphase domain boundaries in pigeonite. *Am. Mineral.*, **77**, 107–114.

Shimobayashi, N. & Kitamura, M. (1991): Phase transition in Ca-poor clinopyroxenes. A high temperature transmission electron microscopic study. *Phys. Chem. Minerals*, **18**, 153–160.

Shirane, G., Minkiewicz, V.J., Linz, A. (1970): Neutron scattering study of the lattice dynamical phase transitions in $KMnF_3$. *Solid St. Comm.*, **8**, 1941–1944.

Skelton, E.F., Feldman, J.L., Liu, C.Y., Spain, I.L. (1976): Study of the pressure-induced phase transition in paratellurite (TeO_2). *Phys. Rev. B*, **13**, 2605–2613.

Slonczewski, J.C. & Thomas, H. (1970): Interaction of elastic strain with the structural transition of strontium titanate. *Phys. Rev. B*, **1**, 3599–3608.

Smelik, E.A. & Reeber, R.R. (1990): A study of the thermal behavior of terrestrial tridymite by continuous X-ray diffraction. *Phys. Chem. Minerals*, **17**, 197–206.

Smith, J.V. & Brown, W.L. (1988): Feldspar minerals. 1: Crystal structures, physical, chemical and microtextural properties (2nd edition). Springer Verlag, Berlin, Heidelberg, New York, 828 p.

Speer, D. & Salje, E. (1986): Phase transitions in langbeinites I: crystal chemistry and structures of K-double sulfates of the langbeinite type $M_2^{++}K_2(SO_4)_3$, M^{++} = Mg, Ni, Co, Zn, Ca. *Phys. Chem. Minerals*, **13**, 17–24.

Spetzler, H., Shen, A., Chen, G., Herrmannsdoerfer, G., Schulze, H., Weigel, R. (1996): Ultrasonic measurements in a diamond anvil cell. *Phys. Earth Planet. Int.*, **98**, 93–99.

Stixrude, L. & Cohen, R.E. (1993): Stability of orthorhombic $MgSiO_3$ perovskite in the Earth's lower mantle. *Nature*, **364**, 613–615.

Stixrude, L., Cohen, R.E., Yu, R., Krakauer, H. (1996): Prediction of phase transition in $CaSiO_3$ perovskite and implications for lower mantle structure. *Am. Mineral.*, **81**, 1293–1296.

Stokes, H.T. & Hatch, D.M. (1988): Isotropy subgroups of the 230 crystallographic space groups. World Scientific, Singapore.

Stokka, S. & Fossheim, K. (1982): Specific heat and phase diagrams for uniaxially stressed $KMnF_3$. *J. Phys. C*, **15**, 1161–1176.

Stokka, S., Fossheim, K., Samulionis, V. (1981): Tricritical behaviour of $KMnF_3$. *Phys. Rev. Lett.*, **47**, 1740–1743.

Sumino, Y. & Anderson, O.L. (1984): Elastic constants of minerals. *in* "Handbook of physical properties of rocks", R.S. Carmichael, ed. CRC Press, Boca Raton, Florida, **III**, 39–138.

Suzuki, I., Anderson, O.L., Sumino, Y. (1983): Elastic properties of a single-crystal forsterite Mg_2SiO_4, up to 1,200 K. *Phys. Chem. Minerals*, **10**, 38–46.

Taylor, M. & Brown, G.E. (1976): High-temperature structural study of the $P2_1/a \rightleftarrows A2/a$ phase transition in synthetic titanite, $CaTiSiO_5$. *Am. Mineral.*, **61**, 435–447.

Terhune, R.W., Kushida, T., Ford, G.W. (1985): Soft acoustic modes in trigonal crystals. *Phys. Rev. B*, **32**, 8416–8419.

Tezuka, Y., Shin, S., Ishigame, M. (1991): Observation of the silent soft phonon in β-quartz by means of hyper-Raman scattering. *Phys. Rev. Lett.*, **18**, 2356–2359.

Tietze, H., Müllner, M., Jex, H. (1983): A new method to determine structural domains. *J. Phys. C*, **16**, 2209–2216.

Tokumoto, H. & Unoki, H. (1983): Investigation of structural phase transition of $BiVO_4$ by Brillouin-scattering measurements. *Phys. Rev. B*, **27**, 3748–3761.

Tolédano, J.C., Errandonea, G., Jaguin, J.P. (1976): Soft acoustic mode in ferroelastic lanthanum pentaphosphate. *Solid St. Comm.*, **20**, 905–907.

Tolédano, P., Fejer, M.M., Auld, B.A. (1983): Nonlinear elasticity in proper ferroelastics. *Phys. Rev. B*, **27**, 5717–5746.

Tomonaga, N., Soejima, Y., Okazaki, A. (1990): A 2θ-resolved HADOX study of $BaTiO_3$. *Phase Trans.*, **28**, 51–61.

Torres, J. (1975): Symétrie du paramètre d'ordre de la transition de phase ferroélastique du phosphate de plomb. *Phys. Stat. Sol. (b)*, **71**, 141–150.

Tribaudino, M., Benna, P., Bruno, E. (1993): $I\bar{1}$ – *I2/c* phase transition in alkaline-earth feldspars along the $CaAl_2Si_2O_8$-$SrAl_2Si_2O_8$ join: thermodynamic behaviour. *Phys. Chem. Minerals*, **20**, 221–227.

Unoki, H., Tokumoto, H., Ishiguro, T. (1984): Brillouin-scattering study of sound velocity of quartz at α-β transition. *in* "Phonon scattering in condensed matter", W. Eisenmenger, K. Lassmann, S. Döttinger, eds. Springer-Verlag, Berlin, Heidelberg, New York, Tokyo, *Springer series in Solid State Sciences*, **51**, 292–294.

Uwe, H. & Tokumoto, H. (1979): Pressure-induced ferroelastic transition and internal displacement mode in TeO_2. *Phys. Rev. B*, **19**, 3700–3707.

Vacher, R. & Boyer, L. (1972): Brillouin scattering: a tool for the measurement of elastic and photoelastic constants. *Phys. Rev. B*, **6**, 639–673.

Vallade, M., Berge, B., Dolino, G. (1992): Origin of the incommensurate phase of quartz: II. Interpretation of inelastic neutron scattering data. *J. de Physique I*, **2**, 1481–1495.

Van Heurck, C., Van Tendeloo, G., Ghose, S., Amelinckx, S. (1991): Paraelectric-antiferroelectric phase transition in titanite, $CaTiSiO_5$ II. Electron diffraction and electron microscopic studies of the transition dynamics. *Phys. Chem. Minerals*, **17**, 604–610.

Vo-Thanh, D. & Diep-The-Hung (1985): Theoretical study of the elastic constants of calcite at the transition calcite I – calcite II. *Phys. Earth Planet. Int.*, **39**, 62–71.

Vo Thanh, D. & Lacam, A. (1984): Experimental study of the elasticity of single crystalline calcite under high pressure (the calcite I – calcite II transition at 14.6 kbar). *Phys. Earth Planet. Int.*, **34**, 195–203.

Wada, M., Nakayama, Y., Sawada, A., Tsunekawa, S., Ishibashi, Y. (1979): Raman scattering and fluorescence spectra of $LaNbO_4$. *J. Phys. Soc. Japan*, **47**, 1575–1580.

Wadhawan, V.K. (1982): Ferroelasticity and related properties of crystals. *Phase Trans.*, **3**, 3–103.

Wang, Y., Guyot, F., Yageneh-Haeri, A., Liebermann, R.C. (1990): Twinning in $MgSiO_3$ perovskite. *Science*, **248**, 468–471.

Wang, Y., Weidner, D.J., Liebermann, R.C., Liu, X., Ko, J., Vaughan, M.T., Zhao, Y., Yeganeh-Haeri, A., Pacolo, R.E.G. (1991): Phase transition and thermal expansion of $MgSiO_3$ perovskite. *Science*, **251**, 410–413.

Wang. Y., Guyot, F., Liebermann, R.C. (1992): Electron microscopy of $(Mg,Fe)SiO_3$ perovskite: evidence for structural phase transitions and implications for the lower mantle. *J. Geophys. Res.*, **97**, 12327–12347.

Warren, M.C. & Ackland, G.J. (1996): Ab initio studies of structural instabilities in magnesium silicate perovskite. *Phys. Chem. Minerals*, **23**, 107–118.

Webb, S.L. (1989): The elasticity of the upper mantle orthosilicates olivine and garnet to 3 GPa. *Phys. Chem. Minerals*, **16**, 684–692.

Webb. S.L. & Jackson, I. (1993): The pressure dependence of the elastic moduli of single-crystal orthopyroxene $(Mg_{0.8}Fe_{0.2})SiO_3$. *Eur. J. Mineral.*, **5**, 1111–1119.

Wennemer, M. & Thompson, A.B. (1984a): Tridymite polymorphs and polytypes. *Schweiz. Mineral. Petrogr. Mitt.*, **64**, 335–353.

———, ——— (1984b): Ambient temperature phase transitions in synthetic tridymites. *Schweiz. Mineral. Petrogr. Mitt.*, **64**, 355–368.

Wentzcovitch, R.M., Ross, N.L., Price, G.D. (1995): Ab initio study of $MgSiO_3$ and $CaSiO_3$ perovskites at lower mantle pressures. *Phys. Earth Planet. Int.*, **90**, 101–112.

Wolf, G.H. & Bukowinski, M.S.T. (1987): Theoretical study of the structural properties and equations of state of $MgSiO_3$ and $CaSiO_3$ perovskites: implications for lower mantle composition. *in* " High-pressure research in mineral physics", M.H. Manghnani & Y. Syono, eds. American Geophysical Union, 313–331.

Wooster, W.A. (1973): Tensors and group theory for the physical properties of crystals. Clarendon Press, Oxford, 344 p.

Worlton, T.G. & Beyerlein, R.A. (1975): Structure and order parameters in the pressure-induced continuous transition in TeO_2. *Phys. Rev. B*, **5**, 1899–1907.

Xiao, Y. & Kirkpatrick, R.J. (1995): Nuclear magnetic resonance investigations of the structural phase transitions of $AlPO_4$ tridymite. *J. Mater. Res.*, **10**, 2586–2591.

Xiao, Y., Kirkpatrick, R.J., Kim, Y.J. (1993): Structural phase transitions of tridymite: a ^{29}Si MAS NMR investigation. *Am. Mineral.*, **78**, 241–244.

——, ——, —— (1994): Nuclear magnetic resonance investigation of structural phase transitions in SiO_2 tridymite. *in* "Solid → solid phase transformations", W.C. Johnson, J.M. Howe, D.E. Laughlin, W.A. Soffa, eds. The Minerals, Metals and Materials Society, 755–760.

——, ——, —— (1995): Investigations of MX-1 tridymite by ^{29}Si MAS NMR – modulated structures and structural phase transitions. *Phys. Chem. Minerals*, **22**, 30–40.

Xu, H. & Veblen, D.R. (1996): Superstructures and domain structures in natural and synthetic kalsilite. *Am. Mineral.*, **81**, 1360–1370.

Yamamoto, A. (1974): Lattice-dynamical theory of structural phase transition in quartz. *J. Phys. Soc. Japan*, **37**, 797–808.

Yao, W., Cummins, H.Z., Bruce, R.H. (1981): Acoustic anomalies in terbium molybdate near the improper ferroelastic-ferroelectric phase transition. *Phys. Rev. B*, **24**, 424–444.

Yeganeh-Haeri, A, Weidner, D.J., Ito, E. (1989a): Elasticity of $MgSiO_3$ in the perovskite structure. *Science*, **243**, 787–789.

——, ——, —— (1989b): Single-crystal elastic moduli of magnesium metasilicate perovskite. *in* "Perovskite, "Perovskite, a structure of great interest to geophysics and materials science", A. Navrotsky & D.J. Weidner, eds. Geophysical Monograph, **45**, 13–25. American Geophysical Union, Washington, D.C.

Zaug, J.M., Abramson, E.H., Brown, J.M., Slutsky, L.J. (1992): Elastic constants, equations of state and thermal diffusivity at high pressure. *in* "High pressure research: application to earth and planetary sciences", Y. Syono, M.H. Manghnani, eds. American Geophysical Union, Washington D.C., 157–166.

——, ——, ——, —— (1993): Sound velocities in olivine at earth mantle pressures. *Science*, **260**, 1487–1489.

Zha, C.-S., Duffy, T.S., Downs, R.T., Mao, H.-K., Hemley, R.J. (1996): Sound velocity and elasticity of single-crystal forsterite to 16GPa. *J. Geophys. Res.*, **101**, 17535–17545.

Zha, C.-S., Duffy, T.S., Downs, R.T., Mao, H.-K., Hemley, R.J., Weidner, D.J. (1998): Single-crystal elasticity of the α and β of Mg_2SiO_4 polymorphs at high pressure. *in* "Properties of earth and planetary materials at high pressure and temperature", M.H. Manghnani & T. Yagi, eds. *Geophysical Monograph*, **101**, 9–16. American Geophysical Union.

Zhang, M., Salje, E.K.H., Bismayer, U., Unruh, H.-G., Wruck, B., Schmidt, C. (1995): Phase transition(s) in titanite $CaTiSiO_5$: an infrared spectroscopic, dielectric response and heat capacity study. *Phys. Chem. Minerals*, **22**, 41–49.

Zhao, Y., Weidner, D.J., Parise, J.B., Cox, D.E. (1993a): Thermal expansion and structural distortion of perovskite – data for $NaMgF_3$ perovskite. Part I. *Phys. Earth Planet. Int.*, **76**, 1–16.

——, ——, ——, —— (1993b): Critical phenomena and phase transition of perovskite – data for $NaMgF_3$ perovskite. Part II. *Phys. Earth Planet. Int.*, **76**, 17–34.

Zubov, V.G. & Firsova, M.M. (1962): Elastic properties of quartz near the α-β transition. *Sov. Phys. Crystallography*, **7**, 374–376.

Received 13 May 1997
Accepted in revised form 27 February 1998